IEAGHG Technical Report 2017-08 August 2017

CO_2 Migration in the Overburden

IEA GREENHOUSE GAS R&D PROGRAMME

International Energy Agency

The International Energy Agency (IEA) was established in 1974 within the framework of the Organisation for Economic Co-operation and Development (OECD) to implement an international energy programme. The IEA fosters co-operation amongst its 29 member countries and the European Commission, and with the other countries, in order to increase energy security by improved efficiency of energy use, development of alternative energy sources and research, development and demonstration on matters of energy supply and use. This is achieved through a series of collaborative activities, organised under 39 Technology Collaboration Programmes. These Programmes cover more than 200 individual items of research, development and demonstration. IEAGHG is one of these Technology Collaboration Programmes.

ACKNOWLEDGEMENTS AND CITATIONS

This report describes research commissioned by IEAGHG. This report was prepared by:

- British Geological Survey (BGS)

The principal researchers were:

- M. C. Akhurst
- R. A. Chadwick
- J. da L. Gafeira
- S. D. Hannis
- D. G. Jones
- K. L. Kirk
- J. M. Pearce
- C. A. Rochelle
- M. A. Stewart
- H. Vosper
- J. C. White
- J. D. O. Williams

To ensure the quality and technical integrity of the research undertaken by IEAGHG each study is managed by an appointed IEAGHG manager. The report is also reviewed by a panel of independent technical experts before its release.

The IEAGHG managers for this report were:

- Lydia Rycroft & James Craig

The report should be cited in literature as follows:

'IEAGHG, "CO_2 Migration in the Overburden", 2017/08, August, 2017.'

Further information or copies of the report can be obtained by contacting IEAGHG at:

IEAGHG, Pure Offices, Cheltenham Office Park
Hatherley Lane, Cheltenham,
GLOS., GL51 6SH, UK

Tel: +44 (0)1242 802911 E-mail: mail@ieaghg.org Internet: www.ieaghg.org

CO_2 MIGRATION IN THE OVERBURDEN (IEA CON/16/237)

Key Messages

- This study was conducted to assess the natural rates of CO_2 and fluid migration that occur in the overburden (defined as the entire geological succession above the target reservoir formation with the lowermost stratum forming the primary seal) and the potential rates that may arise in the unlikely event of unintended migration outside a designated storage complex. The aim was to better inform risk assessments for CO_2 storage sites by providing relevant information on the effect of large-scale features associated with natural fluid migration analogues in the overburden.
- With appropriate site selection and site characterisation risk-based process, CO_2 storage sites are selected to minimise the likelihood and impacts of fluid migration.
- The five case studies in this report highlight that storage sites are likely to have numerous secondary storage formations within the overburden with low permeability sequences (e.g. shale) providing secondary seals, in addition to the primary caprock seal, thereby hindering or preventing migration through the overburden.
- The natural migration of fluid in the overburden over geological timescales is evident from the presence of chimneys, gas hydrates and sediment injections (pockmarks, mud volcanoes and mounds are also present offshore). Generally their formation has been well researched although their current in-situ properties (and their impacts on fluid flow) require further analysis due to the lack of data.
- The principal potential geological pathways which may enable the migration of fluids within the overburden are fractures and faults (chimneys and large-scale geomorphological features such as tunnel valleys and mass-movement deposits may also enhance flow in the overburden).
- Ice-loading on bedrock and sediment deposits can cause rafting, fracturing and faulting. Potential fluid migration pathways are created along faulted surfaces and rafting disrupting lateral seals. Evidence of glacio-tectonic deformation is recorded in areas where CO_2 storage is operational or planned such as onshore in Canada and offshore in the North Sea.
- The large volume and complexity of the overburden makes modelling potential migration pathways difficult. The characterisation of overburden structures should focus on parameterising elements and quantifying potential fluid flow rates.
- From this report, it is recommended that further in-situ data is acquired during future work, directly sampling overburden features such as faults and chimneys. Direct sampling is required to further refine the potential fluid properties of these structure and their implications for fluid migration. Further research, for example the EU funded STEMM project, will investigate these features and is already underway.

Background to the Study

At CO_2 storage sites, large-scale overburden heterogeneities and introduced man-made pathways (e.g. wells) could potentially breach the sealing strata and promote the migration of injected CO_2 in the dense, gaseous or dissolved phase. The ability to fully characterise the overburden would therefore allow identification of the preferred CO_2 vertical migration pathways which will then encourage more complete risk assessments. Overall this will allow for more focussed monitoring efforts and will lead to the deselection of sites prone to vertical migration.

The overburden is very site-specific but at most CO_2 storage projects it consists of a thick sequence of sedimentary rocks and young, poorly consolidated sediments. Heterogeneities in overburden sequences may allow fluids to flow vertically across stratal boundaries and provide fluid flow pathways to shallower depths or laterally beyond the immediate vicinity of the fluid source. In most cases the overburden will inevitably include internal heterogeneities and features (e.g. gas chimneys, and glacial landform) and many of these structures could serve to either hinder or promote fluid migration.

Understanding and quantifying potential migration of fluids within the overburden is difficult because of limited in-situ data from common large-scale features over large areas. Incorporation of overburden heterogeneities into risk assessments, given large uncertainties associated with some structures, presents an additional challenge for site selection and characterisation. IEAGHG published a report in 2016 reviewing the permeability of faults and this report develops on this work to look specifically at the overburden and other associated structures.

Scope of Work

This report documents the subsurface processes that may enable CO_2 to potentially migrate from the storage reservoir to within the overburden sequence. The potential rates of migration for each migration pathway and the implications for leakage are discussed. Secondary trapping mechanisms within the overburden are also discussed within the report. The conclusions are focused on tying overburden characteristics to their impact on developing risk assessments.

As well as specific pathway structures, five CO_2 storage projects were selected for this review and the characteristics of the overburden sequence that promote trapping and hinder migration at each site are a summarised. The projects chosen were the offshore Sleipner and Snøhvit CO_2 storage projects, the planned storage site in the Goldeneye Field, the onshore Ketzin pilot CO_2 injection project in Germany and the Field Research Station in Canada.

Findings of the Study

Case Studies of Overburden Sequences

1. Sleipner

The Sleipner site is divided into Upper, Middle and Lower Seal sections which have all been characterised in detail using seismic techniques and drill cuttings. The Lower Seal has a high clay content with over 80% shale volume and is the most efficient sealing layer. Middle Seal units are generally considered to be fine-grained hemipelagic distal sediments sourced from large river systems. Tunnel valleys are present with the Upper Seal and their infill remains largely untested. Subglacial tunnels are extensive over the Sleipner area but not well characterised.

Caron dioxide is injected into the Utsira sand unit at 1016m depth. Since injection began in 1996 a 200m CO_2 plume has been created between the release point and the top seal. A difference in seismic signal has been noted in the overburden (above the top seal) but has been attributed to background noise and naturally occurring gas pockets rather than CO_2 leakage signals (after conducting an analysis to calculate detection thresholds). Extensive work has been undertaken to calculate leakage detection limits for the Sleipner field and are discussed within the report. They concluded that pore volumes greater than 3000 cubic metres would be detectable anywhere in the succession; this corresponds to a mass of approximately 2000 tonnes, based on a conservative assumption of 100% CO_2 saturation. A feeder chimney is also noted within the CO_2 plume itself which is thought to have been responsible for some upward migration of CO_2 within the plume (i.e within the storage reservoir, but still trapped by the seal). It must be emphasised that although there has been lateral migration beneath the top seal no leakage has been detected in the 20 years of CO_2 injection.

2. Snøhvit

At Snøhvit thick sequences of Cretaceous and Upper Jurassic shale forms the caprock for the CO_2 storage reservoir. Caprock permeability and porosity values have been published for the overburden units in the report, taken from well logs and literature review:

Overburden formation	Average porosity (%)			Average permeability (mD)		
	Low	Medium	High	Low	Medium	High
Torsk	33	36	38	23	31	39
Kveite	30	33	35	16	22	28
Kolmule	28	30	32	11	15	19
Kolje	24	25	27	6	8	10
Knurr	21	24	27	4	7	10
Hekkingen	5	13	20	4	8	12

Table 1 Porosity and permeability values for formations in the overburden to the Snøvhit CO_2 storage site, ordered from deepest (Tork) to shallowest formation.

There have been two distinct phases of injection at Snøhvit, Phase 1 injection was into the Tubåen Formation (2600m depth) and Phase 2 in to the Stø Formation (2450m). Phase 1 ceased in 2011 and Phase 2 commenced shortly after. To date, over three million tonnes of CO_2 have been successfully stored at Snøhvit, with seismic evidence of retention present in both reservoirs.

Several large chimneys have also been mapped using seismic surveying in the vicinity of the field. The seismic data shows large zones of poor reflection which has been attributed to possible residual gas saturations. The mechanisms behind their formation and potential fluid flow rates are not well understood bu these features are not associated with the CO_2 storage at Snøhvit.

3. Ketzin

The lower caprock at Ketzin is overlain by a succession of three sandstone and mudstone Jurassic units. These are then topped with a 100m thick clay separating the storage units from an overlying aquifer system, currently exploited for drinking water. Overall the CO_2 store is overlain by 400m of sealing units with multiple 'barrier' layers. Since the closure of the site in 2013, seismic data reveals no evidence of migration into the overburden.

4. Goldeneye

Injection of CO_2 was planned at the site (now a disbanded project) at 2,400m depth in the Captain Aquifer sandstone. The reservoir is capped with a 60m thick low permeability mudstone with proven hydrocarbon sealing properties over geological timescales. Overlying the primary seal the overburden has been identified as including 4 aquicludes which would prevent the upwards migration of CO_2. Although the upper part of the overburden is glacially influenced (e.g. tunnel valley infill), the flat lying mud-dominated nature of the overburden sequence provides suitable sealing capacity.

Seismic data over the site showed evidence for faulting within the reservoir but this was not present in tertiary deposits. There is no evidence of the faults compartmentalising the reservoir and even the largest fault throws estimated at less than 20m.

5. Field Research Station, Alberta Canada

The Field Research Station is a shallow experimental injection and controlled release site with two injections planned to 300m and 500m depth. The site is being developed to test monitoring techniques with both containment and migration from the planned release points. The CO_2 detection thresholds will also be tested with the migration of CO_2 and CH_4 both monitored.

The 500m injection aquifer is sealed with 50 meters of shale cap rock. The shallow 300m injection is not considered to be effectively sealed with the intention of allowingCO_2

migration to the surface for monitoring research purposes. The overburden may be hydraulically fractured to analyse further migration out of the reservoir subject to regulator's approval.

Mechanisms, Processes and Rates of Migration

1. Faults

A recent review published by the IEAGHG (Nicol et al., 2015) examined the controls on fault zone permeability in detail, and therefore only a summary is presented in this report.

Faults and fractures are highly complex zones of heterogeneous deformation distribution and can either inhibit or promote flow over a range of scale, geometry and temporal changes. This means simple models (based on a fault core with damage zone) are usually adopted but few outcrops are in reality this simple. Overall the nature of deformation and in-situ stresses acting on the fault determine whether it will form a barrier or flow pathway. Areas of structural complexity (such as relays, bends and terminations) are usually zones of local high strain and are therefore considered to be potential areas of elevated fault zone permeability.

The simplest way to evaluate, if cross fault flow is likely to occur, is to assess the juxtaposition of the strata. Whether the reservoir is lower or higher permeability than adjacent rocks will determine the likelihood of flow (if higher permeability, flow is unlikely out of the reservoir). For multi-layered sand-shale sequences fault seal analysis relies on capillary thresholds versus buoyancy driven overpressure. Capillary pressure has to be exceeded by buoyancy to allow for the migration of fluids. In summary, fault rock material with smaller pore throat radii will have higher capillary threshold pressures and are therefore capable of supporting greater column heights of supported or trapped buoyant fluid.

Commonly, shale gouge ratio (SGR) and shale/clay smear factors are used to look at fault composition and sealing potential. After the fault clay volume is calculated the SGR may be converted to permeability and/or threshold pressure. Although this method is relatively easy to implement it has been found that it does not fully account for many observed fault rock heterogeneities.

The formation of deformation bands has also been shown to reduce permeability which may increase fluid flow along-strike although their full impact is unclear given their high variability in three-dimensions. Diagenesis and mineralisation will also impact fault permeability. Re-activating a fault can cause fluid migration, but just because it is critically stressed it does not mean it will be permeable as impermeable fault gouge can form.

With regards to CO_2 injection, further work has shown that the wettability of the injected fluid is important but is only significant if threshold capillary pressure of material is overcome. The CO_2 may also cause dissolution of calcite in cements which will increase permeability, although at low pressures the calcite would re-precipitate reducing the effectiveness of the migration pathway.

Salt structures have been shown to lead to radial fault structures in the overburden above the crest. Shallow gas is also often located above salt domes. In exhumed sedimentary basins the reactivation of faults has been known to cause breach of seal rock in some hydrocarbon reservoirs. Findings show sand incorporation needs to be considered for fault planes in unconsolidated sediment.

2. Geological Fluid Flow Features

A variety of fluid flow features were covered including pockmarks, chimneys or pipes, mud volcanoes, sand mounds, gas hydrates, sediment injections and carbonate mounds. Their formation, distribution, fluid flow properties and implication for migration of CO_2 in the overburden are discussed. The source of the fluid, flow type and structural setting define the nature of structure as shown in Figure 1.

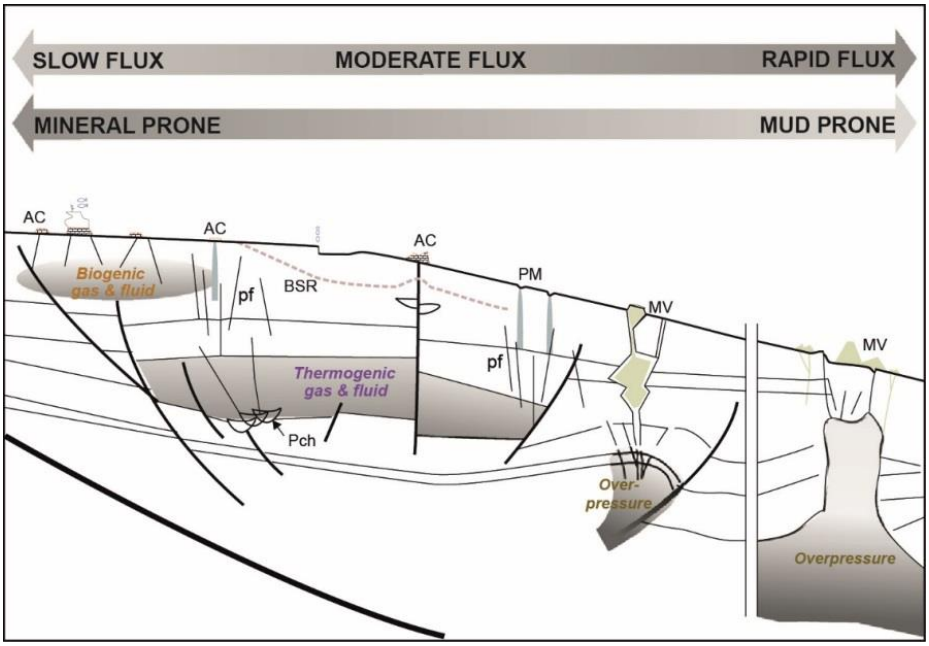

Figure 1 Schematic synthesis of the origins and trigger mechanisms of cold seep systems and the relationships between flow rates and different seeping / venting morphologies observed on the seabed.

Chimneys are a focus of the report given they are common in sedimentary basins and particularly the North Sea. They are of increasing interest in the CCS community as they may have the potential to act as a rapid fluid flow pathways. Current understanding of chimney hydraulic properties and potential fluid flow rates are poor. Three projects have been identified to be investigating chimney structures in the near future:

- The EU funded STEMM-CCS project: its purpose is to use seismic and electromagnetic techniques alongside a drilling and logging program to look at in-situ properties of large deep-rooted chimneys.

- UK NERC funded CHIMNEY project: a geophysical experiment is planned to characterise the internal structure of a chimney (specifically fracture systems) using broadband seismic anisotropy experiments.
- The QICS experiment (Blackford et al., 2014) demonstrated both short-term buoyancy-driven flow in the sedimentary column and also longer term stabilisation as dissolution processes take over with differing rates of dissolution in the dispersed CO_2 of the chimney compared with more highly saturated CO_2 in the layers.

Chimneys are widely considered to be fluid leak-off points from over-pressured sedimentary sequences. Another common theory is that they occur due to rapid depressurisation leading to gas expansion. The in-situ properties of chimneys, and hence their impact on fluid flow, are still poorly understood. Tasianas et al., 2016 wrote a significant report on modelling chimneys using data from a drilled chimney in the East Sea with a 63.7-83.3% porosity range and 0.46-4.85D permeability range. Their work concluded the presence of high permeability chimneys meant that a lower overpressure was needed to drive leakage than to disrupt the sealing overburden. However once the chimney is in place, permeability of the reservoir had a greater impact on fluid migration rates.

The detection of pockmarks is reliant on high-resolution geophysical equipment and hence their known occurrences are currently in economically developed areas. Pockmarks have sizes recorded over 4 magnitudes although most are recorded to be between 10-250m diameter and 1-25m deep. The most common gas to occur within the associated marine sediments is methane as well as carbon dioxide and hydrogen sulphide, the gases are commonly considered to be of biogenic origin. Pockmarks can occur in both random and non-random distribution (the latter are associated with faults and buried channels). The origin, longer-term activity, alteration and preservation of pockmarks still requires further investigation. These features also show the importance of understanding the underlying geology when interpreting seepage features.

Mud volcanoes are the largest surface expressions resulting from fluid flow and are fed by deep gas accumulations and occur mainly in deep waters. They more commonly occur in clusters but can form isolated volcanoes. Submarine mud volcanoes can range from 0.5 to 800 meters in height. The greatest controls on fluid migration are recent tectonic activity (particularly compressional); sedimentary or tectonic loading (due to rapid sedimentation); hydrocarbon generation and the existence of thick plastic sediments in the sedimentary successions.

Sand mound features in North Sea sediments have shown very high amplitude responses in seismic survey datasets. Faulting above the mounds suggest they were formed by post-depositional mobilisation of relatively shallowly buried sands, but there is limited evidence to suggest vertical migration from the mounds into overlying sediments.

Gas seepage data is hard to acquire and although they commonly occur worldwide very few gas seepage rates have been measured, these datasets are therefore limited even on natural sites. The GEOMAR project (Germany) is currently developing new 3D technique called bubble box to calculate overall gas flux.

3. Geomorphological High-Permeability Pathways or Barriers to Flow

Mass submarine movements can cause large quantities of material to be deposited and therefore have the potential to represent significant components of continental margin stratigraphy. A variety of sediments can be deposited (from sand to mud rich) and if comprised of mainly coarse grained material they can form high permeability sequences or they can form baffles if predominantly fine material is deposited.

The 3D seismic data from the northern flank of the North Sea Fan has revealed pipe structures beneath the Tampen Slide Deposits. The structures shown in the seismic profile indicate that the internal structure of the slide deposits interfered with fluid migration through the sedimentary overburden and served as a barrier to fluid-flow through discontinuities within the slide.

Tunnel valleys are the largest structure preserved in the Quaternary succession of the North Sea and range from 500m to 4km wide be up to 100km in length and form erosion features hundreds of metres deep forming significant overburden structures. Currently no CCS projects are thought to be planned within areas where tunnel valleys are present but this may be increasingly likely in the future and hence their importance needs to be understood. At present relatively little is known about the flow properties of offshore buried tunnel valleys as seismic surveys show limited fill structure and a lack of borehole data is available. Most studies agree that coarse sand bodies may be present within the tunnel valley structure which should be considered to enable high permeability flow, but their extent and connectivity remains poorly understood. The large size, linear extent and erosive base of tunnel valleys can either enhance or impede fluid flow within the shallow overburden. As they form conduits for naturally occurring gas their characterisation is important to identify the origin of the seep and prevent false leakage signals being attributed to the site. Ancient tunnel valleys onshore (E.g. Ordovician deposits in Libya and Alegria) are more studied due to potential hydrocarbon sites being present.

4. Hydrofracturing and Glaciotectonic Faulting

Ice sheet loading on sedimentary rocks can cause hydrofracturing and soft-sediment extrusions which are preserved within the overburden sequences. The weight of the ice creates faults and folds in both the bedrock (up to 1500m depth in Netherlands) and unconsolidated sediment at the time of deposition which is then recorded within the rock sequences. Faults within these settings can be laterally extensive at up to 10s of km length. In these sequences deformation is found to be most pronounced at margins of the advancing ice mass. Glaciotectonism can also lead to the detachment and transportation of large blocks although the formation of these rafts is complicated and still debated within the literature reviewed. Overall, structures discussed are shown to vary greatly in scale from tens of meters to kilometres. They can be highly variable (non-uniform and erratic) causing sudden changes in lithology which would directly impact migration pathways.

5. Well Integrity Studies

Potential rates of CO_2 migration due to lack of wellbore integrity are currently unknown although it is currently a very active area of research involving theoretical studies, numerical simulation, laboratory experiments, field-scale experiments and observations from real sites. It is difficult to estimate corrosion caused by CO_2 as it is highly site specific and experiments can make only make a short-term comparison. Accessing wells to do initial analysis without potentially compromising the well integrity by doing so is also an added difficulty to studying well integrity.

The potential defects addressed in the report are:

- Construction defects: when drilling the formation swelling or cavities can form. For installation of the pipe materials need to be non-corrosive, threaded well and centralised in the borehole. Cement defects normally addressed by a 'squeeze job'.
- Mechanical-thermal loading defects: thermal stresses can cause swelling or shrinkage due to the injection of fluids at different temperatures to those in-situ and phase changes (e.g. the Joule-Thompson effect). Mechanical stresses can be caused by the pressure cycling of injection and production as well as natural sources such as earthquakes.
- Chemical loading defects: causing the alteration of the cement or the metal casing due to injected fluids/gases dissolving or precipitating material.

Wells are designed to not leak and therefore within literature there are no potential migration leakage rates defined. The main research focus for wellbore integrity is to look at cement alteration rates and how different alterations can be good or bad for potential leakage risk. Long-term storage analysis can only be investigated via modelling as laboratory experiments can only be conducted on relatively short timescales.

Studies have found that well leakage pathway permeability is the greatest control on leakage volume and rate. Reverse-flow events are likely to have much higher rates than Darcy flow models predict but these events are likely to last for less than a year.

Generally there is very limited data on wellbore leakage rates although data from analogue sites suggests comparatively low leakage rates mostly <0.1 t/year – 100 t/ year. Low level leaks might remain undetected because they are not obvious.

Modelling Studies and Experimental Work

When modelling the overburden a key element is reducing the number of parameters to quantify geological features to prevent the model becoming expensive and excessively detailed. The overburden is usually reduced to a few distinct sequences e.g. aquifers and aquitards.

Assessing the likelihood of leakage through wellbores and faults is also key element. Faults are very site specific, depending on external conditions and therefore can be hard to model.

Usually parameters in the models are estimated then a sensitivity analysis is conducted to establish worst case scenarios. The complexity of modelling the overburden is also added to as CO_2 undertakes phase changes from supercritical to gaseous phase as it migrates upwards towards the surface.

During the characterisation stage, faults fall under two categories for modelling: those large enough to be detected by seismic techniques then smaller faults that are not. Faults are very site specific (stress field, permeability, strength) and hence can incur large uncertainties and be difficult to model. Fault models also need to include geomechanical modelling to incorporate new/ existing fractures as a result of injection. The literature review for fault migration rates in the study showed that in general, increasing the length, aperture and permeability of a fault increases the potential flow rate through it. Leakage rates from 0 to 80 kt/year were simulated, and up to 50% of the simulated injected CO_2 escaped through faults.

Reference	Fault dimensions	Fault permeability	Aquifer permeability and thickness	CO_2 injection rate	Leakage rate (or proportion of CO_2 leaked)
Aoyagi, 2011	50 m x 500 m	10, 100, 1000 mD	100 mD	500 kt/year (30 years)	0, 6, 79 kt/year
Huang et al., (2015)	10 m-wide	0.1 mD	10^{-13} m² (100 mD)	0.3, 0.9, 1.6, 2.2 kt/year	Up to 1.2 x 10^{-4} m³/s
Martinez et al., (2013)	Dynamic	Dynamic	3-5x10^{-14} m² (30-50 mD), >100 m	2.85, 5.5 Mt/year (max 30 years)	(16%, 20%)
Nakajima et al., (2014)	5 m x 1 km	100 mD-1D	10 mD, 40 m	100kt/year	0.2-0.6 kt/year (1% of total)
Ramachandran et al., (2014)	One dimensional	10 mD, 1000 mD	N/A	Continuous source (hydrostatic pressure)	12, 1200 t/year/m²
Vialle et al., (2016)	1 m fault core plus 40–100 m damage zone	10^{-6} mD in fault core, 0.001 mD - 1 mD in damage zone	100mD	Gas initially in place (10 years)	200-320 t/year (0.1-1% annually)
Zahasky and Benson (2014)	3 m x 500 m	1-1000 mD	2.8-280 mD, 68 m	0.25 Mt/year	0.1%-50%

Table 2 A summary of leakage rates through simulated faults (units are converted from source data for consistency in comparison).

Modelling the overburden is difficult given the high variability in a storage site's characterisation and therefore it is challenging to identify a suitable range of parameter values. Wellbore integrity, geochemical processes, reduced order methods and leakage rate modelling are also discussed within the report.

Overburden Trapping Potential

There are three dominant trapping processes physical, hydrodynamic and chemical that occur within the overburden. Physical trapping can be either static (trapped by a barrier to flow) or residual saturation (some CO_2 remains in the pore space as plume moves due to capillary

forces). Hydrodynamic trapping is a combination of physical and chemical trapping as CO_2 migrates to the surface and applies to sites with no stratigraphic trap. Extremely slow migration on geological timescales could lead to possible trapping. There is also a potential for large amounts of CO_2 to become trapped via dissolution. When CO_2 mixes with brine the resulting solution is denser than brine and hence causes the buoyant CO_2 reservoir to diminish (as the dense mixture sinks to the bottom of the storage reservoir) and over long-time scales reduces the risk of leakage. Chemical trapping is the result of CO_2 reaction with the pore fluid and reservoir matrix (mineral formation, adsorption onto coal surfaces and hydrate formation). Field evidence from south-east Utah shows that feldspar dissolution occurs adjacent to faults that have conducted CO_2 saturated groundwater. This process is also likely to occur in diffusion controlled migration in mudstones.

Once CO_2 leakage occurs, self-enhancing and prohibiting processes occur which are dominant within different timescales. These are summarised in the report and the timescales for each trapping mechanisms are summarised in Figure 3.

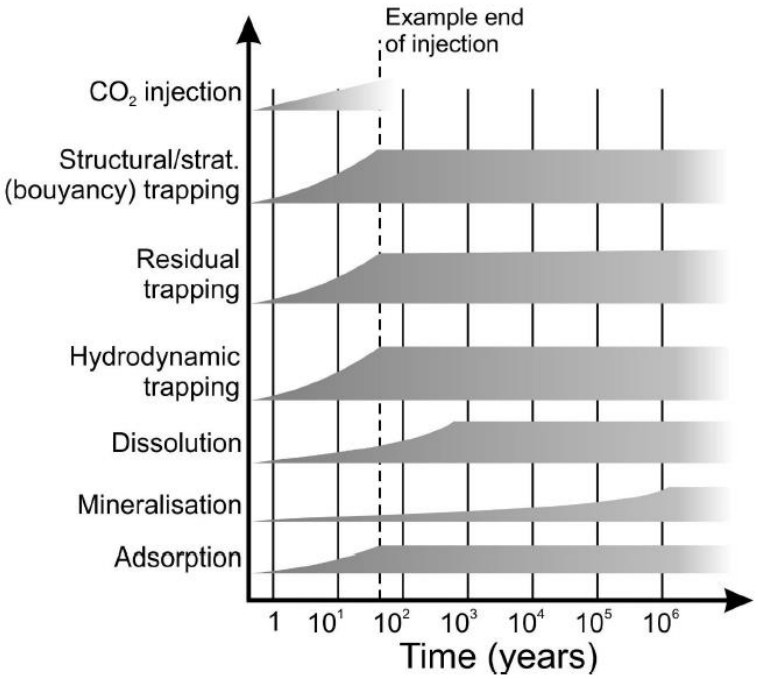

Figure 3 Operating time frame of the various trapping mechanisms (modified from IPCC, 2005) Structural/ stratigraphic trapping relates to buoyancy-driven trapping.

This review showed there is a potential for hydrate formation within the overburden if CO_2 were to migrate from deep geological storage under the required pressure and temperature conditions (hydrate forms under cool but elevated pressure scenarios). Under present day conditions CO_2 hydrate formation should not occur in shallow parts of the North Sea. There is the potential for hydrate formation to occur in shallow overburden and prohibit further upwards migration by reducing permeability due to precipitation. However, quantitative data are needed to inform an assessment of the processes involved and prediction of CO_2 trapping by hydrate formation.

Characterisation and Monitoring Methods

1. Shallow-Focused Characterisation Methods

Dependant on whether the site in onshore or offshore, the techniques implemented to characterise and monitor the site vary significantly. There has been no significant leakage from any onshore storage sites and hence research of monitoring migration and leakage come from natural and experimental seepage sites. For large-scale storage sites, being able to accurately predict where a leakage may occur and assess its impacts, will help improve the monitoring scheme design. Natural seepages and experimental sites often have a number of small discrete leakage points which once detected, makes monitoring (and therefore quantification) easier. Predicting where leakage will occur at experimental sites has proven difficult which has implications for larger storage sites as leakage detection is likely to require locating small features in a large search area.

Remote sensing has been shown to cover a large area, but is prone to detecting false positives. Drones have also been able to cover large areas but take longer to cover sites and can be restricted by ground conditions and flight restrictions. Continuous methods have been developed (usually at wellheads) and include soil gas monitoring, automated chambers or eddy covariance to measure fluxes and fixed scanning of atmospheric changes. Direct flux measurements will be required for accurate quantifications to be made as well as identifying the gas source. Deducing the natural background flux makes baseline monitoring difficult. Different near-surface methods have been reviewed by Klusman (2011).

Methods commonly used to characterise shallow (less than 200 m beneath seabed) offshore potential CO_2 storage sites include: seabed imaging; subsurface imaging; sea bed morphological monitoring; gas bubble/water column monitoring; chemical analysis; and biological analysis.

Seismic data is particularly effective in characterising the overburden and assessing the sealing capacity in the shallow sub-surface. The optimum 2D seismic data for characterising the topmost section (up to 100 m) of overburden is likely to be acquired using Boomer, Pinger or Chirp systems, which allow for imaging of horizons at a centimetre to metre scale.

Multi-beam echo-sounder (MBES) also allows up to centimetre scale resolution and enables an assessment of sediment hardness/softness to be made. This may then give an indication to natural leakage pathways and has been used to map natural pathways such as pockmarks and polygonal faulting. Active acoustic surveying techniques were used for all the offshore sites described in Section 3 of the report. These tools are often equipped with instrumentation able to detect gas bubbles which may be a sign of gas leakage from the seabed. The Ocean Acoustic Tomography (OAT) tool uses sound monitoring to detect bubbles and involves the placement of a network of transponders on the sea bed.

Chemical and biological indicators can also be monitored as gas leakages impact the local environment. Water column samples can be taken from the ship which are analysed to give

an indication of pH, CO_2 partial pressure, salinity and other anomalies. Water samples were also taken at all offshore sites analysed in the report. Video observation and direct seabed sampling can allow analysis of biological changes that may occur if seawater chemistry is altered, these include bacterial mats and methane derived authigenic carbonates.

2. Deep-Focused Onshore and Offshore Methods

For detailed deep sub-surface analysis 3D seismic surveying is required. Resolution is generally 10s meters horizontally and vertically but depends on acquisition parameters. This enables small changes in the fluid content volume to be detected above the storage reservoir and is most effective in thick unconsolidated sequences (compared to thin lithified successions). The repeatability (matching) of the seismic surveys is key in having an accurate time-lapse detection capability. Accumulations of CO_2 are likely to form in high permeability areas (e.g. chimneys) or pond and grow laterally, as shown in the modelled leakages in Figure 4.

As 3D seismic surveys are expensive to undertake, a useful approach, especially for baseline monitoring of proposed sites, is to re-process legacy datasets with parameters that optimise imaging of the upper section of the overburden. A major drawback of 2D seismic survey data for leakage detection is the lack of continuous subsurface coverage.

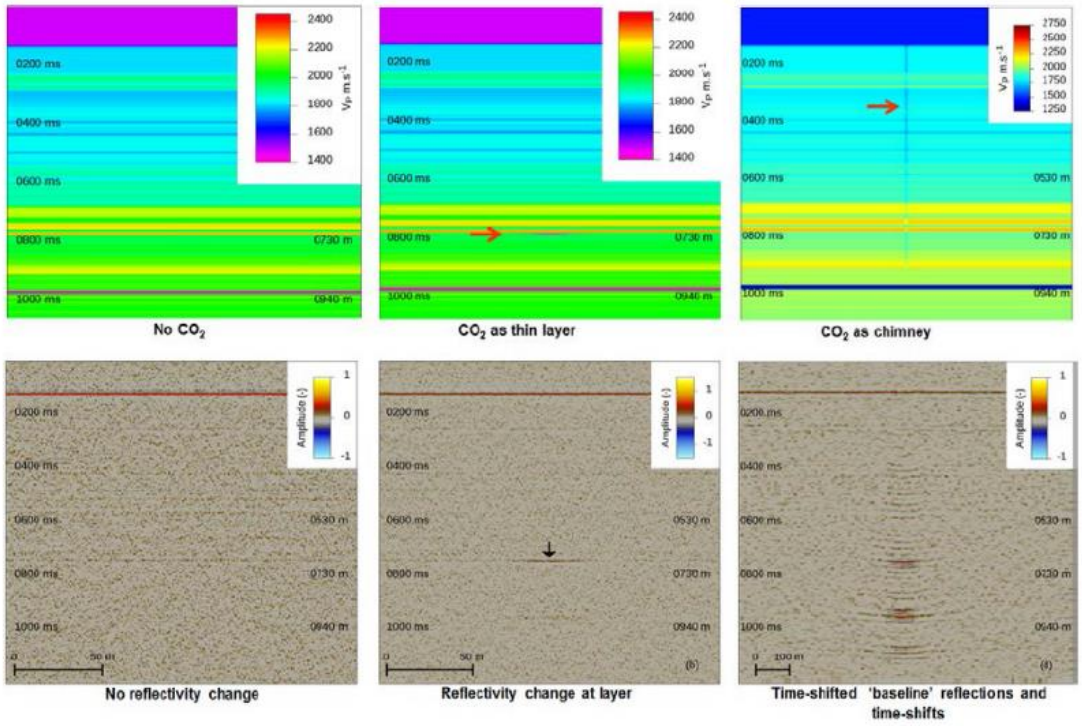

Figure 4 Overburden velocity models (top) with the reservoir top surface at about 900 ms (two-way time). Models have no CO_2 (left), a thin wedge of CO_2 (middle) and a vertical CO_2 chimney (right). Synthetic difference seismic profiles (bottom) show difference noise (left) and changes induced by the CO_2 either as a reflection (middle) or as a time-shift difference response (right) (from Chadwick et al., 2013).

Controlled Release Experiments and Natural Leakages

1. Onshore Field Tests

These field tests can be divided into two main categories, shallow tests at 1-3m to examine the impact of leaks on near-surface ecosystems and tests at 10-50m researching monitoring techniques for leakage into aquifer systems. Where seepage has reached the surface it occurred in specific areas due to CO_2 flowing in the higher permeability pathways. Given the shallow injection at the sites and their small area, detecting leaks has not proven difficult, predicting where they occur has been though. The Field Research Station in Alberta and the GeoEnergy Test Bed site in the UK are now planning deeper (200-500 m) test injection. The Otway site in Australia and the Sulcis Fault experiment in Italy will be looking at injecting into faults in order to take direct measurements of transmission.

2. Natural CO_2 Seepage Sites

Italy has the greatest density of natural seepages studied (especially in volcanic areas) and other sites from Europe and the USA are also reviewed in this report. Natural seepage is usually associated with faulting and continuous monitoring has shown high variability with near surface changes such as temperature, pressure, soil moisture and seismicity. This variability and patchy nature of seepages makes the quantifications of emissions difficult.

There are few observations of offshore CO_2 seepages and most recorded are of volcanic origin (due to the degassing of magma chambers). The leaked CO_2 reduces the pH levels of the seawater creating more acidic conditions which can effect local ecosystems.

Controlled release sites and natural seepages showed similar patterns of distribution with leaks initially localised to between 1-10 meters in diameter. The flux rates measured at natural seepage sites were highly variable but research concluded that high rate leakage around boreholes, fault and fractures would be easily detectable via monitoring. One of the experiments reviewed, the CO_2 Field Lab Project, highlighted the difficulties of accurately predicting a leakage point (although monitoring allowed for a thorough appraisal of the overburden). The biggest challenge highlighted at a majority of sites is calculating the quantity of CO_2 released as monitoring alone will not take into account natural variations and hence modelling will also need to be conducted.

Expert Review Comments

Six experts were invited to review the study, all of which returned comments. The general consensus was that the report was comprehensive and of excellent quality. The reviewers commented that the study provided a good reference document for the characterisation of overburden sequences at CO_2 storage sites. It was emphasised that the report needed to relate back to risk assessment impact to further support the reports value to industry and regulatory purposes. This was addressed in the final copy of the report with the executive summary and conclusions becoming more succinct and focused.

The chapter on trapping mechanisms was re-written based on reviewers' comments that the physics initially referred to in the physical trapping section was outdated and needed additional referencing. At points it was felt the report could be too repetitive and hence certain chapters were combined and re-distributed within the report to reduce the repetitive nature.

Conclusions

- The largest challenge in modelling fluid migration the overburden is characterising a large and complex area. Identifying appropriate parameters is the most difficult and expensive stage in modelling to predict rates of leakage.
- Although characterisation methods can now accurately identify chimneys and their associated pockmarks, the lack of in-situ sampling to date makes estimations of potential fluid migration rates difficult.
- The conductivity of glacio-tectonic structures is also poorly understood. There is the possibility that hydrofractures may be reactivated if over-pressured but quantifying the pressures required and the flow rates possible within these systems is not currently achievable.
- Information on well integrity is often difficult to acquire unless the operator is required to make data available by regulations. Long-term observations will be required to validate predictive models as currently only relatively short-term experimental data is readily available.
- Although only an initial scoping study, there is some evidence that the formation of hydrates as CO_2 migrates from the reservoir may act as a secondary trapping mechanism.

Areas for Further Investigation

- There is no evidence that the development of a large-scale pockmark feature has been directly observed and hence little is known about their long-term activity, persistence and demise.
- The in-situ fluid flow properties of chimney structures is currently unknown with no in-situ samples having been taken.
- The long-term effects of cement degradation on wellbore integrity and hence potential fluid migration rates are unknown.
- The comparison and verification of numerical models is currently very difficult given the wide range of overburden properties and hence parameter values.
- Although glacio-tectonic and hydrofracturing features are known to potentially allow fluid flow pathways to form, the nature of the systems and potential fluid flow rates remain unknown.
- One point of interest will be to investigate the impacts of O&G production on the overburden.

Recommendations

The following are recommendations for future overburden characterisations:

- If high-resolution 3D seismic data has identified faults, the data should be combined with high frequency 3D or 2D seismic surveys. This will allow better characterisation of the fault in the shallow burden and help determine the placement of monitoring equipment.
- Although not currently common practice, if an understanding of overburden fault properties are deemed critical to the storage operation, drilling through faults and acquiring core should be an option.
- Further work is required on the in-situ fluid flow characteristics of chimneys to better characterise the vertical fluid conduits and estimate potential migration rates (as planned in the CHIMNEY, STEMM-CCS and QICS projects).
- For the characterisation of glacio-tectonic structures, accurate surveying in 3D (plan and cross-section view) is required due to the complex nature of the structures. The lateral and vertical extent of large-scale glacio-tectonic structures both onshore and offshore can also be investigated by using high-resolution 2D and 3D seismic reflection data.
- Monitoring of any wellbores considered as potential CO_2 flow pathways is recommended and might include, for example, downhole and annular pressure monitoring of accessible boreholes and surface-based subsurface monitoring targeted within the vicinity of abandoned wells. Integration of monitoring and modelling results, to regularly update the understanding of the enhanced migration potential, and to detect 'early warning' of unexpected migration is also recommended.
- Extensive baseline data will be required to fully understand natural gas concentrations and flux conditions (including both temporal and spatial variability). This will prevent anomalous gas measurements being incorrectly attributed to injected CO_2 leakage.

REVISED FINAL REPORT

CO_2 MIGRATION IN THE OVERBURDEN

IEA/CON/16/237

Revised report delivered: 31st March 2017

Acknowledgements and citations

This report describes research sponsored by the IEAGHG and was prepared by the British Geological Survey (BGS).

The principal researchers were:
M. C. Akhurst
R. A. Chadwick
J. da L. Gafeira
S. D. Hannis
D. G. Jones
K. L. Kirk
J. M. Pearce
C. A. Rochelle
M. A. Stewart
H. Vosper
J. C. White
J. D. O. Williams

The report was compiled and edited by:
M. C. Akhurst

To ensure the quality and technical integrity of the research undertaken by the IEAGHG each study is managed by an appointed IEAGHG manager. The report was also reviewed by a panel of independent technical experts before its release.

The IEA GHG managers for this report were:
James Craig and Lydia Rycroft

The expert reviewers for this report were:
G. A. Williams, BGS;
Six external reviewers from five countries.

The report should be cited in literature as follows:
'IEAGHG, 2017. Review of CO_2 migration in the overburden'.

Further information or copies of the report can be obtained by contacting the IEAGHG:
IEAGHG, Pure Offices, Cheltenham Office Park, Hatherley Lane, Cheltenham, Glos. GL51 6SH, UK
Tel: +44 (0)1242 802911
E-mail: mail@ieaghg.org
www.ieaghg.org

EXECUTIVE SUMMARY

This report summarises the characteristics and processes that can influence the retention and migration of CO_2 above a deep geological storage site.

Fluid migrates through geological strata within hydraulically connected pore space driven by pressure and density differences. Fluids migrate laterally and vertically within permeable rocks but they may be contained within the subsurface by impermeable strata and structures. The presence of natural oil, gas and CO_2 fields proves that strata can contain fluids and gasses over extended periods of geological time. The presence of natural seeps of oil, gas and CO_2 also shows that, in some cases, the overburden containment system fails to retain buoyant fluids.

The site selection process and associated risk and consequence assessments for a CO_2 storage project need to identify those strata that will contain the required volumes of CO_2, and understand the potential rates and environmental signatures of seepage. Vertical and lateral fluid flow within a layered sequence of sedimentary strata may be substantially enhanced by high-permeability flow pathways. Conversely, geological features and structures may be present that are barriers to subsurface fluid migration within the strata above a storage formation, defined here as the 'overburden'.

Large-scale overburden heterogeneities or anthropogenically introduced pathways (such as wellbores and induced or reactivated faults) have the potential to breach the sealing strata, which could influence CO_2 migration. Faults, fractures, wellbores and large-scale geomorphological features can act as either geological pathways for CO_2 to bypass potential secondary storage strata or can hinder migration to retain fluid in the subsurface, depending on their characteristics.

The overburden sequences at five operational or planned CO_2 storage sites illustrate those characteristics that promote trapping and hinder migration. The strata overlying the offshore Sleipner, Snøhvit and Goldeneye Field sites, also the onshore Ketzin project, Germany, and Field Research Station, Canada, all have a number of features in common. A porous and permeable sandstone storage formation is usually capped by a series of low-permeability shale or clay lithologies, which seal the storage formation, preventing upwards migration. Additionally, there are multiple secondary sealing units within the overburden, which are typically low-permeability shale, clay or evaporite lithologies, and porous secondary storage formations to contain any injected CO_2 should it bypass the primary seal rocks. The structure of the overburden sequence is commonly flat lying or shallowly inclined, and little affected by faulting; if faults are present, site characterisation investigations indicate they are sealing to fluid flow and pressure propagation.

Evidence of the processes of migration and rates of fluid flow through the overburden is drawn from studies of faults and fractures and other natural fluid-flow structures. Discontinuities generated by large-scale erosional geomorphological features, tens of kilometres or more in extent, are potentially either high-permeability pathways or barriers to overburden fluid migration. Submarine mass movement deposits and glacial tunnel valleys are large-scale features in the shallow overburden that are both associated with evidence of fluid flow. Mass movement deposits have a worldwide distribution whereas tunnel valleys are known to occur in recently glaciated terranes,

both offshore and onshore, where geological CO_2 storage is in operation and is planned. The influence of large-scale geomorphological discontinuities to enhance or hinder migration in the overburden is dependent on the character of the strata below or above the erosional discontinuity. Hydrofracture systems and glacitectonic fault structures are also evidence of pressurised fluid migration and are known to occur in recently glaciated terranes considered for CO_2 storage.

Wells are designed, constructed and abandoned to preserve hydraulic isolation between intervals penetrated by the well and prevent undesired fluid flow into or out of the wellbore. However, wellbores also represent one of the main threats to storage containment since all CO_2 storage sites will contain at least one well and some may be penetrated by hundreds of wells. Despite careful design, potential losses in wellbore integrity that could occur as a result of subsequent physical and chemical changes in and around the wellbore and/or construction defects, require further mitigation assessments to reduce the potential for leakage. Wells abandoned prior to the inception of CO_2 storage at a locality will need to be assessed to determine their ability to withstand such operations. Pathways may exist along the interfaces between the well cement and geological formation, through the cement, along the cement or abandonment plug and well casing interface and through the abandonment plug itself. Abandoned wellbores may maintain their integrity and not necessarily provide a direct pathway for migration of CO_2 through the overburden to the surface. Potential wellbore leakage rates, for risk assessment purposes, can be drawn from laboratory and field-scale experiments, observations of hydrocarbon and CO_2 Enhanced Oil Recovery wells and numerical simulation predictions. The risk of leakage may best be understood from simulations that predict the behaviours of well barriers for long-term containment of CO_2 rather than the shorter timescale over which CO_2 injection well operations are known.

The three dominant processes that can affect the natural attenuation of CO_2 migrating through the overburden are physical trapping, mineral precipitation, and hydrodynamic trapping. Field studies in areas of natural CO_2-rich groundwater provide evidence for physical and dissolution trapping mechanisms and the processes of mineral trapping. The results of field studies also inform modelling needed to predict fluid migration and long-term efficacy of trapping within overburden strata. CO_2 hydrate formation has potential as a containment mechanism within the overburden to storage sites beneath deep cold oceans and below permafrost regions in higher latitude regions.

Seepage of CO_2 has been studied at natural sites, mostly offshore, and rates of flux have been measured. Five of six sites studied are within volcanic regions and so do not provide suitable baseline values against which CO_2 storage sites can be compared but are useful to establish characterisation and monitoring methods. By contrast, all but one of seven experimental controlled releases of CO_2 are onshore, where implementation of an experimental method and monitoring of environmental impact is more readily achieved. Key lessons learned by comparison of the experimental releases and natural sites are that surface seepage is most likely to be localised, within areas metres to tens of metres across. The migration pathways, and hence the precise location of surface seeps, are very hard to predict even for well-characterised sites. Flux rates measured at natural seepage sites, experimental and accidental releases

are highly variable, from very low rates close to background levels to high rates around boreholes, faults or fractures. Flux rates vary over time in natural systems and even in subsurface release experiments with constant injection rates. Estimates of total emissions will need to account for both spatial and temporal variability.

Methods are recommended that are judged as effective and of adequate resolution to characterise the overburden of a CO_2 storage site, based on the experience of practitioners, to assess overburden containment or migration of fluids. High-resolution seismic surveys, both 2D and 3D, specifically focused to acquire data at the appropriate depth are recommended for all geological features, and to aid interpretation of features. Recommendations are made for data acquisition, observations and surveys for onshore sites in glaciated terranes. Acquisition of borehole datasets is essential to characterise overburden properties, including core samples and geophysical logs, however such data are not commonly collected and targeted drilling is likely to be required. Characterisation methods can benefit from numerical modelling which is recommended to enable assessment of the dependence of leakage rates on particular parameters. The integrity of wellbores that have the potential to enhance CO_2 migration through the overburden should be characterised from documentary information of the design, completion and abandonment of the identified wellbores. Original casing tests and logs of cement presence and bond quality and other information should be used if available. However, the effort required to achieve wellbore characterisation from legacy data should not be underestimated. Knowledge gaps in the characterisation and risk of fluid migration via wellbores are associated with the challenges of access to legacy well records, in particular, for abandoned wellbores. There is a lack of understanding of methods to effectively mitigate poor well integrity in abandoned wells and the cost-benefit of possible options to do so.

Gaps in current knowledge to characterise the overburden to CO_2 storage sites highlight the need to obtain data on the properties of the strata. In particular, in the shallower overburden within the uppermost few hundred metres of the surface. A number of research projects seek to address the sparsity of data on chimney structures by a suite of geophysical and electromagnetic methods. However, information is especially needed of the properties of overburden strata to retain and contain CO_2. Borehole logging and monitoring within the shallow and deep overburden sequences is essential to increase confidence in the capacity of the overburden to contain CO_2 and to inform predictive modelling of the long-term migration and trapping processes. Pressure data is required to assess the likelihood that faults may allow along-fault flow, inform assessment of geomechanical stability and reactivate hydrofracturing in glaciated terranes.

Table of Contents

List of Tables

List of Figures

1 Introduction

The presence of natural oil, gas and CO_2 fields proves that geological strata can contain fluids and gasses over extended periods of time. But the presence of natural seeps of oil, gas and CO_2 also shows that, in some cases, the overburden containment system fails to retain buoyant fluids. The site selection process and risk/consequence assessments for a CO_2 storage project need to identify those strata that will contain CO_2 and understand the potential rates and environmental signatures of seepage. This report reviews potential pathways and overburden migration processes which may enable CO_2 to leak from the storage reservoir and its subsequent attenuation in the overburden. The report focuses on defining potential migration pathways and assessing the likely rates of migration of CO_2 in dense phase, gaseous phase or dissolved in groundwater via these routes. In this context the **overburden is defined here as the entire geological succession above the target reservoir formation with the lowermost stratum forming the primary seal**.

This report details findings from a review of migration in the overburden above CO_2 storage sites. **Section 2** illustrates the overburden structure at five large-scale operational or planned offshore storage sites and two onshore pilot CO_2 injection projects and discusses the typical structures and lithologies present at these sites. These case studies are used to illustrate characteristics of the overburden favourable for CO_2 storage. **Section 3** reviews the mechanisms, processes, rates and timescales of migration through the overburden. In **Section 4** the trapping potential of the overburden is discussed from the perspective of modelling and experimental efforts which have investigated the efficacy of various CO_2 trapping mechanisms. This section also provides an introduction to hydrate trapping. **Section 5** presents a short review of the techniques currently employed to characterise the overburden and **Section 6** reviews controlled CO_2 release experiments and natural leakages and appraises lessons learnt from onshore and offshore field tests. Additionally, a review of studies at natural CO_2 seepage sites is included, focusing on flux rates through the overburden at each site. **Section 7** summarises the report findings, provides recommendations for overburden characterisation methods and identifies knowledge gaps from existing literature.

1.1 Overview of CO_2 migration pathways and barriers in the overburden

Geological and anthropogenic pathways can bypass sealing strata and promote migration of CO_2 through the overburden. Evidence is reviewed for recent fluid migration within the overburden, via geological and man-made pathways, and also large-scale geomorphological features within the overburden that form either potential high-permeability pathways (or termed ‘thief zones’) or prospective barriers to migration.

Pathways and barriers to migration in the overburden are outlined in Chapter 1. Geological migration pathways, which include faults and fractures (Section 1.1.1), and fluid flow structures, and associated structures (Section 1.1.2), are described. Large-scale buried geomorphological features that can be either potential high-permeability pathways, such as tunnel valleys, or barriers to migration within the overburden (for

example, submarine mass movement deposits) are introduced in Section 1.1.3. Hydrofracturing and faulting within strata over-ridden by recent glacial ice are outlined in Section 1.1.4. Man-made migration pathways associated with the wellbores drilled for CO_2 storage, the exploration or production of hydrocarbons or water, are introduced in Section 1.1.5. Although wellbores are designed to be hydraulically isolated, if they are faulty or degraded they could potentially allow fluid flow pathways to develop.

1.1.1 Faults and fractures as potential migration pathways

Fractures and faults are present at a variety of scales in the subsurface, and as such are likely to be present within the overburden above many potential CO_2 storage sites. Faults are known to be pathways for fluid movement, often at low rates over the geological timescale, or can be sealing and prevent fluid movement. The presence or absence of major features is likely to be known from seismic reflection data, and therefore sites where faults might facilitate unwanted migration of CO_2 can be avoided. Therefore, initial site characterisation can help to avoid sites containing significant through-going faults connecting the reservoir to the shallower overburden sequence or to the seabed, which these may pose a risk of leakage. Much of the overburden in a selected storage site is therefore likely to be devoid of such faults. However smaller faults, below resolution on seismic profile data, can be abundant in some structures and it is important to consider their likely effect on CO_2 migration.

Fractures and faults commonly act either to inhibit or promote flow through the subsurface. Upward or lateral escape of fluids can occur from geological traps via faults, which in these circumstances act as effective seal bypass mechanisms, and so impose a risk to subsurface CO_2 storage activities. In assessing the security of geological traps for CO_2 storage, it is important to consider the likely sealing, or non-sealing behaviour, of faults under the range of expected pore-pressure conditions that are likely to occur during and following injection activities (Bretan, et al., 2011).

In simplistic terms, the ability of a fault to act as a lateral trap to buoyant fluids such as dense-phase CO_2 depends on the juxtaposition of lithologies in the fault-wall blocks, the composition of the fault zone rocks and any differential pressure across the fault. Vertical conductivity of faults is commonly associated with the effective in situ stress conditions, with a wide range of case studies worldwide suggesting that critically stressed or active faults are more likely to be hydraulically conductive (Barton, et al*.,* 1995; Wiprut and Zoback, 2000; Hennings, et al., 2012; Williams and Gent*,* 2015). Pore pressure and its influence on the effective in situ stress is therefore a critical factor that can influence the stability of a given fault, and it is important to understand the prevailing in situ stress conditions in regions where CO_2 is to be stored (Williams, et al., 2015). This is true not only at the level of the reservoir to evaluate trap and seal integrity, but also within the overburden in the event that the primary seal is breached.

A recent literature review conducted for IEAGHG (2016) evaluated how fault permeability is controlled by fault zone properties and in situ stresses of both anthropogenic and geological origin. A brief review of natural CO_2 seeps along faults is included here and the outline findings are applied to the evaluation of fault zones in storage sites, and overburden strata. In particular, one aspect investigated from

available literature is the permeability of faults in relatively unconsolidated rocks (Sections 3.1.2.5 and 3.1.2.6), such as those expected to be encountered in the sedimentary overburden above some, but not all, prospective storage sites.

1.1.2 Fluid flow pathways

Fluid flow through a sedimentary sequence can occur at a range of depths and via distinct flow pathways, from near-seafloor features that chiefly reflect the escape of biogenic and diagenetic fluids to larger subsurface conduits for thermogenic fluids. Seismic survey data can reveal near-vertical chimneys (also termed 'pipes'), that may culminate in sea bed pockmarks (Figure 1.1), or gas-bearing mound features on the sea floor. Chimneys are identified from seismic records, as vertical features characterised by chaotic low-amplitude seismic reflections. Chimneys may represent paleo- or modern fluid flow pathways, within the subsurface from a source to a reservoir, or from a source to the surface. Chimneys are common in some sedimentary sequences and are believed to be a consequence of fluid migration or hydraulic fracturing. These large-scale overburden heterogeneities offer the means to breach sealing sequences by allowing fluids to flow vertically across stratal boundaries, providing fluid flow pathways to shallower depths (Figure 1.1).

Little work has been undertaken to determine the physical properties of these structures and their effectiveness as conduits for CO_2 is unknown, and likely to be highly variable. Currently, studies are ongoing which attempt to determine the in situ permeability of chimneys in the North Sea and address the question of how long, and under what conditions, the structures might be conduits for CO_2 migration (Section 3.2.1).

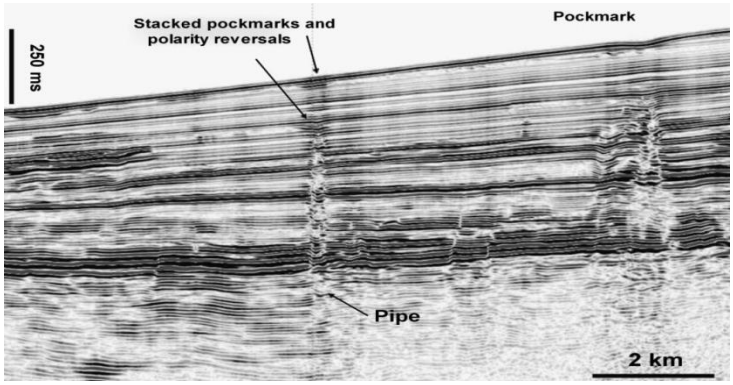

Figure 1.1 Small chimneys imaged on a seismic profile (from Cartwright et al, 2007)

1.1.3 Large-scale buried geomorphological features as pathways or barriers to migration

Large-scale submarine mass movements have shaped the morphology of continental slopes and shelves around the world. The internal structure and composition of the deposits will influence their ability to enhance or hinder fluid migration through the overburden.

Tunnel valleys are large-scale features within unconsolidated strata and bedrock over-ridden by Pleistocene ice sheets that have the potential to act as high-permeability pathways. Pressurised glacial water flow beneath ice sheets erodes elongated channels or tunnel valleys that are tens of kilometres in length and hundreds of metres deep. Buried tunnel valleys preserved in the subsurface have the potential to affect fluid flow in the overburden of storage sites in glacially over-ridden areas such as the European North Sea and onshore Canada, which were covered by ice sheets during the Pleistocene.

1.1.4 Hydrofracturing and glacitectonic faulting

Glacitectonism refers to the deformation of material by over-riding ice including rafting, fracturing and faulting. The effects of glacitectonism have been observed onshore and high-resolution seismic provides evidence that parts of the offshore Quaternary succession may have undergone glacitectonic deformation in places such as the North Sea. As with tectonically-driven faulting (Section 1.1), the main effect of this more localised deformation, which would affect pathways for fluid flow, is the potential for migration directly along faulted surfaces, and the potential to displace stratigraphic sequences and disrupt lateral seals to allow flow through more permeable material.

Loading by glaciers and ice sheets typically results in the development of a pressurized hydrogeological system which can trigger hydraulic fracturing of the underlying sediments and bedrock (van der Meer et al., 2008; Phillips et al., 2013; Phillips and Hughes, 2014), as well as create specific landscapes of soft-sediment extrusion (Piotrowski, 2006). Hydrological modelling of subglacial groundwater systems in the Netherlands indicates that the pressure transient induced by loading from major ice masses has penetrated to a depth of up to 1500 metres into the sub-glacial bedrock (Piotrowski, 2006).

Hydrofracture systems (also referred to as water-escape features or clastic dykes) provide clear evidence for the passage of pressurised meltwater beneath both former and contemporary glaciers and ice sheets. They range from just a few millimetres across, through to much larger structures (up to several metres wide) which can be traced laterally for several tens of metres (van der Meer et al., 1999; van der Meer et al., 2008; Phillips and Merritt, 2008; Phillips et al., 2013; Phillips and Hughes, 2014). The marked fluctuation in hydrostatic pressures encountered during hydrofracturing leads to brittle deformation of the sediment and/or bedrock beneath the ice, accompanied by the penecontemporaneous liquefaction and introduction of the sediment fill. Due to the pressurised nature of the meltwater, this sediment infill can be introduced from structurally above (downward injection) or below (upward injection) the developing hydrofracture system. Hydrofractures range from simple features in which initial fracture propagation was immediately followed by the injection of the fluidised sediment fill (cut and fill), through to highly complex multiphase systems, which were active over a prolonged period and accommodated several phases of fluid flow and sedimentation (Phillips et al., 2013). These hydrofracture systems comprise a complex sequence of laminated clay, silt and sand with the grain size variation recording major changes in flow regime. The presence of graded bedding (normal and reverse), cross-lamination, small-scale scours and erosion surfaces preserved within

the sediment-fill demonstrates that hydrofractures can behave like temporary, small-scale, fluviatile drainage systems focusing fluid flow beneath the ice mass.

1.1.5 Wellbores as potential fluid flow pathways

All wellbores will have been designed to maintain hydraulic isolation between permeable geological units, to protect interests in hydrocarbon fields or aquifers for supply of potable water. Wells that penetrate the storage cap rock have the potential to provide a direct path from the reservoir to the surface. This means that wells often represent one of the main threats to storage containment. All CO_2 storage sites will have at least one well and potentially tens or even hundreds. The wells may be operational or may have been previously plugged and abandoned. They will have been drilled, completed and abandoned to fulfil a particular purpose, within a particular budget, to be in accordance with the relevant regulations at the time. This means that wells abandoned prior to the inception of CO_2 storage will not have been designed specifically to withstand such operations. In particular, casings may not be fully cemented to surface and abandonment plugs may not be set across all the permeable intervals within the overburden that are now being considered as secondary containment for CO_2 storage. Abandoned wellbores may maintain their integrity and not necessarily provide a direct pathway for migration of CO_2 through the overburden to the surface, but it can be a very challenging process to establish this. Characterising the wells to understand the potential risks they pose can be difficult with the sometimes less-than-satisfactory record-keeping, or record-retrieval of wellbore completion design and abandonment details. Mitigating the risks of poor or unknown integrity can be an expensive process.

Despite careful design, losses in wellbore integrity can occur as a result of subsequent physical and chemical changes in and around the wellbore and/or construction defects. In a CO_2 storage site, CO_2 or reservoir brine could exploit potential pathways along the interfaces between the well cement and geological formation, or the cement and well casing, and through the cement and the metal casing itself. These pathways may exist, and be opened or closed due to construction defects in the well or subsequent physical (mechanical and thermal) and chemical loading.

2 Review of storage site overburden sequences

The common feature of all the major CO_2 storage demonstration sites is injection into a porous and permeable sandstone reservoir. This unit is usually capped by a series of shale or clay lithologies, which act to seal the storage complex. Typically, the overburden is dominated by lower permeability rocks providing multiple seals. Here, we review several major CO_2 storage operations, selected by IEAGHG, and address the commonalities and differences between the broad overlying strata. The Sleipner and Snøhvit CO_2 storage projects in the Norwegian North Sea (Sections 2.1 and 2.2), the Ketzin pilot CO_2 injection project onshore near Berlin in Germany (Section 2.3), the planned CO_2 storage site in the Goldeneye Field[1] in the UK North Sea (Section 2.4) and the onshore Field Research Station in Alberta, Canada (Section 2.5) are reviewed.

2.1 Sleipner CO_2 Storage Project

Sleipner is the world's longest running offshore CO_2 storage project. Approximately one million tonnes of CO_2 per year has been stored since injection commenced in 1996. Now, over 16 million tonnes have been successfully stored (Chadwick et al, 2016).

Dense phase CO_2 is injected at 1016 metres depth below sea level into the Utsira Sand – a permeable and porous sandstone reservoir in the Norwegian North Sea. The storage complex includes both the Miocene Utsira Formation and an overlying Pliocene sand wedge (Furre et al., 2015). The Utsira Sand comprises the mainly sandy, lower part of the Utsira Formation (Isaksen and Tonstad, 1989) and lies within the Nordland Group. The top of the Utsira sand unit is generally smooth and, regionally, varies in depth between 550 and 1500 metres below sea level (Kirby et al., 2001).

The seismic technique is particularly suitable for monitoring CO_2 aquifer storage since the replacement of formation water by CO_2 produces significant acoustic impedance changes. At Sleipner, a number of time-lapse 3D seismic surveys have been acquired to study the development of the growing CO_2 plume (e.g. Arts et al., 2004; Chadwick et al., 2004, 2009). The overburden is also imaged during these surveys; no leakage of CO_2 has been observed at Sleipner. The CO_2 plume itself is around 200 metres high and imaged in cross-section as a series of bright sub-horizontal reflections each representing a trapped layer of dense phase CO_2.

The cap rock is generally considered as comprising three main units (Gregersen and Johannessen, 2007), the Lower-, Middle- and Upper Seal (Figure 2.1), based on the response seen in seismic data. The units are shale dominated with a series of small

[1] The Goldeneye Field was proposed and investigated as a prospective storage site for CO_2 captured from power generation. Initially, detailed plans were presented for storage of CO_2 from the coal-fired Longannet power plant in 2011. Subsequently, plans were prepared to an advanced stage for CO_2 storage from gas-fired power generation by the Peterhead CCS project until the withdrawal of funding for the UK CCS Commercialisation Competition in 2015.

local sandy deposits. The sequence comprises Pliocene, prograding deltaic wedges overlain by Pleistocene deposits.

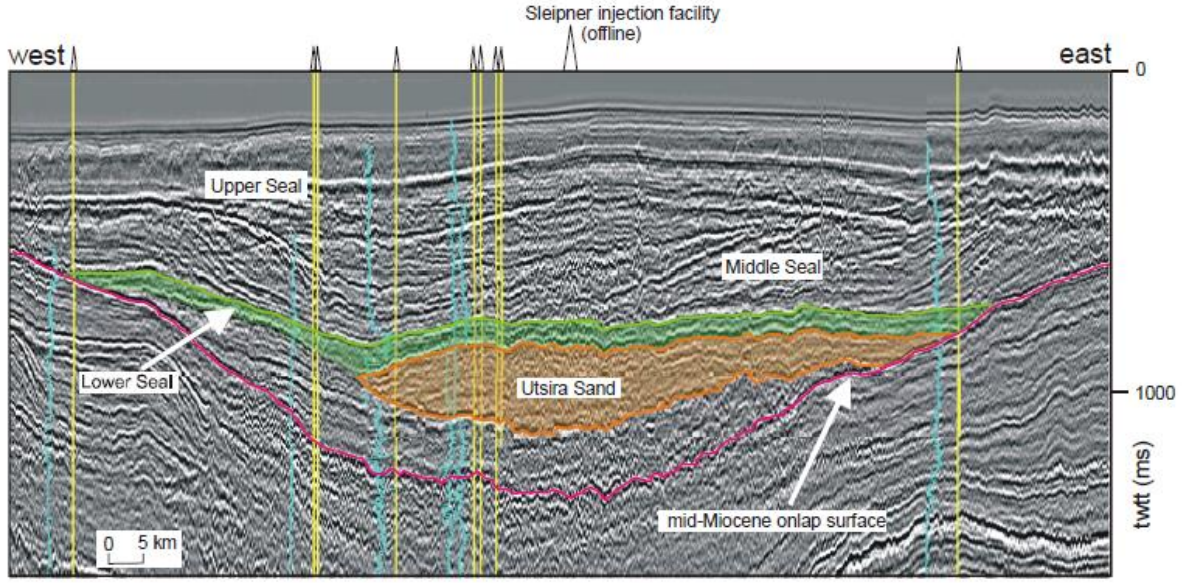

Figure 2.1 Seismic section through the Utsira Sand highlighting the main cap rock units (From the SACS2 final report – Chadwick et al., 2002)

The Lower Seal, of the order of 50 to 100 metres thick, is composed of shaly, basin-dominated sediment and immediately overlies the storage reservoir; it is identified as the lowermost part of the Nordland Group in the UK (Stoker et al., 2011) and the lowermost Naust Formation in Norwegian waters (Ottesen et al., 2009). Regional drill cuttings indicate high clay content in the unit and logs suggest over 80 per cent shale volume (SACS2 final report, Chadwick et al., 2002; Harrington et al., 2010). This suggests that the Lower Seal offers the most efficient sealing properties of the Sleipner overburden.

The thick, Middle Seal is defined on the seismic data by inclined reflections down-lapping onto the Lower Seal; the seismic architecture indicates a series of clinoform seismic units infilling the central and northern North Sea Basin, originating largely from the east and south-east. Middle Seal units are generally considered to be fine-grained hemipelagic distal sediments sourced from the large river systems of northern Europe (Gibbard, 1988; Eidvin et al., 2000; Moreau and Huuse, 2014). BGS cores (Fyfe, 1986; Stoker and Bent, 1987) in the UK sector prove marine and prodeltaic muds with thin sands. Higher-amplitude reflectors which appear to onlap the base of the clinoforms may be interpreted as sandier material and probably formed as mass flow or turbidite deposits. The limited lateral extent (< 10 km) of such features makes them unlikely to risk the sealing capacity of the remainder of the Middle Seal (Chadwick et al., 2002, fig. 26).

The upper parts of the Middle Seal are truncated by the erosive base of the Upper Seal; generally identified in the UK sector as the top Aberdeen Ground Formation (Stoker et al., 2011) and in the Norwegian sector as the Upper Regional Unconformity (URU, Ottesen et al., 2009). The Upper Seal comprises a Pleistocene unit and is imaged between the URU unconformity and the sea floor. Upper Seal sediments have

been repeatedly influenced by significant glacial episodes with geomorphological evidence for glacial landforms (i.e. tunnel valleys, iceberg plough marks, mega-scale glacial lineations and glaciotectonism) most recently imaged in 3D seismic data (see summary in Graham et al., 2007; Ottesen et al., 2009). Borehole material shows that Upper Seal sediments largely comprise marine and glacimarine muddy and clayey material, with some sands and glacially influenced diamicts (Fyfe, 1986; Stoker and Bent, 1987; Sejrup et al., 1991; Stoker et al., 2011). The largest of the glacial landforms, subglacially formed tunnel valleys, are present extensively across the Sleipner area (Fichler et al., 2005; Van der Vegt, 2012, fig. 1; Stewart et al., 2013). The infill of buried tunnel valleys in the central and northern North Sea remains untested; bright and chaotic reflector packages identified towards the base of some tunnel valleys are tentatively interpreted to comprise coarser-grained materials (Kristensen et al., 2008; Van der Vegt, 2012, fig. 4; Stewart et al., 2012; Benvenuti and Moscariello, 2016) but these packages are not observed systematically. Further sandy material may be present nearer to the sea bed surface relating to fluvial or subglacial deposition during subaerial exposure, but are not laterally or stratigraphically extensive (Fyfe, 1986; Stoker et al. 2011).

Seismic difference signal in the overburden is not attributed to leaking CO_2 but to random noise and the effect of poorly matched reflectivity from geology and naturally occurring gas pockets. Chadwick et al. (2014) determined the leakage detection limits of CO_2 in the overburden at Sleipner using a wavelet decomposition methodology. After adding random reflectivity to slices extracted from the seismic data, the reflectivity was converted to layer thickness using an amplitude-thickness tuning relationship. By statistically examining the seismic response, to see if the associated reflective anomaly would be distinguishable from the background noise, they were able to set thresholds of detectability that varied within the overburden. They concluded that pore volumes greater than 3000 cubic metres would be detectable anywhere in the succession. This corresponds to a mass of approximately 2000 tonnes, based on a conservative assumption of 100% CO_2 saturation. Since CO_2 becomes more reflective at shallower depths, as it moves from dense phase into a gaseous state, the threshold of detectability decreases closer to the sea bed. In the quiet zone around 500 metres depth, Chadwick et al. (2014) reported that as little as 315 tonnes of CO_2 would be detectable.

One further noteworthy attribute of the Sleipner CO_2 plume is a vertical ‘feeder chimney’ evident within the CO_2 plume itself (Figure 2.2). This feature appears to be responsible for the upward migration of CO_2 in the plume and is being investigated by the NERC-funded ‘Migration of CO_2 through North Sea Geological Carbon Storage Sites: Impacts of Faults, Geological Heterogeneities and Dissolution’ project. It should also be stated that the topmost layer CO_2 at a depth of around 800 metres has been in contact with the reservoir top seal for 17 years (since 1999) and as it has migrated laterally has impinged on a number of small naturally occurring gas chimneys or gas pathways in the overburden with no leakage observed.

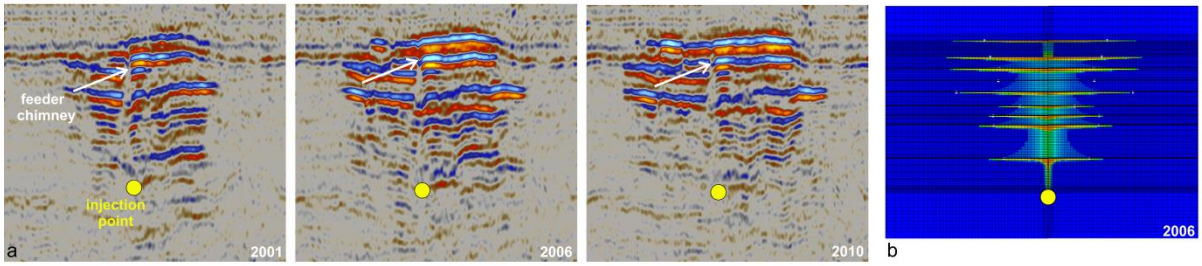

Figure 2.2 a) Time-lapse seismic images of the Sleipner CO_2 plume showing brightly reflective individual CO_2 layers and the induced feeder pipe. b) Preliminary numerical flow model of the plume with a feeder pipe in the upper reservoir, BGS © NERC (2016). CO_2 saturation output from a simulation of CO_2 injection. Saturation from 0 (blue) to 1 (red). High amplitude seismic reflectors in Figure 2.2a correspond to high saturation layers in Figure 2.2b.

2.2 Snøhvit CO_2 Storage Project

Snøhvit is the second large-scale offshore CO_2 storage demonstration project under Norwegian waters. Statoil operates both projects (Snøhvit and Sleipner). The CO_2 injected at Snøhvit comes from natural gas extracted from the Snøhvit Gas Field. The gas contains around 6% CO_2 and is processed on shore before being returned by pipeline for injection through infrastructure located on the sea bed.

Snøhvit has seen two distinct phases of injection – both injecting into sandstone reservoirs of Early to Middle Jurassic age (Figure 2.3). The units are buried beneath a thick Upper Jurassic to Quaternary overburden at depths of around 2600 and 2450 metres below sea level, respectively. Initially, CO_2 was stored in the Tubåen Formation, a fluvial-deltaic to tidal sandstone which is around 100 metres thick. Injection commenced in 2008, and prior to injection ceasing in early 2011 over one million tonnes of CO_2 had been sequestered (Hansen et al., 2013). Phase 1 was stopped as the downhole pressure gauge continually reported steady increases in pressure associated with injection (Hansen et al., 2013). Phase 2 injected into the overlying Stø Formation, a shallow-water marine sandstone typically 85 metres thick (Osdal et al., 2013, 2014), and separated from the Tubåen Formation by the sealing Nordmela Formation. The Stø Formation is the gas reservoir of the Snøhvit Field and injection takes place into a separate fault-bounded segment. Injection recommenced in summer 2011 and, prior to the most recent seismic survey in 2012, over half a million tonnes was successfully injected. Presently, over three million tonnes of CO_2 have been successfully stored at Snøhvit. In 2017, an additional injection well was drilled into an adjacent fault block with the aim to increase storage capacity and operational flexibility.

Two major collision events governed the tectonic development in the region, the Caledonian orogeny and the collision of Laurasia and western Siberia (Dore, 1995). These give rise to the platform and basin regime that define the geology beneath the Barents Sea. East-west-trending normal faults (Figure 2.3) which penetrate the Upper Jurassic - Lower Cretaceous strata (Dore, 1995), dominate the Hammerfest Basin, which contains the Snøhvit Field. Grude et al., (2013, 2014) and White et al. (2015) used the seismic data acquired during the Tubåen injection phase to suggest the faults were sealing to fluid flow and pressure propagation, based on the extent of the seismic anomalies.

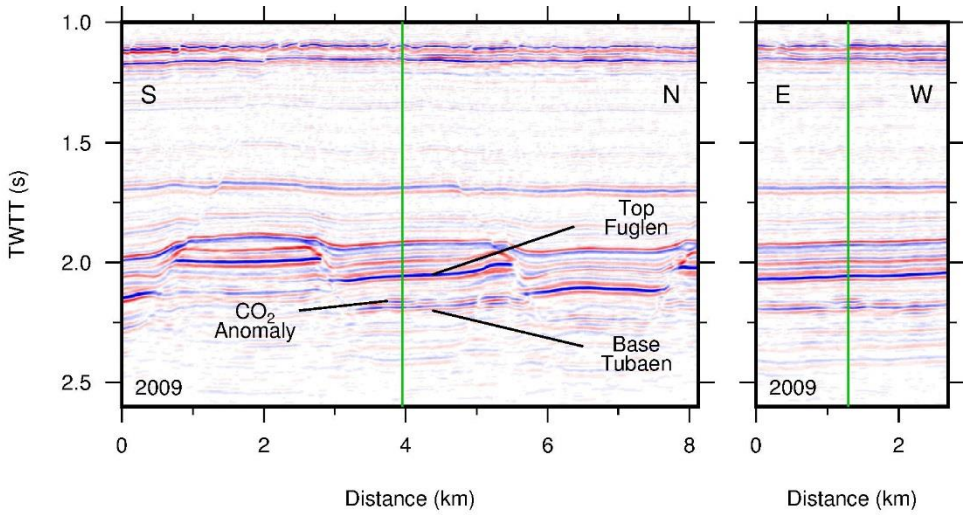

Figure 2.3 Orthogonal seismic lines from the 2009 3D survey over the Snøhvit CO_2 storage operation. Green lines delineate the intersection between N-S and E-W lines. The base of the Tubåen Formation is highlighted alongside the Top Fuglen reflector, a key regional surface that directly overlies the Stø Formation.

A thick sequence of Cretaceous and Upper Jurassic shale acts as the cap rock for CO_2 storage and hydrocarbon plays throughout the Barents Sea. The stratigraphy of the region was defined by Worsley et al. (1988) with the Palaeocene-Eocene age Torsk Formation overlaying the Cretaceous sequence. Cap rock permeability and porosity values have been published for the overburden units (Buenz et al., 2012; Tasianas et al., 2016) after analysis of well logs and a literature review. Permeability values of the order of several millidarcies are observed in the immediate cap rock (Torsk Formation) and the low permeability sequence extends from depth to very near to the seabed (Table 2.1).

Overburden formation	Average porosity (%)			Average permeability (mD)		
	Low	Medium	High	Low	Medium	High
Torsk	33	36	38	23	31	39
Kveite	30	33	35	16	22	28
Kolmule	28	30	32	11	15	19
Kolje	24	25	27	6	8	10
Knurr	21	24	27	4	7	10
Hekkingen	5	13	20	4	8	12

Table 2.1 Porosity and permeability values for formations in the overburden to the Snøvhit CO_2 storage site, ordered from shallowest (Torsk) to deepest formation.

In the vicinity of the Snøhvit Field, several large chimney features have been mapped (Ostanin et al., 2013). The timescales for leakage and the mechanisms for occurrence are both poorly understood (Tasianas et al., 2016) but have been attributed to spilling of reservoirs during the regional uplift of the Barents Sea region (Makurat et al., 1992; Duran et al., 2013). On seismic data the features form wide zones with poor reflection continuity and a loss of reflected signal. Løseth et al. (2009) attribute this character change to a reduction in, and variability of, the velocity field – possibly a consequence of residual gas saturations. The sea bed overlying the Snøhvit region is characterised

by pockmarks of the order of 10 to 20 metres in diameter and approximately three metres deep (Chand et al., 2012).

2.3 Ketzin Pilot CO2 Injection Site

Ketzin is the largest onshore CO_2 storage operation in continental Europe and is located approximately 25 kilometres west of Berlin, Germany (Schilling et al., 2009). Previously the site was used for the safe storage of natural gas in Jurassic aquifers buried to 400 metres depth (Norden and Frykman, 2013). CO_2 is stored in the deeper Triassic Stuttgart Formation (Figure 2.4) and injection commenced in June 2008. During the five-year operational period, injection of almost 68,000 tonnes of CO_2 occurred. The site boasts excellent well control with three wells drilled to over 750 metres depth - serving as a single injection and two observation wells, respectively. The injection site sits on the southern flank of an anticline ensuring that the injected CO_2 will flow towards the crest of the structure.

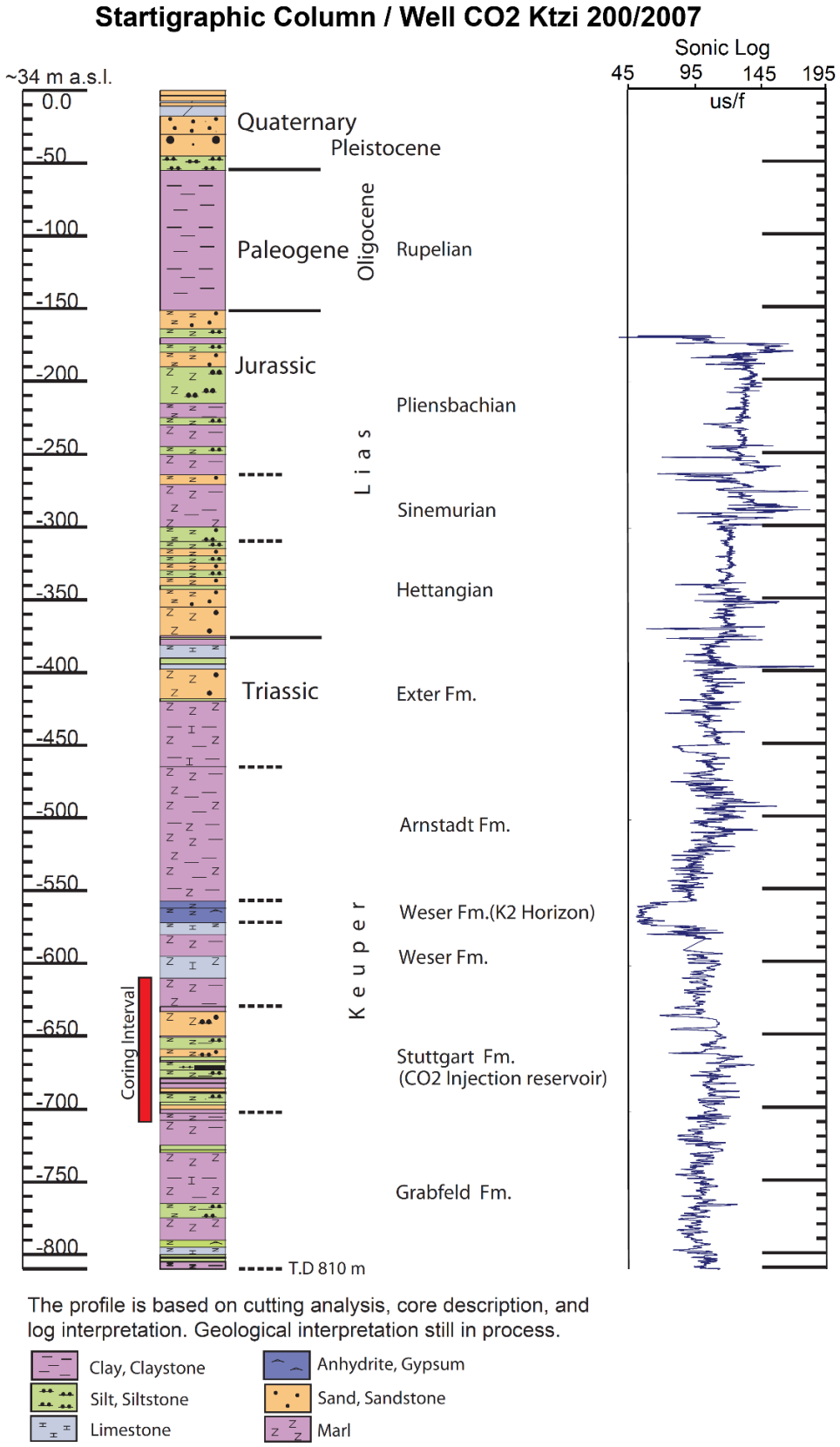

Figure 2.4 Stratigraphic log illustrating the lithological profile at the Ketzin site (Kazemeini et al., 2010).

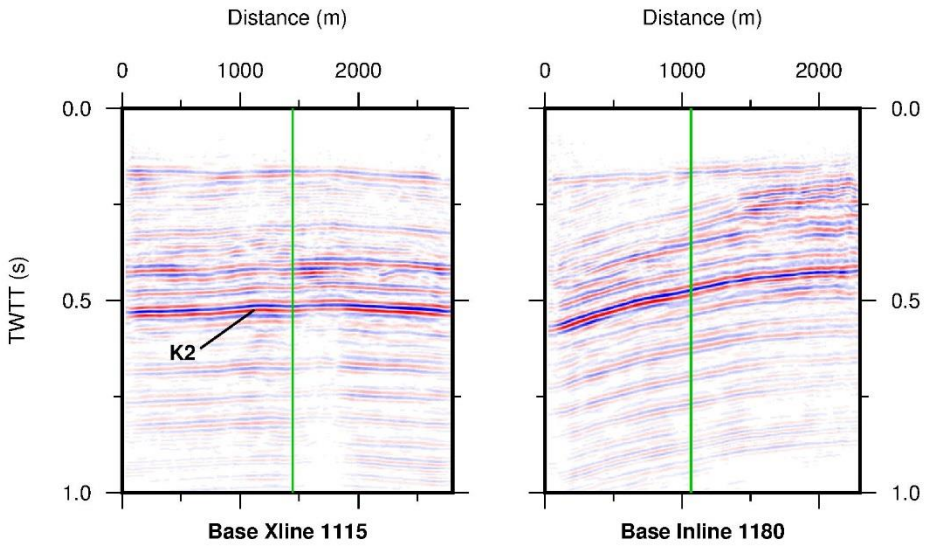

Figure 2.5 Orthogonal cross-sections from the seismic baseline data at the Ketzin CO_2 storage site highlighting the anticlinal structure. Label indicates the dominant K2 reflector. Green lines delineate the intersection between the two sections.

The Stuttgart Formation is a reasonably heterogeneous sandstone aquifer at 630 to 700 metres depth interspersed with siltstone baffles of poor reservoir quality (Ivanova et al., 2012). The Weser and Arnstadt formations (Kempka et al., 2010) constitute the immediate cap rock, both consisting predominantly of marly mudstone, silty claystone, anhydrite and nodules of dolomite. Collectively, these two units comprise an approximately 200 metres-thick playa facies sequence (Norden et al., 2006). An anhydrite layer, 20 metres thick, which provides a strong and persistent reflective horizon in the seismic data, separates the two formations (at depths of 560-629 m). Juhlin et al. (2007) refer to this marker as the K2 reflector (Figure 2.5).

The Weser and Arnstadt formations are described as lime-rich muddy and evaporitic in the well analysis. They have an average porosity of 17% and low permeability (of the order of 0.1 mD, Norden et al., 2006). This is a consequence of the high clay content observed in both lithologies.

Overlying the lower cap rock succession three Jurassic units (Hettangium, Sinemuriam and Pliensbachian in age) contain an alternating sandstone and mudstone sequence (Figure 2.4) used previously for the gas storage operation. These are topped by a 100-metre-thick Tertiary clay that separates the storage units from an overlying aquifer system, exploited for drinking water. As such the CO_2 store is overlain by about 400 metres of sealing units in a multiple barrier configuration. Following closure of the site, analysis of post-closure seismic data reveals no evidence of migration into the overburden.

2.4 Goldeneye CO_2 Storage Site

The Goldeneye CO_2 storage complex was planned to operate as the CO_2 storage site for the Peterhead CCS Project. Unfortunately, due to withdrawal of funding from the UK government's CCS Commercialisation Competition in November 2015, the project was disbanded.

Led by Shell and SSE (Scottish and Southern Energy) the CCS operation had planned to capture and store between 10 and 15 million tonnes of CO_2 over a 10 to 15-year period. During the development, the storage complex and overburden were studied to ensure safe storage of CO_2. Unlike the other sites considered in this study, injection was intended to re-pressurise a depleted hydrocarbon field - the Goldeneye Field in the UK Central North Sea. Previously, a gas condensate accumulation had been produced between 2004 and December 2010.

CO_2 injection was planned into the Lower Cretaceous Captain Sandstone reservoir at around 2400 metres depth. The Captain Sandstone comprises large, blocky, high-density turbidites deposited in a sandy shelf-edge depositional environment. Throughout the early and mid-Cretaceous the regional deposition was influenced by the depocentre's location. The Outer Moray Firth region was dominated by an emerged Horst block, resulting in turbidite deposition on the flanks of the structure throughout this period. Alongside the accumulation of sandy turbidites, periodic deposition of marl, shale and limestone also occurred. The regional stratigraphy is shown in Figure 2.6.

Figure 2.6a)

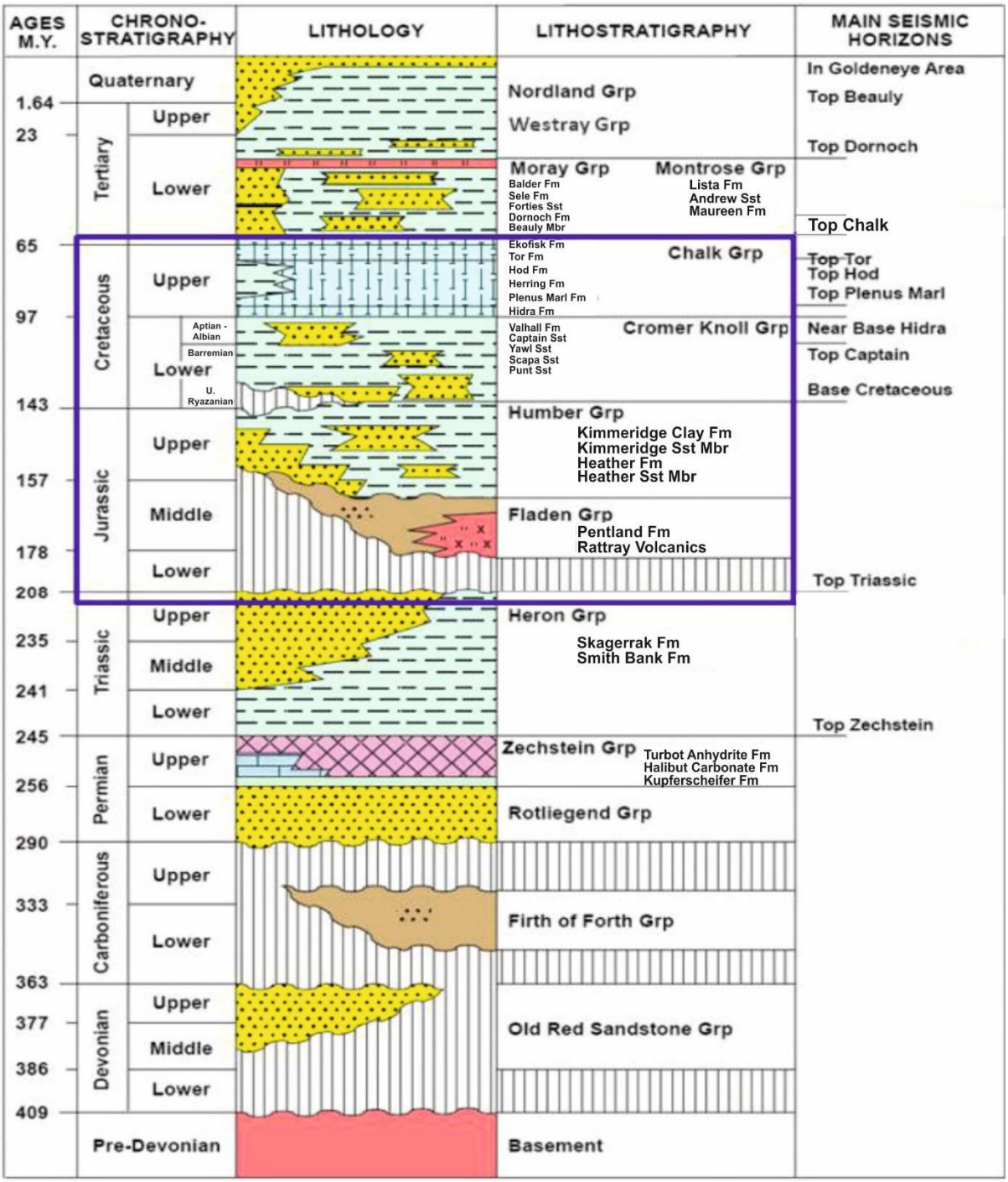
AGES M.Y.
CHRONO-STRATIGRAPHY
LITHOLOGY
LITHOSTRATIGRAPHY
MAIN SEISMIC HORIZONS
Quaternary
1.64
23
Tertiary
Upper
Lower
65
Cretaceous
Upper
97
Aptian - Albian
Barremian
Lower
U. Ryazanian
143
Jurassic
Upper
157
Middle
178
Lower
208
Triassic
Upper
235
Middle
241
Lower
245
Permian
Upper
256
Lower
290
Carboniferous
Upper
333
Lower
363
Devonian
Upper
377
Middle
386
Lower
409
Pre-Devonian
Nordland Grp
Westray Grp
Moray Grp
Balder Fm
Sele Fm
Forties Sst
Dornoch Fm
Beauly Mbr
Montrose Grp
Lista Fm
Andrew Sst
Maureen Fm
Ekofisk Fm
Tor Fm
Hod Fm
Herring Fm
Plenus Marl Fm
Hidra Fm
Chalk Grp
Valhall Fm
Captain Sst
Yawl Sst
Scapa Sst
Punt Sst
Cromer Knoll Grp
Humber Grp
Kimmeridge Clay Fm
Kimmeridge Sst Mbr
Heather Fm
Heather Sst Mbr
Fladen Grp
Pentland Fm
Rattray Volcanics
Heron Grp
Skagerrak Fm
Smith Bank Fm
Zechstein Grp
Turbot Anhydrite Fm
Halibut Carbonate Fm
Kupferscheifer Fm
Rotliegend Grp
Firth of Forth Grp
Old Red Sandstone Grp
Basement
In Goldeneye Area
Top Beauly
Top Dornoch
Top Chalk
Top Tor
Top Hod
Top Plenus Marl
Near Base Hidra
Top Captain
Base Cretaceous
Top Triassic
Top Zechstein

Figure 2.6b)

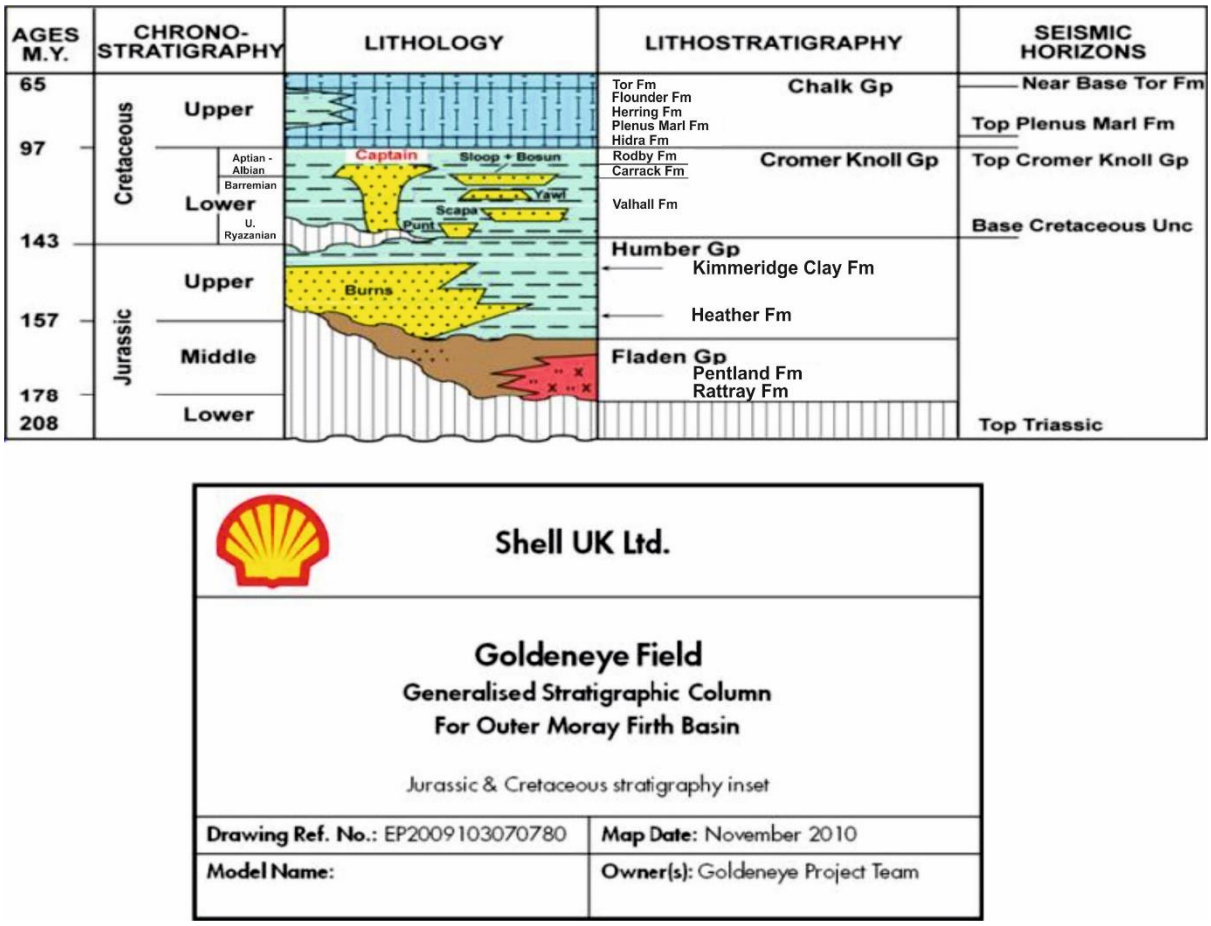

Figure 2.6 a) Stratigraphy of the Goldeneye area, blue lines are inset shown in Figure 2.6b) Jurassic and Cretaceous lithostratigraphy, with storage reservoir of the Captain Sandstone shown in red text (partly redrawn from Shell, 2011).

The reservoir is capped by the mudstones of the Rødby Formation; with an average thickness of 60 metres and average permeability values below 0.1 milliDarcy. This primary seal rock for the CO_2 is composed of chalky mudstone that acted as the seal to the Goldeneye hydrocarbon field over geological time periods. Overlying the primary seal rock is a thick Upper Cretaceous and Tertiary sequence of clay, shale, sand and lignite and Quaternary sediment up to the sea bed. Within this sequence four aquicludes were identified which would restrict upward migration of CO_2 through the overburden sequence. These are the Dornoch Mudstone Unit, the Lista Formation, the Plenus Marl Formation and the Hidra Formation.

The Plenus Marl and the Hidra Formation directly overly the Rødby seal rock and offer an additional 100 metres-thickness of low permeability mudstone and interbedded limestone to enhance the primary trap. The Lista mudstone, which acts to trap natural gas in hydrocarbon fields in the Central North Sea, provides the secondary seal. Regionally it varies in thickness between 60 and 120 metres and is composed of non-calcareous mudstone and claystone.

The Lista Formation mudstone overlies a stratigraphic sequence, one kilometre in thickness, containing aquifer-quality reservoirs (e.g. the Mey Sandstone). This sequence was intended to provide secondary containment for any CO_2 leaking from the primary reservoir.

The Dornoch Mudstone does not provide a structural trap in the region but its properties suggest it would provide a suitable tertiary seal. The Goldeneye storage site was chosen due to a multiple barrier configuration of thick sealing units with the potential for secondary storage above the primary seal (Figure 2.7).

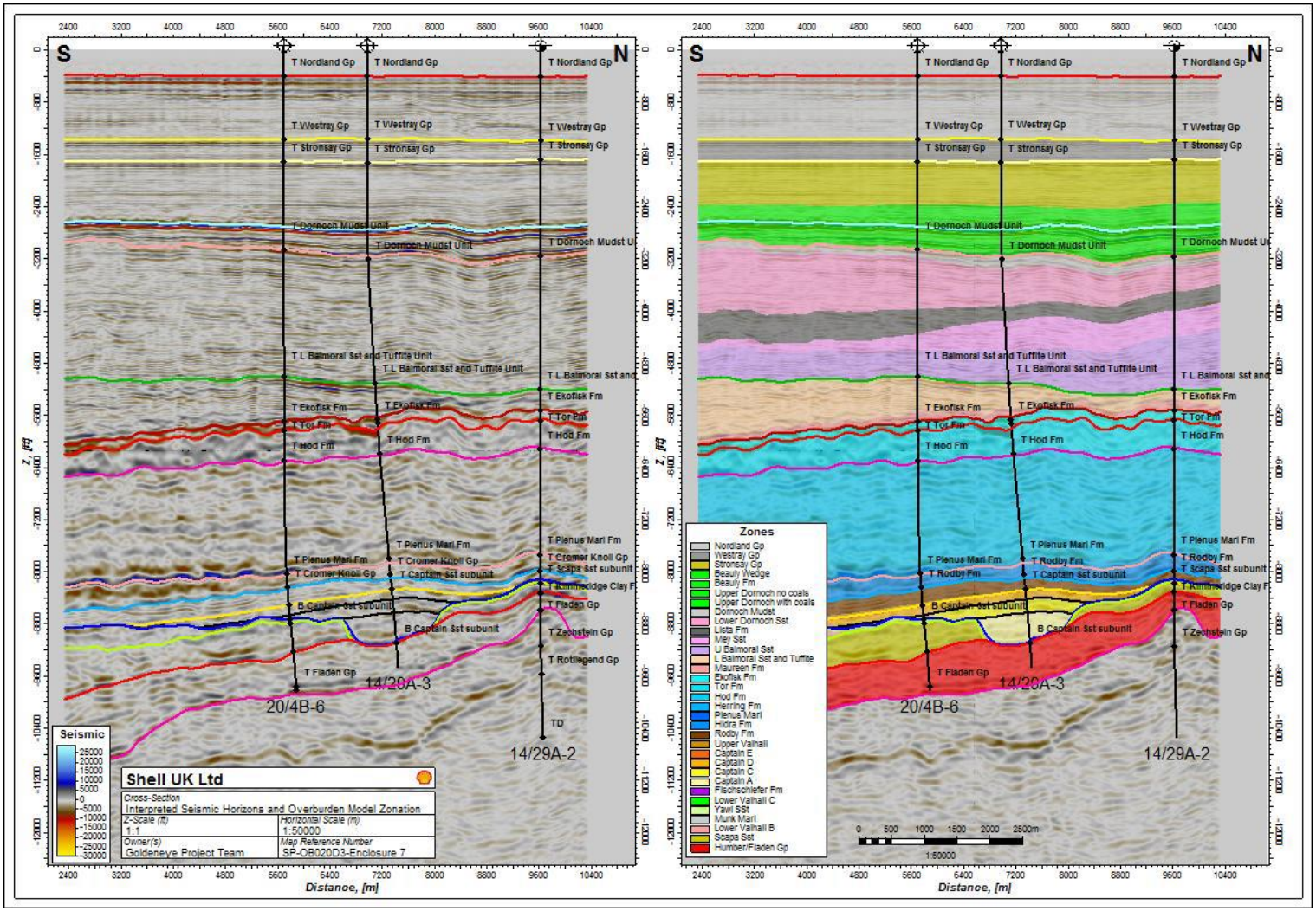

Figure 2.7 Seismic cross-section showing interpreted seismic (left) and overburden stratigraphy (right) (from Shell, 2011). The Figure on the right shows the top Rødby Formation cap rock in pink, overlying the Captain Sandstone, and the secondary seal rocks of the Lista Formation in dark grey.

An analysis of the 3D seismic data over the site identified reservoir-level faulting of limited vertical extent and with a dominant west-north-west to east-south-east trend. The faulting does not appear to have compartmentalised the reservoir and fault throws of less than 20 metres are attributed to the larger features. Interestingly, two different fault sets can be mapped within the Cretaceous overburden. Interpretation of these features suggests they were decoupled from the faults at reservoir level. No significant faulting was observed in the Tertiary sequence.

The uppermost part of the Goldeneye overburden comprises Nordland Group sediments (Stoker et al., 2011), largely dominated by clay and mud, with a glacially influenced upper part. BGS cores (Fyfe, 1986; Stoker and Bent, 1987) near the area describe marine and prodeltaic muds with thin sand overlain by glacimarine mud with occasional sand and diamict units (Graham et al., 2011). These sediments are Pleistocene in age and have been repeatedly influenced by significant glacial episodes with geomorphological evidence for glacial landforms (i.e. tunnel valleys, iceberg plough marks, mega-scale glacial lineations, glaciotectonism) most recently imaged in 3D seismic data (see summary in Graham et al., 2007; Ottesen et al., 2009). The largest of the glacial landforms, subglacially formed tunnel valleys, are present extensively across the Goldeneye area (Fichler et al., 2005; Van der Vegt, 2012, fig. 1; Stewart et al., 2013). The infill of buried tunnel valleys in the central and northern North Sea remains untested; bright and chaotic reflector packages identified towards the base of some tunnel valleys are tentatively interpreted to comprise more coarse-grained materials (Kristensen et al., 2008; Van der Vegt, 2012, fig.4; Stewart et al., 2012; Benvenuti and Moscariello, 2016) but these packages are not observed systematically.

Further sandy material may be present near to the sea bed, likely relating to fluvial or subglacial deposition during subaerial exposure, but are not laterally or stratigraphically extensive in the vicinity of the Goldeneye Field (Fyfe, 1986; Stoker et al., 2011). Overall, the relatively flat-lying and mud-dominated nature of the upper part of the overburden (Nordland Group) provides good sealing capacity.

2.5 Field Research Station, Alberta, Canada

The Field Research Station (FRS) differs from the other storage sites in this section in that it is a relatively shallow experimental injection site, under development, where both containment and migration out of containment, are being evaluated. The site is about 180 km south-east of Calgary in southern Alberta, Canada. An initial controlled release of CO_2 is planned at 300 m depth, with a later injection proposed at 500m. Injection rates are expected to be up to 1,000 tonnes per year. The experimental objectives include the determination of CO_2 detection thresholds for different monitoring techniques and monitoring of migration of both CO_2 and CH_4 at intermediate to shallow depths. It is hoped that the first injection will take place in 2017.

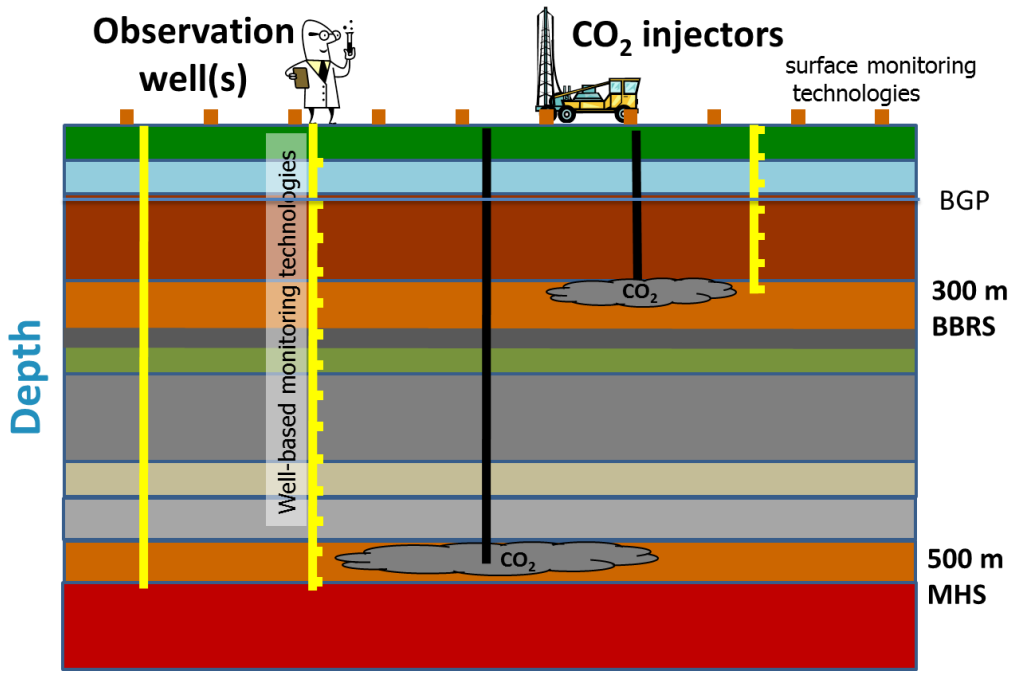

Figure 2.8 Schematic diagram of the FRS (MHS – Medicine Hat Sand; BBRS – Basal Belly River Sand). Diagram courtesy of Don Lawton.

The proposed storage formations are aquifer sandstones within the Upper Cretaceous sequence; the Medicine Hat Sand at about 500 metres depth and the Basal Belly River Formation at about 300 metres depth (Figure 2.8). The Medicine Hat Sand is overlain by about 50 metres of shale cap rock, which is expected to form an effective seal. The Basal Belly River Formation is six metres thick and comprises shoreface-facies sandstone with an overburden sequence including mudstone, sandstone and thin coal. There may be upward migration out of this storage formation and potential for leakage to surface. It is also possible that, if the regulator approves, the overburden could be hydraulically fractured to investigate the effect on migration out of the storage reservoirs.

3 Review of mechanisms, processes and rates of migration through the overburden

Large-scale overburden heterogeneities or anthropogenically induced pathways offer the means to breach the sealing strata that contain geologically stored CO_2 and promote migration of the injected CO_2 into the overburden. Heterogeneities in overburden sequences may allow fluids to flow vertically across stratal boundaries and provide rapid fluid flow pathways vertically to shallower depths or laterally beyond the immediate vicinity of the fluid source. These 'seal by-pass' features (Cartwright et al., 2007) are of three main types: geological faults; seismic or gas 'chimneys'; and injected bodies of sedimentary or igneous material. Here we also include and review large-scale sedimentary features within the overburden strata, related to recent marine and glacial processes and deposits, that have the potential to act as high permeability pathways. The processes that operate and the resulting structures and features generated differ, dependent on whether the strata are consolidated or not, and are considered separately in this review. Ultimately, a key issue for CO_2 storage is to assess whether the allowable temporal CO_2 flux via a particular bypass mechanism or permeability pathway would be sufficient to compromise the integrity and efficacy of the storage site over extended periods of time.

The processes and rates of migration through the overburden are considered for the following migration pathways: geological faults and fractures (Section 3.1); geological fluid flow pathways (Section 3.2), large-scale geomorphological features that are potential pathways or barriers to fluid migration (Section 3.3); hydrofracturing and glacitectonic faults (Section 3.4); wellbore-related pathways (Section 3.5); modelling of migration and experimental work (Section 3.6). The rates of migration and their ranges presented in this section are deemed to be representative of both natural processes and anthropogenic subsurface activities. The processes and rates set the context for migration of geologically stored CO_2 within the overburden sequence.

3.1 Geological faults and fractures

Faults are roughly planar fractures or discontinuities within a volume of rock, formed by external stresses that cause deformation of the rock mass. Generally, there is a degree of displacement across faults due to relative movements of the opposing rock volumes on either side of the fault. Fractures and faults commonly act either to inhibit or enhance the flow of fluids in the subsurface, and are commonly present at a range of scales. In the context of CO_2 storage, faults are likely to consist of large faults separating basins and highs within or at the margins of sedimentary basins, or smaller faults related to local structural configurations and pore pressure history. While larger faults are more likely to offset potential storage reservoirs and their overburden sequences, smaller faults are preserved within more limited stratigraphic windows without significant offset of strata. The nature of faulting within potential storage site overburden sequences is highly variable, so overburden faults in typical settings cited for storage in the North Sea and UK Continental Shelf are described in Section 3.1.2.3. Although larger faults can be easily identified using seismic reflection methods, it is

unlikely that pre-existing faults and fractures can be avoided altogether within a storage complex and some degree of faulting can be expected within storage site overburden sequences.

An understanding of fault properties in relation to fluid-flow is therefore critical for any practical application where fluids are injected into, or produced from the subsurface. Faults form a critical structural component to hydrocarbon traps, and to prospective CO_2 storage sites. At a CO_2 storage site, the presence of pre-existing faults could prove to be beneficial or deleterious to the storage operation, depending on the specific geological and operational site conditions. A recent review published by the IEAGHG (Nicol et al., 2015) examined the controls on fault zone permeability in detail, and therefore only a summary is presented in this report.

A large volume of literature provides evidence for fluid flow along faults; however there are also examples of faults acting as effective capillary seals (Caine et al., 1996; Yielding et al., 1997; Aydin, 2000; Fisher and Knipe, 2001; Bjørlykke et al., 2005; Faulkner et al., 2010). In the context of CO_2 storage, cross-fault transmissivity is important as many traps suitable for storage are fault-bounded in the same way that faults form the trap to a large proportion of natural hydrocarbon accumulations. Alternatively, faults that do not form an effective capillary seal might allow injected CO2 to migrate across the fault to permeable strata in the opposing fault block. Faults and fractures that cut the storage reservoir, if permeable, might increase bulk reservoir permeability and therefore injectivity, proving beneficial to storage. Conversely, faults less permeable than the undeformed rock might act to compartmentalise the reservoir or form internal baffles, reducing storage capacity. Indeed, faults could impede the displacement of brine or other resident pore fluids during injection, resulting in higher-than-anticipated reservoir pressure increase, such as was the case at Snøhvit, where reservoir heterogeneities are believed to have played a role in addition to fault compartmentalisation (Hansen et al. 2013; Chiaramonte et al. 2015). Permeability anisotropy caused by faults could also lead to preferential along-fault migration, either laterally or vertically. Preferential along-fault lateral migration could result in CO_2 being diverted towards the storage complex or trap boundary, while vertical migration up faults could result in loss of CO_2 from the primary storage reservoir to the overburden. Indeed, faults commonly act as seal bypass mechanisms, allowing buoyant fluids such as hydrocarbons to migrate through otherwise low-permeability top-seals to the overburden and in some cases to the surface (Haney et al. 2005; Schroot et al. 2005; Finkbeiner et al. 2001; Langhi et al. 2014). Along-fault migration may occur in response to geomechanical effects, such as fault reactivation, which could act to increase fault zone permeability or decrease it if there is extensive generation of fine-grained fault gouge. Alternatively, migration could occur within the fault zone where permeabilities can be higher than that of the surrounding rock by up to several-orders of magnitude (Ishii, 2015).

Fault zone permeability is also known to be temporally dependent. Mechanical processes during deformation mean that fault zone permeability can be greater during deformation than afterward (Barton et al., 1995; Fossen et al., 2007; Ballas et al.,

2015). Fluid flow, either across or along faults is also known to be affected by pore fluid pressure. Differential pressure depletion in adjacent fault blocks has modified the cross-fault flow characteristics in numerous UK gas fields (Hillier, 2003; McCrone et al., 2003), with fault baffling breaking-down during production because differential pressure across faults increases the driving force resulting in increased cross-fault flow. Sibson (1990) discussed the concept of fault valve behaviour. Here, faults exhibit episodic fluid-flow resulting from mechanical reactivation during periods of increased pore fluid pressures. As pressure increase is widely expected to occur during CO2 injection, such a mechanism is important both in terms of breaching of the primary seal rock, and in terms of how any 'leaked' CO_2 is likely to migrate within the overburden. Diagenetic effects also impact fault zone permeability, as mineral dissolution and carbonate precipitation can effectively heal a fault rock by porosity reduction (Kampman et al. 2014a; 2016). Strain hardening and later diagenesis also commonly acts to decrease fault zone permeability (Bjørlykke et al. 2005).

3.1.1 Fault characteristics

Faults are not simple planar features, but are highly complex zones of heterogeneous deformation distribution over a range of scales (Childs et al., 2009). Numerous studies of fault zone architecture and fluid-flow characteristics have been presented in the scientific literature, and so it is useful to define some basic terminology pertaining to fault zone structure. A commonly adopted and simple representation is the fault core and damage zone model (Figure 3.1a). Displacements are largely accommodated by the fault core, which is generally accepted to consist of low permeability fault gouge material. The fault gouge may also be referred to as fault rock. The core is surrounded by a thicker zone of deformation known as the damage zone, which comprises subsidiary faults and small-scale joints. In the case of the Punchbowl Fault, an exhumed and inactive part of the San Andreas Fault System, the fault core comprises a single layer of ultracataclasite several tens of centimetres thick, and is bounded by an extensively damaged zone in the order of 100 metres thick (Chester and Logan, 1986). Although it is convenient to consider faults in such a way, few faults observed in outcrop adhere to this simple model, but rather exhibit significant complexity and variable displacement distribution (Childs et al., 2009; Faulkner et al., 2003; Faulkner et al., 2010).

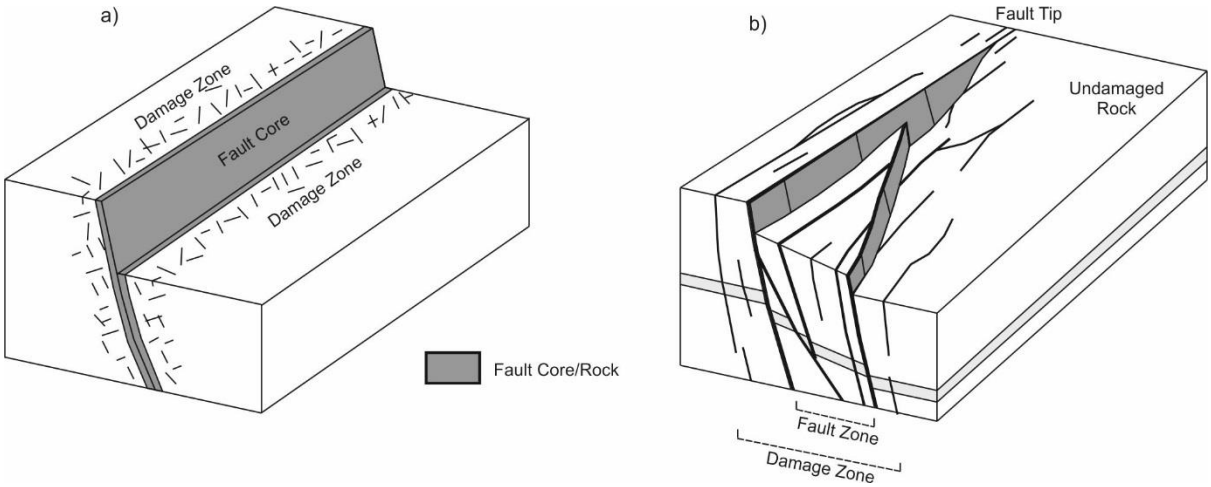

Figure 3.1 a) Simple fault core and damage zone model, where low permeability fault rock is surrounded by a wider damage zone with associated smaller faults and fractures. b) More complex model with multiple fault cores, where the number and thickness of individual fault cores vary along the fault surface. The model also shows that the damage zone extends beyond the tip of the fault slip surface. BGS © NERC (2016).

Fine-grained fault rocks result from processes such as intense fracturing or grain crushing, or by entrainment or smearing of fine-grained host-rock into the fault. In addition to associated smaller faults and joints these may be referred to as the fault zone, which itself might have a corresponding wider damage zone consisting of variably fractured host rock (Figure 3.1). Childs et al. (2009) provide a useful discussion of fault zone terminology, but it is important to note that a fault zone might consist of a number of anastomosing and intersecting slip surfaces with numerous fault cores (Faulkner et al., 2003). When faults form, they propagate through a rock volume as irregular and segmented surfaces, with the volume between individual genetically-related fault segments being termed relay-ramps (Figure 3.2). These are zones of high strain (Chadwick, 1986; Walsh and Watterson, 1991) and, where continued displacement causes failure of the relay zone, a new linking fault will be formed and the relay ramp is deemed to be breached (Peacock and Sanderson, 1994). Such a relay zone can be preserved as an irregularity along the length of the fault, or can be entrained into the fault and eventually reduced to fault rock during further or future displacement. Fossen and Rotevatn (2016) provide an in-depth review of fault linkage and relay structures and their impact on fluid flow.

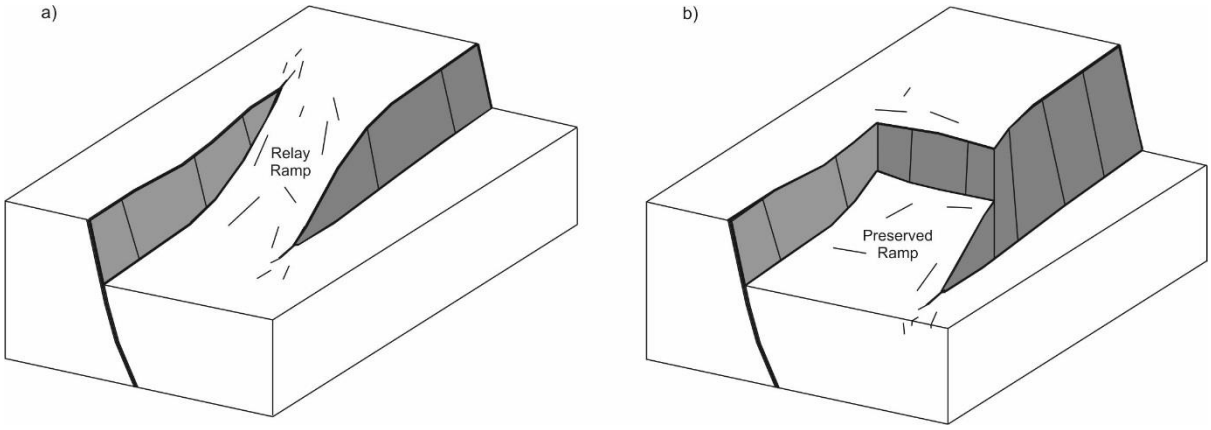

Figure 3.2 Block diagrams showing a) relay ramp between two fault segments, and b) breached relay ramp where subsequent extension has resulted in development of a transfer fault, linking the two previously separate fault segments. In the case shown a portion of the relay ramp is preserved. BGS © NERC (2016)

Both fault rock and fault zone thickness varies in cross-section and plan view. Numerous studies have sought to correlate fault displacement with thickness, broadly finding that larger displacement faults tend to have wider fault zones (Robertson, 1983; Hull, 1988; Evans, 1990; Marrett and Allmendinger, 1990; Shipton et al., 2006). However, there is significant heterogeneity in fault zone thickness for any given fault displacement, and fault zone thickness can vary by an order of magnitude over a distance of several meters (Childs et al., 2009; Nicol et al., 2013). Areas of structural complexity such as fault or fault segment intersections, relays, bends and terminations tend to be the widest parts of faults, and are often considered to be local zones of high strain with increased density of smaller-scale faults, fractures and joints. Consequently, they are considered to be areas of elevated fault zone permeability, a notion supported by a number of studies (Hermanrud et al., 2014; Gartrell et al., 2003; Gartrell et al., 2004; Teige and Hermanrud, 2004; Dockrill and Shipton, 2010). As a result, these features can be considered as specific targets for risk assessment and monitoring for CO_2 storage.

3.1.2 Migration through faults

The factors affecting the migration of fluids along faults, or fault zones in the overburden are broadly the same as relevant to a breach of the primary seal rock, where migration occurs between the reservoir and top seal formations. These factors are outlined, along with a brief description of faulting observed in the overburden of potential storage sites in typical North Sea settings and issues relating to potential migration in such areas. Additionally, potential migration rates are discussed based on natural leakages of CO_2 from the subsurface.

3.1.2.1 Controls on cross-fault migration

Stratigraphic juxtaposition is the simplest way to evaluate whether a fault is likely to allow across-fault flow of fluid. If a hydrocarbon-bearing reservoir rock or CO_2 storage reservoir is offset against a fine-grained low-permeability rock type then it can be expected that cross-fault fluid-flow will be impeded. Conversely, if the reservoir rock is juxtaposed against a permeable rock layer then it can be assumed that cross-fault flow is a possibility. Cross-fault juxtaposition can be determined from 2D seismic reflection profiles normal to the strike of faults, or if adequate seismic data coverage is available to allow for the 3D interpretation of the faults and affected horizons. Stratigraphic juxtaposition across faults may be mapped using Allan Diagrams (Allan, 1989), which display the distribution of units with contrasting lithological characteristics in the footwall and hanging wall of the fault surface (Figure 3.3).

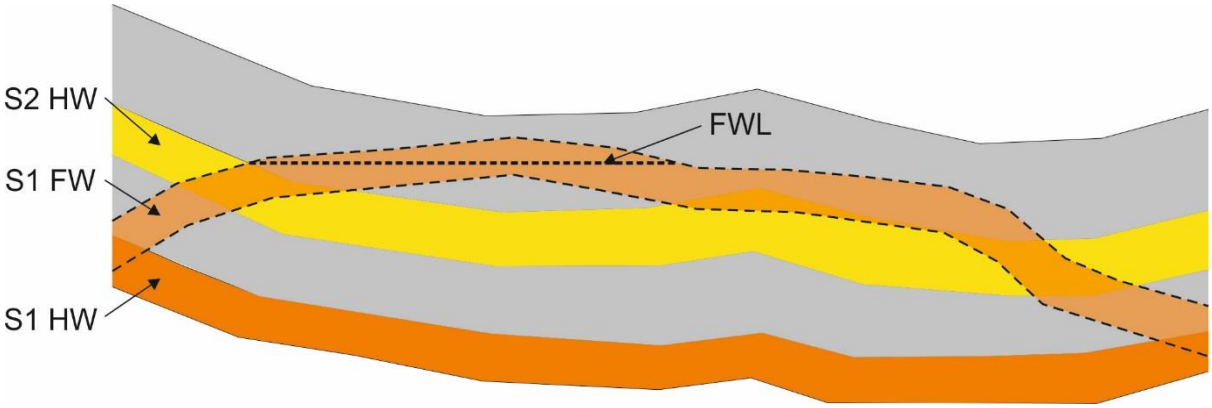

Figure 3.3 Example of Allan diagram, showing sandstone S1 reservoir in footwall (FW) juxtaposition against lithologies in the hanging wall (HW). The height of the Free Water Level (FWL) in the S1 reservoir in the footwall trap is limited by juxtaposition of the S1 reservoir in the footwall trap is limited by juxtaposition of the S1 reservoir against the younger S2 sandstone in the hanging wall. Above the Free Water Level the S1 reservoir is juxtaposed against shale (grey). BGS © NERC (2016)

The formation of clay-rich fault rock is commonly understood to impede cross-fault fluid flow (Yielding et al*.,* 1997; Sperrevik et al., 2002; Freeman et al., 2008; Manzocchi et al*.,* 2010). Therefore, in an interbedded sequence of sandstones and mudstones, if a sandstone is self-juxtaposed across a fault, or offset against another sandstone the fault may either be sealing or non-sealing depending on the properties of the fault rock. Given the likely complexities of any given fault, the transmissibility of the fault rock can vary spatially across the fault surface, and also temporally depending on reservoir pressure conditions in relation to the capillary or membrane seal capacity of the fault rock. In fault-seal analysis methods developed for multi-layered sand-shale sequences, the concept of capillary thresholds and buoyancy-driven overpressure is important (Yielding et al., 1997; Yielding, 2012; Bretan and Yielding, 2003; Bretan and Yielding, 2005; Sperrevik et al*.,* 2002; Freeman et al., 2008; Manzocchi et al., 2010). Here, the fault effectively seals a column of buoyant non-wetting fluid, such as hydrocarbon or CO_2, until the capillary threshold pressure of the water-wet fault rock is exceeded by the buoyancy-driven overpressure exerted by the column. Once the fault rock capillary threshold pressure is exceeded the fluid will migrate, or leak into and across the fault. The sealing capacity of the fault is therefore limited by the capillary pressure (Pc) of the non-wetting fluid and the capillary threshold pressure (Pct) of that part of the fault rock above the buoyant fluid–water contact. This limit will

constrain the height of the supported or trapped buoyant fluid column. The limiting point is where Pc exceeds Pct. Conventional fault seal prediction techniques assume, therefore, that the capillary-pressure threshold of the fault rock controls lateral migration across faults, and that this is a function of pore-throat size. Fault rock materials with smaller pore throat radii will have higher capillary threshold pressures and are capable of supporting greater column heights.

Several conceptual models have been developed to estimate the composition of fault rocks (Figure 3.4), their fluid-flow properties and sealing potential (in terms of critical pressure thresholds and/or column height potential). Shale Gouge Ratio, or SGR (Yielding et al., 1997), is commonly used to estimate the degree of mixing of host rock-derived material within faults using the fault displacement and clay content of the affected strata that has been displaced past a given point. Clay or shale volume interpreted from downhole geophysical logs are generally up-scaled or attributed to different layers in a geological model and the SGR of faults is calculated based on the clay volume attribute and fault displacement. After the calculation of fault clay volume, SGR may be converted to permeability and/or threshold pressure based on empirical relationships derived for specific conditions, such as the time–temperature history of the formation (Sperrevik et al., 2002) and the properties (interfacial tension and contact angle) of the fluid-rock system (Bretan et al., 2011). Although relatively straightforward to implement for individual reservoirs where site characterisation data are available (wells and seismic reflection data), outcrop studies (Farrell et al., 2014, see especially fig. 2) suggest that the mixing of lithologies as described by the SGR method does not fully account for the observed fault rock heterogeneities (Childs et al., 2007; Dockrill & Shipton 2010).

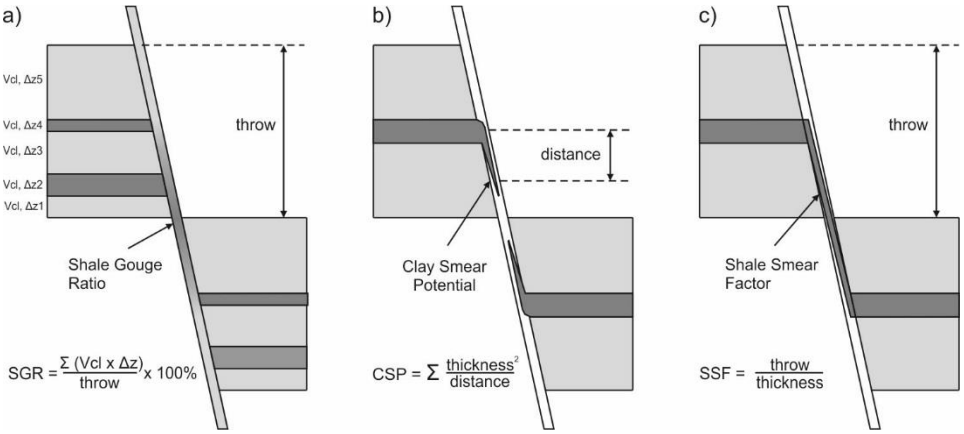

Figure 3.4 Schematic diagram illustrating conceptual fault seal models in interbedded sand-shale sequences. a) Shale Gouge Ratio (SGR), b) Clay Smear Potential (CSP) and c) Shale Smear Factor (SSF). Figures re-drawn after Yielding et al., (2010) and Jolley et al. (2007).

Shale or clay layers in some interbedded sequences are observed to flow into the fault during shearing, forming continuous down-fault 'smears' between the un-deformed footwall and hanging wall shales (Lehner and Pilaar 1997; Fulljames et al., 1997). Shale Smear Factor, or SSF (Lindsay et al., 1993), and Clay Smear Potential (CSP), account for the smearing of shale or clay layers down the fault plane, depending on the burial depth and degree of consolidation. In SSF the clay layers are continuously smeared along the fault during shearing (Figure 3.4), until a critical value is reached

at which point the smeared clay layers become discontinuous and the fault-seal is broken.

Cataclastic processes involve the progressive fracturing of mineral grains and rock comminution during faulting, which results in the formation of angular clasts set within a fine-grained material. In extreme cases, ultracataclasites are formed, where the fine-grained matrix comprises more than 90% of the material. Such grain-size reduction is associated with a significant reduction in porosity and permeability (Tueckmantel et al., 2012).

Deformation bands (Figure 3.5), also known as shear bands or granulation seams, form as small strain-accommodating structures that develop in porous granular materials (Fossen et al., 2007; Antonellini et al., 1994; Aydin, 1978; Underhill and Woodcock, 1987). The width of individual bands is commonly in the range of less than one millimetre to a few centimetres, and each band accommodates a small offset of the same order. Deformation bands are commonly observed in rock adjacent to faults and are particularly prevalent in relay ramps where significant strain localisation occurs. Wide zones of deformation bands are present at some localities, where they can accommodate significant offsets due to cumulative small offsets across many individual deformation bands, despite the absence of a well-defined fault slip surface. Deformation bands are characterised by distinct zones of porosity reduction due to grain sliding, rotation and/or fracture, or crushing and cataclasis. Fossen et al., (2007) describe different types of deformation bands, and define categories based on the deformation mechanism. These include disaggregation bands, phyllosilicate bands, cataclastic bands and solution and cementation bands. Deformation bands that form without cataclasis (compactional deformation bands) tend to form either at low confining pressure (shallow depth) or in overpressured sandstones and are common in unconsolidated sands and in weakly cemented sandstones. In well-sorted sands, initial dilation occurs followed by compaction, with granular flow contributing towards the development of the deformation band. In such non-cataclastic bands, fault slip surfaces can form following the development of several tens of individual bands. In the case of cataclastic deformation bands, hundreds of bands may develop before a fault will form.

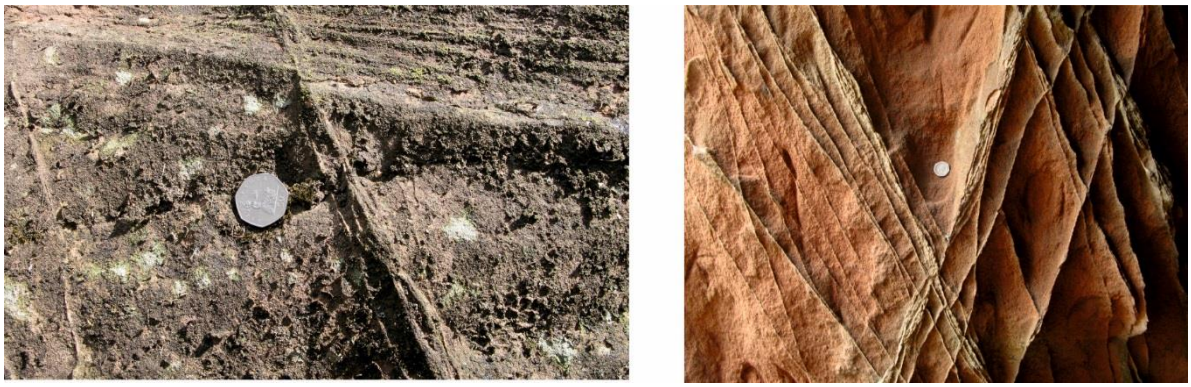

Figure 3.5 Examples of deformation bands from northern England. Photographs courtesy of Andy Chadwick. British Geological Survey.

The development of deformation bands can have a detrimental effect on cross-fault fluid flow due to permeability reduction (Fossen et al., 2007; Pittman et al., 1981;

Fisher and Knipe, 2001), and may therefore serve to promote fluid-flow along strike. Their thickness and permeability is highly variable in three dimensions, and their practical effect on fluid flow at the reservoir scale is currently unclear (Fossen et al., 2007).

Other processes that can influence cross-fault transmissibility are diagenesis and mineralisation of fault zones. In Lower Permian Rotliegend sandstone reservoirs of the Southern North Sea, the prevalence of both deformation bands and cementation affect cross-fault fluid-flow in otherwise 'clean' sand-on-sand juxtapositions (Leveille et al., 1997; Corona, 2005; Van Hulten, 2010). Where pore-space within fault zones is occluded by diagenetic cement it is clear that this can result in porosity and permeability reduction. This process can also lead to fault zones being mechanically stronger than the surrounding undeformed rock, reducing the potential for dilation of the fault zone relative to the undeformed rock during further episodes of deformation.

3.1.2.2 Controls on vertical fault migration

Many of the same factors that influence cross-fault fluid flow are also relevant to vertical migration of fluids along fault zones. Stratigraphic juxtaposition, fault zone geometry, fault rock composition and post-deformation diagenesis all influence the likely along-fault flow properties. A key additional consideration in terms of vertical migration along faults is the concept of mechanically active faults, which are hydraulically active and facilitate vertical fluid flow (Sibson, 1990). Positive normal stresses will inhibit slip along a fault plane by pushing the opposing blocks together, counter-acting the effect of shear stresses that act parallel to the fault. Increasing fluid pressure during CO_2 injection reduces the effective stress (normal stress minus pore pressure) acting on a fault plane (Figure 3.6) effectively reducing the strength of a fault (Streit and Hillis 2004). Once a fault has failed, it is broadly assumed that in the absence of strain-hardening behaviour or the formation of fine-grained fault gouge, the fault will then become transmissible to along-fault fluid flow in response to a pressure gradient (Sibson 1990; Barton et al. 1995). The relationship between in situ stress and fluid flow has been shown to be relevant to a number of applications worldwide, in flow processes relating to fractured aquifers and geothermal fields in crystalline rock (Barton et al., 1995), in understanding naturally constrained hydrocarbon column heights (Wiprut and Zoback, 2000; Finkbeiner et al., 2001), and in optimising productivity of hydrocarbons or groundwater by targeting fractures experiencing high ratios of shear to normal stress (Ferril et al., 1999; Hennings et al*.,* 2012). Faults that are on the verge of failing, and cannot, therefore, support any additional pore pressure increase are termed to be critically stressed. The build-up of fluid pressure over time can, therefore, cause faults to fail episodically, releasing pressure through valve-like behaviour (Finkbeiner et al., 2001; Sibson, 1990).

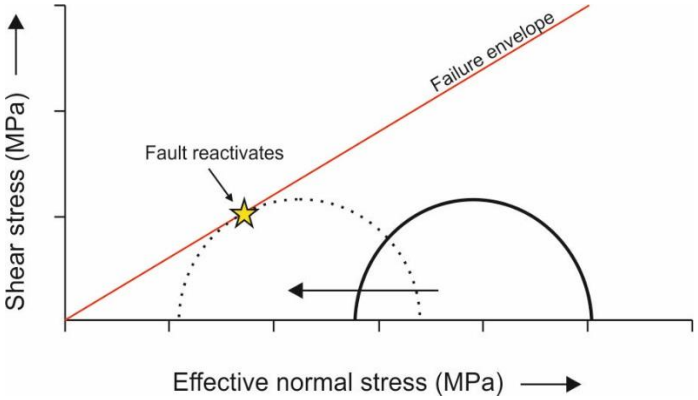

Figure 3.6 Mohr-circle representation of failure on a pre-existing, optimally oriented and cohesionless fault. Pore pressure increase above initial pressure (solid circle), results in reduction of the effective normal stress (dotted circle), moving the stress state towards the failure envelope (Streit and Hillis 2004). MPa, megaPascal.

Using knowledge of fault geometry, rock physical properties and pore pressure, together with principal stress orientations and magnitudes, it is possible to estimate the stability of faults in a given stress regime. It is also possible to estimate the pore pressure perturbation at which faults of given orientations will slip (Ferril et al., 1999; Morris et al., 1996; Mildren et al., 2005; Worum et al., 2004). Such geomechanical models include slip tendency, the ratio between the shear and effective normal stress acting on the fault, a measure of whether the fault is preferentially oriented for failure in the given stress regime. Another measure related to the structural permeability of faults is dilation tendency, which describes the likelihood of faults to dilate under particular stress conditions, the assumption being that dilated or open faults are more likely to exhibit fluid-flow (Ferrill et al. 1999). Fracture stability is another commonly used metric to describe the pore pressure perturbations that would induce slip at given locations on a fault plane (Mildren et al., 2005). Numerous studies have used such principles to assess the structural integrity of potential CO_2 storage sites (Lucier et al., 2006; Chiaramonte et al., 2008; Bretan et al., 2011; Williams et al., 2016), and the same techniques may also be used to assess the likelihood for flow in overburden successions.

It is widely assumed that faults that are critically stressed in the current stress regime will potentially allow vertical migration of fluids such as CO_2 due to an increase in along-fault permeability during slip or pressure-induced reactivation. However, it has been shown that fault orientation does not always control the flow properties of hydraulically conductive faults and fractures (Laubach et al., 2004; Cuss et al., 2015). Sathar et al., (2012) present a case where shear stress hysteresis appears to control the ability of faults to conduct fluids. Barr (2007) shows that deformation and inversion history has affected fault sealing in the West Sole gas fields, UK Southern North Sea. In this case, Jurassic rifting resulted in the formation of sealing lithified cataclastic fault rocks during burial and extension, which were subsequently breached by inversion-related brittle deformation which took place in reducing temperature and effective stress regimes (Barr 2007). Therefore, the burial and exhumation history of faults can exert a control on fault permeability, even if those faults are not critically-stressed in the current stress state, necessitating an understanding of past fault movements and stress history. Laboratory experiments have shown that fault orientation does not

always control fluid-flow through a synthetic fault gouge (Cuss et al., 2015). Evans (2005) investigated fluid-flow and its relationship to fractures in the Soultz-sous-Forets hot dry rock geothermal project in France, where all of the naturally flowing fractures were confirmed to be critically stressed. Despite this, a significant number (approximately 500) of other critically stressed fractures were found to be non-conductive. This suggests that while the ability of a fracture to conduct fluid at the site is dependent on it being critically-stressed, the flow properties of the overall fault population were inadequately predicted using critically stressed fault principles (Evans, 2005). Although initial dilation may occur during failure of a fault, the formation of low-permeability fault gouge can result in significant permeability reduction (Bjørlykke et al*.,* 2005; Yielding et al., 1997). The notion that critically stressed faults will facilitate along-plane migration of CO_2 should, therefore, be considered to be conservative (Williams et al*.,* 2014).

Underschultz (2016) explored the link between capillary processes and mechanical fault reactivation, theoretically concluding that a water-wet fault rock will not experience an elevated pore pressure unless its threshold capillary pressure for a particular fluid is reached. It follows, therefore, that if potential upward migration of CO_2 via a fault is of concern, the wettability properties of the injected fluid may be of importance because the fault zone will not 'feel' the increased fluid pressure until the threshold capillary pressure of the material for CO_2 is overcome. Understanding the capillary entry pressure of the fault material itself is, therefore, important in considering the potential for fault reactivation and any subsequent along-fault CO_2 migration.

In the presence of a CO_2-brine system it is possible that acidification could result in the dissolution of calcite cements, leading to additional porosity and permeability development within an otherwise tightly cemented fault zone (Kampman et al., 2014a). In such cases, supersaturation of the pore fluids with respect to the dissolved cement can prevent subsequent dissolution, effectively self-healing the fracture. Where CO_2-saturated fluids migrate vertically to lower pressures, as would be expected if escaped CO_2 migrated upward into the overburden, degassing CO_2 can drive carbonate mineral supersaturation and rapid deposition rates, limiting the extent to which it continues to migrate upwards via the fracture system (Kampman et al., 2014a).

3.1.2.3 Faulting and fluid-flow in overburden successions

Most CO_2 storage studies address the risk of faulting in terms of trap failure, breach of the seal rock or the limiting effects of fault compartmentalisation (Lucier et al., 2006; Chiaramonte et al., 2008, 2015; Bretan et al*.,* 2011; Williams et al*.,* 2016). Few published studies seek to examine how faults overlying CO_2 storage sites will influence CO_2 migration in the overburden in the event that migration occurs above the reservoir top seal. The principles of fluid flow through overburden faults are similar to those that determine how faults influence CO_2 migration in reservoir-cap rock systems. It is, however, useful to consider faulting styles prevalent in typical overburden successions in terms of how these might affect overburden migration processes. The example of the North Sea and surrounding regions where CO_2 storage is in operation or planned is used here.

The nature of overburden faulting differs in different parts of the North Sea. Significant (large-offset) overburden faults affecting the Tertiary succession over the buried Mesozoic Central and Viking grabens are generally fairly localised in their nature (Morton, 1979). Zones of pervasively, polygonally faulted, slope and basin-floor facies are present in Eocene to Mid Miocene intervals, and to a lesser extent in the more sand-prone Palaeocene succession (Lonergan et al., 1998). Such faults tend to be constrained to particular stratigraphic intervals and do not commonly constitute continuous migration pathways from reservoir to surface. Above potential storage sites in the UK sector of the Southern North Sea, faulting is mainly related to the growth of Zechstein salt swells in the basin centre (Griffiths et al., 1995; Williams et al., 2014). In exhumed regions, such as the East Irish Sea and Moray Firth (Hillis et al., 1994; Argent et al., 2002), Cenozoic inversion has resulted in reactivation of existing Mesozoic and older faults (Argent et al., 2002; Corcoran and Doré, 2002; Zanella and Coward, 2003), with major faults extending through the overburden stratigraphy towards the seabed. The following discussion will focus on faults affecting the post-rift sequence of the North Sea, faults related to halokinesis, and processes resulting from faulting and inversion in exhumed sedimentary basins.

3.1.2.4 Faulting in the post-rift sequence of the North Sea

The post-rift overburden sequence of the North Sea largely comprises Cretaceous and Cenozoic rocks and rift-related faulting is generally restricted to strata beneath the base Cretaceous unconformity, except at the basin margins. Faults that significantly offset the stratigraphy are not generally observed in Cretaceous and Cenozoic strata unless associated with halokinesis in the Permian-aged Zechstein evaporites or due to Cenozoic basin inversion. In the Central North Sea region, the Tertiary succession includes a number of saline aquifer storage prospects and hydrocarbon fields. Sandstone fairways are overlain by largely argillaceous overburden rocks, which in turn are overlain by Pleistocene glacial and glacimarine sediments and Holocene superficial sediments (Gatliff et al., 1994). The Sleipner CO_2 storage site is situated in a similar setting in the Norwegian North Sea, with CO_2 injected since 1996 into a basinal deposit of Mio-Pliocene age, the Utsira Sand (Chadwick et al., 2004). The reservoir and overburden are devoid of significant faulting, although small-scale faults are present in abundance within restricted stratigraphic intervals.

The most common form of faulting in the post-rift succession of the North Sea is polygonal faulting within fine-grained slope and basin-floor Tertiary deposits. Such faults pervasively deform specific depth intervals (Figure 3.7), giving rise to a chaotic zone of non-tectonic faulting exhibiting a crudely polygonal pattern in plain view. Throw on such faults occurs in a normal sense, with typical offsets amounting to less than 100 metres, with fault spacing of the order of one kilometre or less (Cartwright, 2014). As the polygonal fault systems are layer-bound, both over- and underlain by strata unaffected by the same mode of deformation, it is clear that they are non-tectonic features. This is supported by the isotropic strain distribution they represent, which precludes a tectonic origin. The origin of polygonal fault systems remains an area of much debate, with proposed genetic mechanisms including fluid overpressure, gravity collapse, density inversion, syneresis and compactional loading (Cartwright et al., 2003). Vejbaek (2008) suggests that a polygonal fault system in the Danish North Sea

corresponds with the transition to normal hydrostatic pressure conditions at the top of an overpressured zone of Lower Cenozoic sediments. Goulty (2008), after Vejbaek (2008), shows that these rocks have an exceptionally low coefficient of residual friction, meaning that the weak mechanical properties are coincident with the zone of effective stress minimum at the top of the overpressured zone. Crucially, characterisation of polygonal faulting is only possible with 3D seismic data as it is not possible to appreciate the polygonal geometry using 2D data alone (Cartwright, 2014).

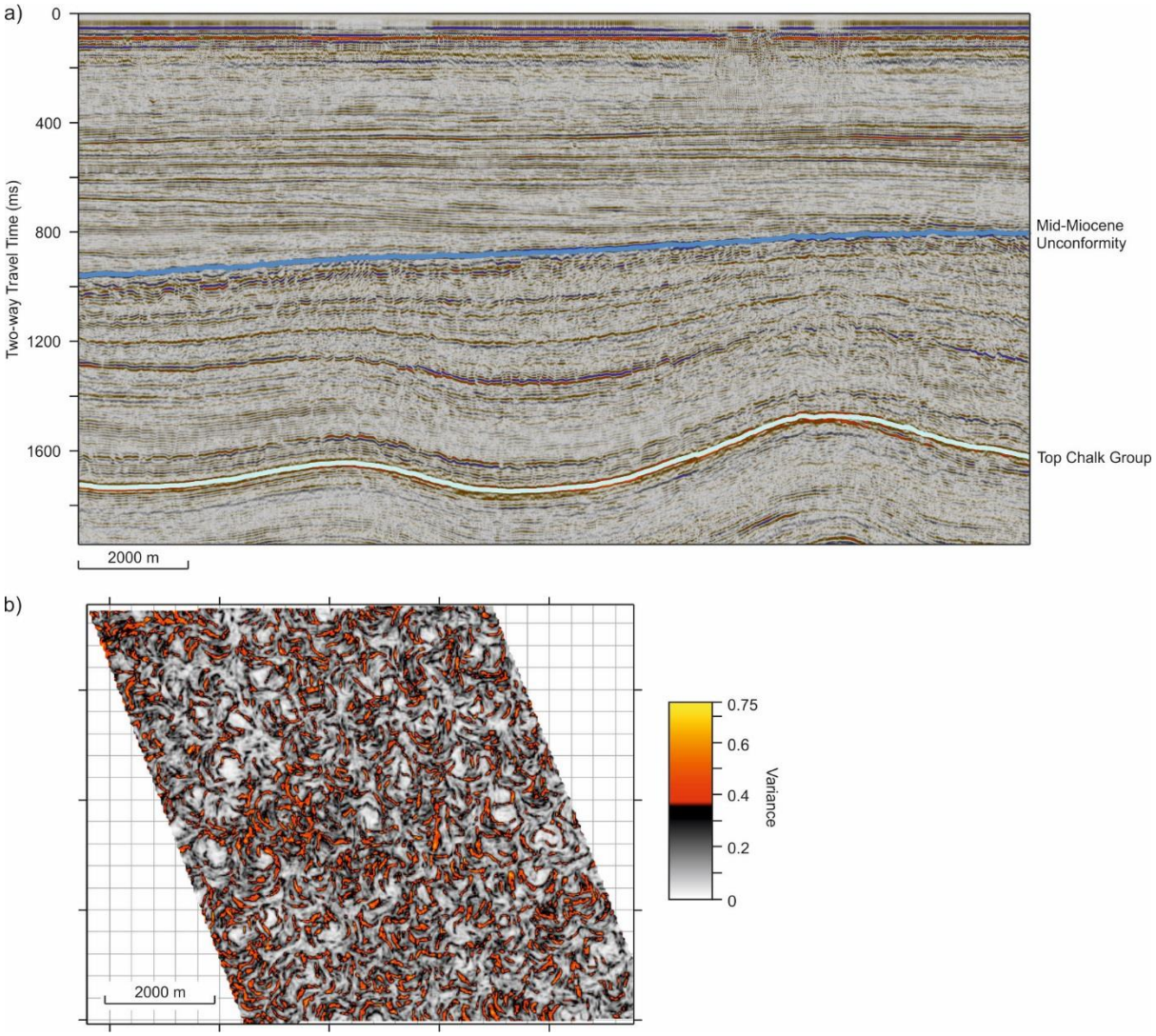

Figure 3.7 a) Seismic reflection section showing nature of polygonal faulting restricted to Lower North Sea Group (Palaeogene–Neogene) beneath the Mid-Miocene Unconformity offshore Netherlands. The polygonal faults can be observed in the chaotic seismic character beneath the unconformity. b) Plan view of horizon slice (100 ms TWT beneath the Mid-Miocene Unconformity surface) showing distribution of polygonal faults highlighted by the seismic variance attribute. Seismic data shown courtesy of www.nlog.nl. BGS © NERC (2016).

In terms of CO_2 migration through the overburden following an unexpected release of CO_2 from a storage reservoir, it is unclear whether a zone of polygonal faulting would encourage upwards migration of buoyant CO_2. Gay et al. (2004) and Berndt et al. (2003) show an apparent association of polygonal fault systems with overlying fluid escape structures, however, as many polygonal fault systems are not spatially coincident with such features, the relationship between polygonal faulting and fluid flow remains unclear (Cartwright, 2014). Tewksbury et al. (2014) present a study of an

exposed polygonally faulted chalk formation in the western desert of Egypt. Their study documents extensive polycyclic vein calcite which suggests a link between fault development and fluid expulsion, and they infer that the steep dips of faults are suggestive of failure under significant overpressure. Circular to sub-circular basin-like features in overlying strata shown by Tewksbury et al. (2014) are inferred to be fluid-escape features. It is also possible that where such evidence of fluid escape is located above zones of polygonal faulting that the fluid escape structures represent relic features that are no longer active (Section 3.2). As polygonal fault systems are associated with low-permeability argillaceous sediments, it is not known if the faults would provide upwards fluid conduits because the fault gouge would similarly be expected to be clay rich. The degree of throw on individual faults will be insufficient to pose a risk of upwards flow to shallower stratigraphic horizons. If the faulted zone is interbedded with thin and possibly impersistent sand- or siltstone beds, such pervasive faulting could feasibly lead to upward migration via fault juxtapositions or thief zones. However, this could be considered somewhat unlikely to occur over depth intervals spanning several hundreds of metres. If, however, the zone is subject to pore fluid overpressure, as suggested by Vejbaek (2008), individual faults might be critically stressed or even openly dilated to facilitate upwards migration of buoyant fluids such as CO_2. Conversely, if the storage reservoir and its cap rock are normally pressured, an overlying overpressured zone could actually impede upwards buoyant fluid migration (Miocic et al., 2013).

Faults related to halokinesis

Halokinesis, the process of salt tectonics, has occurred in large regions of the North Sea, resulting in the formation of faulting in overburden successions overlying potential CO_2 storage sites. Movement of the Permian Zechstein evaporites is responsible for many of the present day structures of interest for CO_2 storage in the southern parts of the North Sea (Figure 3.8). Numerous hydrocarbon traps in the southern and central North Sea sectors were also formed by diapirism. In the UK sector, CO_2 storage is considered in the Bunter Sandstone Formation (Furnival et al., 2014), a reservoir of Triassic age, which has been gently folded to form a series of four-way dip-closed structures. Overburden faults are commonly associated with these structures (Bentham et al., 2013; Williams et al., 2014), formed by extensional stresses over the crests of the structures as they developed during salt movement. The overburden stratigraphy consists of Triassic and Jurassic strata, predominantly mudstone with thin interbedded limestone, anhydrite and several halite members. Mesozoic strata are variably removed beneath the base Cretaceous Unconformity, above which the mudstone dominated Cromer Knoll Group sits beneath the Chalk Group. This is overlain by Cenozoic strata in the eastern parts of the UK sector, which thicken considerably into the offshore Netherlands to the east where a major deltaic system drained the Fennoscandian and Baltic shields during the Miocene–Pliocene (Overeem et al., 2001).

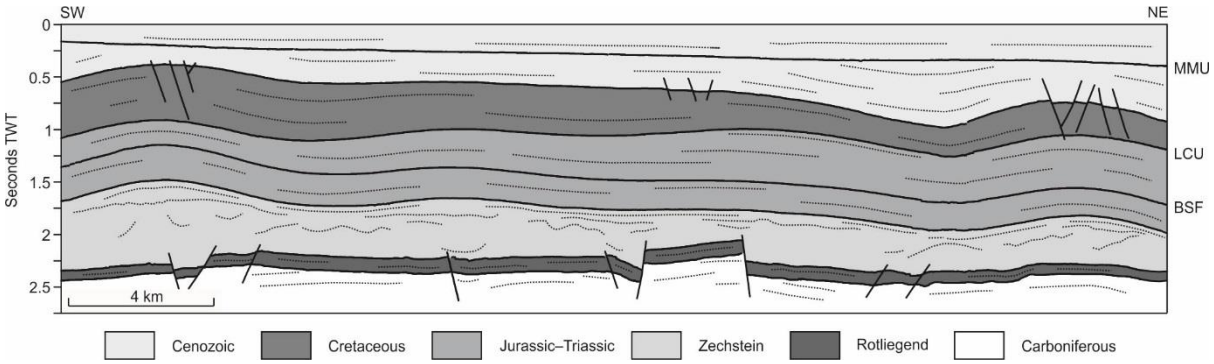

Figure 3.8 Representative line drawing across part of the UK Southern North Sea, showing different structural domains below and above the Permian (Zechstein) salt swells in two-way travel time. The Mid-Miocene Unconformity (MMU), Late Cimmerian Unconformity (LCU) and the Bunter Sandstone Formation (BSF) are marked. Reproduced from Williams et al., (2015). BGS © NERC (2016).

Faults affecting the overburden above salt domes and diapirs often exhibit a radial pattern around the structural crest, related to the stresses caused by flexure of the brittle overburden during salt movement. Due to the mud-prone nature of the overburden, the nature of fault-gouge materials is likely to be fine-grained unless there is some associated micro-porosity enhancement. However, there is some uncertainty regarding the current state of stress affecting the strata at post-salt levels. Williams et al. (2014, 2015) proposed that stresses over salt-related structures in the Southern North Sea could be related to their structural growth. Recent activity of some salt domes indicates that stresses will have been affected by halokinesis in the Netherlands sector as recently as the Late Pleistocene and Holocene (Harding and Huuse, 2015). This has implications for the potential for fault reactivation. If both the overburden faults and the prevailing in situ stress conditions are related to the growth of the structures, the faults would therefore be close to optimally oriented for failure, reducing the pore-pressure increase they are able to support before fault reactivation occurs.

The presence of shallow gas within Pliocene–Pleistocene sediments in the Netherlands North Sea is well documented, and occurs coincidently with overburden faults over several salt structures, and is imaged on seismic reflection data as high amplitude anomalies (Schroot and Schüttenhelm, 2003). It is not possible to determine the origin of the gas in the majority of the accumulations, due to lack of fluid sampling. However, it has been shown that the gas variably comprises both thermogenic gas from depth and biogenic gas generated within the deltaic deposits in situ (Schroot et al., 2005). Figure 3.9 shows an example of shallow gas indicators coincident with overburden faulting. While it is difficult to draw conclusions regarding the origin of the gas and whether the faults have allowed the migration of thermogenic gas from depth (Williams and Gent, 2015), the image indicates the effectiveness of the seismic reflection technique in identifying changes in pore-fluid content within the Cenozoic sediments of the North Sea.

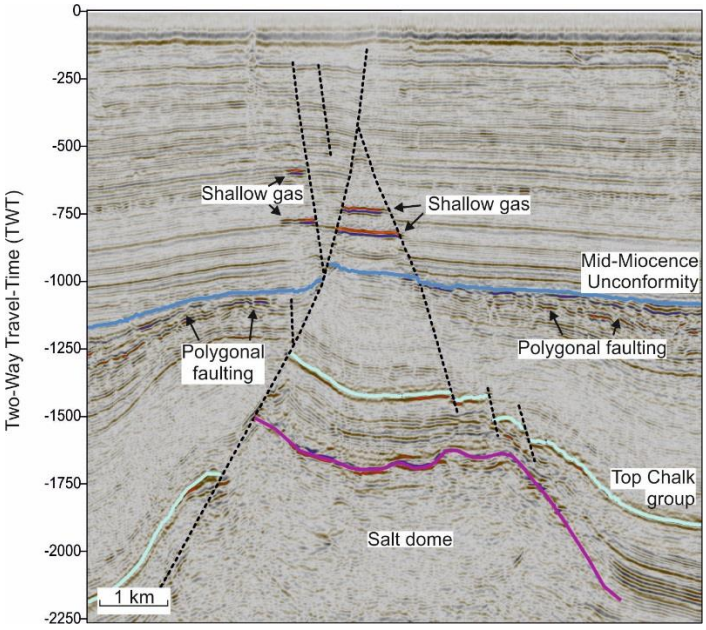

Figure 3.9 Shallow gas accumulations imaged on seismic reflection data, associated with faults over a salt dome, from the Netherlands Sector of the Southern North Sea. Depth in two-way travel time in milliseconds, Seismic data shown courtesy of www.nlog.nl. BGS © NERC (2016).

Faults in exhumed sedimentary basins

In exhumed sedimentary basins such as the East Irish Sea and the Moray Firth, Tertiary basin inversion has resulted in fault reactivation and the exposure of Mesozoic structures at, or at least very near to the seabed (Argent et al., 2002; Corcoran and Doré, 2002; Zanella and Coward, 2003). Reactivated faults are known to have caused breach of the seal rock in some hydrocarbon reservoirs (Mildren et al., 2005; Wiprut and Zoback, 2000), which supports the notion that faults can leak when they are mechanically activated. Whether previously reactivated, but currently inactive faults constitute fluid-flow conduits is unclear, however, and they are commonly assessed similarly to faults that have not undergone significant reactivation (Sections 3.1.1 and 3.1.2). Barr (2007) presents a case study where reactivation of faults during uplift has affected the sealing capacity of some faults, reducing their sealing efficacy. Formation leak-off test data from the East Irish Sea Basin show that exhumed claystone and siltstone possess high tensile strength which is characteristic of the higher mechanical compaction experienced at maximum burial depth prior to uplift (Corcoran and Doré 2002). However, if the shale rocks have been buried sufficiently deeply to have been subjected to embrittlement prior to exhumation, the anomalously high shear strength may result in the development of dilatant shear fractures under lower confining pressures during exhumation. What effect these processes have on the hydraulic properties of reactivated faults is unclear and likely to be variable, but some degree of mechanical deformation would be expected to occur during fault reactivation and exhumation of faulted strata to shallower depths. Whether this results in permeability enhancement or reduction is likely to vary locally along the length of any given fault.

3.1.2.5 Discussion of fluid flow and overburden faults

Most fault-seal analysis techniques have been developed with a focus on sand-shale sequences in order to assess the risk of trap integrity for hydrocarbons or CO_2 storage

(Yielding et al., 1997; Sperrevik et al., 2002; Bretan et al., 2011). As a result, few published studies have sought to identify the hydraulic properties of faults in largely shale-prone or clay-dominated sequences devoid of reservoir quality rocks. In the oil and gas sector, such faults are typically considered to be impermeable unless critically stressed. Clay-rich overburden successions are likely to comprise an element of ductile deformation. Even large faults observable on seismic reflection data have been shown to have developed continuous and thick shale smear between shale-rich lithologies with throws of up to 250 metres (Færseth, 2006). If the overburden rocks are composed of fine-grained minerals, it follows that the fault material will also be composed of fine-grained material with little porosity and permeability. However, it is possible that the fine-grained fault rock material can become fragmented, enhancing permeability between the fragments. If there is a network of connected fractures along the length of the fault zone, reduction of the effective stress could promote their dilation allowing buoyant fluid to migrate vertically along the fault trace. If the fault zone was mechanically weaker than the undeformed rock, and given a sufficient fluid pressure gradient, new micro-fractures could develop parallel to the fault leading to preferential along-fault flow. Experimental results show that the Mohr-Coulomb approach to assessing fault reactivity and fluid flow does not capture the full complexity observed, and suggests that some caution needs to be exercised in assessing fault reactivation potential (Cuss and Harrington, 2016). Complex pore-pressure distributions result from flow localisation in clay-rich fault gouge materials during gas injection. The full extent of a fault will not experience an increase in fluid-pressure during gas injection because of the formation of dilatant pathways that localise flow, meaning only a small proportion of the fault (approximately 15% in the experiment) experiences elevated gas pressures, which is insufficient to initiate reactivation. However, a more evenly dispersed pore pressure distribution results from fluid injection (Cuss and Harrington, 2016). It is clear that fracture transmissivity, even in idealised planar fractures in clays, is highly complex and dynamic, being a function of hydro-mechanical coupling, saturation state, mineralogical composition and time-dependent features of the clay material (Cuss et al., 2011; Cuss and Harrington, 2016).

Many overburden faults formed in poorly consolidated sediments. Lewis et al. (2002) present a study of syn-sedimentary faults in Pennsylvanian-aged strata in Kentucky, USA. Field observations identified three key deformation styles that have important implications for fluid-flow prediction for faults formed in unconsolidated sediments:

1) Shearing of sands along the fault plane form disaggregation bands parallel to the fault plane.
2) Fault plane refraction due to significant strength contrast at sand–shale interfaces, in faulted sand–shale sequences. Further fault development tends to ‘smooth’ the fault plane and produces shortcut faults and slivers of sandstone that are incorporated into the fault zone.
3) Sand injection into the fault plane and into planes of weakness in the footwall, leading to increased sand on sand juxtaposition across fault planes.

The above findings of Lewis et al. (2002) highlight that traditional fault seal analysis methods such as SGR (Yielding et al., 1997) do not account for processes that incorporate sand into fault planes during faulting in unconsolidated sediments. Similar

effects have been observed from the Britannia Field in the North Sea along with dewatering structures that can be traced across fracture arrays with no offset (Porter et al., 2000). This proves that soft sediment deformation processes do influence present-day fluid migration across faults formed in unconsolidated or semi-lithified sediments. Analysis of overburden faults should account for the possibility of such processes if the overburden comprises mixed sand–shale sequences affected by faulting during or soon after deposition. In another study of faults in poorly lithified sediments, Torabi (2014) identified cataclastic deformation bands with intense cataclasis formed in sandstone rich in phyllosilicate and clay minerals. This indicates that intense cataclasis can occur during shallow burial regardless of the rock mineralogy at the time of deformation. The deformation bands were associated with listric normal faults with displacements of up to ten metres. The observation of brittle deformation of phyllosilicate and clay-rich materials during shallow burial (and low stresses) is counterintuitive in light of the expected ductile response of such materials. While the slip surfaces were found to be conduits for fluid-flow, permeability reduction in the damage zone was reduced by up to two orders of magnitude (Torabi, 2014).

Another consideration in terms of CO_2 migration via faults in the overburden is the degree of associated pore pressure increase. Unless a catastrophic breach of the primary cap rock was to occur, small-scale emission of CO_2 into the overburden is not likely to be associated with a significant increase in formation fluid overpressure. CO_2 migration would be driven primarily by buoyancy, which would not exert a significant overpressure on any overburden faults encountered unless the CO_2 becomes trapped and a column accumulates. In the absence of permeable fault materials that might preferentially facilitate upward migration, the column height accumulated may not be sufficient to exceed the capillary threshold pressure of the fault material or to initiate fault reactivation. As a result, the CO_2 may become trapped within the overburden. Therefore, even if a connected network of faults existed, between the source of the CO_2 above the cap rock and the surface, it is not necessarily the case that leakage will result in migration to the surface. If the faults did facilitate migration, it is still possible that some, if not all, of the CO_2 would find its way to shallower ‘thief’ horizons, permeable strata overlain by fine-grained rocks that would act as secondary or tertiary reservoirs for CO_2 as it migrates within the overburden.

3.1.2.6 Natural CO_2 seeps along faults

Natural CO_2 seeps are reviewed in Section 6.2, and provide an indication of the volumes and rates of CO_2 emission. Faults and fractures provide vertical migration conduits for some of the natural seep sites (Panarea, Florina and potentially the Juist Salt Dome), along with others identified in IEAGHG (2016). Studies of leakage rates facilitated by faulting can aid understanding of flow processes along fault zones in overburden successions, between breached CO_2 reservoirs or magmatic sources and the surface. Table 3.1 contains known surface leakage rates to provide representative flux rates associated with fluid-flow via faults.

Site	Country	Detection Method	Surface leakage rate	Source	References
Paradox Basin	USA	Soils, springs	0.0365 t/m^2/year	Clay-carbonate reactions, also potential carbonate decomposition	Shipton et al., 2004, 2005; Burnside et al., 2007; Lewicki et al., 2007; Jung et al., 2014; 2015.
Crystal Spring (in Paradox Basin)	USA	Springs	13.234 t/m^2/year	Clay-carbonate reactions	Baer and Rigby 1978; Shipton et al., 2004; 2005; Gouveia et al., 2005; Jung et al., 2014; Watson et al., 2014.
Mammoth Mountain	USA	Soil, aerial gas flux	0.19 t/m^2/year	Magmatic	Lewicki et al., 2007.
Solfatera, Phlegraean Fields	Italy	-	average 0.41 t/m^2/year, max 2 t/m^2/year	Magmatic	Lewicki et al., 2007; Voltattomi et al., 2009.
Albani Hills, Tor Caldera	Italy	Gas seeps and springs	0.44 t/m^2/year, max 11.6 t/m^2/year	Magmatic and decarbonisation of fractured carbonates	Chodini and Frondini 2001; Lewicki et al., 2007; Voltattomi et al., 2009.
Latera Caldera	Italy	Soil, gas vents, springs	0.039 t/m^2/year	Meta-carbonates	Cavarretta et al., 1985; Astorri et al., 2002; Annunziatellis et al., 2004; Pearce et al., 2004; Lewicki et al., 2007; Arts et al., 2009; Pettinelli et al., 2010; Bigi et al., 2013.
Mátraderecske	Hungary	Gas seeps and springs	0.073–0.146 t/m^2/year (to 0.62 t/m^2/year)	Geothermal/karst	Pearce et al., 2004; Lewicki et al., 2007.
Poggio dell'Ulivo and Torre Alfina	Italy	Springs	$1.76x10^{-5}$ – $3.96x10^{-4}$ t/m^2/year	Geothermal/Mesozoic carbonates	Chiodini et al., 2009; NASCENT 2005; Streit and Watson 2005.
Otway	Australia	Soil	<1 kg/m2/year, but likely rates up to 1000 t/year after	Magmatic, in sandstones and fractured Belfast Mudstone	Watson et al., 2004; Streit and Watson 2005; 2007.

Site	Country	Detection Method	Surface leakage rate	Source	References
			earthquakes. $3.7–7.5x10^{-3}$ to $1.5x10^{-2}$ t/m^2/year rates from diffusion		
Panarea	Greece	Seabed vents	≤$4.14x10^4$ m^3/year per vent. 1670–8500 t/ year, >>1600 t/year CO_2	Volcanic/hydrothermal	Italiano et al., 2001; IEAGHG 2005; Voltattorni et al., 2009; Caramanna et al., 2011; Kirk 2011.
Juist Salt Dome	Germany	Point source above dome	-	Likely to be biogenic	McGinnis et al., 2011.
Southern North Sea	Netherlands	Shallow seismic amplitude anomalies and pockmarks	-	Biogenic and thermogenic	Schroot and Schüttenhelm 2003; Schroot et al., 2005; IEAGHG 2005.
Florina	Greece	Gas vents and carbonated springs	7.3–3650 t/year	Magmatic/hydrothermal	Ziogou et al., 2013; Koukouzas et al., 2015

Table 3.1 Flux rates, surface (or near-surface) expressions and source of naturally occurring CO2 leakages along faults. Table re-produced from IEAGHG (2015 – Fault Permeability report) with some additional data. See given references, IEAGHG (2015) and Section 6.

In the Paradox Basin, low permeability fault rocks do not fully occlude leakage because pressure builds-up sufficiently within shallow strata, which act as reservoirs to upward migrating CO_2. As a result, leakage to surface occurs due to the continuous CO_2 accumulation, promoting the opening of fractures and/or exceeding the capillary threshold pressure of the low permeability fault rocks (Jung et al., 2015). The flux rates at some leakage sites such as Crystal Geyser are very high, as a result of rapid and continuous charging of the shallow gas reservoirs.

Salt Dome Juist provides a potential analogue for leakage along faults over a salt dome; however, it is unclear whether the faults actually provide the conduit by which CO_2 migrates towards the surface (McGinnis et al., 2011). The shallow gas observed on seismic survey data, and sea bed seeps offshore Netherlands (Schroot et al., 2005) is also difficult to attribute to faults over salt domes, despite their coincidental locations. Shallow gas could equally be migrating upwards through the relatively unconsolidated Palaeogene deltaic sediments, becoming trapped in thin folded reservoirs over the salt domes.

Leakages along faults derived from magmatic and hydrothermal sources are useful in that they give a range for the flux rates that can be transmitted along faults. However, it is not clear whether they provide good analogues for migration of CO_2 through overburden above CO_2 storage sites. The high rates at which CO_2 is expelled from such sources, high temperatures and fluid chemistry are likely to differ significantly compared with sites cited for geological storage: average gas flux rates are highest along faults at Mátraderecske (increased from an average of 5–10 L/hour/m^2, up to 400 L/hour/m^2 along faults, Pearce et al., 2004), while annual discharge can be very high in some cases (Table 3.1). It isn't clear what kind of flux rates would occur if a primary cap rock was breached, but discharge rates from the reservoir might be determined by considering if the breach occurs during the injection period when reservoir pressure would be at its greatest, the height of the accumulated column and resulting buoyancy forces and the flow-properties of the fault zone.

The natural seep studies do provide some useful indications of how CO_2 might migrate through overburden faults. Diffuse leakage occurs to the surface along a fault at Mammoth Mountain, while shallow groundwater is saturated with CO_2 in the Albani hills, Italy. Some of the surface leakage has been associated with faults and low-level seismicity, indicating either that seismic activity is responsible for facilitating along-fault migration due to external stresses on the faults, or that excess fluid-pressures cause reactivation of the faults and subsequent along-fault fluid flow, giving rise to the detected seismic events. A major CO_2 gas eruption occurred at the Panarea site in 2002 and this, along with variable discharge rates, suggests that the rates of along fault migration are likely to vary considerably over timescales of years to decades. Episodic leakage also indicates temporally variable flux rates at Florina, a naturally occurring CO_2 field, where lack of an effective cap rock allows CO_2 to migrate upwards before it subsequently leaks along faults and fractures until reaching the water table and, in places, the surface (Koukouzas et al., 2015). In some respects, the Florina case appears to be a good analogue for overburden migration, however, high heat-flow and the active magmatic- hydrothermal source are likely to promote the upward migration of CO_2. What is clear from the studies is that the conditions under which fluid

will migrate via faults is site specific, in terms of the properties of the faults, the seal bypass mechanism and dynamic nature of the subsurface fluids.

For comparison with the measured rates of natural leakage (Table 3.1), modelling studies of CO_2 leakage along faults suggest variable fluxes, accounting for significant uncertainty in fault parameters and different injection rates between 0–79 kt/year (Ayogi, 2011), up to 3784 m^3/year (Huang et al., 2014), 0.2–0.6 kt/year and 12–1200 t/year/m^2 (Ramachandran et al., 2014), and 200–320 t/year (Vialle et al., 2016)). Section 3.6.2.3 describes flux rates from modelling studies which suggest leakage rates of the order of several thousand tonnes per year, comparable to some of the natural leakage rates, but these tend to consider very high (1000 mD) fault zone permeability values (Aoyagi, 2001; Ramachandran et al., 2014).

*3.2 **Fluid flow pathways***

Fluid flow processes can develop a wide range of geological structures such as pockmarks, chimneys or pipes, mud volcanoes, sand mounds, gas hydrates, sediment injections and carbonate mounds. The type of structure generated depends on a variety of parameters such as the source of fluid, the flow type, the structural setting and the nature of the sediment through which the fluid flows (Figure 3.10).

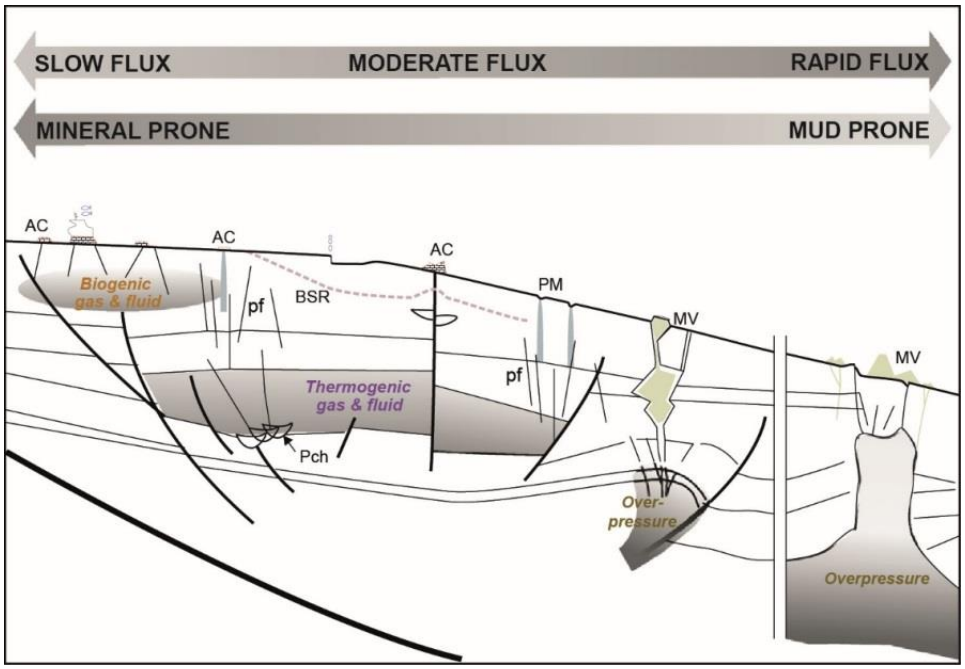

Figure 3.10 Schematic synthesis of the origins and trigger mechanisms of cold seep systems and the relationships between flow rates and different seeping/venting morphologies observed on the seabed. Modified from Talukder (2012). AC, authigenic carbonate; BSR, bottom simulating reflector; MV, mud volcanoes; Pch, palaeo-channel; pf, polygonal faults; PM, pockmarks.

The diagram produced by Reeburgh (2007), schematically displays the range of methane flux to the ocean water column from several sources (Figure 3.11), plus an indication of the depth of the origin of the methane. On this diagram, emission magnitude and variability, increases from left to right, with diffusion and small seeps being relatively constant and with larger seeps and mud volcanoes showing a more episodic behaviour.

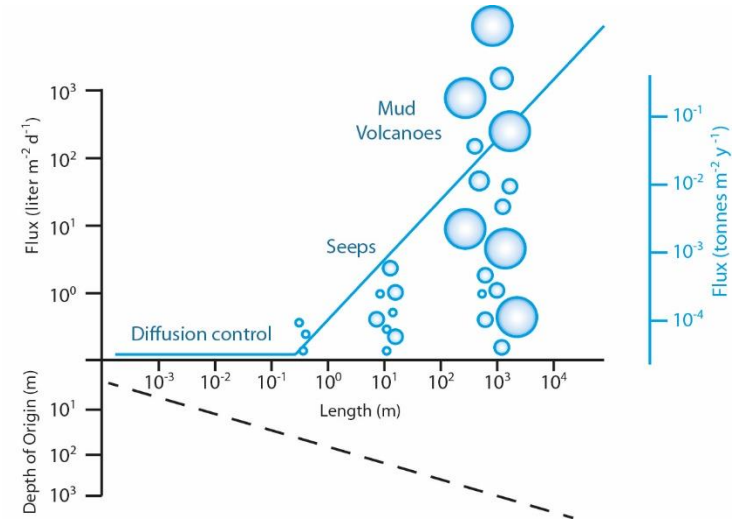

Figure 3.11 Schematic diagram showing the length, origin depth, and flux scales of methane in litres per square meter per day (upper left vertical axis), from a range of sources to the ocean water column. Image modified from Reeburgh (2007) to include an approximate equivalent indication of flux in tonnes per square metre per year (right vertical axis) to permit comparison with measured CO_2 flux in this report.

3.2.1 Chimneys

Chimneys are vertical structures linked to hydrofracturing and fluid migration, often attributed to overpressure in the subsurface (Osborne and Swarbrick, 1997). Common in sedimentary basins, they are being studied increasingly worldwide with particular interest in the North Sea, Western Europe. The cause of increased interest in chimneys by the CCS community is the expectation that they may act as seal bypass features, providing fluid flow pathways to shallower depths.

Chimneys are identified as one of three key seal-bypass mechanisms, along with faults and injected bodies of sedimentary and igneous material (Cartwright et al., 2007). These features are often called pipes or vertical fluid conduits and have long been of interest to the hydrocarbon industry as they represent potential conduits for hydrocarbon migration. In addition, the presence of gas pockets in the near surface above chimneys present a significant risk to drilling operations.

Chimney structures have been primarily recognised in seismic survey data. High amplitude gas accumulations, vertical pathways in the seismic sections or clearly visible sediment mobilisation are the key attributes used to pinpoint chimneys (Figure 1.1). Additionally, pockmarks on the sea floor are attributed as visible expressions of the tops of chimney structures. Chimneys are typically tens to hundreds of metres in diameter and can be in excess of one kilometre in height, providing a pathway through thick, low-permeability overburden successions. Exhumed structures, thought to represent chimneys, have been sampled (Løseth et al., 2011), but examples of chimney features sampled in situ are lacking in the scientific literature (with the notable exception provided by Kim et al. 2011). Consequently, current understanding of hydraulic properties and potential fluid flow rates in chimneys is poor. The inability to parameterise reservoir models with suitable transmissibility values for gas chimneys makes it difficult to quantify the leakage risk associated with these features. The lack

of suitable data has been identified as a key research target and several studies are now planning to investigate chimney structures:

- In April/May 2017 the EU Horizon 2020-funded STEMM-CCS project will attempt to parameterise a chimney using controlled-source electromagnetic techniques and seismic reflection studies. Alongside this work a programme of geological drilling and logging will be undertaken to ground-truth the geophysics whilst geochemical experiments will back up the drilling program. This project should contribute significant new data on the in situ properties of large deep-rooted chimneys.

- The UK NERC-funded CHIMNEY project (Characterisation of Major Overburden Leakage Pathways above Sub-sea floor CO_2 Storage Reservoirs in the North Sea) is investigating potential for leakage through vertical fluid pathways. A geophysical experiment, planned for Autumn 2017, will attempt to characterise the internal structure of a chimney using a broadband seismic anisotropy experiment. This study aims to provide information on fracture orientation and geometry and hopes to ascertain if the fracture system remains open or closed. The key deliverable of the project is a clear estimate of the permeability of a North Sea chimney. Alongside the geophysical experiment the group hope to undertake a geochemical characterisation of the chimney. Sampling beneath the sea bed should allow the timing of fluid flow, and the length of time the feature was active, to be determined.

- A key experiment charting the development of a vertical fluid flow system for CO_2 was the QICS experiment (Blackford et al., 2014). Here, high-resolution seismic data were used to image CO_2 accumulating in shallow marine sediments directly above an injection point (Cevatoglu et al., 2015), both as thin layers and within a ‘gas-chimney’ (Figure 3.12). Significant acoustic blanking also occurred, with a vertical unreflective zone beneath the injection point. The experiment demonstrated both short-term buoyancy-driven flow in the sedimentary column and also longer term stabilisation as dissolution processes take over with differing rates of dissolution in the dispersed CO_2 of the chimney compared with more highly saturated CO_2 in the layers.

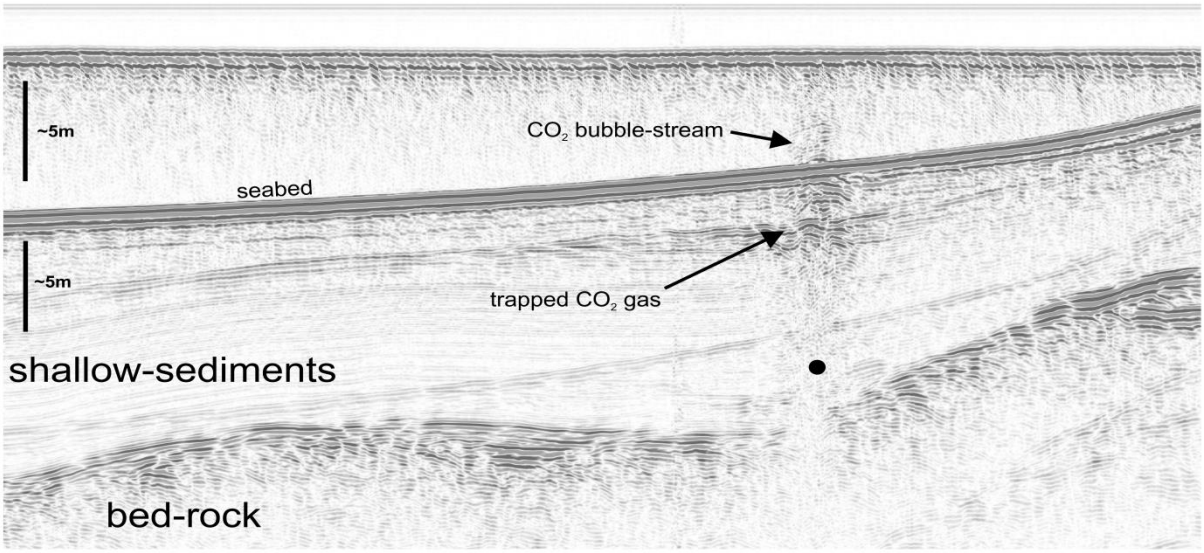

Figure 3.12 High-resolution seismic image of the QICS experiment in 2012 during injection (BGS data).

Gas chimneys or pipes are manifested on seismic data as vertical to sub-vertical columnar zones where the seismic reflections are disrupted (reflection may be offset, deformed, attenuated, or have their amplitudes enhanced). They are the result of highly focused fluid flow via vertical conduits that can range in height from tens of metres to several kilometres. Gas chimneys/pipes can be differentiated from seismic artefacts (such as velocity push down and migration anomalies) by the presence of vertical variations in the type and degree of disruptions and by considering their geologic context. They occur commonly throughout the shallower overburdens of the North Sea Basin (Karstens and Berndt, 2015). They are enigmatic features whose genesis and in situ properties are poorly understood. Seismic reflection data provide the main evidence for their existence and they are characteristically imaged as narrow vertical or sub-vertical zones of disrupted stratal reflections, with strong spatial variation in reflectivity (Figure 1.1). In some examples, the seismically imaged features are linked to overlying pockmark features at the seabed (Section 3.2.2), indicating significant fluid flux and high transient permeability. The integration of seismic and water column data from the North Sea indicates the presence of gas flares in the water column. Twenty-five acoustic gas flares, up to 125 metres in height in the Viking Graben and 19 flares on the Utsira High up to 70 metres in height are partly connected to deeper sediments through faults and chimney structures extending up to the sea bed from Oligocene strata in the overburden (Chand et al., 2016).

3.2.1.1 Chimney formation and observation

It is widely believed that these chimneys represent fluid leak-off points from overpressured sedimentary sequences. They may also have formed in response to rapid depressurisation leading to in situ expansion of naturally occurring gas accumulations. Depressurisation might occur in response to removal of an overlying load - either by rapid tectonic uplift and erosion or (pertinent to the North Sea) melting of a thick overlying ice-sheet (Vadakkepuliyambatta et al. 2013). The in situ properties of these features are poorly-understood, so, for example, the amount of natural gas currently residing within them might have a strong effect on capillary flow processes

that would control leakage of CO_2, and hence their effective (and relative) permeability. Another uncertainty is in their true geometry. A wide range of apparent seismic morphologies have been observed on seismic data (Karstens and Berndt 2015), but it is clear that strong seismic imaging artefacts are present. A consequence of this is that both the radial and vertical extents of many pipes might be significantly overstated, since high amplitude bright spots in the near subsurface are capable of producing shadowing, pushdown features, attenuation and null zones that give the appearance of vertical pathways. Utilising long offset pathways and taking care during processing should allow interpreters to distinguish artefacts from true chimney structures. Numerous studies have verified the disrupted and discontinuous sediments associated with chimney structures (Heggland, 1997, 1998; Gay and Berndt, 2007; Loseth et al., 2009, 2011, Gay et al, 2012) on seismic data. These fluid flow features are a key component of hydrocarbon plumbing systems (Heggland, 1998; Gemmer, 2002). In many cases the continuing leakage of hydrocarbons has been observed and reported (e.g. Hovland and Sommerville, 1985).

Chimneys and pipes have been documented across the globe e.g. Gulf of Mexico (Heggland, 2000), offshore Namibia (Moss and Cartwright, 2010), offshore South Africa (Kuhlmann et al., 2011) and repeatedly in the North Sea, Western Europe (Løseth et al., 2009, 2011; Hustoft et al., 2010; Tasianas et al, 2016;), where dramatic blow-out events that generate large scale fluid conduits through the overlying sequence are reported (Buez et al., 2003). The variability in imaging these features can be attributed to sediment type, fluid source, and flow regime (Van Rensbergen, 2003).

Whilst investigating sedimentary basins in the Danish North Sea and offshore Angola to improve basin analysis tools, Andresen (2012) highlighted sedimentary loading in the basin, coincidence of maturation and migration of major regional source rocks and expelled pore water as drivers for creation of vertical fluid pathways.

Baristeas et al. (2012) mapped the distribution of seal bypass features in the Malvinas Basin, offshore Argentina and documented numerous chimney and pockmark structures linked to the presence of maturing hydrocarbons. The distribution of features was associated with an underlying polygonal fault system. Additionally, the location of vertical fluid conduits has been shown to coincide with deeper mud volcanism, sediment injection or carbonate mounds (Cartwright, 2007; Huuse, 2010)

Gay et al. (2012) used 3D seismic data from the Gjaller Ridge, offshore Norway in the Voring Basin where numerous pockmarks on the sea floor are attributed to fluid migration in the sub-surface (Bunz et al. 2003; Nouzé et al., 2004). Here, long-standing hydrothermal vent systems transport fluid from depth to the seabed. Since the structures reach the modern seafloor, the authors argue that the plumbing mechanism has remained active over geological timespans, or reactivation of existing pathways has occurred. By combining their regional analysis with sand-box experiments Gay et al. (2012) demonstrated that highly deformed sediments remoulded into v-shaped structures, increasing in diameter as they move up the sequence and often providing relief at the sea bed.

The region of the Southern Viking Graben, Norwegian North Sea, that contains the Sleipner Field is extensively studied (e.g. Karsten and Berndt, 2015; Nicol, 2011; Furre et al., 2015; Heggland, 1997). Shallow gas accumulations and chimneys are well imaged on seismic data and numerous authors have mapped the locations of vertical fluid conduits (Nicol, 2011; Lothe and Zweigel, 1999; Jackson and Stoddart, 2005; Judd and Hovland, 2007). Karsten and Berndt (2015) catalogued the vertical fluid pathways in Southern Viking Graben using regional seismic data and found features aligned along distinct trends, suggesting a deep-lying control on chimney formation. Karsten and Berndt (2015) discuss the different types of chimney structure based on their seismic appearance. These features relate the continuity of reflections in the chimney, the degree of chaotic reflectivity observed and the terminations of coherent reflections at the edges. The type A, type B and type C categorisation of the structures they adopt (Figure 3.13) is a simple methodology for characterising the broad features seen in chimney structures. Type-A is believed to represent the seismic image of large-scale pipe-structures, which have formed due to comparably rapid fluid expulsion. They contain reversed phase high amplitude reflections with bright spots at variable depths. The seismic image of type-B anomalies suggests the presence of slowly developed, gas-filled fracture networks. They are chaotic in nature with diffuse boundaries and have irregular structures that do not always form columnar pipes. Type-C anomalies have complex internal structures and tend to form linear structures, when mapped in plan-view, which correlate with overlying tunnel valleys. Type-C anomalies have the potential to be artefacts in the seismic image generated by overlying events in the succession (Karstens and Berndt, 2015).

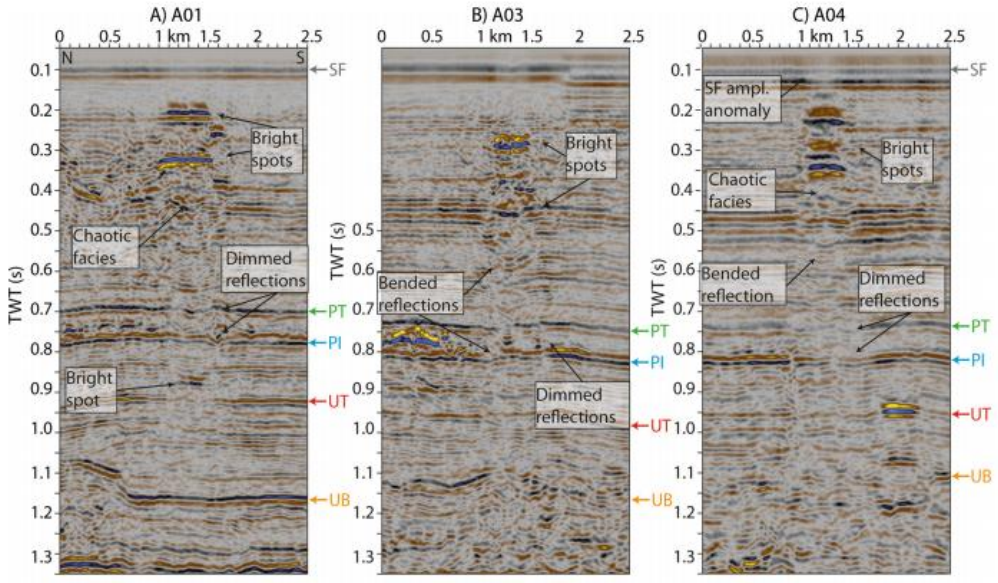

Figure 3.13 Seismic profiles showing A-, B- and C-type vertical anomalies (left to right), from Karsten and Berndt (2015).

3.2.1.2 Modelling CO_2 migration in chimneys

A key on-going research goal is the development of flow modelling schemes to accurately model the migration of CO_2 through chimney structures into the shallow overburden. This represents a key opportunity for the scientific community. Tasianas et al. (2016) undertook a modelling study using the mapped pre-existing fluid pathways

in the Snøhvit area. The modelling assigned each of the seven overburden units a range of porosity and permeability values, taken from analysis of literature and well logs (Buenz et al., 2012). For the chimney hydraulic properties, Tasinas et al. (2016) used results directly from the drilled chimney in the Ulleung Basin in the East Sea (Kim et al., 2011) which resulted in a reported porosity range between 63.7% and 83.3%, horizontal permeability values between 0.46 and 4.84 D and vertical permeability values of 0.34 to 3.35 D.

The authors concluded that the presence of high permeability chimneys meant that the overpressures required to drive CO_2 leakage were much smaller than those required to disrupt competent sealing overburden. However once a chimney was in place, the permeability of the reservoir had the greatest influence on migration rate. The chimney permeability had little effect on the rate of leakage at reservoir level, but controlled the volume of CO_2 reaching the upper region of the fluid flow conduit. Higher permeabilities lead to faster movement through overburden. The spatial extent of the chimney also played a part in the migration rate, as the area of the capturing region had significant influence. The primary conclusion from the study highlighted the need for detailed knowledge of the hydraulic properties of chimneys in order to improve modelling studies.

3.2.2 Surface structures associated with fluid flow

Sea bed structures, such as pockmarks, mud volcanoes, sand mounds and methane-derived authigenic carbonate precipitation, have been recognised as evidence of migration and sea bed leakage of fluid from deeper sources and reservoirs. Most of the sea bed is not characterised by features associated with fluid flow. However, the numerous descriptions of such features worldwide reflect their scientific interest and importance, rather than their frequency. Fluid flow structures are of great interest for a number of reasons including: 1) their relevance to the oil and gas industry, as they can provide information on present or past migration routes for hydrocarbons; 2) their effect on local biodiversity; 3) as a conduit for methane and its emission, as a greenhouse gas, to the environment.

Particular attention is given here to pockmarks (Section 3.2.2.1) because they are considered the most frequent expression of focused fluid seepage at the sea bed of hydrocarbon gases, such as methane. Mud volcanoes (Section 3.2.2.2), sand mounds (Section 3.2.2.3) and methane-derived authigenic carbonate precipitation (Section 3.2.2.4), as less frequent evidence of fluid migration to the sea bed, are considered in lesser detail. Rates of marine methane gas flux are reviewed in Section 3.2.3.

3.2.2.1 Pockmarks

Pockmarks are concave crater-like depressions formed at the sea bed. They were first reported by King and Maclean (1970) offshore Nova Scotia (Canada), who suggested that gas and/or water from the underlying bedrock was released in sufficient quantities to put fine-grained material into suspension and that this material could then drift away from the venting point. Since then, pockmarks have been found worldwide, from water depths of less than 10 metres in estuaries (e.g. Martínez-Carreño and García-Gil,

2013) to over 3,000 meters in offshore canyons (e.g. Olu-Le Roy et al., 2007). However, they occur only where the sediments are suitable for pockmark formation. For example, in the UK sector of the North Sea the majority of pockmarks have been found in the Witch Ground Basin and those areas of the sea bed in which pockmarks are known to occur and compiled by Brooks et al. (2011) represent less than 5% of the entire UK sector of the North Sea.

Various gasses occur within marine sediments, usually dissolved within the pore fluids but occasionally as free gas, dependent upon pressure, temperature, gas concentration, and degree of gas saturation. These gasses can include carbon dioxide and hydrogen sulphide but methane is the most common and is mainly the gas escaping at the sea bed and associated with pockmarks (Hovland and Judd, 1988; Hovland and Sommerville, 1985). The average methane content in natural gas bubbles collected from active seeps worldwide ranges between 72% and 99% (Tizzard, 2008). Even though many documented pockmark fields occur in hydrocarbon-bearing basins, such as the North Sea and Gulf of Mexico, the gas escaping from pockmarks has been demonstrated to be from a biogenic origin as revealed by isotopic analysis (Hovland and Judd, 1988; Hovland and Sommerville, 1985). Additionally, there are numerous cases where pockmarks were identified in non-hydrocarbon provinces (e.g. Martínez-Carreño and García-Gil, 2013).

The nearly exponential increase in pockmark discoveries is mostly due to the improvements and increased use of high-resolution echosounder, sidescan sonar and 3-D seismic surveys during the exploration for hydrocarbons. During seabed site investigation studies particular attention is given to the presence and distribution of pockmarks at the sea bed since the existence of these features needs to be considered in the development of any sea bed infrastructure. Therefore, it is not surprising that there is a biased distribution, the known areas with pockmarks are mainly within more economically developed areas of the world (northern hemisphere, northern margin of the Mediterranean) since the detection of these features are dependent upon the availability of high-resolution geophysical equipment. This apparent distribution is evident in compilations of the worldwide distribution of pockmarks based on scientific literature, as presented by Ingrassia et al. (2015) tabulated in

Appendix 2. For instance, of over 43 sites mentioned in the compilation (Ingrassia et al. (2015) only two are reported from the southern hemisphere (Figure 3.14). With the increased exploration of hydrocarbons in challenging environments and the

collaboration between industry and academia, it is anticipated that the distribution of reported pockmarks will become more widespread.

Figure 3.14 Worldwide and Mediterranean distribution of shallow water (<200 m) fluid-escape sea bed depressions reported in the literature. Figure modified from Ingrassia et al. (2015)

Pockmark fields, which may contain several hundreds of pockmarks per square kilometre, mostly occur in areas of recent, fine-grained, unconsolidated sediment (silt and clay) (Hovland and Judd, 1988). One of the best known areas with extensive pockmark coverage and the highest density of pockmarks per square kilometre is the Barents Sea. These features are believed to have been formed by the expulsion of gas due to dissociation of gas hydrates during the last deglaciation (Rise et al., 2015). However, when present, pockmarks tend to occur in smaller numbers and confined to more restricted areas. For example, in the Chatham Rise of New Zealand an area of more than 20 000 square kilometres was investigated by multibeam surveys. Here several gas escape features were found, but pockmarks only occur between 500 and 700 metres water depth and about 1% of the sea bed (Davy et al., 2010).

The range of pockmark size, covering more than four orders of magnitude, from diameters of less than one metre to hundreds of metres, is well illustrated by the compilation of pockmarks described in the literature by Pilcher and Argent (2007). Most pockmarks described are between 10 and 250 metres in diameter and are 1 to 25 metres deep (Figure 3.15). However, this does not imply that these are the typical dimensions of pockmarks, since pockmarks with smaller dimensions may not be reported in the literature due to insufficient resolution of the survey equipment used to display smaller features.

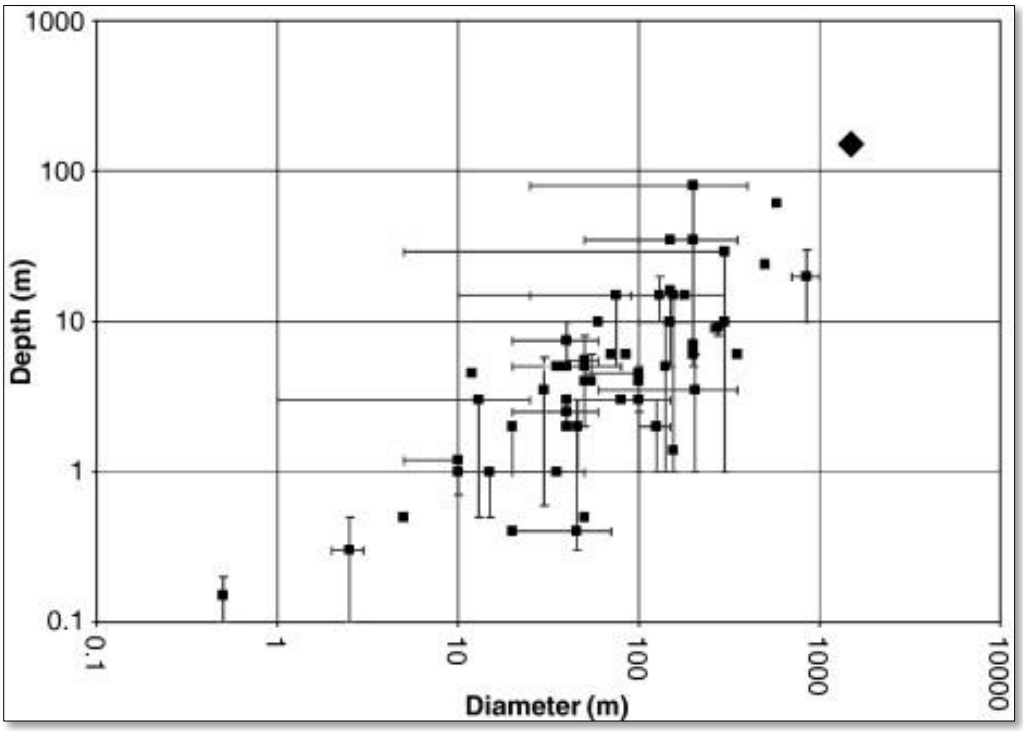

Figure 3.15 The size of the seabed pockmarks, from around the world, compiled from the literature by Pilcher and Argent (2007). Single points represent either measurement of single pockmarks or average measurements where no range is given. Error bars represent the range of sizes in a pockmark field or region, with the associated point representing either the average or maximum values as quoted in the source.

Almost 4150 pockmarks were semi-automatically mapped by Gafeira et al. (2012) across an area of the central North Sea, where the sea bed comprises a thick sequence of mud and sandy mud of the glacial Witch Ground Formation (Figure 3.16). These are inactive pockmarks, typically 20 to100 metres in diameter and three to four

metres deep and the density of pockmarks can reach almost 30 pockmarks per square kilometre. The mapping and morphometric characterisation of such a vast number of pockmarks allowed the identification of morphological trends reflecting the hydrodynamic regime, whereas the pockmarks density and spatial distribution in this area appeared to be related to differences in shallow gas availability and deeper geologically controlled fluid migration pathways (Gafeira et al., 2012).

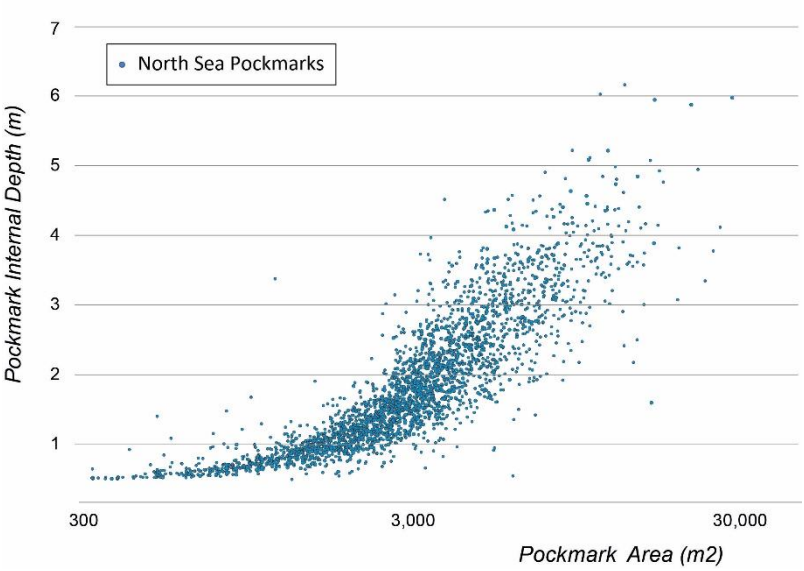

Figure 3.16 Plot of pockmark internal depth vs. area of the depression for pockmarks in seven site survey areas in the North Sea (blue dots) studied by Gafeira et al. (2012).

In addition to the smaller, probably inactive pockmarks present in the central North Sea, several unusually large pockmarks (e.g. the Scanner and Scotia Pockmark Complexes, Challenger and Alkor Pockmark) are still sporadically active (e.g. Dando, 1990; Dando et al., 1991; Judd and Hovland, 2007; Pfannkuche, 2005). A compilation of evidence of active seepage in four of these largest pockmarks is presented in Gafeira and Long (2015), that include the visual observation of bubble streams during ROV-based surveys. Based on visual observations within the Scanner Pockmark Complex, a maximum volume of gas released by bubble streams was estimated to be 1 m^3 per day from the entire pockmark (Hovland and Sommerville, 1985).

Pockmarks are found to occur in both random and non-random distributions, as stated by Pilcher and Argent (2007). These authors use the term ‘random’ to describe areas where the pockmarks are either isolated occurrences or with no recognisable spatial relationship to each other or to a resolvable surface or sub-surface feature. This type of distribution occurs preferentially within flat-lying or gently dipping, homogenous, mud-prone sediments in structurally simple geological substrates. Non-random pockmarks occur in a range of settings and in different spatial distributions, such as clusters or chains of pockmarks.

The distribution of non-random pockmarks has been associated with different underlying structures, such as: faults and buried channels, e.g. in the Lower Congo Basin (Gay et al., 2003); mud diapirs, e.g. in the eastern Mediterranean (Dimitrov and Woodside, 2003); mass movement deposits, e.g. in Gabon (Sultan et al., 2004);

iceberg scours, e.g. Canadian Margin (Fader, 1991); polygonal faulting, e.g. Norwegian Margin, (Berndt et al., 2003).

Pockmarks associated with faults can be referred to as fault-strike pockmarks or fault hanging-wall pockmarks. The fault-strike pockmark designation is assigned where the fault plane acts as a fluid conduit to the surface and pockmarks form along its strike, e.g. Gulf of Corinth (Soter, 1999). Whereas the fault hanging-wall pockmark designation is used where the pockmark development is offset from the fault trace on the hanging-wall side, e.g. Ebro Delta, (Maestro et al., 2002). The fault creates a change in structural elevation of a fluid-charged layer in the sub-surface, locally tilting the layer and bringing the footwall side closer to the sea bed.

The Athena development area in the central North Sea operated by Ithaca Energy (UK) Ltd provides a good example of how the presence of a buried tunnel valley effects the local gas distribution and pockmark development in the area. This area is situated on the western edge of the Witch Ground Basin, where almost 6% of the seabed has been shaped by pockmarks. Here the pockmark distribution is not uniform across the area and their density decreases eastwards until they are absent in the extreme east of the survey area where the late glacial/post-glacial Witch Ground Formation deposits are also virtually absent (Figure 3.17).

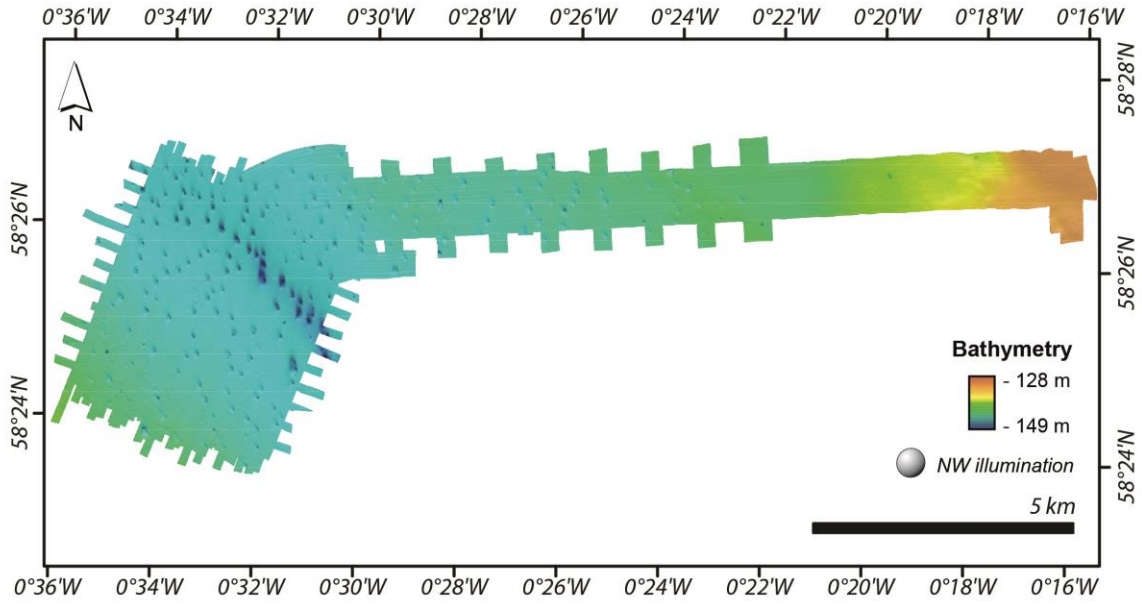

Figure 3.17 Multi-beam bathymetry from the Athena development area, showing eastward decrease in the number of pockmarks and increase of pockmark dimensions along the gentle, elongated sea bed depression oriented north-west—south-east within the study area.

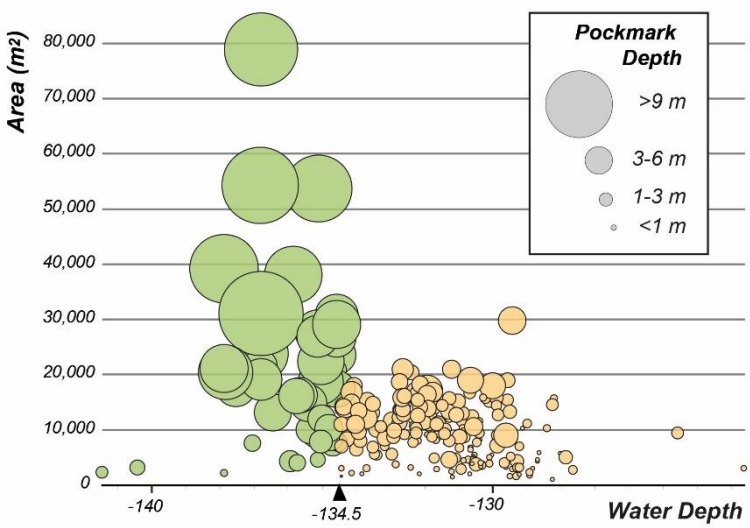

Figure 3.18 Plot showing the area, pockmark internal depth and minimum water depth of 225 pockmarks mapped from the multi-beam within the Athena development area. Pockmarks are represented in green if at water depths below 134.5 m and in orange if at shallower water

The deepest pockmarks (*Figure 3.18*) were found within or in close proximity to a gentle, elongate, sea bed depression oriented north-west to south-east within the study area where water depth reaches more than 134.5 metres, this depression is due to the presence of a buried tunnel valley. The internal depth of these pockmarks can reach almost 12 metres, well above the depth average of three metres for the surrounding pockmarks and the ten deepest pockmarks are aligned along the centre of the depression. The pockmarks with areas greater than 50,000 square metres are more than five times the average size of the pockmarks outside the depression. The dimensions of the sea bed pockmarks are directly affected by the underlying buried tunnel valley, either by the increased thickness of the Witch Ground Formation or by greater amounts of free gas available within the tunnel valley infill (Figure 3.19).

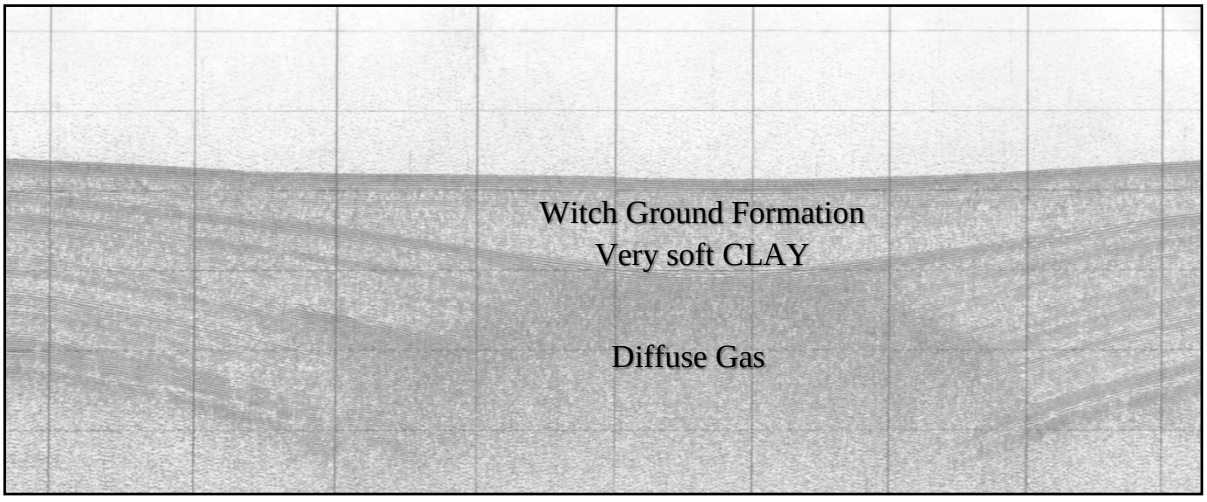

Figure 3.19 Pinger seismic profile across the buried channel present in the Athena development site area. Image from a Gardline Report (Mosawy et al., 2006) with permission of Ithaca Energy (UK) Ltd.

Though pockmarks are usually assumed to be long-lasting sea bed features, sustained by a combination of fluid flow processes and minimal sediment

accumulation, pockmarks can persevere in more active depositional settings, for example, in a dynamic estuarine setting that exhibits minimal modern fluid venting (Brothers et al., 2011). For such settings, it has been suggested that other mechanisms may also play a role in maintaining these sea bed depressions (Brothers et al., 2011). Iglesias et al. (2010) describe pockmark-like sea bed features located on the Landes Plateau, Bay of Biscay, which are relict 'pockforms' rather than present day pockmarks. The authors, suggest that the shape of these Late Miocene features has been preserved because sedimentation in the area mainly comprised mud deposited from low-energy transportation (diluted gravity flows) and settling from hemipelagic suspension.

Therefore, the observation of pockmark-like depressions at the sea bed should not be immediately interpreted as evidence of modern fluid flow. However, active fluid seepage associated with pockmarks can be detected directly from: acoustic evidence, e.g. mid-water reflections in the water column above the pockmark; geochemical evidence, e.g. elevated concentrations of methane in pore water samples; visual evidence, e.g. gas bubbles emerging from the bottom of the pockmark. However, fluid escape can be an intermittent process, and the observations of actual seepage could be fortuitous (Judd, 2001). Consequently, the observation of other indirect evidence or indicators, such as the presence of bacterial mats on the sea bed, can play a fundamental role in the identification of gas seeps, assuming the bacterial mats are correctly identified as thiotrophic. The presence of Methane-Derived Authigenic Carbonate (MDAC) or stacked subsurface pockmarks, at several stratigraphic levels, indicate a long-term fluid flow system even if there is no evidence of present day activity.

Seepage sites at the sea bed are often important sites of biological activity as these habitats may host a highly specialized fauna exploiting the released fluid, hence these habitats are listed under Annex 1 of the European Habitats Directive. For example, two species found on the Scanner Pockmark Complex had not previously been reported in the northern North Sea (Dando et al., 1991). Additionally, exposed MDAC may provide a habitat for a diverse benthic fauna that requires the presence of hard substrate and fish, such as hagfish, haddock, wolf-fish and small redfish, appear to use the pockmark depressions and the carbonate structures for shelter (Dando et al., 1991).

Almost fifty years have passed since pockmarks were first reported by King and MacLean (1970), and there is still a great deal that is unknown about their origin, longer-term activity, persistence and the role of other mechanisms, besides to fluid flow, in the formation, alteration and preservations of these seabed features. However, most studies of pockmark fields demonstrate the importance of understanding the underlying geology when interpreting seepage features.

3.2.2.2 Mud volcanoes

Mud volcanoes are the largest surface expression of the migration of fluid flow and are large, rimmed sea bed features that have kilometre-scale diameters and are fed by deep gas accumulations and hydrates (Milkov, 2000). Mud intrusion and extrusion occurs when buoyant fluid-rich, fine-grained sediments ascend through a lithological

succession (Kopf, 2002). They occur worldwide on continental shelves, slopes and in the abyssal parts of inland seas (Table 3.2) and it is estimated that the total number of current submarine mud volcanoes could be between 1 000 and 100 000, mostly occurring in deep waters (Milkov, 2000).

Region	***References***
Black Sea, deep-water part	*Limonov et al., 1994*
Black Sea, Sorokin Trough	*Woodside et al., 1997.*
Caspian Sea	*Ginsburg and Soloviev, 1994*
Gulf of Cadiz	*Kenyon et al., 2000*
Gulf of Mexico, lower continental slope	*Prior et al., 1989*
Gulf of Mexico, upper continental slope	*Kohl and Roberts, 1994*
Norwegian Sea	*Bogdanov et al., 1999*
Offshore Barbados Island	*Lance et al., 1998*
Offshore Crete	*Ivanov et al., 1996*
Offshore Cyprus (Anaximander Mountains region)	*Woodside et al., 1997*
Offshore Greece (Prometheus area)	*Cita et al.,1981*
Offshore Nigeria	*Heggland, R., Nygaard, E., 1998*

Table 3.2 Regions where submarine mud volcanoes are known and example first reported publications.

Mud volcanoes are often described as cone shaped structures produced over faults by the upwelling of sediments fluidised by gas and water. They may develop as single isolated cones and craters or, more frequently, as groups of cones and crater systems (Etiope, 2015). Submarine mud volcanoes range in size between 50 centimetres and 800 metres in height (Murton and Biggs, 2003). Three-dimensional seismic has allowed identifying a set of structures associated with the constructional edifice, i.e. the mud volcano. This set of structures is designated as a ’mud volcano system’ and connects the mud volcano to its source stratigraphic unit (Stewart and Davies, 2006). Figure 3.20 shows the synthetic model presented by Somoza et al. (2012) that summarises the structural elements and seismic signatures of mud volcanoes imaged on high-resolution seismic profiles.

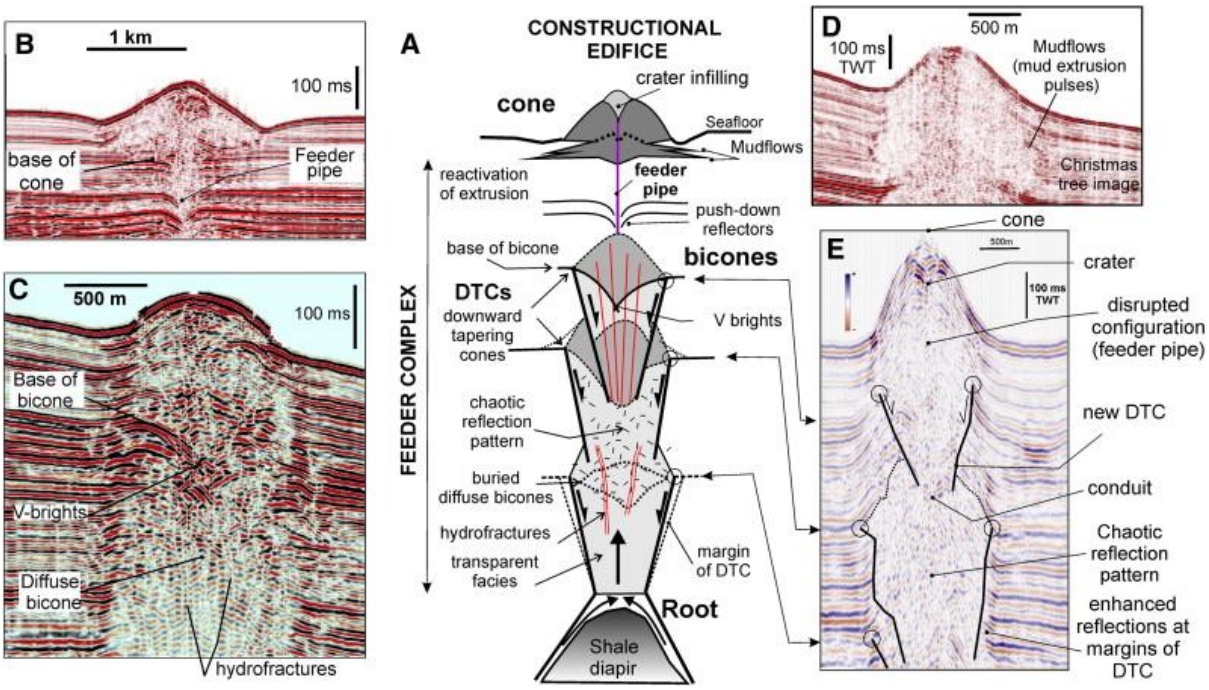

Figure 3.20 Synthesis of the structural elements of a mud volcano system and seismic signatures observed on the mud volcanoes (MV) of the Ceuta Drift. Partial sections correspond to Dhaka MV (B), Carmen MV (C), Granada MV (D) and Perejil MV (E). Extracted from (Somoza et al., 2012).

The principal controlling factors of fluid migration associated to formation of a mud volcano (Dimitrov, 2002) include: *1)* recent tectonic activity, particularly compressional activity, *2)* sedimentary or tectonic loading due to rapid sedimentation, accreting or overthrusting, *3)* continuous active hydrocarbon generation; *4)* the existence of thick, fine-grained, soft, plastic sediments deep in the sedimentary succession. It has also been suggested that sea-level variations may also contribute to explain episodic reactivations of mud volcanoes (*e.g.* Perez-Garcia et al., 2011; Somoza et al., 2012), as major sea-level lowstands could alter the neutral buoyancy conditions of the overburden above the shale units.

3.2.2.3 Sand mounds

Gas-bearing mounded sand features are described by Brooke et al., (1995) amongst others, in the Fisher Bank Basin of the central North Sea. They provide direct evidence for gas migration from older geological systems (i.e. Jurassic strata) into the Late Pliocene/Early Pleistocene succession. The mounded features display a very high amplitude response in seismic survey datasets. The mounds are generally around 500 metres to one kilometre in diameter, and up to 20 metres in height. Radial and listric faulting above the mounds suggest they were formed by post-depositional mobilisation of relatively shallowly buried sands, but there is limited evidence to suggest vertical migration from the mounds into overlying sediments. Brooke et al., (1995) suggest that the mounds are only formed when the overlying material successfully seals upwards migration of gas and discourages discharge to the sea bed and the formation of pockmarks (Section 3.2.2.1).

3.2.2.4 Authigenic carbonate

Methane-derived authigenic carbonate (MDAC) has been documented on continental shelves around the world (Judd and Hovland, 2007). MDAC is a common feature of methane seepage where rising methane is anaerobically oxidised by a microbial community of methane-oxidizing archaea and sulphate-reducing bacteria (Boetius et al., 2000). Carbonate cement (typically $CaCO_3$ as either calcite or aragonite) precipitates within the upper part of the sediment column if there is sufficient dissolved methane in the fluids, low bioturbation, and low sedimentation rates. Subsequent erosion of the sea bed will expose the MDAC, since the carbonates tend to be more resistant to erosion than the uncemented surrounding sediment. MDAC can be found within pockmarks (*e.g.* Judd, 2001) and salt diapirs (*e.g.* Hovland and Judd, 1988) in a variety of forms including concretions, pillars, chimneys and slabs. MDAC can also form larger-scale pavements, such as the Croker Carbonate Slabs that cover an area of eight square kilometres in the Irish Sea (Van Landeghem et al., 2015). The association with methane escape can be confirmed by the distinct carbon isotopic composition of the MDAC cement (Schoell, 1980).The occurrence of MDAC is specific evidence of methane seepage but does not necessarily imply current active gas escape. However, it does imply that methane seepage has occurred over a prolonged period.

3.2.3 Gas flux via geological fluid flow features

Gas seeps are a globally widespread phenomenon (Judd and Hovland, 2007), however, very few gas seepage rate measurements have been made. The sparsity of measured observations is due to a number of challenges associated with the acquisition of seepage rate data. In addition to technical challenges, there are difficulties associated with the nature of the process itself; fluid flux can be spatially and temporally variable with several seeps exhibiting periodic and discontinuous ('on–off') flow rate characteristics. Seepage rates reflect a response to external forcing such as tides, ocean swell, and potentially others, such as earthquakes (e.g. Boles et al., 2001; Leifer and Boles, 2005). Despite these challenges, the number of direct flux measurements and studies of temporal flux variability is steadily increasing (Figure 3.21). Flux rates from a single seep are mostly small (e.g. 62.3×10^{-3} mol s^{-1}, approximately 3.15×10^{-6} tonnes per year, Leifer and MacDonald, 2003) but the total marine contribution of methane gas flux has been estimated at about 50 million tonnes per year of methane from sea bed seeps of which 30 million tonnes per year of methane reaches the atmosphere (Kvenvolden et al., 2001).

The escaping bubble streams are detected either visually or acoustically (Section 5.1.2) and provide an identifiable source of active seepage. Bubbles streams have been analysed from video records to seep-tents equipped with dedicated sensors set at a seepage location (Leifer and Boles, 2005). Acoustic echosounding has been demonstrated to be a suitable technique for remotely sensed seepage quantification (Section 5.1.2). One of the most recent developments for investigating natural gas seepage bubbles in-situ is a 3D sensor called Bubble Box (Jordt et al., 2015). The aim of this sensor, under development at GEOMAR, is the automated determination of bubble size-distribution and rise velocity, as well as overall gas flux.

To address the limitations of each individual approach and to accurately study and characterise a seepage site often video, hydroacoustic, sub-bottom profile and chemical data are acquired during the same period time. For instance, this combined approach was adopted by Schneider Von Deimling et al. (2011) to study the methane seepage area of Tommeliten in Norway (estimated methane flux of 1.5 $x10^6$ mol per year, approximately 26 tonnes per year, see also Table A2).

Estimates of methane emissions from natural seepages			
CH_4 flux (tonnes per year)	***Area***	***Comment***	***Reference***
8×10^6 - 6.5×10^7	Global	Does not take in account loss within the hydrosphere	*Hovland et al. (1993)*
1.9×10^6	Continental shelves		*Trotsyuk and Avilov (1988)*
1.4×10^7 - 1.7×10^7	Global		*Lacroix (1993)*
4×10^5 – 1.22×10^7	Global	Extrapolated from UKCS data	*Judd (2000)*
1.8×10^7 – 4.8×10^7	Global	Based on Coal Point seep, California	*Hornafius et al. (1999)*
1×10^6 – 1×10^7	Global	Includes methane from gas hydrates	*Cranston (1994)*
1×10^7 – 3×10^7	Global	Based on oil/gas ratios and lifetime of methane	*Kvenvolden (2005)*
6.6×10^6 – 1.95×10^7	Continental margins	4×10^5 – 1.22×10^7 t y^{-1} from natural gas seeps 3.2×10^6 – 4.3×10^6 t y^{-1} from mud volcanoes 3×10^6 t y^{-1} from gas hydrates	*Judd et al. (2002)*
17	North Sea	Single pockmark	*Hovland and Sommerville (1985)*
$3.6 x10^5$ – $1.6 x10^6$	Black Sea	Black Sea Continental Shelf	*Dimitrov (2002)*
$1.2 x10^5$ – $3.5 x10^5$	UK continental Shelf		*Judd et al. (1997)*
13.3	Toney River, Canada		*Cranston (1994)*
$5 x10^2$ – $1.9 x10^4$	Rias Baixas, Spain		*Garcia-Gil et al. (2002)*
$3.5 x10^2$ – $5 x10^4$	Coal Oil Point, California		*Hornafius et al. (1999)*

Figure 3.21 The contribution to atmospheric methane from sub-sea bed sources compiled and references by Tizzard (2008). Methane flux values are presented here in tonnes of methane per year. For cited references see Tizzard (2008).

3.3 Geomorphological high-permeability pathways or barriers to flow

Discontinuities generated by large-scale erosional geomorphological features, tens of kilometres or more in extent, are potential high-permeability pathways or barriers to overburden fluid migration. Two types of overburden erosional geomorphological discontinuity, tens of kilometres or more in extent and associated with evidence of fluid flow are considered here; submarine mass movement deposits (Section 3.3.1**Error! Reference source not found.**), which have a worldwide distribution, and glacial tunnel valleys (Section 3.3.2**Error! Reference source not found.**) that are known to occur in onshore and offshore areas where geological CO_2 storage is in operation and is planned.

3.3.1 Submarine mass movement deposits

Submarine mass movement deposits can represent a significant stratigraphic component of many ancient and modern continental margins. Newton et al., (2004) recognised that locally up to 94% of the Quaternary sedimentary column of the Nile Fan is comprised of submarine mass movement deposits. Mass movement processes have occurred intermittently throughout geological history, being responsible for the remobilization of vast amounts of sedimentary material, even on slopes of less than 1° (*e.g.* Locat, 2001; Locat and Lee, 2002; Canals et al*.,* 2004).

The mass movement of sediment results in a vast spectrum of deposits, from sand-rich gravity flows that form many of the world's largest oil and gas reservoirs, to mud-rich deposits that may sequester globally significant volumes of organic carbon. The composition of the sediment matrix, its effective porosity and permeability will vary markedly between each type of deposit.

Mass movement deposits may act as high-permeability pathways if they are predominantly coarse-grained or baffles if they contain fine-grained, low-permeability mud layers. For example, 3D seismic data from the northern flank of the North Sea Fan revealed recognisable internal pipe structures within the strata beneath the Tampen Slide deposits (Gafeira et al., 2010). Figure 3.22 shows one of the pipe-shaped features observed beneath the Tampen Slide, where doming of the acoustic reflectors, labelled INS and TNS, might have been caused by fast-flowing vertical movement of fluidised sediment rather than diffusive fluid migration processes. The observed doming could also be an artefact caused by a seismic velocity increase in the overlying sediment in response to precipitation of carbonate cement within the pipe or gas hydrates (Gay and Berndt, 2007). On Figure 3.22 an amplitude decrease can be seen beneath the TNS reflectors, whereas the reflectors above TNS do not show any significant evidence of disruption or alteration in their geometry or seismic character. This structure indicates that the internal structure of the Tampen Slide deposits interfered with fluid migration through the sedimentary overburden and served as a barrier to fluid-flow through discontinuities within the slide.

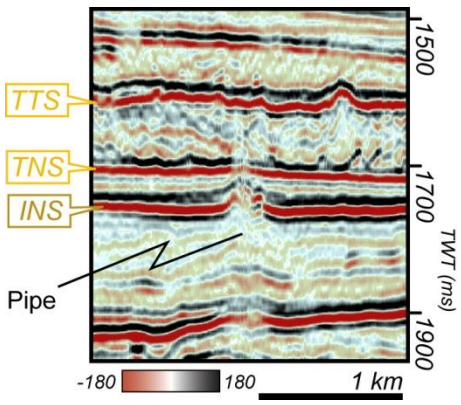

Figure 3.22 Seismic line from a 3D volume showing pull-up and disruption of the INS and TNS reflectors due to fluid migration, which do not appear to propagate beyond the TTS stratigraphic level. INS: Naust S internal reflector; TNS: Top of Naust S reflector, which on this location corresponds to the base of the Tampen Slide deposits; TTS: Top of the Tampen Slide.

Sediments within the slide were deposited in a stable state in which their shear strength exceeds the shear stress induced by the slope on which they were deposited. Nonetheless, any modification of this state, through either a decrease in sediment shear strength, an increase in shear stress operating on the sediment, or a combination of both, can lead to slope failure (Hampton et al., 1996). Many different triggering mechanisms have been presented in the literature. Table 2.1 shows some examples of known slope failure events that have been attributed to at least one specific triggering mechanisms associated with fluid flow: gas charging, e.g. Caspian Sea, (Newton et al., 1980); gas hydrate dissociation, e.g. Beaufort Sea (Kayen and Lee, 1993) and North Atlantic Ocean (Maslin et al. 2004); salt diapirism, e.g.Gulf of Mexico, (Prior and Hooper, 1999); and mud volcanoes, e.g. Offshore Trinidad (Moscardelli and Wood, 2008).

Triggering Mechanisms	Examples
Earthquakes	Grand Banks, Piper et al. (1988); Papua New Guine Tappin et al. (2001);North Aegean Trough, Lykousis et al. (2002)
Wave loading	Mississippi Fan (Hurricane Camille), Bea et al. (1983)
Tides	Terzaghi (1956); Fraser River delta (Canada), Atigh and Byrne (2003)
Rapid sediment accumulation	Mississippi Fan, Coleman et al. (1993); offshore Mauritania Krastel et al. (2006)
Gas charging	Caspian Sea , Newton et al. (1980)
Gas hydrate dissociation	Beaufort Sea Kayen and Lee (1993); North Atlantic, Maslin et al. (2004)
Glacial loading	Scotian Shelf, Mulder and Moran (1995); Laurentian Channel, Piper and Macdonald (2001); Nyk Slide, Lindberg et al. (2004)
Erosion	California canyons, McAdoo et al. (2000)
Salt diapirism	Off North Carolina, Cashman and Popenoe (1985);Gulf of Mexico, Prior and Hooper (1999)
Volcanic processes	Canary Islands, Watts and Masson (1995) & Gee et al. (2001); Hawaiian, Moore et al. (2008)
Water seepage	New Jersey, Dugan and Flemings (2000)
Mud volcanoes	Gulf of Mexico, Prior and Doyle (1993); Offshore Trinidad, Moscardelli and Wood (2008)
Sea-level fluctuations	Madeira Abyssal Plain, Weaver and Kuijpers (1983)
Human activity	Nice, Assier-Rzadkieaicz et al. (2000)

Table 3.3 List of the main mechanisms triggering slope failure and examples, For references cited see Gafeira (2010).

3.3.2 Tunnel valleys

Tunnel valleys are kilometre-scale geomorphological features typically 500 metres to four kilometres wide, up to 100 kilometres in length and eroding to depths of as much as several hundred metres. In the North Sea they are mapped as open geomorphological features at the sea bed and as infilled and buried features to depths of 500 metres below the sea bed. They form beneath ice sheets and are preserved as suites of elongated features, oriented in response to the mechanics of the overlying ice sheet (Figure 3.23). Successive cycles of ice advance and retreat generate superimposed and cross-cutting suites of tunnel valleys that may intersect. Tunnel valleys are the largest geomorphological glacial features preserved in the Quaternary succession of the North Sea where CO_2 storage projects are in operation or planned. The large size, extent and erosive base of tunnel valleys and understanding of their potential to enhance or impede fluid flow are essential when assessing migration potential migration pathways in the shallow overburden to CO_2 storage projects.

Most high latitude areas of the northern hemisphere, including those areas under consideration for storage sites offshore the UK and Norway have undergone repeated glaciations over the last two million years. The overburden in these regions have

therefore been affected by the repeated advance and retreat of significant ice sheets, reflected by geomorphological landforms within the overburden left behind after ice sheets retreated. As ice sheets generally create erosive environments, many older geomorphic features are subsequently eroded; thus, within most of the overburden, large landforms are generally restricted to the upper part of the succession, preserved from the last glacial maximum, around 26 000 years ago. In the case of the UK and Norway, this is generally within the upper few hundred metres of the subsurface. Background sedimentation in these conditions will normally comprise of relatively high rates of deposition with heterogeneous muds, sands, gravels and iceberg dropstones. Tunnel valley features associated with the Quaternary glaciations of the northern hemisphere are also described onshore (Livingstone et al., 2016) and offshore (see Todd et al., 2016, and references therein) in North America.

Understanding the influence of tunnel valleys on potential fluid flow in the overburden requires an understanding of their distribution, morphology and fill. Very little is known about potential rates of fluid flow through buried tunnel valleys in the North Sea, as no offshore buried tunnel valleys have been comprehensively investigated by methods which would reveal internal sedimentological properties; no scientific boreholes penetrate buried tunnel valleys in the North Sea where potential CO_2 storage sites are proposed. Commercial well data, which may have penetrated tunnel valleys during oil and gas exploration, do not record or report the shallow overburden succession.

Analysis of subsurface seismic data suggests many of the buried valleys in the Quaternary overburden succession of the North Sea are characterised by an approximately tripartite fill pattern. A chaotic basal fill with a 'chaotic' seismic character is overlain by sequences with dipping reflectors and a final package in which the reflectors illustrate a drape character (Huuse and Lykke-Andersen, 2000; Kristensen et al., 2007, 2008; Lutz et al., 2009; Stewart et al., 2012; Van der Vegt 2012; Benvenuti and Moscariello, 2016). Many studies find evidence for the second component of the fill as dominated by clinoform packages (Praeg, 2003; Lonergan et al., 2006, Kristensen et al., 2007, 2008; Benvenuti and Moscariello, 2016) although this is not universal (see summary in Van der Vegt, 2012). However, many buried tunnel valleys contain no evidence for a structured fill when observed within seismic survey data, and the lack of borehole information precludes correlation between seismic characteristics and sediment description.

Tentative correlation with borehole data from tunnel valleys mapped onshore in the Netherlands, Germany and Denmark indicate the sedimentary character of the tripartite packages observed in offshore seismic data. The basal component may comprise glaciofluvial sands and gravels overlain by glaciofluvial sands/clays and topped with finer grained marine or lacustrine sediments (Jørgensen et al., 2003; Kluiving et al. 2003; Jørgensen and Sandersen, 2006; Andersen et al., 2012; Sandersen and Jørgensen 2012). Most studies agree that coarse-grained gravels and sands, with potentially high permeability and porosity, may be present within tunnel valleys, with implications for potential routes of fluid flow. However, the extent of these potential sandy bodies, and their connectivity, remains poorly understood. The majority of buried tunnel valleys in the central and northern North Sea are present

within the relatively muddy Aberdeen Ground or Nordland Formations and overlain by more recent mud-dominated facies (Stoker et al., 2011).

Buried tunnel valleys form very extensive networks in north-west Europe (**Error! Reference source not found.**) (Van der Vegt, 2012, fig.1); individual valleys display lengths of 125 kilometres or greater (Van der Vegt, 2012; Stewart et al., 2013) with implications for potential migration routes over large distances. North Sea tunnel valleys are also observed to cross-cut one another (Figure 3.24), with multiple generations of valleys forming the apparently complex networks observed today (Stewart et al., 2013).

Tunnel valley features related to ancient glaciations, such as those of Ordovician age in Libya (Le Heron et al., 2004) and Algeria (Hirst et al., 2002) are present onshore and their fill architecture has been more closely examined with respect to fluid flow because they represent potential hydrocarbon reservoirs. Davidson et al*.,* (2000) and Le Heron et al., (2004) report laterally extensive fan sands comprising the basal fill of the tunnel valley, with moderate reservoir potential, but these are separated by basal muddy sands which would restrict vertical fluid flow (see Le Heron et al., 2004, fig. 9). In Algeria, Hirst et al., (2002) report analogous sands with a permeability of up to 1000 milliDarcy (mD). Overall, fill architecture is characterised by 'seaward dipping, alternating metre to tens of metre-thick units of poor and moderate quality', which the authors suggest will direct fluid flow upwards or downwards, crucially, *through* the tunnel valley (Le Heron et al., 2004). It should be noted that the internal architecture of more recently formed tunnel valleys in the North Sea has not been directly compared to these ancient palaeovalleys; however, their formation processes beneath extensive ice sheets are expected to be the same (Van der Vegt, 2012).

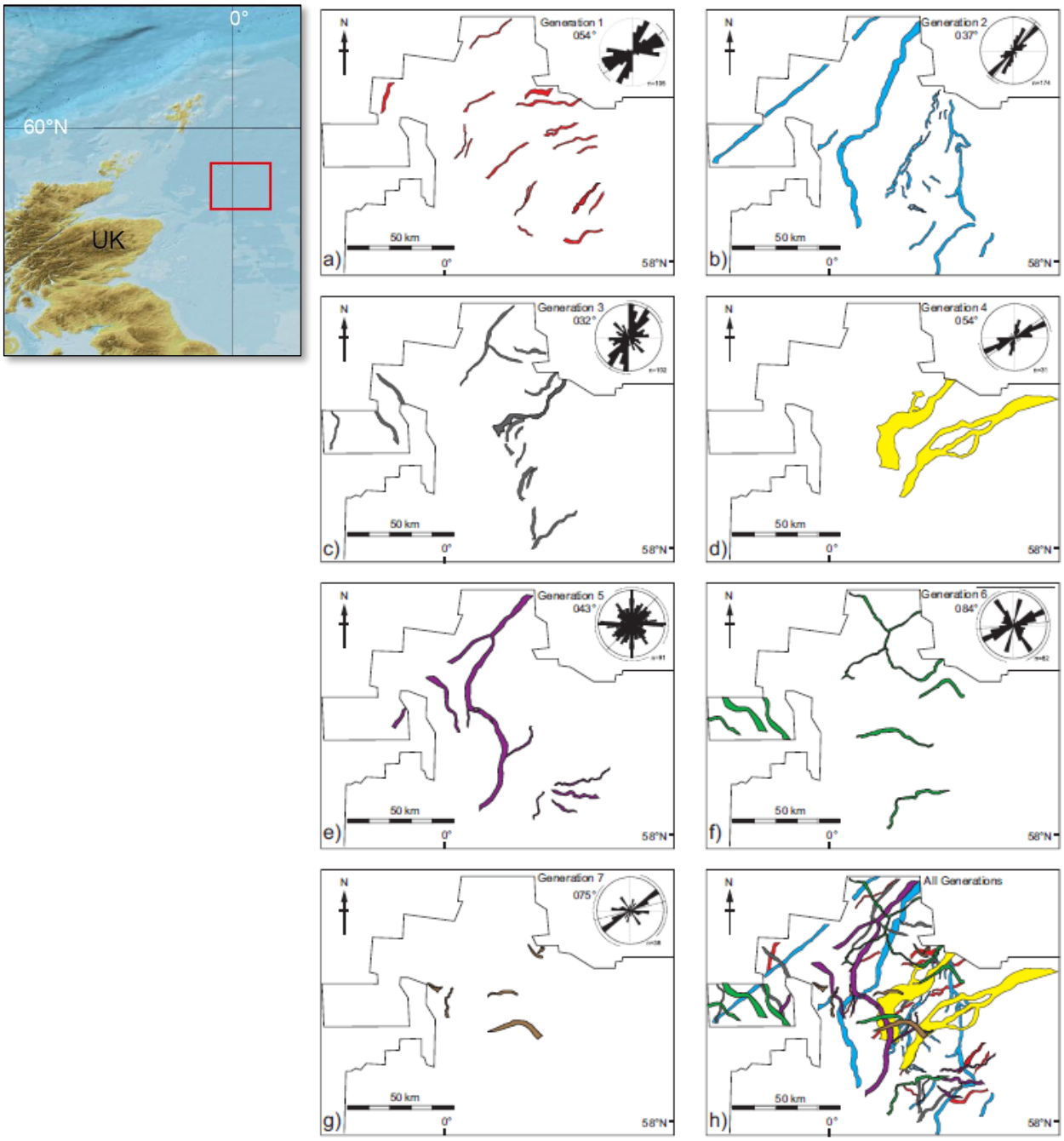

Figure 3.23 Cross-cutting tunnel valleys in the UK sector of the central North Sea (study area outlined in red in inset) from a) oldest to g) youngest emphasising superimposition of generations over time. Figure adapted with permission from Figure 8 of Stewart et al. (2013). Bathymetric data from GEBCO_08.

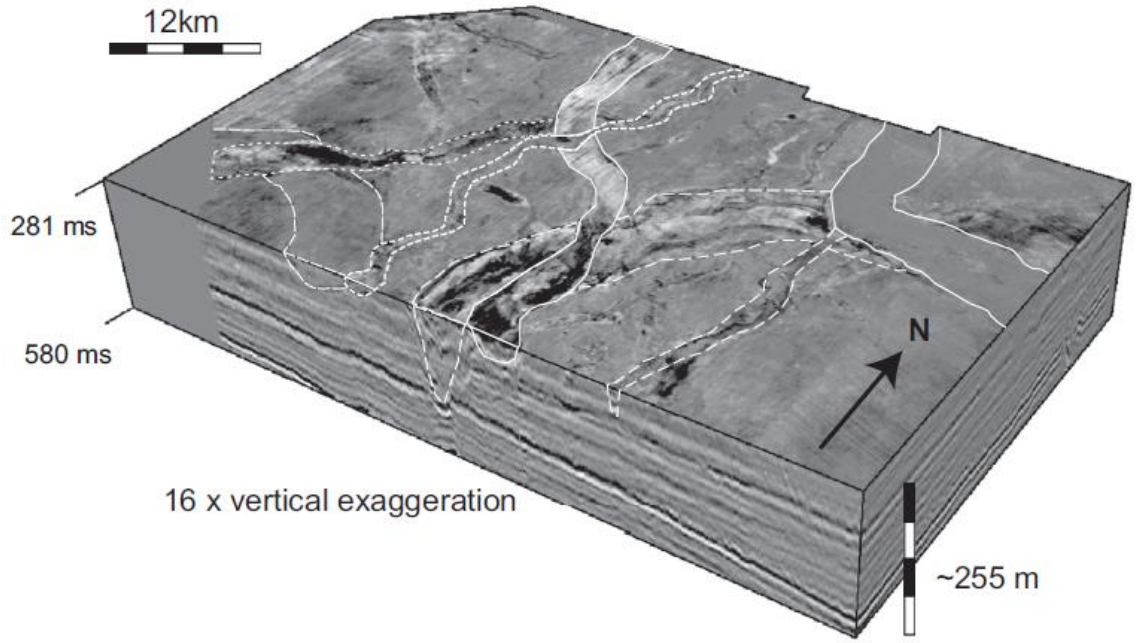

Figure 3.24 Example 3D seismic cube in the UK central North Sea demonstrating the cross-cutting, stacked nature of buried tunnel valleys. Adapted from Figure 3 of Stewart et al. (2013).

3.4 Hydrofracturing and glacitectonic faulting

Structures associated with hydrofracturing (e.g. sediment-filled fractures and fluid escape features) and glacitectonic deformation (e.g. folding and faulting) are relatively common within areas of former glaciated terrane such as the UK, northern Europe, Canada, Scandinavia and Russia). However, in areas which have not encountered geologically recent glacial activity, the impact on the near surface geology as a result of hydrofracturing and glacitectonic deformation will not be an issue.

Evidence of hydrofracturing is preserved in sediment and bedrock subject to ice sheet loading. Loading by glaciers and ice sheets typically results in the development of a pressurised hydrogeological system which can trigger hydraulic fracturing of the underlying sediments and bedrock (van der Meer et al., 2008; Phillips et al., 2013; Phillips and Hughes, 2014) and create specific landscapes of soft-sediment extrusion. Hydrological modelling of subglacial groundwater systems indicates deep penetration of the effect of loading by major ice masses, up to a thickness of 1500 metres in the Netherlands, into the underlying subglacial sediments and rocks (Piotrowski, 2006). Over-riding by ice also deforms the underlying sediment and rock (Phillips et al., 2011); glacitectonic deformation generates faults and folds in both bedrock (e.g. Mud Buttes, Alberta, (Slater 1927; Phillips et al., in press)) and unconsolidated strata (e.g. North Sea, (Vaughan-Hirsch and Phillips, 2016; Pedersen and Boldreel, 2016)). The extent of glacitectonic thrust zones mapped from seismic data indicates that glacigenic fault zones can be tens of kilometres in length (Phillips, in press). Faulting typically occurs at a range of depths from just a few metres (Phillips et al., 2002), through several tens of metres (40-150 m) (Phillips et al., 2008; Vaughan-Hirsch and Phillips, 2016), up to hundreds of metres (approximately 500 m, Pedersen and Boldreel, 2016). The largest

examples can be laterally extensive ranging from tens to hundreds of metres across, and tens of kilometres in length.

Glacitectonic deformation caused as a glacier or ice sheet pushes into and over-rides a pre-existing sequence of sediments and/or bedrock (Phillips et al., 2011) is most pronounced at the margins of the advancing ice mass. It typically involves both folding and thrusting, and therefore results in a similar range of structures to those found in orogenic mountain belts (Croot, 1987; van Gijssel, 1987; Pedersen, 1987; Aber et al., 1989; Harris et al., 1997; Bakker, 2004; Andersen et al., 2005; Phillips et al., 2008; Phillips et al., 2011; Vaughan-Hirsch and Phillips, 2016). Well-documented examples include: the deformed Quaternary glaciofluvial sediments within the composite ridges of the Dammer and Fürstenauer Berge region of Germany (van der Wateren, 1987; 1995); folded and thrust Cretaceous chalk bedrock and associated Pleistocene sediments on the Isle of Rügen, northern Germany (Steinich, 1972; Gehrmann et al., 2016) and at Fur Knudeklint and Møns Klint, Denmark (Pedersen, 2005; 2014); imbricated and folded Quaternary sediments at St. Bees, Cumbria, England (Williams et al., 2001), Dinas Dinlle, northwest Wales (Harris et al., 1997; Thomas and Chiverrell, 2007, 2011) and the Bride Moraine on the Isle of Man (Slater, 1931; Thomas et al., 2006; Roberts et al., 2006; Thomas and Chiverrell, 2011). Large-scale glacitectonic thrust complexes are increasingly being identified using high-resolution, 2D and 3D shallow seismic data (Huuse and Lykke-Andersen, 2000; Vaughan-Hirsch and Phillips, 2016; Cotterill et al., in press) and ground penetrating radar studies (Bakker and van der Meer, 2003; Bakker, 2004). These geophysical techniques not only make it possible to map out these features in the marine environment, but also investigate their deeper structural architecture both onshore and offshore (Harris et al., 1997; Williams, et al., 2001; Vaughan-Hirsch and Phillips, 2016; Pedersen and Boldreel, 2016). These thrust complexes deform both bedrock (e.g. Mud Buttes, Alberta, Slater 1927; Phillips et al., in press) and unconsolidated strata (e.g. North Sea, Andersen et al., 2005; Vaughan-Hirsch and Phillips, 2016; Pedersen and Boldreel, 2016) with their basal detachments occurring at depths ranging of from just a few metres (Phillips et al., 2002), to several tens or metres (40 to 150 m) (Phillips et al., 2008; Vaughan-Hirsch and Phillips, 2016), up to several hundred metres (c. 500 m, Pedersen and Boldreel, 2016). The largest thrust complexes can be laterally extensive ranging from tens to hundreds of metres across, and tens of kilometres in length where they are associated with the development of a complex system of linear landforms. These landforms comprise a series of arcuate, subparallel ridges separated by depressions which in general preserve the shape of the former ice margin. The individual ridges correspond to either the crests of large-scale folds or the ends of the tilted thrust blocks/sheets.

Glacitectonism can also result in the detachment and transport of large blocks or “rafts” of bedrock and/or pre-existing unconsolidated sedimentary strata some distance from their original site of deposition (Burke et al., 2009). They are typically thin (up to a few tens of metres) when compared to their aerial extent, which can be up to several hundreds of square kilometres. The base of the raft is marked by a prominent thrust or décollement surface which may show evidence of locally intense ductile and/or brittle deformation associated with their displacement (transport) within the hanging-wall of these glacitectonic structures. Once detached, the blocks may be transported

for a relatively short distance (tens of metres) or up to several hundred kilometres from their source (Bluemle and Clayton, 1983; Phillips and Merritt, 2008). Examples include: the Interior Plains of North Dakota (USA), where rafts of shale and sandstone bedrock have been thrust upwards into younger sediments (Bluemle and Clayton, 1983); detached sandstone blocks occurring across extensive tracts of the prairie regions of Alberta and Saskatchewan, Canada (Moran et al., 1980); and thrust-stacked blocks of chalk within the highly glaciotectonised sequences in north Norfolk, eastern England (Phillips et al., 2008; Burke et al., 2009; Vaughan-Hirsch et al., 2013) and Denmark (Jakobsen, 1996). Several models have been proposed to explain the generation of glacial rafts. However, recent studies have argued that failure leading to detachment is associated with elevated pore-water pressures occurring along water-rich décollement surfaces located either beneath the ice (Moran et al., 1980; Aber, 1985; Broster and Seaman, 1991; Kjær et al., 2006), or as a consequence of subglacial hydrofracturing and forceful water escape (Boulton and Caban, 1995; Rijsdijk et al., 1999), and/or associated with the propagation of water lubricated décollement surfaces in response to ice-marginal to proglacial thrusting (Phillips and Merritt, 2008).

3.5 Wellbore-related pathways

Wellbore-related flow paths are potential seal rock bypass mechanisms for CO_2 and brine migration in the overburden. Here the flow pathways are introduced (Section 3.5.1) and the mechanisms which can detrimentally affect well bore integrity are described (Section 3.5.2). These include construction defects and subsequent physical and chemical changes in and around the wellbore. Well integrity studies, pathway development and potential rates of fluid migration through the overburden afforded by a leaking wellbore are presented in Section 3.5.3. Modelling studies to determine potential leakage rates are reviewed in Section 0.

3.5.1 Introduction

Wellbores that penetrate sealing units in the overburden are often perceived as representing the greatest risk to storage containment (Bachu and Watson, 2009; Pawar et al., 2015). All CO_2 storage sites will contain at least one well and some may be penetrated by hundreds of wells. Each has the potential to connect the storage reservoir with overburden strata. However, wells are constructed and abandoned to preserve hydraulic isolation between intervals penetrated by the well and prevent fluid flow into or out of the wellbore itself. Once drilled, the wellbore is lined with casing of metal pipe that is screwed together in sections, and cemented in by pumping cement slurry (of a purpose-designed mix and volume) down the casing and up into the gap between the casing and formation where it solidifies (Figure 3.25). Once the cement has set, hydraulic tests may be performed to ensure the wellbore integrity is sufficient to withstand the subsequent expected pressures, and geophysical logs may be run to assess the cement presence and quality. Any significant fluid-flow pathways discovered can be sealed by a ‘squeeze job’ by perforating the casing and forcing cement or sealant into the pathway to restore hydraulic isolation. During well operation the inside of the casing will contain additional flow barriers such as tubing and packers, and on abandonment, these will be removed and replaced with strategically positioned

cement plugs designed to maintain hydraulic isolation indefinitely (Azar and Samuel, 2007; for a simple article in layman's terms see Nelson, 2012,).

Despite their careful design, losses in wellbore integrity can occur as a result of subsequent physical and chemical changes in and around the wellbore and/or construction defects (Figure 3.25). In a CO_2 storage site, CO_2 or reservoir brine could exploit potential pathways along the interfaces between the cement and formation, or the cement and casing, as well through the cement and the metal casing itself (Figure 3.25). These pathways may exist, and be opened or closed as a result of construction defects in the well, and its subsequent physical (mechanical, thermal) and chemical loading. There has been considerable focus on research aimed at determining well integrity in recent years with extensive recent review studies (for example Huerta et al., 2016; Carroll et al., 2016; Bai et al., 2016; Zhang and Bachu, 2011).

Characterising well integrity prior to CO_2 injection may be challenging. There may be significant uncertainty in the current or long-term integrity of wells, particularly for plugged and abandoned wells where borehole access is no longer possible and records of previous integrity assessments and abandonment procedure may not be available. Record retention and retrieval systems depend on company and regulatory policies and access to these legacy documents for the CO_2 storage site operator may be difficult. A conservative approach to risk assessment is generally taken, so wells may be classified as 'higher risk' because there is insufficient information available to characterise and assess their integrity. Predicting future well integrity will also be challenging because of the highly site-specific conditions to be incorporated in short-term laboratory scale investigations and numerical models, and the lack of long-term relevant field-scale data to validate predictions (Caroll et al., 2016). In terms of field-scale information, Manceau et al. (2016) describe observations from a short-term, around one year CO_2 exposure, controlled field-scale experiment. Longer-term well-integrity investigations of wells exposed to CO_2 for around 30 years include an Enhanced Oil Recovery (EOR) site (e.g. Carey et al., 2007) and a natural CO_2 production site (e.g. Crow et al., 2010). Although observations of field-scale systems can only provide information over decadal timescales, cement mineral carbonation over a timescale of ten thousand years has been investigated using a natural analogue of rock cementing minerals (Rochelle and Milodowski, 2013). For CO_2 storage projects where wellbore leakage is considered to be a risk, monitoring of those wellbores and plans for any potential remediation should be considered.

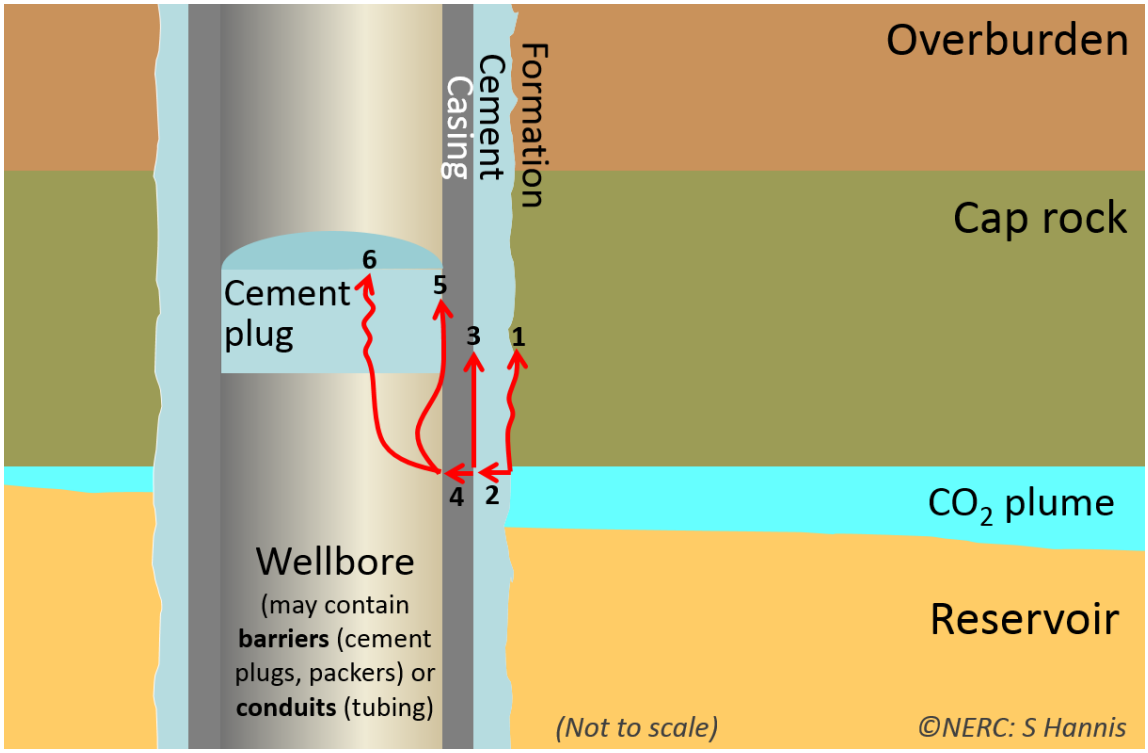

Figure 3.25 Wellbore schematic showing possible fluid-flow leakage pathways: 1, along the well cement-formation interface; 2, through the cement; 3, along the cement-casing interface; 4, through the casing into the wellbore; 5, along the cement-casing interface of an abandonment cement plug; 6, through the cement of an abandonment plug.

The numbered arrows in Figure 3.25 indicate potential leakage pathways for CO_2 or brine as follows:

1: Along the cement-formation interface

2: Through the cement

3: Along the cement-casing interface

4: Through the casing into the wellbore

5: Along the cement-casing interface of an abandonment cement plug

6: Through the cement of an abandonment plug

In an operational well, packers or tubing may create additional pathways or barriers, and abandoned wells also contain multiple cement plugs, which may be set on top of packers. Many of the pathways may be sequential, for example, pathways 5 and 6 (Figure 3.25) would not be relevant unless 4 has been breached.

3.5.2 Wellbore-related pathways and mechanisms

Wells are constructed and abandoned to preserve hydraulic isolation, both between intervals penetrated by the well and into or out of the wellbore itself (Section 3.5.2.1). However, defects introduced during the wellbore completion or resulting from subsequent physical or chemical loading during its operation or abandonment can result in the development or sealing of potential leakage pathways (Sections 3.5.2.2and Section 3.5.2.3). Understanding the interaction between the physical and chemical stressors of the system and the transport properties through time is

challenging, and currently little evidence of potential migration rates through time exists. However, improved understanding in this area could ultimately reduce uncertainty in the leakage risks and avoid unnecessary remediation (Caroll et al., 2016). This is an area of active research involving theoretical studies, numerical simulation, laboratory experiments, field-scale experiments, and observations from real sites.

3.5.2.1 Construction Defects during Wellbore Completion

Potential difficulties can arise during the wellbore drilling and completion that can adversely affect wellbore integrity (either by directly creating potential leakage pathways or causing damage or weaknesses that can compromise integrity later during well life). The steps involved in completing a well and how, when and where defects can arise are explained sequentially below:

a. Well drilled to avoid formation damage

i. Drilling strategy and drilling fluid (mud) system designed to avoid damaging the borehole wall. Design should avoid, for example, the borehole becoming enlarged ('washed out'), fractured or deformed, as certain lithologies may swell in the presence of the drilling mud. Otherwise, these processes could alter the strength and permeability characteristics of the borehole walls to create fluid leakage pathways behind the cement (Figure 3.25, pathway 1).

ii. Efficient mud removal prior to cementing. Efficient removal would avoid leaving mud channels or pockets that could affect the quality of the cement and the cement-formation bond, and consequent potential leakage pathways through the cement or along the cement-formation interface (Figure 3.25, pathways 1 and 2).

b. Correct installation of casing pipe

i. Appropriate selection of materials to provide mechanical support and avoid excessive corrosion of intervals that may be exposed to chemical attack. This is to avoid the creation of potential leakage pathways through the casing via corrosion holes or fractures (Figure 3.25, Pathway 4).

ii. Casing pipe sections properly screw-threaded together to avoid thread leaks which are a potential leakage pathway through the casing (Figure 3.25, Pathway 4).

iii. Casing pipe sufficiently centralised in the borehole, to allow cement slurry to access the complete circumference of the pipe and avoid potential leakage pathway through the cement, or along the cement/formation or cement/casing interfaces, (Figure 3.25, pathways 1, 2, 3). This may be especially challenging in deviated wellbores.

c. Correct installation of well cement

i. Correct installation of a suitable cement slurry designed with appropriate density, additives and mixing to ensure the cement will be of good quality to provide structural support and chemical protection to the casing and provide hydraulic isolation between geological intervals.

ii. During the solidifying process the cement can be vulnerable to gas-migration ingress creating through- or behind-cement pathways (Figure 3.25, pathways 1, 2, 3). When the setting cement forms a gel the borehole pressure is reduced and as the cement sets further the hydration processes draw in water thereby reducing cement pore pressure. Connected pores at lower pressure within the cement can form a gas-migration pathway during the cement curing process, which remains once the cement is fully hardened potentially allowing hydraulic connectivity.

iii. Sufficient volume of cement to ensure good cement coverage and placement, i.e. the top of the cemented interval is placed where it is designed to be, to provide hydraulic isolation over the required intervals.

iv. Cement delivery set up for effective drilling mud removal. Remaining mud, which fills the borehole prior to cement delivery, or mudcake (which coats the borehole wall) can dehydrate as the cement sets and form channels within the cement or along the cement-formation interface, respectively. This is more common in wells with formation drilling damage and improperly centralised casing (see above).

d. Hydraulic isolation test

A hydraulic isolation test can be carried out after the cement is sufficiently cured by pressuring up the casing and cement to see if it withstands the pressures required for well operation or deeper drilling. Pressure (and temperature) changes at this stage and later in the well lifetime can sometimes cause a small gap to form along the cement-casing interface. This small gap is known as a microannulus.

i. If cement defects are discovered that are detrimental to zonal isolation, either at the time of well completion or at later stages in the lifetime of the well, it is commonly addressed by a ‘squeeze job’. Here an additional cement is squeezed into the affected area, sealing it to fluid flow and is usually sufficient to fix the isolation around the treated area, but smaller pathways may remain. Purpose-designed compounds to improve penetration and sealing efficiency are being developed.

3.5.2.2 Mechanical-thermal Loading

All wells will experience pressure and temperature changes throughout their lifetime, as a result of operation and abandonment, or external changes in the subsurface environment. External changes can result from other subsurface uses or regional hydrogeological and tectonic effects. Understanding the stresses affecting a wellbore through time is complex, particularly at material interfaces (Caroll et al., 2016). These stresses can be focused and exacerbated by existing damage created during the wellbore construction (Section 3.5.2.1). Wellbores are designed to address and withstand these stresses and maintain integrity; however the main sources of thermal and mechanical stresses and their effect on potential pathway creation are outlined below:

a. **Thermals stresses** can cause swelling or shrinkage in the casing and cement, influencing the geomechanical stress state and creating radial strains) and leading

to the potential creation of leakage paths (Figure 3.25, pathways 1 to 6) such as fractures pathways or microannuli.

i. Temperature changes can be introduced as result of injection or production of fluids at different temperatures to those in-situ down hole.

ii. Phase changes of the fluids in the borehole or reservoir can also cause thermal stress. (such as the Joule-Thompson cooling effect).

b. **Mechanical stresses** have the potential to cause tension, compression or shear failure in the casing and cement and debonding at their interfaces, leading to the creation of potential leakage paths (Figure 3.25, pathways 1 to 6).

i. Anthropogenic operations in the well or neighbouring pore space alter the stress state in the well and the reservoir. For example, pressure cycling resulting from repeated production and injection or overburden uplift /subsidence induced by injection/production, respectively.

ii. Regional tectonic stresses can cause sudden or gradual stress changes, for example, by earthquakes or salt creep, respectively.

3.5.2.3 Chemical reactions

Chemical reactions or 'loading' can occur inside or outside the wellbore as a result of interactions with fluids and gases that have been injected, produced, or are already present within the host rock (native or previously injected). The fluids and gases can react with the host rock and wellbore materials to dissolve and/or precipitate material. The net result can act to create, open or seal leakage pathways over time, dependent on the chemistry of the components, environmental conditions, flow rates and fluid residence times. Existing weaknesses or pathways can focus and enhance chemical alteration, similarly to the effects of thermo-mechanical stresses (Section 3.5.2.2). Many stresses generated by chemical reactions can be avoided through wellbore design. The design could incorporate the use of appropriate materials in the wellbore construction, installation of cathodic protection arrays to reduce subsurface metal corrosion, introduction of corrosion inhibitors or control of the CO_2 stream composition. The latter would remove elements that might enhance corrosion, such as water or oxygen, from the CO_2 stream.

a. **Alteration of the cement** matrix materials can change the cement porosity and permeability, thereby altering its strength, hydraulic conductivity properties and propensity to allow leakage. This can allow, enhance or reduce flow along cement interfaces or along pathways through the cement to contact the casing. (Figure 3.25 pathways 1, 2, 3, 5 and 6). Leakage into uncemented annuli would allow free flow of fluids towards the surface.

i. As cement matrix alteration proceeds, a series of reaction fronts form, because the reactions are limited by the rate of transport of the reaction inputs and products through the matrix. The hydrated cement matrix materials may dissolve with carbonic acid formed when CO_2 dissolves in water. The portlandite minerals in the cement dissolve at the fastest rate giving a portlandite-depleted zone at the reaction front that penetrates deepest into the

unaltered cement. Dissolved components may then re-precipitate behind this front, for example forming a calcium carbonate zone, and leaving a zone of amorphous silica behind, closest to the interface between the cement and reactive fluid (reviewed in Carroll, 2016). Zhang and Bachu (2011) explain that the 'carbonation' process described reduces cement porosity and permeability, but if fresh reaction inputs are provided, e.g. through extensive flushing, the re-precipitated calcite can be re-dissolved, leading to 'cement degradation'.

ii. Cement additives and impurities in the CO_2 stream or native to the reservoir (e.g. O_2, H_2S and H_2S) can change both the reactions and the rates of reaction compared to those for standard portlandite cement reacting with pure CO_2.

b. **Alteration of the metal casing** can change its strength and hydraulic conductivity. If completely penetrated the alteration can allow across-casing flow, i.e. flow in or out of the casing (Figure 3.25, pathway 1) or weaken it sufficiently that mechanical-thermal stresses can cause the casing to fracture (Section 3.5.2.2). Good quality cement should protect the outside of the casing from contact with the chemicals that can alter it.

i. Corrosion of the casing can occur through reaction with carbonic acid, formed when CO_2 dissolves in water, which causes the dissolution of iron. H_2S, O_2 or chloride ions can increase casing corrosion rates. Iron carbonate can precipitate to form a scale which can potentially slow further corrosion.

ii. Embrittlement can occur if oxygen or hydrogen is present, which can enhance cracking resulting from thermo-mechanical stressors.

iii. Metal erosion can occur from high velocity gas bubbles or from the entrainment of sand, for example from the proppants used to 'prop' open fractures in hydraulic fracturing operations, or from friable formations.

3.5.3 Review of well integrity studies: pathway development and potential migration rates

This is an area of active research involving scientific theory, laboratory experiments, field-scale experiments, observations from real sites and numerical simulation predictions, to calculate potential leakage rates for risk assessment purposes.

Effects of leakage on pathway development have been analysed using laboratory-scale experiments with wellbore-specific materials. As the wells are designed not to leak, migration rates are often not defined, rather, observations such as cement alteration rates through time for different scenarios are presented, often with depth of carbonation reported (e.g. reviewed in Zhang and Bachu, 2011). However, cement alteration does not necessarily equate to degradation in barrier properties and experiments are reported in which barrier properties improve with alteration, or that open fractures become sealed. The interplay and coupling between the in situ conditions of the wellbore and any existing pathways, with the stresses (thermo-mechanical and chemical) and transport properties through time are important to understand migration pathway behaviour and potential leakage rates (Carroll et al., 2016). Carroll et al. (2016) concluded that alteration rates by diffusion through the cement matrix are extremely slow when there is no flushing or through-flow of the

reacting fluids, which is thought to be more typical of the storage scenario. Therefore, this mechanism would be insufficient to pose a threat to well integrity. In addition, in regard to flow pathway development, Carroll et al. (2016) conclude that over the timescale of geological storage, fracture sealing may be more common behaviour than fracture opening, because of the long residence times of the reacting fluids. Few experiments directly study flow behaviour along cement-casing-rock interfaces and the potential protection-effect of altered cement or iron carbonate scale on casing corrosion in a CO_2 storage environment.

In parallel to the laboratory-scale experiments, field-scale studies directly examining retrieved samples of wellbore cements and casings from wells exposed to CO_2 have been carried out. Field-scale studies have been conducted at a purpose-designed study site (e.g. Manceau et al., 2016), a CO_2 production well from a natural CO_2 field (e.g. Crow et al., 2010) and CO_2 injection wells from CO_2-EOR at the SACROC site (e.g. Carey et al., 2007), USA and at Cranfield, USA (Duguid et al., 2014). Direct tests of hydraulic isolation have also been carried out across zones in the wells identified as having questionable integrity from their geophysical log responses using vertical interference tests at Cranfield (e.g., Duguid et al., 2014) and at Weyburn (Gasda et al., 2011). This involves temporarily piercing the casing above and below the questionable zone and isolating the piercings inside the wellbore with packers. The well is pressured-up from surface and held at a constant pressure. The pressure change 'transient pressure response' in the lower zone is measured. From this, the effective wellbore permeability can be estimated. In the well investigated by Duguid et al. (2014) evidence pointed towards poor-quality, unconsolidated cement over the interval to be tested. However, on testing the interval was found to maintain zonal isolation. Time-lapse logging data from the same interval suggested surprisingly large changes in integrity had occurred over short timescales of approximately five years. However, given the infrequency of such measurements, it is not known whether such changes can be considered 'normal' or whether they identify an increased risk of leakage (Duguid et al., 2014).

Well integrity and potential failure modes are often studied at hydrocarbon or CO_2-EOR wells, given the relatively few CO_2 storage sites and their short exposure times, to gain a more statistically representative understanding of well integrity. For example, Bachu and Watson (2009) found that well age, operational mode, completion intervals, or presence of acid gas (H_2S, CO_2) in the produced fluids did not have a statistically detrimental effect on integrity. Anecdotally, unanticipated wellbore-related leakage has occurred in the USA via 'lost wells', where past records were inadequate to properly locate all wells in the area of interest. Studies on operating CO_2 injection wells suggest that most CO_2-release incidents relate to surface components rather than subsurface leakage paths. Checkai et al. (2013) and Tao et al. (2014) examined leakage rates from hydrocarbon wells by measuring the pressure or flow rate from intermediate casing valves. They inferred that any pressure or flow at this point represented flow via wellbore-related leakage pathways and used this to estimate effective wellbore permeability (study 1 in Figure 3.26 and Table A1). Learnings from wellbore reverse flow (blow-outs) from CH_4 gas wells, CO_2 producers and geysering behaviour (Figure 3.26 and Table A1) suggest that it is not always straightforward to bring a reverse-flowing well back under control (IEAGHG, in press).

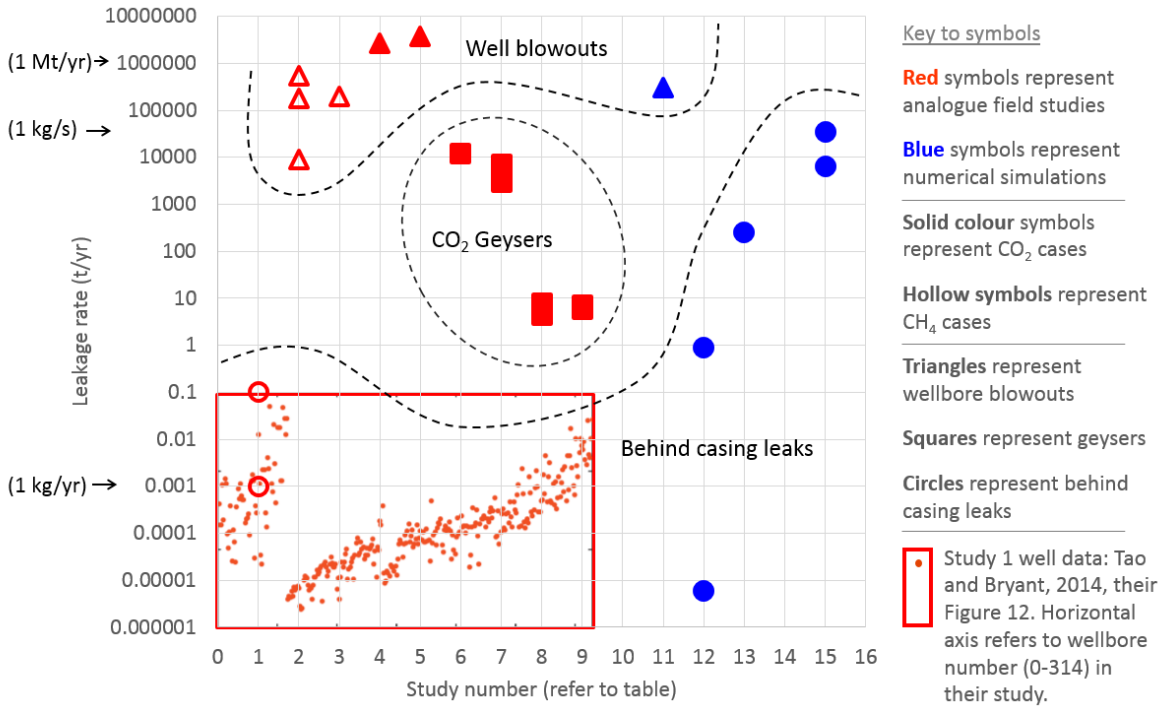

Figure 3.26 Selected leakage rates along wellbores at various analogue sites (gas storage or CO2 producers) and those calculated by numerical simulations, see Appendix 1. Inset (red box) reproduced from Tao and Bryant (2014). (Dotted lines are to indicate groups of points and do not represent boundaries). (permission needed for Tao and Bryant)

Even hydrocarbon wells, particularly those involving CO_2-EOR, have been in operation for relatively short timescales compared to the period anticipated to demonstrate long-term containment at a CO_2 storage site. Therefore, laboratory- and field-scale understanding is incorporated into numerical simulations that can predict the behaviours of well barriers over much longer time periods to understand the risk of leakage. For example, Brunet et al., (2016) developed a numerical model calibrated to experimental results and found that there is a critical fluid residence time for each fracture aperture size, beyond which they tend to self-seal (Figure 3.27).

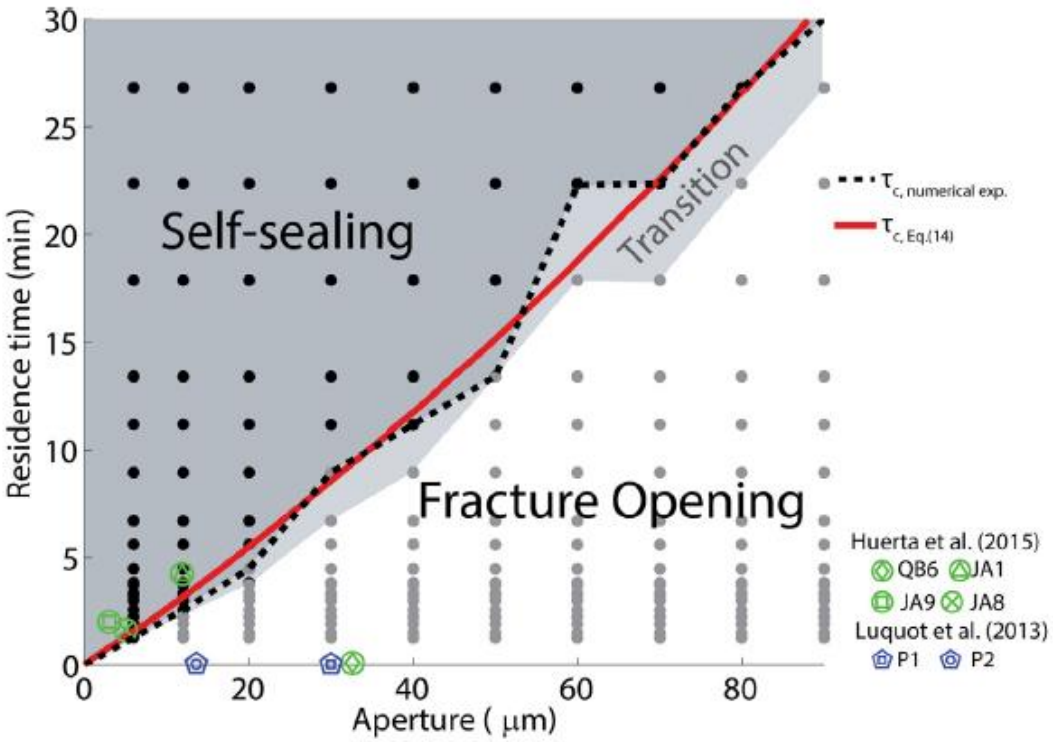

Figure 3.27 Numerical model indicate fracture opening or closing behaviour depends on fracture aperture and fluid residence time, from Brunet et al. (2016) (need to get IPR permission to reproduce)

Recent publications by NRAP (Huerta et al., 2016) and Harp et al. (2016) review the various types of models designed to examine well integrity and potential leakage rates through time. These vary from analytical solutions and systems-level models that attempt to simplify and incorporate the relevant leakage processes and may be computationally expensive and time consuming. Harp et al. (2016) describe a more computationally efficient reduced-order model extracted from a few hundred computationally expensive 3D multi-phase finite-element numerical simulations. This reduced-order model can be used to estimate CO_2 and brine leakage rates along wellbores, including abandoned wellbores (study 13 in Figure 3.26 and Table A1). The model found that extremely small amounts of the total injected CO_2 flow up the wellbore (at rates in the order of $<1 \times 10^{-2}$ kg/s). Note that this model uses Darcy-flow and so would be unsuitable for modelling very high leakage rates, such as reverse-flow wellbore scenarios. For reverse-flow a two-phase drift flux model would be more appropriate. Most workers have found that the permeability of the well leakage pathway is the most important parameter controlling the predictions of the volume and the rate of leakage (e.g., Tao et al., 2014; Harp et al., 2016).

In general, there are relatively few records relating to actual wellbore leakage rates although data examined from analogue sites suggest that both the rate and duration should be assessed. Although the rate of leakage in a blow-out event could be high (in the order of 0.3 Mt/year) they are likely to leak for much less than a year (Lindeberg, et al., in press). Smaller cement or casing leaks could be lower (mostly less than 0.1 t/year but up to 100 t/year, Duguid et al., in press) but potentially of longer duration if not detected or mitigation is not cost-effective. A selection of rates examined for this study are shown in Figure 3.26 and explained in more detail in Table A1.

3.6 Review of modelling studies

The relationship between the mechanism and expected rates of migration, and review of computational modelling undertaken to assess this is considered here. However, this review of modelling of migration mechanisms and rates excludes: leak detection and monitoring, e.g. through pressure signals, surface monitoring; modelling of CO_2 once it has reached the surface/sea bed; probability estimation of leakage (Zhang et al 2009); consequences of leakage.

3.6.1 Introduction

The overburden is often very complicated and includes a large volume of rock encompassing a variety of geological strata. Detailed geological models of the overburden are expensive to produce and can easily become excessively detailed and specific to the site modelled, reducing applicability to only the final stages of site characterisation. Although a wide range of geological features may be present in the overburden, it is important to maintain a good balance between capturing the important geological features and focusing on the questions that the modelling aims to answer. Simplified overburden models generally categorise strata into homogeneous layers with distinct properties. The strata are often grouped into aquifers and aquitards, enabling the computational expense of flow modelling to be reduced and worthwhile predictions of CO_2 flow to be simulated at a reasonable scale. Sites with overburden sequences with multiple layers of low permeability strata are preferred as these may provide additional trapping for CO_2 in the event of leakage from the target reservoir. The simplification of the overburden into a small number of distinct layers also allows for CO_2 migration in shallower aquifers to be modelled (Aoyagi et al., 2011; Harp et al., 2016) and lateral spreading of CO_2 leading to flow through additional leakage pathways (Cavanagh and Rostron, 2013; Hou et al., 2014; Huang et al., 2015; Wang et al., 2015).

Modelling of the migration of CO_2 in the overburden above a storage site is difficult because the leakage is always, to an extent, unexpected; permitting of the operation would not have been possible if there was a known flow pathway through the overburden to the surface through which CO_2 was predicted to travel. As a result, the models considered in this review are either used to estimate maximum amounts of leakage from small, unpredictable pathways or, with hindsight, to determine further information about a known leak from an existing operation.

Appraising the potential for leakage through faults and historical wellbores is an important component of site characterisation and selection. Excessive leakage not only undermines the purpose of CO_2 storage but might also have an adverse impact on the local environment. However, the obligation for proven zero leakage from every operation is unrealistic, if only in terms of the monitoring systems required for such a high level of confidence. Hepple and Benson (2005) recommend a maximum allowable leakage rate below which the CO_2 storage operation is viable. The quantification of probable leaks and likely flow paths is therefore essential to assess the severity of any observed leakage and facilitate suitable interventions, as required. Modelling of CO_2 leakage in the overburden can provide insight where other sources of information are not available.

Back-modelling of detected CO_2 leaks is used to build on observed data regarding the leak, for example pressure drops during an injection operation, to estimate other properties of the leak (such as flow rate; size and permeability of the flow pathway). In connection with this are controlled release experiments in the shallow subsurface (e.g. QICS, CO_2 Field lab in Section 6).

The overburden can extend hundreds to thousands of metres deep and CO_2 travelling from a given reservoir to the surface is likely to experience large changes in both pressure and temperature. The resulting phase changes in the CO_2 can have a significant effect on its migration in the overburden. During leakage CO_2 moves from a supercritical phase in the storage reservoir to a gaseous phase nearer the surface. The rapid changes in density associated with this phase change should be accounted for in any mathematical model of CO_2 flow from the reservoir to the surface. This adds additional complexity to numerical and analytical models of the system. In applicable circumstances, including sufficiently low temperatures and pressures, condensation of CO_2 can reduce leakage flow rates by up to 50% when compared to isothermal conditions (Ramachandran et al., 2014).

The aim of this section is to review existing computational modelling of CO_2 leakage and flow in the overburden and explore the relationship between mechanism and expected rates of CO_2 migration. The section is divided to focus on flow through faults and fractures (Section 3.6.2) and abandoned wellbores (Section 0); for modelling of fluid migration via chimneys see Section 3.2.1.2.

3.6.2 Fault modelling

Faults in the cap rock and overburden of a CO_2 storage site can provide permeable pathways for CO_2 leakage through an otherwise sealing cap rock, as discussed in Section 3.1. This has also been observed at natural CO_2 reservoirs, for example in Utah, USA (Dockrill and Shipton, 2010) see Section 6.2.

There are two general categories of large or small faults that are modelled in relation to CO_2 storage and the overburden, based on whether or not they are imaged on seismic data. Large faults are detected and analysed at the site characterisation stage of an operation while smaller sub-seismic faults, although not visible in seismic surveys, might also provide migration pathways for CO_2. These sub-seismic faults are much more likely to occur in the field without prior knowledge and therefore pose some level of risk to almost all CO_2 storage operations (Zahasky and Benson, 2014).

The standard method for modelling CO_2 flow in porous media uses Darcy's law as the constitutive equation that describes fluid flow. Darcy's law is valid for the moderate to high flux rates encountered during active CO_2 injection operations, particularly in the region surrounding the injection well. An alternative modelling approach is to use invasion percolation theory (e.g., Cavanagh and Rostron (2013)), which assumes capillary-limit conditions to simulate the CO_2 migration; this theory is valid for low flux rates at the basin scale.

3.6.2.1 Static modelling of fault geometry

One of the most difficult aspects of modelling flow along and through faults is the characterisation and quantification of the properties of the fault and surrounding

geology. Parameters such as the in situ stress field, fault location, extent, permeability and strength all have a large impact on rates of leakage (Vialle et al., 2016). This can easily become fault specific and includes a large amount of uncertainty with parameters, which often can only be accurately deduced by reverse-modelling of observed leakage. The usual methodology for approximating these parameters is to use estimated initial values and carry out a sensitivity analysis to assess the impact of the uncertainty and best or worst case scenarios (Zahasky and Benson, 2014).

There is a wide range of geometric approaches to modelling flow of CO_2 along a fault published in scientific literature; however, modelling of the majority of fault systems is based around idealised, linear faults and fault systems. The most simplified models consider a fault as a one-dimensional feature with a single permeability value that is higher than the surrounding host rock along its entire length. The most popular geometrical representation of a fault is a continuous row of cells, which represents a fault with planar geometry. This may be as a link between the reservoir and a shallower aquifer (e.g. Aoyagi et al., 2011) or a two-dimensional addition to the model of the reservoir (e.g. Nakajima et al., 2014).

3.6.2.2 Fault geomechanical modelling

Faults are geomechanical features that respond to the stress field of the rock and strain can occur within faults as a response to pressure increases caused by CO_2 injection. This can lead to the opening of new or reactivating existing leakage pathways and allow for the migration of buoyant CO_2 from the storage reservoir through the cap rock and into overlying strata. The leakage of CO_2 from the reservoir to shallower geological units is often accompanied by a decrease in pressure, which might present the first opportunity for the leak to be detected. In turn, the reduction in pressure has a corresponding effect on the stress field in the fault, which may allow the pathways to close. This close coupling of the CO_2 plume and pressure field with the stress and strain in the fracture provides a computational challenge to model the fluid flow and geomechanical processes in a fully coupled simulation. A review of geomechanical issues relating to CO_2 storage is provided by Rutqvist (2012) which includes geomechanical and wellbore-related leakage, as well as notable seismic events. That study has a particular focus on the In Salah project, Algeria.

Ideally, the modelling of flow along fractures requires coupling to a geomechanical model to incorporate opening of new and/or existing fractures as a result of increased injection pressures. Huang et al., (2015) use pre-chosen fault locations with given properties that respond to pressures from the CO_2 injection operation as well as allowing new fractures to open/existing fractures to extend in a fully coupled numerical simulator. Similarly, geomechanical opening of (pre-existing) joints is included by Martinez et al., (2013) who use separate packages to simulate fluid flow and geomechanics, coupled at every time step.

3.6.2.3 Fault flow modelling and leakage rates

A sample of computational studies on CO_2 leakage through faults has been taken from published modelling studies and some of the relevant parameters presented in Table 3.4.

In general, increasing the length, aperture and permeability of a fault increases the potential flow rate through it. This is not obvious from the results collected in **Error! Reference source not found.** because the rate of leakage through a fault is dependent on many parameters. The supply of CO_2 to a leakage pathway is fundamental for any flux of CO_2 through the fault – if there is no CO_2 in the vicinity of the fault, then there will be no CO_2 leakage through the fault. This means that a number of factors all play a part in determining the final leakage rate of CO_2 through a fault: proximity of the injection site to the potential leakage pathway; amount of CO_2 injection; permeability of the reservoir (to allow the CO_2 to migrate to the fault); the presence of any flow barriers within the reservoir; dissolution of CO_2 into resident brine. For example, Zahasky and Benson (2014) found that the aquifer permeability was one of the most important parameters in their simulations because it ensured CO_2 supply to the leakage pathway. The aquifer permeability also has an impact on the amount of pressure that is generated from the injection operation, this can then have a knock-on effect on the geomechanics and enable wider opening of fractures.

The large number of variables involved in modelling CO_2 leakage through faults adds much complexity to the comparison of studies. Leakage rates from zero to 80 kt/year were simulated, and up to 50% of the simulated injected CO_2 escaped through faults (Table 3.4). Nakajima et al., (2014) created a conservative model with a vertical fault close to the centre of a CO_2 plume. The authors found that increasing the fault permeability didn't significantly increase leakage as expected, because dissolution of CO_2 into brine prevented buoyant CO_2 reaching the leakage pathway. The dissolution of CO_2 into resident brine in the reservoir is a well-known trapping mechanism (Section 86 which removes buoyant CO_2 from the base of the cap rock and allows gravity to draw it towards the base of the reservoir (IPCC, 2005). This process can be greatly enhanced by convection in the reservoir.

Reference	Fault dimensions	Fault permeability	Aquifer permeability and thickness	CO_2 injection rate	Leakage rate (or proportion of CO_2 leaked)
Aoyagi (2011)	50 x 500 m	10, 100, 1000 mD	100 mD	500 kt/year (30 years)	0, 6, 79 kt/year
Huang et al., (2015)	10 m-wide	0.1 mD	100 mD	0.3, 0.9, 1.6, 2.2 kt/year	Up to 1.2 x 10^{-4} m^3/s
Martinez et al., (2013)	Dynamic	Dynamic	30-50 mD, >100 m	2.85, 5.5 Mt/year (max. 30 years)	(16%, 20%)
Nakajima et al., (2014)	5 m x 1 km	100 -1000 mD	10 mD, 40 m	100 kt/year	0.2-0.6 kt/year (1% of total)
Ramachandran et al., (2014)	One dimensional	10 - 1000 mD	N/A	Continuous source (hydrostatic pressure)	12, 1200 t/year/m^2
Vialle et al., (2016)	1 m fault core plus 40−100 m damage zone	10^{-6} mD in fault core, 0.001 - 1 mD in damage zone	100 mD	Gas initially in place (10 years)	200-320 t/year (0.1-1% annually)
Zahasky and Benson (2014)	3 m x 500 m	1-1000 mD	2.8-280 mD, 68 m	0.25 Mt/year	0.1%-50%

Table 3.4 A summary of leakage rates through simulated faults (units are converted from source data for consistency in comparison)

3.6.3 Wellbore Modelling

Abandoned wellbores present potential leakage pathways through the overburden for CO_2 escaping from storage sites. The state of abandoned wellbores can be very variable depending on the date and quality of abandonment and the state of the cement (Bachu and Watson, 2006). Leakage through wellbores is generally considered as more localised than through faults and more predictable providing that the locations of historical wellbores are known.

The key assumption to determine leakage rates through wellbores is the permeability of the wellbore. Permeability is increased by degradation of the cement (Section 3.5) which can vary greatly within a single wellbore. A popular approach to incorporating uncertainty in the cement degradation is to define two distinct categories, either intact, well-bonded cement segments or degraded and/or poorly bonded cement segments. A bi-modal distribution for the permeability is then applied to the appropriate sections of wellbore (Celia et al., 2006; Nogues et al., 2012).

Some authors correlate the distribution of permeability in a wellbore to the formation it penetrates against depth (Nogues et al., 2012). Aquitards give rise to lower permeability sections than aquifers and in some studies are removed from the computation (Harp et al., 2016). Other authors use a distribution of values for the

permeability across the depth of the wellbore without correlation to the formations through which the well is drilled (Celia et al., 2006). High variability in the distribution allows for both high and low permeability segments and any low permeability segments significantly reduce leakage rates.

Stochastic methods such as Monte Carlo simulation are the method of choice for simplified models with low computational cost to analyse the impact of uncertainty in wellbore permeability and provide confidence intervals for leakage rates. Also, working backwards, likely parameter ranges for degraded cement, constrained to not produce leakage rates greater than an imposed limit, can be established (Nogues et al., 2012).

3.6.3.1 Geochemical wellbore modelling

Processes of CO_2 dissolution in water and water in CO_2 can enhance geochemical reactions which degrade the casing and cement of wells (Section, 3.5.2), as mentioned by Wang et al., (2015). A small pathway through the cement of a wellbore in a CO_2 reservoir can bring acidic waters to previously inaccessible places and increase the size of the pathways (see also Deremble et al., 2011). This is self-enhancing leakage and requires the coupling of chemical processes with CO_2 flow, adding an additional layer of complexity to the model. Self-sealing leaks are also modelled and occur through the precipitation of solid material/minerals from CO_2 flow and can be relevant to other flow pathways as well as wellbores (Huerta et al., 2016).

3.6.3.2 Reduced Order Methods

Many attempts to find computationally cheap solutions to the complex system of CO_2 leakage have been sought (Harp et al., 2016; Nordbotten et al., 2004; Nordbotten et al., 2005). For example, the focus of Wang et al. (2015) is on a collocation method. The Euler-Lagrangian method is an attempt to reduce the computational expense of full numerical modelling of a CO_2 plume spreading under a cap rock, migrating up a permeable wellbore and forming a plume in a shallower aquifer. This is one of many attempts to find computationally cheap solutions to the complex system of CO_2 leakage (Harp et al., 2016; Nordbotten et al., 2004; Nordbotten et al., 2005).

3.6.3.3 Modelled wellbore leakage rates

A summary of wellbore leakage rates arising from models in the literature is given in**Error! Reference source not found.** Table 3.5. Wellbore permeability values are widely ranging (0.01 µD – 100 D) giving rise to a correspondingly large range of leakage rates.

Source	Wellbore dimensions	Wellbore permeability	Aquifer properties	CO_2 injection rate (duration of injection)	Other information	Leakage rate (proportion of CO_2 leaked by end of simulation)
Aoyagi *et al.,* (2011)	Productivity index: $3x10^{-13}$, $1x10^{-12}$, $6x10^{-12}$ m^3		100 mD	500 kt/year (30years)		27, 76, 200 kt/year
Celia *et al.,* (2006)		0.01 µD-0.1 mD (mean values)		1.58 t/year (50 years)	502 wells in total; uncorrelated	0.1% -1%
Harp *et al.,* (2016)	0.1 m square	10 m D-10 D	10 -1000 mD	6.3 - 63 kt/year		16 - 250 t/year (10^{-8}% - 0.1%)
Nogues *et al.,* (2012)	0.15 m (radius)	10 µD (intact sections), 1 mD -100 D (degraded sections)		12.3 Mt/year (50 years)	39 wells	10^{-5}% - 12% per year
Wang *et al.,* (2015)	0.15 m (radius)	1000 mD	30 m	280 kt/year (approximately 2.7years)		0.1 m^3 (30 days)

Table 3.5 A summary of simulated leakage rates through abandoned wellbores from the literature. Units have been converted for consistency. The ranges of wellbore permeability values typically refer to the parameterisation of different sections along the length of the wellbore

4 Overburden trapping potential

When CO_2 is injected into a geological storage site it will migrate through the reservoir and displace some of the native pore fluids and therefore the CO_2 needs to be injected at a greater pressure than the existing reservoir pore pressure. Once in the reservoir rock the CO_2 will be retained by one or more trapping mechanisms. The trapping mechanisms are introduced in Section 4.1, an overview of processes and relative timescales of overburden trapping mechanisms is presented in Section 4.2. Overburden trapping by CO_2 hydrate formation is summarised in Section 4.3.

4.1 Trapping Mechanisms

There are three main types of trapping mechanism that can occur during the geological storage of CO_2: 1) physical, related to retention of buoyant fluids by stratigraphic/structural seals; 2) residual or capillary trapping; and 3) dissolution and mineralisation (IPCC, 2005). These mechanisms occur over different timescales during the lifetime of CO_2 storage (Figure 4.1).

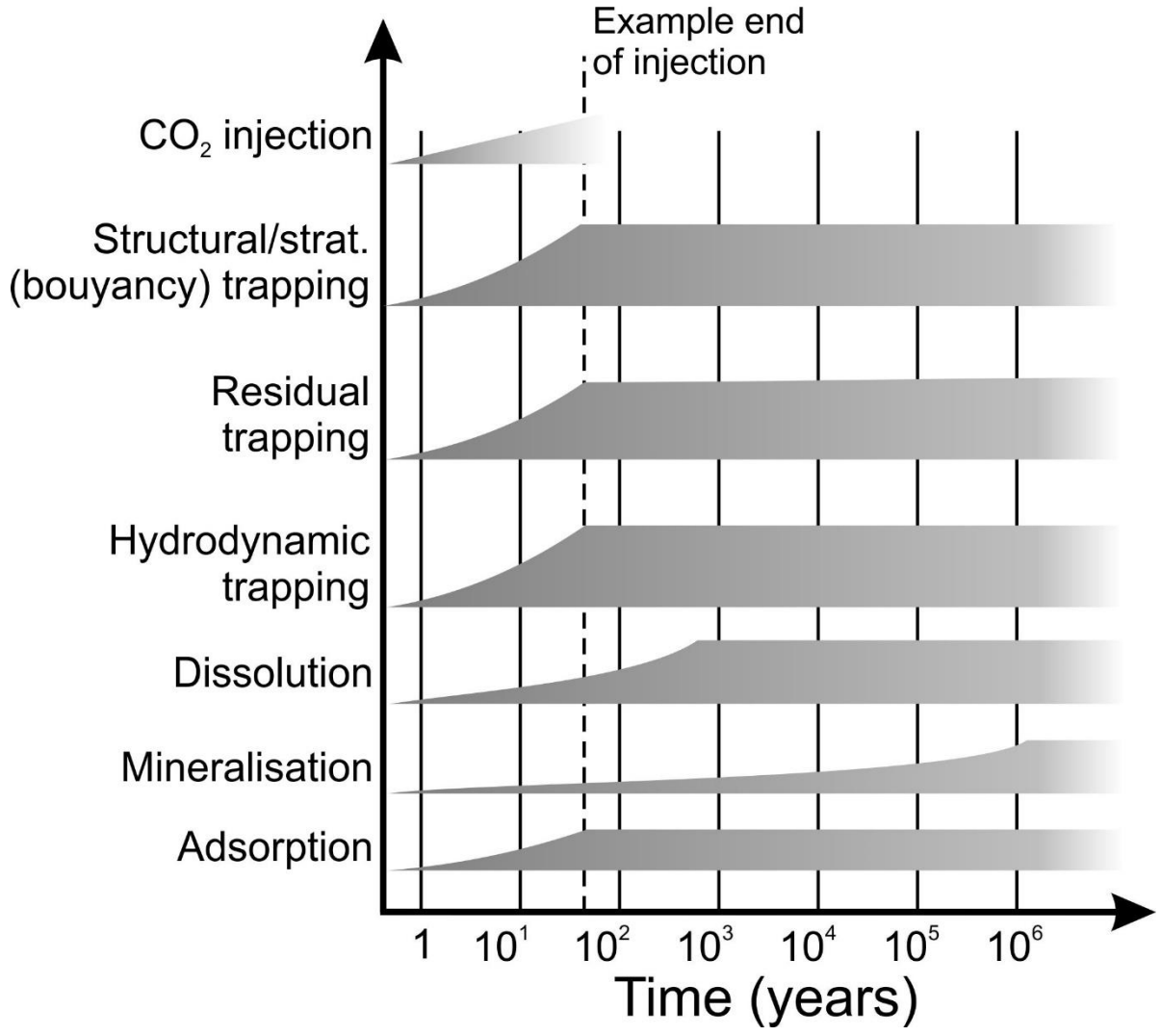

Figure 4.1 Operating time-frame of the various trapping mechanisms (modified from IPCC, 2005) Structural/ stratigraphic trapping relates to buoyancy-driven trapping.

4.1.1 Physical Trapping

Physical trapping is the result of CO_2 being stored as either a free gas or supercritical fluid. There are two types of physical trapping:

1. *Static trapping* is storage within a closed trap such as a stratigraphic or structural trap that confines the CO_2 due to presence of a low permeability barrier, creating a larger capillary entry pressure which prevents CO_2 from migrating vertically (e.g. Bachu 2015; Heath et al.2012; Krevor et al., 2011). This process is similar to the way in which hydrocarbons may be trapped by low permeability barriers. The pore space is occupied by native pore fluids that need to be displaced.
2. *Residual-saturation trapping* in pore spaces occurs as CO_2 moves through the reservoir. Some of the CO_2 remains trapped in the pore spaces, by snap-off of the non-wetting CO_2 (e.g. Akbarabadi and Piri 2013, Bachu 2013, El-Maghraby and Blunt 2013, Ruprecht, Pini et al. 2014, Soroush, Wessel-Berg et al. 2014, Zuo and Benson 2014, LaForce, Freifeld et al. 2015, Trevisan, Pini et al. 2015, Dance and Paterson 2016, Herring, Andersson et al. 2016, Rahman, Lebedev et al. 2016, Zeidouni, Hovorka et al. 2016). .

4.1.2 Dissolution trapping

The rate of CO_2 dissolution into pore water is dependent on the temperature, pressure and salinity of the native fluid. Once the CO_2 has dissolved it remains trapped in solution in the pore water (CSLF, 2007). This pore water is slightly denser than the surrounding CO_2-free pore water which can lead to gravitationally instabilities and which can lead to downwards migration of CO_2-charged formation water. There is potential for large masses of CO_2 to be dissolved, but it is dependent on the solubility of the CO_2 and the extent to which mixing occurs within the reservoir. Exposure to ‘fresh’ non-saturated brine will enhance dissolution trapping and convectional mixing is one process that increases exposure to unsaturated brine.

4.1.3 Hydrodynamic trapping

Under certain conditions CO_2 may migrate in the subsurface extremely slowly and/or over long flow pathways. It could become trapped via a combination of physical or chemical trapping, known as hydrodynamic trapping (e.g. Altman 2014). This mechanism is active when CO_2 is injected into an aquifer. If aquifer flow is present, the CO_2 will migrate in the same direction as the natural flow in the reservoir. Hydrodynamic trapping occurs via a combination of any of the above described mechanisms which may be simultaneous but at different rates and is not specific to physical or chemical trapping. Eventually, possibly after millions of years, no mobile free-phase CO_2 will remain in the system as it is trapped by residual-saturation trapping, dissolution and mineral precipitation.

4.1.4 Chemical trapping

1. Chemical trapping is the result of CO_2 reaction between the CO_2 and pore fluid and reservoir matrix. There are three types of chemical trapping: mineral

trapping; adsorption trapping; hydrate trapping. Mineral trapping requires initial dissolution of CO_2 in pore water. *Mineral trapping* occurs when there is a chemical reaction either between the pore water or the reservoir rock leading to the formation of new minerals. Chemical reactions with the reservoir rock will occur over much longer timescales than reactions with pore water. These chemical reactions are dependent upon the pore water chemistry, rock mineralogy and the length of the migration path.

2. *Adsorption trapping* where CO_2 is adsorbed onto coal surfaces. CSLF (2007) state that storage through adsorption is the only significant trapping mechanism for coal storage.
3. *Hydrate trapping* where CO_2 forms a white, ice-like solid (or hydrate) when mixed with water under appropriate pressure and temperature conditions. Hydrates form rapidly (in a matter of minutes) and hydrate trapping is particularly relevant to migration of CO_2 within the overburden to storage sites in high latitudes: it is considered in more detail in Section 4.3.

4.2 Overview of processes and timescales of overburden trapping mechanisms

An overview is presented of the processes and timescales of overburden trapping mechanisms. Selected analogue studies of physical and chemical (dissolution and mineral) trapping mechanisms and the factors that aid or hinder increased trapping are reviewed in Sections 4.2.1 and 4.2.2, respectively.

The three dominant processes that can affect the natural attenuation of CO_2 that is migrating through the overburden are physical trapping, dissolution and potential mineral precipitation (typically carbonate precipitation) and capillary trapping, as with trapping in the storage reservoir. The physical migration of CO_2 through the overburden will be controlled by viscous, capillary and gravity forces which will determine the potential for secondary accumulation and lateral migration within a highly permeable lithology or fault (Manceau et al., 2014; Nordbotten et al., 2005; Pruess, 2008).

The physical and chemical properties of CO_2 indicate the potential for self-enhancing leakage. Relevant properties include: (1) lower density than the aqueous phase, enabling buoyant flow and pressure increases at shallow depth; (2) much lower viscosity than water, providing for much greater volumetric flow rates for given driving pressures; (3) notably larger compressibility than aqueous fluids, providing for much greater volume expansion upon depressurisation with associated potential for cooling which can limit CO_2 fluxes (see Pruess, 2008 for discussion). Natural analogues indicate that self-limiting processes can also occur.

Simulations of fault-controlled CO_2 migration indicate that the greatest attenuation is likely to occur in permeable layers near to the storage reservoir (Chang et al., 2009). Chang et al. (2009) concluded that the rate of attenuation of CO_2 leakage depends on geometric and/or petrophysical properties of highly permeable structures as well as reservoir properties (such as permeability). Where groundwater flow predominates over any regional pressure gradient, for example under pressure management to

control flow or leakage, viscous effects can enable continued CO_2 mobility in secondary aquifers (Manceau et al., 2013). Heterogeneity within the overburden, i.e. a wide range of permeability values, will increase the rate of dissolution (e.g. Farajzadeh et al., 2007). Furthermore, Manceau et al. (2013) also concluded that, as may be expected, higher capillary threshold pressure increases the trapping potential of secondary aquifers through residual trapping and dissolution.

The formation of secondary accumulations, whilst providing secondary trapping potential, may also provide further routes to leakage if high-permeability pathways connect these secondary accumulations to the surface. Fluxes to the surface are balanced by the size of these secondary accumulations and the permeability of connecting pathways (Pruess, 2008, 2011).

4.2.1 Analogue for physical trapping in the overburden – south-east Utah

Some evidence for attenuation can be drawn from studies of natural CO_2-rich springs with fault-controlled fluid migration in the Colorado Plateau of south-east Utah (Jung et al., 2014). Chemical and isotopic evidence (Assayag et al., 2009; Baer and Rigby, 1978; Heath et al., 2009; Kampman et al., 2009, 2012; Mayo et al., 1991; Shipton et al., 2004; Wilkinson et al., 2009) and a borehole drilled to a depth of 322 metres through CO_2-containing aquifers (Kampman et al., 2014a,b) indicate that free CO_2 is formed by exsolution from within the aquifer and fault system. This enables migration of free CO_2 from deeper reservoirs (>2 km depth) which mixes with meteoric water being fed from nearby recharge in the San Rafael Swell (Hood and Patterson, 1984). The recent summary on the distribution of CO_2 accumulations across the south-east Utah analogue by Jung et al. (2014) provides an instructive case study of the implications this has for both formation and fault-controls on potential trapping mechanisms. Here, the Little Grand Wash Fault in the wider CO_2 system of south-east Utah, located in an uplifting extensional setting, has been shown to be a major conduit of free CO_2 and CO_2-rich brines. However, this and other faults can also act as a barrier to lateral flow where low permeability rocks occur in the hanging wall. Jung et al. (2014) postulate that the vertical migration of CO_2 is likely to be hampered by low permeability zones and localised fault gouges that would also enable lateral migration. This creates local pools of CO_2 within the anticlinal trap. These pools control the distribution of surface expressions of CO_2 leakage, namely the many well-known CO_2-rich springs in the area, such as Crystal Geyser. As the CO_2 migrates upwards its solubility decreases significantly (Wilkinson et al., 2009) and, with the local geothermal gradient, this exsolution increases significantly at depths of less than 650 metres.

4.2.2 Dissolution and mineral trapping in the overburden

During its migration, CO_2 will dissolve (Section 4.1.2) to form weak acid which may react with the rocks through which it passes, including clay seal rocks (e.g. Gaus *et al*., 2005, Johnson *et al*., 2005 and Liu et al., 2012). This CO_2-rich fluid could react with any carbonate and oxy-hydroxide (mainly ferrous) phases which will equilibrate the pH of the CO_2-rich fluid to around a value of 5. Subsequent reaction with silicate minerals (feldspars and phyllosilicates) will be significantly slower but result in increased pH and possible re-precipitation of carbonate minerals (mainly siderite and calcite). Kampman *et al.* (2009) provide field evidence for the dissolution of feldspars

along a groundwater flow-path that intersects the CO_2-conducting faults in south-east Utah. Although such reactions may also occur in low-permeability mudstone, the reaction rate in such rocks is controlled by diffusion. Recent investigation from field studies suggest that this self-healing mechanism, dissolution followed by carbonate precipitation, is likely to occur in diffusion-controlled mudstone (Kampman et al., 2016).

CO_2 dissolution into pore water will increase the natural attenuation potential of the overburden, though this is dependent on the temperature, pressure and salinity of the native fluid. Once the CO_2 has dissolved it can remain trapped in solution in the pore water. This CO_2-saturated or partially saturated pore water is more dense than unsaturated formation water and will sink to the bottom of the formation (e.g. Lindeberg and Wessel-Berg 1997, Ennis-King and Paterson 2003, Ennis-King and Paterson 2005). There is potential for large volumes of CO_2 to be trapped in this way, but it is dependent on the solubility of the CO_2 and whether mixing occurs within the formation. This mechanism of trapping can take thousands of years to achieve maximum dissolution and CO_2 saturation within the pore water. In dynamic flow systems, such as under active groundwater migration in the overburden, dissolution trapping could be more extensive. However, if such CO_2-rich water migrates to shallower depths then the CO_2 in solution can exsolve, as has been observed in some analogue systems (see below). Snippe and Tucker (2014) also showed that the faster a CO_2 plume migrates, the more undersaturated water it contacts and hence the greater the dissolution. Therefore, greater lateral migration will lead to more dissolution of CO_2.

Simulations of leakage along faults suggest that variable permeability values along a fault, due either to changes in stress, fault geometry or the presence of fault fills can reduce the rate of fracture flow. Variable permeability values also increase the potential for CO_2 dissolution as the surface area between the CO_2 and the surrounding brine increases (e.g. Carneiro 2009; Watson et al., 2012). Simulations by Iding and Blunt (2011) led them to conclude that the relative increase in CO_2 dissolution in a system is reduced as more fractures are added to the system. Chang et al. (2009) proposed that the amount of CO_2 reaching the surface after leaking through a highly permeable fracture can be reduced if the fracture intersects suitably permeable formations within the subsurface. Their modelling indicated that the amount of CO_2 reaching the surface after leaking from the storage formation is lower when the fracture intersects a greater number of rock layers with high permeability values. Watson et al. (2012) concluded that convection-enhanced dissolution, following much slower diffusion-driven dissolution, can occur in fractures that pass through permeable strata, although the rate of dissolution will decrease over time.

4.3 Hydrate trapping of CO_2

Carbonate minerals are not the only potential secondary solid phases/minerals that could trap CO_2. Under elevated pressures and cool temperatures (typically <10°C and >35 bar pressure) CO_2 hydrate is stable and there are geological situations where this may play an important role in trapping CO_2 within the overburden to the CO_2 storage site. This ‘cool storage’ approach has received relatively little attention, even though it

may offer certain advantages in terms of long-term containment of CO_2 (e.g. Koide et al., 1997, Rochelle et al., 2009; Burnol et al., 2015).

Geographical locations where CO_2 hydrate might form include: within shallower sediments below the floors of deep, cold oceans surrounding continental landmasses; and below permafrost. For the latter, glacial and periglacial processes will play an important role in determining subsurface pressure and temperature conditions , and these need evaluation when considering CO_2 storage complexes beneath permafrost. In this section, we only consider present day permafrost (appropriate to northern, high-latitude regions), although the processes could be extended to far future conditions.

Here we concentrate on conditions where CO_2 hydrate might play a role limiting CO_2 migration through the overburden above a CO_2 storage complex. CO_2 hydrate formation would provide a back-up trapping mechanism should deeper barriers be breached, effectively building 'redundancy' into the storage scheme. If the CO_2 storage complex lay below a deep enough and cold enough body of water, or below a region of thick permafrost, then upward-migrating CO_2 could enter a zone of CO_2 hydrate stability within the sediments. The formation of CO_2 hydrate could then enhance any natural low permeability cap rock, slowing the ascent of CO_2, or even possibly blocking flow pathways. Once in the CO_2 hydrate stability zone, this would be facilitated by the ability of CO_2 hydrate to form relatively rapidly under appropriate conditions (e.g. Sakai et al., 1990; Brewer et al., 1999; Riestenberg et al., 2004; Someya et al., 2006).

Many gases form hydrates and hydrates of mixed composition can be formed. Impurities present in the CO_2, such as SO_2, H_2S etc., can also form hydrates, and these can be more stable than CO_2 hydrate. However, even if included in the CO_2 waste stream, we anticipate that their relative chemical reactivity will limit their abundance in a deep geological CO_2 store. In this review we consider pure CO_2 hydrate as a limiting case.

4.3.1 Stability of CO_2 hydrate in the North Sea under present-day conditions

An assessment of the location and thickness of sediments offshore Western Europe that exist within the CO_2 hydrate stability zone is presented by Rochelle *et al.,* (2009). In summary, key requirements are overlying cold and deep waters, and so CO_2 hydrate is not stable in sediments below the relatively shallow waters around the UK and north-west Europe (Figure 4.2). Thus, for example, under present-day conditions CO_2 hydrate should not form within or above CO_2 storage facilities below the North Sea (although see comments at the end of the hydrates text section).

For present day conditions at a site such as Sleipner, Rochelle and Long (2008) found that CO_2 hydrate is not stable, even for the most dilute fluids. Even adjusting for an extra 80 metres of hydrostatic head and a reduction in surface temperature to 7°C (to account for conditions on the sea bed at Sleipner), CO_2 hydrate would remain unstable.

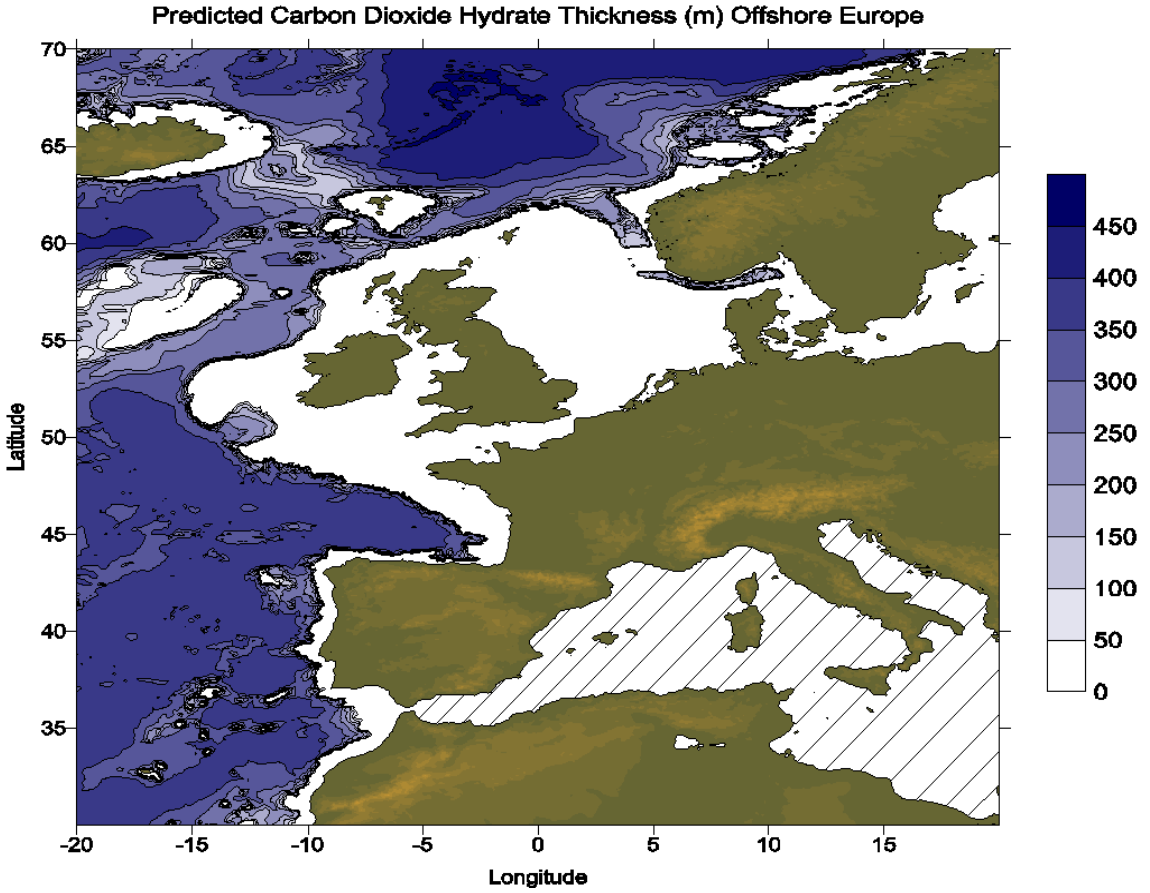

Figure 4.2 Map of predicted thickness (in metres) of the CO_2 hydrate stability zone within seabed sediments offshore Western Europe (from Rochelle et al., 2009). Note that the Mediterranean Sea is not covered by this study.

4.3.2 Stability of CO_2 hydrate in permafrost areas

Rochelle and Long (2008) undertook hydrate stability calculations with reduced temperatures to represent permafrost conditions that could be present in high latitude regions. CO_2 hydrate was found to be stable within the relatively shallow geosphere. The depth below surface varied with temperature and groundwater salinity, but for dilute groundwaters could form over a depth range from less than 200 metres deep to over 800 metres deep, given average annual subsurface temperatures from -3°C down to -10°C.

It should be noted that the reduction in temperature in the subsurface could also affect the phase of free-phase CO_2, even if it lies at depths outside hydrate stability. Consequently, for the geothermal gradient used by Rochelle and Long (2008), liquid CO_2 could be the stable phase of CO_2 down to approximately 1600 metres. In such circumstances, free-phase CO_2 stored at shallower depths would be a liquid, rather than a supercritical fluid, and have a consequent reduction in volume and increase in density. Both of the latter would reduce further the potential for upward migration and escape of CO_2.

4.3.3 Uncertainties regarding CO_2 hydrate trapping

CO_2 hydrate requires only gas and water to form and will do so relatively readily in the appropriate conditions of pressure, temperature and fluid composition. However, whether it will form will also depend on there being a sufficient supply of CO_2 to exceed

local CO_2 hydrate saturation (see Rochelle et al., 2008). Thermodynamic constraints mean that it is slightly easier to form in larger pores compared to very fine-scale pores. However, once it begins to form, exactly what morphology it will take is less clear. If it behaves like methane hydrate, then it might form pore- or fracture-filling cements, or as nodular masses that displace sediment. We are still some way from understanding the control of hydrate morphology.

Ultimately, whilst the formation of CO_2 hydrate is controlled by thermodynamic and kinetic constraints, there can be situations where it may be stabilized in regions apparently outside its expected stability zone. Hence, it may also be able to form locally, within sediments seemingly too warm to form hydrate. A preliminary study by Pruess (2003) modelled what would happen if liquid CO_2, rising along a flow pathway, such as a fracture, started to boil off as it depressurized. The latent heat of vapourization required to boil off the CO_2 would cool the surrounding rocks, possibly to the point at which CO_2 hydrate, or even ice, would form. As a result, flow pathways could be reduced or even blocked. In the Pruess (2003) model, a cool zone several hundreds of metres thick was predicted to form, which could slow the ascent of the CO_2 and cause it to spread out laterally. This might help retard the ascent of CO_2, allowing it more time to dissolve in pore waters, and potentially precipitate as carbonate minerals. However, the preliminary model was somewhat idealized, and needs to be improved with more realistic geological structures, and is a model without experimental verification. Further work is needed to investigate localized cooling during CO_2 ascent.

5 Evaluation of current characterisation methods

The principal objective of overburden characterisation is to determine the nature of the strata overlying a CO_2 storage site and inform an assessment of the potential of those strata to retain or enhance migration of CO_2. The information gained from overburden characterisation is used to drive an assessment of the potential risk for CO_2 migration through the overburden. Ideally, characterisation would indicate layered, undisturbed strata that might contain fluids, or provide evidence of containment of fluids, over geological timescales. If there is an indication of any features in the overburden that disrupt the strata, appropriate for that specific environment and setting, they will be identified as part of a risk assessment process. Any consequent risk reduction activities would be targeted to reduce or mitigate the potential for CO_2 migration through the overburden.

The techniques and methodologies employed for overburden characterisation can be similar, but more shallowly focused, than those used for characterisation and monitoring of the underlying storage reservoir and the primary seal formations.

Characterisation of the overburden for site assessment will also provide a baseline of observation for any future operation and monitoring of a storage site (see also IEAGHG, 2015). For ‘baseline’ characterisation it is essential that temporal (diurnal, seasonal, non-systematic) and areal variations are established. A key requirement in the characterisation of overburden strata is the necessary spatial coverage to adequately ensure any features that disrupt the overburden are observed. In particular, where there may be overburden features that have the potential to promote lateral migration, due to their extent and geometry, away from those strata directly above a storage site.

Characterisation techniques and methodologies can be considered under two main categories according to depth below surface: surveillance of the shallow subsurface, near seabed, sea bed and water column; deep-focused surveillance of the deeper overburden. Shallow–focused characterisation methods are reviewed in Section 5.1 and deep-focused methods are reviewed in Section 5.2.

5.1 Shallow-focused characterisation methods

Shallow-focused characterisation methods differ significantly dependant on where they are deployed. Techniques that are effective in terms of deployment, accessibility and cost for onshore sites (Section 5.1.1) may not be suitable for use in offshore sites (Section 5.1.2). The monitoring review by IEAGHG (2015) provides detail on offshore techniques and some comparison with onshore methods that are relevant to characterisation of the overburden since the techniques and methodologies employed are similar.

5.1.1 Shallow onshore characterisation

A variety of geophysical and geochemical methods have been applied to shallow site characterisation onshore. So far there has been no significant leakage from any pilot or large-scale storage sites so experience of monitoring migration is limited to natural gas seeps and experimental injection sites.

The tools for onshore shallow-focused characterisation are essentially those also deployed at natural seepage and experimental release sites that are reviewed in the following sections.

5.1.1.1 Near-surface gas characterisation and monitoring

Shallow-focused tools for characterisation and monitoring have been tested at a variety of onshore sites of natural CO_2 seepage. Those studied in Europe include: Latera, Italy (Bateson et al., 2008; Beaubien et al., 2008; Lombardi et al., 2008), Laacher See, Germany (Gal et al., 2011; Govindan et al., 2013; Krüger et al., 2011), Sainte Marguerite, France (Battani et al., 2010; Gal et al., 2012) and Florina, Greece (D'Alessandro et al., 2011; Ziogou et al., 2013). More recently CO_2 emissions have been examined along the Bongwana Fault in South Africa (Johnson et al., In press).

Shallow experimental injection has been carried out at a number of sites worldwide, several of which have been deliberately designed to cause migration and/or leakage to the surface. These range from very shallow injections (2 m depth or less) such as ZERT, USA (Spangler et al., 2010), Ginninderra, Australia (Feitz et al., 2014a), ASGARD, UK (Smith et al., 2013), Resacada Farm, Brazil (Moreira et al., 2014) and Grimsrud Farm, Norway (Moni and Rasse, 2014) to deeper tests. A shallow aquifer test in Denmark injected at 10 metres depth (Cahill and Jakobsen, 2013), the Maguelone site, France at 15 m (Pezard et al., 2016), the CO_2 Field Lab in Norway at 20 metres (Barrio et al., 2014; Jones et al., 2014) and a Mississippi aquifer experiment at 50 metres (Trautz et al., 2012). Currently sites are planning further injection tests, such as those proposed at Otway (30 m depth), at a number of sites in South Korea (e.g. Lee et al., 2016), the GeoEnergy Test Bed, UK (up to 200 m), Sulcis, Italy (fault and pilot scale injections) and Field Research Station, Canada (300 and 500 m depths).

Near surface gas monitoring encompasses measurements of soil gas, gas flux through the soil to the atmosphere and atmospheric gas concentrations close to the ground surface. The primary objectives are the detection of seepage and quantification of any emissions to the atmosphere. There are several approaches to this monitoring; spatial coverage to detect potential anomalies, continuous monitoring at selected sites and source attribution. Anomaly detection normally relies on an adequate definition of temporal and spatial baseline variability.

Industrial-scale CO_2 storage sites have a potentially large surface footprint (typically hundreds of square kilometres). However, leakage at both natural and experimental sites tends to occur most obviously at seeps with a small surface area, normally metres to tens of metres across, (Feitz et al., 2014b and natural and experimental site references above). Where leakage might occur is difficult to predict; faults or fractures usually only leak at small numbers of discrete seeps (e.g. Annunziatellis et al., 2008; Johnson et al., In press); leakage associated with wells might occur at or near the well head, but if it is related to casing defects then it could follow any higher permeability pathway away from the well. For example, the surface manifestation of leakage from gas storage at Hutchinson, Kansas in 2001 was several kilometres away from the leaking well (Allison, 2001). Thus leakage detection is likely to require the location of small features in a large search area.

Wide-area methods have been attempted with some success, but without yet coming close to a single definitive approach. Remote sensing can detect vegetation changes caused by CO_2 seepage. It has excellent areal coverage but is prone to false positives (Bateson et al., 2008; Govindan et al., 2013). Ground-based mobile methods (Jones et al., 2009), or the use of sensors on low-flying Unmanned Aerial Vehicles (UAVs) (de Vries and Bernardo, 2011; Neumann et al., 2013) can detect seepage but take longer to cover large areas and may be restricted by ground conditions or flight regulations.

Continuous measurements have typically been deployed at wellheads or other locations selected for baseline definition. It has included soil gas monitoring (Schlömer et al., 2014), flux measurement using automated chambers or eddy covariance (Lewicki and Hilley, 2012) and fixed or scanning instruments for atmospheric monitoring (Hirst et al., 2004; Kuske et al., 2013; Luhar et al., 2014). Methods such as scanning open-path lasers (e.g. Shell's LightSource) and networks of atmospheric or eddy covariance sensors can cover a larger area, which effectively varies in size and location with wind speed and direction, as well as the number of instruments and paths scanned. The area covered with such an approach can span at least a few hundred metres. On the other hand, buried soil-gas probes, or accumulation chambers on the surface, are essentially point measurements usually at a relatively small number of locations.

Flux methods are required to quantify emissions. These could be direct chamber measurements linked to statistical analysis, modelling and mapping, as applied to volcanic emissions (e.g. Cardellini et al., 2003; Chiodini et al., 1999) or derived from eddy covariance (Lewicki and Hilley, 2009) or fixed or scanning atmospheric sensors again with significant use of statistics and modelling (Hirst et al., 2013; Kuske et al., 2013).

Whatever approach is used to identify potential leakage the source of the gas needs to be determined. If leakage does occur then any natural background flux needs to be removed before the amount of leakage can be calculated. Gas ratios have been shown to be a useful tool in source attribution (Beaubien et al., 2013; Jones et al., 2014; Romanak et al., 2012; Schroder et al., 2016). Stable isotope analysis of gas samples can also be effective, but only if the injected CO_2 has a signature distinct from that of shallow biogenic CO_2. Radiocarbon and noble gas isotopes have also been used to good effect but are notably more expensive. A range of such methods was applied by three separate teams to investigate suggested leakage at the Weyburn site in Canada (Beaubien et al., 2013; Romanak et al., 2014; Sherk et al., 2011; Trium Inc. and Chemistry Matters, 2011). Isotope ratios, or trace components in the injected gas, can act as natural tracers. Alternatively, naturally occurring or artificial tracers can be added to the injected gas to determine the source.

Sometimes, combinations of wide area, continuous and source attribution monitoring have been deployed, such as the use of isotope analysers on mobile platforms (Krevor et al., 2010) or to continuously monitor soil or atmospheric gas (Moni and Rasse, 2014). Different near-surface methods have been reviewed by Klusman (2011).

5.1.1.2 Aquifer characterisation and monitoring

The other major focus of shallow characterisation and monitoring is concerned with the protection of subsurface drinking water supplies. While dissolved and free gas measurements can be made using similar techniques to those applied for soil gas, a much wider range of both geochemical and geophysical parameters can be measured. Many of these measurements can only be made in boreholes so they are of restricted areal extent. Some geophysical methods can be applied cross-hole, providing 2-D coverage or used in a tomographic mode (e.g. Electrical Resistivity Tomography) to provide 3-D coverage. Keating et al. (2014) have shown that pressure monitoring may be more effective in detecting a leakage plume than groundwater sampling and analysis. Other geophysical methods evaluated include ground penetrating radar, electrical conductivity/resistivity and electromagnetic surveys. Some of these methods are also applicable to deep-focused monitoring and are covered in more detail in Section 6.2. A range of different techniques have been tried at a small number of experimental sites including the CO_2 Field Lab (Denchik et al., 2014), Maguelone (Pezard et al., 2016) and in Denmark (Auken et al., 2014; Lassen et al., 2015) and have been reviewed for possible use in South Korea (Lee et al., 2016).

Variation in ground water chemistry, pH, or resistivity and other geophysical parameters need to be evaluated in the context of the natural variability of the aquifer system. They must be ascertained through baseline characterisation and monitoring, before they can be ascribed to CO_2 leakage with any confidence. Characterisation baseline values vary both spatially and temporarily and with factors such as climate, geology, soil type, depth and residence time (Jones et al., 2015). The background conditions, for example pH and total dissolved solids, may dictate whether a particular monitoring approach is likely or not to be able to successfully detect leakage. Aquifers can be stratified vertically, such that techniques may not be equally effective at different depths within the same aquifer system.

As well as migration of CO_2 there exists the possibility of brine displacement into the overburden from the storage reservoir or another deep saline aquifer. This further increases the number of parameters that might need to be measured to detect migration.

A high density of characterisation and monitoring wells is unrealistic, so higher risk locations are typically targeted to keep costs reasonable. The best parameters to observe and monitor vary from site to site and they may differ for carbonate and sandstone aquifers. Yang et al., (2014) have suggested that the concentration of CO_2 (more usually expressed in water as the partial pressure, pCO_2) and pH may be a good general compromise for leakage detection. A much wider range of major and trace elements will be required to demonstrate that drinking water quality has not been impacted. A more thorough understanding of processes and source has been gained through the use of stable isotopes including C, Sr, B, Li, O and H (Humez et al., 2014; Lions et al., 2014; Newell et al., 2014). Detection of brine incursion may be possible using Cl, Br, B or Li or a proxy for salinity, such as electrical conductivity (Jones et al., 2015).

As for near surface gas characterisation and monitoring, both survey approaches, for example periodically measuring parameters in a series of wells, and continuous monitoring can be undertaken. Monitoring strategy is frequently developed after completion of a conceptual model of the aquifer(s). Continuous monitoring has the advantage that transient changes in aquifer properties can be detected that might be missed by periodic surveys. Short-lived variations have occurred in controlled field experiments, due to dissolution or desorption, but buffering or slower rate reactions may later dampen down these effects (Cahill et al., 2014; Trautz et al., 2012).

5.1.2 Shallow offshore characterisation

Methods commonly used to characterise shallow (less than 200 m beneath sea bed) overburden to potential offshore CO_2 storage sites include: sea bed imaging; subsurface imaging; sea bed morphological monitoring; gas bubble/water column monitoring; chemical analysis; and biological analysis. The above techniques and applications are discussed below, followed by a brief summary of their effectiveness, limits of resolution, and use in the three offshore sites described in Section 2.

5.1.2.1 Video and Camera Imaging

High-resolution video and still camera technology are widely available and may be towed or deployed on Autonomous Underwater Vehicles (AUV), landers and Remotely Operated Vehicles (ROV). Imaging systems provide direct visual evidence for conditions at the sea bed and in the water column and are particularly important for the assessment of sea bed morphology, gas bubbles, and biological indicators for site characterisation, as discussed in the following sections. The usability of the resulting images is dependent, however, on a number of factors including suspended sediment, weather conditions, and variation in distance from target when towed or attached to equipment. Video and still camera technology for deployment underwater is relatively inexpensive. Visual images from towed underwater cameras have been recently used, for example, to identify bacterial mats indicative of natural seepage sites hundreds of kilometres to the west of the UK (Stewart et al., in press).

Video and still camera imaging is routinely collected in any underwater infrastructure project, including, for example Slepiner, where continuous video footage obtained from the ROV used to deploy equipment was obtained in 2002, 2005 and 2009. The results of monitoring the seabed during this time revealed normal sea bed conditions (Chadwick and Eiken, 2013).

5.1.2.2 Subsurface imaging

Acoustic methods commonly used to image the subsurface are crucial to characterisation of the shallow overburden, particularly because they are very likely to detect fluid flow evidence due to the large acoustic impedance contrast between gas/brine and sediment. Features indicative of natural and human-influenced migration are well documented within numerous examples from 2D and 3D seismic data. Seismic data also characterise the architecture of the subsurface and are particularly useful for assessing the sealing capacity of the shallow overburden in regions, such as the central and the northern North Sea, which comprise thick sequences of relatively unconsolidated sediments (Lumley et al., 1997). 3D seismic

data, in particular, are key to identifying buried landforms in the shallow subsurface, which may affect sealing capacity, for example the glacial tunnel valleys or pockmarks discussed in Section 3, which are more challenging to image using 2D profiling.

The presence of fluids and gas in the shallow section within seismic data are usually indicated by acoustic blanking, enhanced reflectivity and/or the presence of gas chimneys. The presence of shallow gas leads to increased attenuation of sound, scattering of acoustic energy and changes in velocity which are reflected in the seismic imaging (Taylor, 1992). High-frequency seismic profiles, usually acquired to image the top few hundred metres of the subsurface, often show evidence for gas blanking (sometimes referred to as 'blanketing') (Barkan et al., 2009), where acoustic reflections are completely or partly obscured, as mapped across the UK continental shelf from 2D seismic in Holmes et al., (1993). Gas or fluid accumulations may also result in increased reflectivity within seismic data, sometimes referred to as 'gas brightening'. Lateral and vertical variations in brightness may be used to map potential migration pathways or gas accumulations. Finally, gas chimneys or columns are observed within seismic data as vertical or near-vertical disruptions of seismic reflectors (Figure 5.1) at scales of tens of metres to kilometres in vertical extent (see a recent summary in Andresen, 2012).

The resolution limits of seismic data are highly dependent on the acquisition parameters; in general, lower frequency sources with large source-receiver offsets, used for imaging deeper in the subsurface (i.e. >1 km) are less optimal for resolving sea bed and near sea bed features. The optimum 2D seismic data for characterising the topmost section (up to 100 m) of overburden is likely to be acquired using Boomer, Pinger or Chirp systems, which provide excellent vertical resolution allowing for imaging of horizons at a centimetre to metre scale (Bull et al., 1998; Bull et al., 2005; Vardy et al., 2008).

5.1.2.3 Acoustic sea bed morphological characterisation

Detailed active analysis of the sea floor may reveal geomorphological evidence for natural leakage pathways and/or monitor potential leaks at proposed CO_2 storage sites. Multi-beam echosounder (MBES) provides up to centimetre-scale (but usually metre-scale) three-dimensional mapping of the sea bed surface. Incorporation of backscatter data provides further information on the nature of the sediments at the sea bed, usually indicative of the degree of hardness or softness. Time-lapse MBES and other sea bed surface data may reveal changes in sea floor morphology, elevation or hardness indicative of migration to the sea bed. MBES surveys acquire data suitable to map natural landforms or detect features indicative of natural fluid flow, such as pockmarks (e.g. Gafeira et al., 2012) or polygonal faulting (e.g. Berndt et al., 2012). Side-scan sonar (SS) may also be used to image the sea floor at very high resolution (millimetre to centimetre scale) and in time-lapse mode can pick up very small changes in the sea floor for monitoring purposes (e.g. Judd, 2005). AUV deployments for sea bed monitoring are becoming more common.

Sea bed surface mapping derived from subsurface imaging techniques, particularly 3D seismic, also provide a good overview of landforms. However, they are dependent

on lateral seismic resolution, usually in the tens of metres, and therefore will not pick up more subtle features (Cartwright and Huuse, 2005).

The cost of ship time is the main logistical issue when obtaining acoustic sea bed survey data. Smaller vessels can operate up to about 80 kilometres offshore, but beyond this distance larger, more costly vessels are required. An acoustic survey could also include multiple techniques (e.g. sampling of sea-water and sea bed). Autonomous Underwater Vehicle-deployed surveying equipment is less expensive but is a less well-developed technique.

Active acoustic surveying techniques were used for all the offshore sites described in Section 3. For example, at Sleipner, a range of ship-borne sea bed imaging profiles, side-scan sonar and single and multi-beam echosounder data were acquired in 2006. The side-scan sonar proved the highest resolution imaging, able to detect features on the sea bed 1.5 metres in diameter and 0.3 metres in height. Analysis of sea bed features using this data at Sleipner found no evidence of gas leakage to the seabed.

5.1.2.4 Gas bubble and water column characterisation

Active acoustic tools such as MBES and SS (above) are often equipped with instrumentation to identify gas bubbles in the water column which may be used to detect leakage of gas from the sea bed (e.g. Judd, 2005). Bubbles may also be imaged and measured by camera, either from ship-board equipment or as part of ROV/AUV equipment or towed platforms, although quality may vary (Dando, 1990). Recent developments have used stroboscopic methods to identify bubbles, bubble size and rate of flow (Leighton et al., 2012a, b). Bubble streams may also be monitored using more permanent sensors; acoustic tomography, also known as Ocean Acoustic Tomography (OAT), involves the placement of a network of transponders on the sea bed which pick up sound. A change in the travel-time of sound between the monitors provides information on changes in temperature, pressure and current processes and can be used for bubble detection (Kargl and Rouseff, 2002). Measurement over time can provide a good baseline for potential storage sites but OAT systems are also affected by environmental conditions such as sediment input and interference from wildlife, and by the impact of shipping or infrastructure projects. Simple hydrophone listening systems can also be used to detect bubble noise, but are also affected by conditions, and may not detect ‘quiet’ systems.

Bubble columns can also be detected by acoustic techniques directed at the subsurface (i.e. seismic data) due to the high impedance contrast between gas and water. Gas bubbles may be imaged in the water column within seismic data (Hovland and Sommerville, 1985; Judd and Hovland, 2007; Schneider Von Deimling et al., 2015) unless the survey is designed for very deep imaging with very low seismic frequencies. Acoustic disturbance caused by schools of fish may be picked up using such acoustic techniques, but tend to display a more dispersed nature than plumes associated with gas (Hammer et al., 2009).

Costs are largely part of those required for site surveys (i.e. MBES, SS, see above) but extra effort may be required to use the techniques associated with bubble plumes (‘fish finders’). Divers may be employed to monitor test sites (Blackford et al., 2014).

Bubble streaming identification techniques were employed at all the offshore sites reviewed in this study (Section 2). For example, no bubble streams were identified at Sleipner or Snøhvit, but natural sea bed features including pockmarks were clearly identified (Bünz, 2011, 2013).

5.1.2.5 Chemical characterisation

Geochemical anomalies in the water column, such as high levels of dissolved gasses, may result from seepage from the sea bed. In the shallow overburden section, subsurface sediments will display an associated higher concentration of gas or fluid, dependant on the sediment porosity and permeability (Hovland et al., 2012).

Chemical monitoring methods for the shallow overburden sequence detect and characterise changes in sea bed or near-sea bed sediments or sea water indicative of gas or fluid leakages. Shipboard samples of the water column and measurements of Conductivity, Temperature and Depth (CTD) enable measurements of parameters such as pH, partial pressure of CO_2 (pCO), dissolved oxygen, inorganic and organic carbon, nitrogen, phosphate, salinity and, potentially, isotopic carbon and tracers, in order to assess if any anomalies or variations may be the result of emitted CO_2 or associated fluids.

Direct sampling of material at or near sea bed can also be used to characterise potential storage sites. Methods may include dredging/grabbing, or collection of material from shallow boreholes. Further geochemical analysis, including information on the concentration of CO_2 or methane, stable isotopes, alkalinity, pH, rare metals, and carbonate will indicate the likelihood of migration. The method of collection is very dependent on the nature of the sea bed, with rocky and sandy substrates being more difficult to sample. Any sampling programme which aims to analyse gasses within shallow sediments must employ specific techniques to prevent samples degassing on recovery.

Geochemical analysis was carried out at all of the offshore sites discussed in this report. For example, at Snøhvit, water was sampled at water depths between 310 and 355 metres, and analysed on the ship for dissolved oxygen concentration and pH, and in the laboratory for pH, CO_2, CH_4, dissolved inorganic carbon (DIC), dissolved organic carbon (DOC), nutrients, dissolved organic nitrogen, phosphate and salinity. A Conductivity, Temperature and Depth (CTD) probe was also used to measure the speed of sound in water, fluorescence, turbidity, salinity and oxygen, in addition to the standard temperature, conductivity and pressure (converted to depth). Six sampling stations also monitored water geochemistry and temperature during the 2013 cruise; no evidence for CO_2 emission was detected by either method (Bünz et al., 2013).

The costs of techniques such as CTD sampling are largely related to ship time and equipment, with further costs from lab analysis, which may be performed on board to achieve swift results.

5.1.2.6 Biological characterisation

A number of biological indicators in the shallow overburden and at seabed are indicative of anomalous chemistry which may be used to characterise and monitor potential CO_2 storage sites. Methane derived authigenic carbonates (MDAC) are

strongly suggestive of methane seepage over a relatively long period, and may be imaged by multi-beam or sidescan sonar, although visual confirmation is considered to be required to prove their presence. Bacterial mats at seabed result from communities of sulphide-oxidising bacteria, most commonly found at sites of marine methane seeps. The most common species are *Beggiatoa sp* (Judd and Hovland, 2007; Hovland *et al.,* 2012) which produce thick mats on the sea floor best observed using underwater camera technology. All biogenic indicators are, however, inherently variable, and highly sensitive to human impacts.

Techniques used to identify biological markers are largely restricted to sea bed sampling or video observation. Video and camera imaging is routinely collected in any underwater infrastructure project, including, for example Sleipner, where continuous video footage obtained from the ROV used to deploy equipment was obtained in 2002, 2005 and 2009. The results of monitoring the sea bed during this time did not reveal any biological evidence for seepage.

5.2 Deep-focused onshore and offshore monitoring

Surface seismic methods offer the potential for high-resolution imaging and characterisation of the subsurface over wide areas, including the detection of changes in fluid distributions and pressure. Robust subsurface monitoring of the overburden requires comprehensive spatial coverage and 3D seismic surveys are unique in their ability to provide uniform and continuous three-dimensional spatial surveillance of the overburden. For 3D seismic data vertical resolutions may be at the metres to tens of metre scale, with horizontal resolution dependent on acquisition parameters but generally at tens of metres. 3D seismic specifically acquired to image relatively shallow CO_2 storage site overburden sequences might achieve vertical resolutions in the order of a few metres, with thin layer detectability of around one metre.

Controlled source 3D seismic methods provide the best imaging in order to characterise the sub-surface over CO_2 storage sites. Offshore, using a ship travelling at speeds of up to 10 kilometres per hour, large swathes of data can be acquired in a single pass. Large spatial coverage is possible due to the use of long receiver streamers in arrays up to 500 metres wide. This acquisition approach keeps costs down once initial deployment fees are covered. Onshore, acquisition costs are dependent on the terrain and environment since they require significantly more man-power to place sources and receivers. In difficult regions, the costs may reach ten times those of a standard offshore survey. Once data has been acquired, processing and interpretation costs are similar for on- and offshore seismic data.

In time-lapse mode 3D seismic surveys provide a very powerful leakage monitoring tool because of their ability to detect small changes in fluid content of the rock volume above the storage reservoir. Resolution and detection capability depend on subsurface conditions; shallow, thick, unconsolidated sedimentary sequences are more suitable for seismic monitoring than thin, deep lithified ones (Lumley et al., 1997). Survey repeatability (the accuracy with which successive surveys can be matched) is also a key determinant of time-lapse detection capability.

Accumulations of CO_2 in the overburden are likely to occur within higher permeability regions, either as sub-vertical columns ('chimneys') of vertically migrating CO_2, or as thin sub-horizontal layers of ponded CO_2, which grow laterally. In both cases 'difference' signal will be produced on time-lapse seismic survey data, either via a reflection from the accumulation itself, or by velocity-pushdown inducing measurable time-shifts in the underlying reflector sequence that produce a difference response (Figure 5.1).

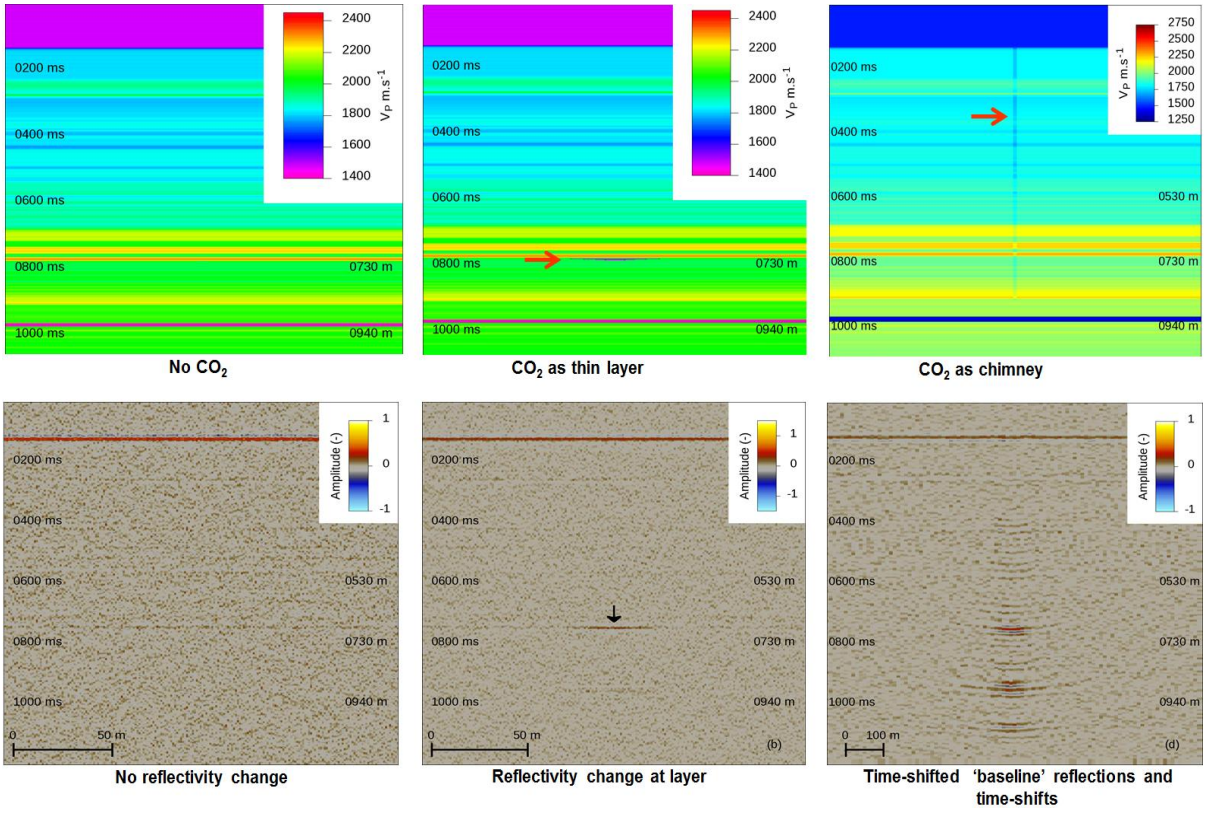

Figure 5.1 Overburden velocity models (top) with the reservoir top surface at about 900 ms (two-way time). Models have no CO_2 (left), a thin wedge of CO_2 (middle) and a vertical CO_2 chimney (right). Synthetic difference seismic profiles (bottom) show difference noise (left) and changes induced by the CO_2 either as a reflection (middle) or as a time-shift difference response (right) (from Chadwick et al., 2013).

Time-shifts are a notably robust time-lapse seismic parameter and it has been shown (White, 2014) that statistical analysis of very small time-shifts on 3D seismic data can constrain CO_2 amounts in the overburden over a wide spatial extent.

An alternative approach is to focus on induced reflectivity changes in the overburden due to small CO_2 accumulations. This involves the detection of small reflectivity changes attributable to CO_2 within a 3D cloud of repeatability noise, which is not related to the presence of CO_2. Chadwick et al. (2013) introduced a novel statistical methodology to determine the detectability of small reflectivity changes based upon their brightness and spatial extent. Analysing the Sleipner time-lapse datasets, they concluded that at depths of around 800 metres with CO_2 in the dense phase, accumulations with pore volumes greater than about 3000 cubic metres should be robustly detectable. With a conservative assumption of full CO_2 saturation, this corresponds to a CO_2 mass detection threshold of around 2100 tonnes. At shallower depths within the overburden as it passes from the dense phase into a gaseous state,

CO_2 becomes progressively more reflective, less dense, and correspondingly more detectable. Chadwick et al. (2103) concluded that the detection threshold at Sleipner falls to around 950 tonnes of CO_2 at 590 metres depth, and to around 315 tonnes at 490 metres depth, where repeatability noise levels are particularly low. These particular numbers are very site-specific, depending on both the seismic repeatability and the local rock physics. They are also quite preliminary estimates based on a first deployment of the statistical technique. More ground-truthing is required, particularly from pilot-scale experiments such as at Otway and the FRS in Canada (Section 2.5), where known amounts of CO_2 are being injected into the relatively shallow subsurface and monitored with time-lapse 3D seismic surveys.

Conventional 3D seismic surveys are designed to achieve imaging at reservoir depths and coverage of the shallow overburden is generally sub-optimal. P-cable is a high-resolution 3D seismic system using small airguns in conjunction with a seismic cable towed perpendicular (cross-cable) to the streaming direction. It is designed for imaging the shallow subsurface beneath the sea bed, where conventional seismic data lose quality and coverage. Targets are typically gas chimneys, shallow gas and gas hydrate reservoirs typically within the top 500 to 1000 metres of the seabed (Petersen et al., 2010). Two P-cable surveys have been acquired at Snøhvit in 2011 and 2013 by the ECO_2 project (Bünz et al., 2011, 2013); however, the time-lapse performance of P-cable, which depends on accurate positioning and source/receiver reproducibility, has not yet been demonstrated.

3D seismic surveys are expensive to undertake. A useful approach, especially for baseline monitoring of proposed sites, is to re-process legacy datasets with parameters that optimise imaging of the upper section of the overburden.

For example, high resolution ‘site-survey’ 2D seismic was deployed at Sleipner in 2006 and showed useful improvements in resolution in the overburden and upper part of the storage reservoir compared with the conventional 3D survey (Williams and Chadwick, 2012). A major drawback of 2D seismic survey data for leakage detection is the lack of continuous subsurface coverage.

6 Review of controlled release experiments and natural leakages

There have been many studies of natural occurrences and experimental releases of CO_2. The lessons learned from the study of onshore controlled CO_2 release experiments are outlined in Section 6.1. Six natural CO_2 seepage sites from around the world are summarised and the rates of seepage from monitoring of natural analogue sites, both onshore and offshore, are tabulated in Section 6.2. The processes and rates of migration through the overburden from investigations at seven controlled release sites is summarised and the sites compared in Section 6.3. The lessons learned distilled from the controlled releases and monitoring of natural leakage sites are summarised in Section 6.4.

6.1 Review of lessons learnt from onshore field tests

There have been a number of onshore controlled release experiments at field sites around the world (Section 6.3). The depth of the release has ranged from 50 metres to less than one metre. The deeper tests (10-50 m) assessed the possible impact of CO_2 leakage on drinking water aquifers and evaluated monitoring technologies (Cahill et al., 2014; Pezard et al., 2016; Trautz et al., 2012). The shallow releases (<1 to 3 m depth) were also designed to test monitoring techniques, and examine potential impacts on near-surface ecosystems (Barrio et al., 2014; Feitz et al., 2014a; Goudinho, In press-a; Jones et al., 2014; Moni and Rasse, 2014; Moreira et al., 2014; Smith et al., 2013; Spangler et al., 2010).

Both shallow and deeper experiments have found the surface or subsurface impacted areas to be restricted in extent (e.g. Feitz et al., 2014b; Jones et al., 2015; Pearce et al., 2014). Seepage at the surface has occurred as small patches (typically metres to tens of metres across). These appear to form as a result of the CO_2 following higher permeability pathways of restricted extent. When experiments have been repeated, the pattern of leakage/seepage has not always been consistent because of changes in the overburden properties, especially the moisture content and position of the water table (Feitz et al., 2014a).

Given the restricted size of the test sites, and the relatively shallow depths of injection, there has been little difficulty in detecting the seepage and measuring the flux rates using soil gas, flux or atmospheric measurements (mobile or continuous fixed techniques). However, there have been problems in predicting where leakage will occur with significant differences between the modelled and actual behaviour of the injected gas, for example in the CO_2 Field Lab experiment (Jones et al., 2014).

Plumes of affected groundwater are seen, or modelled, to also be of limited volume such that there is likely to be a low probability of their detection using downhole techniques (Carroll et al., In press; Carroll et al., 2014) except for measurement of the pressure response, which modelling suggests would have a better chance of success (Keating et al., 2014; Keating et al., In press). There has also been some success with cross-hole or wider area geophysical techniques, including electrical conductivity/resistivity, ground-penetrating radar and electromagnetic surveys (Auken et al., 2014; Dafflon et al., 2012; Denchik et al., 2014; Lassen et al., 2015; Pezard et al., 2016). Whilst downhole changes in pH or chemistry may be readily apparent in

any boreholes that penetrate the CO_2 plume, the effects can be reduced by water-rock reactions, particularly the buffering effect of carbonate minerals. Elements, such as heavy metals, may be released from the rock into the fluid but this can be offset by processes such as sorption. The potential impacts of leakage and implications for monitoring have been recently reviewed by Jones et al. (2015).

The focus of current and future experiments appears to be somewhat deeper, with injections proposed at depths ranging from tens to hundreds of metres. The deepest of these are potential injections at 300m and 500m depth at the Field Research Station in Alberta, Canada. Proposals for the GeoEnergy Test Bed site in the UK include injection at around 200 metres depth. A number of sites are planning injection into faults in order to obtain direct measurements of the transmission (or otherwise) of migrating gas. They include the Otway site in Australia (Feitz et al., In Press) and the Sulcis Fault experiment in Sardinia, Italy. This should help to fill a recognised research gap (IEAGHG, 2016). Shallow experiments (2-3 m depth) continue at sites in Brazil and South Korea (Goudinho, In press-b; Jun et al., In press) with a number of deeper tests also planned in S Korea (e.g. Lee et al., 2016).

A key potential contribution of onshore pilot injection sites is in the calibration of time-lapse seismic methods for leakage detection (see Section 6.2). Statistical methods for CO_2 detection in 3D overburden rock volumes have been proposed (Chadwick et al. 2013) but these have not been properly calibrated yet, in terms of establishing a robust relationship between seismic repeatability, rock physics and detection thresholds. Experiments that inject a small quantity of CO_2 and monitor the process with time-lapse seismic data have been proposed at Otway (Phase 3) and also at the Field Research Station in Alberta, Canada; these provide an opportunity to achieve this calibration.

6.2 Review of monitoring and rates at natural CO_2 seepage sites

Natural seepage sites have been studied particularly in Europe and the USA. Italy has the greatest concentration of studied seeps, particularly in volcanic areas, but there has been research in other countries, including the Czech Republic, France, Germany, Hungary and Greece, and volcanic and geothermal areas worldwide. The European project NASCENT examined a number of sites (Pearce et al., 2004; Pearce et al., 2003; Pearce, 2006). In the USA there have been many studies in the Green River Valley in the Paradox Basin, Utah (e.g. Burnside et al., 2013; Dockrill and Shipton, 2010; Jung et al., 2014; Jung et al., 2015; Kampman et al., 2014; Shipton et al., 2004) and at the Mammoth Mountain site in California (Evans et al., 2002; Gerlach et al., 2001; Lewicki and Hilley, 2014; Werner et al., 2014). Seepage has also been examined more recently along the Bongwana Fault in South Africa (Bond et al., In press; Johnson et al., In press).

Monitoring at natural sites has often involved the measurement of CO_2 flux using accumulation chambers, or, more rarely, eddy covariance. The emphasis has been to quantify total emissions and delineate potential hazards, especially in volcanic areas. Flux surveys have sometimes been supplemented by soil gas measurements and continuous monitoring has been established at a small number of locations. Sampling of the soil gas has been undertaken in some cases to determine the gas composition

in more detail and for isotopic analysis. This has helped to understand processes and to attribute the source of the gas. The areas of natural CO_2 seepage tend to be small, typically metres to tens of metres across (Annunziatellis et al., 2008; Byrdina et al., 2009; Chiodini et al., 2010; Mazzini et al., 2011; Perrier et al., 2009; Rogie et al., 2000; Vodnik et al., 2006). However, they can extend to a few hundred metres in some cases (Carapezza et al., 2009; Chiodini et al., 2010; Lewicki et al., 2008).

In many natural seepage studies, from a CO_2 storage perspective, the migration of CO_2 and other gases has been linked to faults. As for the experimental sites, the surface expression of leakage is notably patchy. Fluid movement occurs along only a very small proportion of the total fault length leading to isolated small seeps, along the fault (Annunziatellis et al., 2008; Johnson et al., In press; Krüger et al., 2011; Ziogou et al., 2013) or elongated in the direction of the fault (Carapezza et al., 2009; Gerlach et al., 2001).

The recent IEAGHG report on fault permeability (IEAGHG, 2016) suggests that the likelihood that faults at a given storage site will leak can be assessed. However, because of the heterogeneity of fault zones and the variability of the shallow overburden, prediction of where migration may occur along a fault, or where seepage might appear at the surface, is very challenging. This makes the choice of locations to monitor problematic. A detailed analysis might suggest sections of the fault with a particular orientation could be more likely to leak or higher priority could be given to more populated areas or more sensitive ecosystems.

The rates of natural seepage of CO_2 vary across several orders of magnitude. Background flux rates vary from usually less than 50 grammes per square metre per day (50 g m^{-2} d^{-1}) and often lower (20-30 g m^{-2} d^{-1}), whereas natural seepage rates can exceed 10 000 grammes per square metre per day (e.g. Annunziatellis et al., 2008; Beaubien et al., 2008; Krüger et al., 2011; Ziogou et al., 2013). Soil gas CO_2 concentrations at seeps are often greater than 80% and can reach close to 100%. The high concentration of CO_2 causes depletion of O_2 and N_2 through dilution. The CO_2 can be accompanied by other trace gases, depending on the site characteristics, such as CH_4, H_2S, He and Rn, although more reactive gas species tend to only accompany the CO_2 if flux rates are high (Annunziatellis et al., 2007). The coincidence of higher levels of several gas species can be an indicator of leakage from depth. Ratios of CO_2 to O_2 and N_2 can be a powerful way of distinguishing deep leakage from shallow biogenic processes. Source attribution can also be made using stable C isotopes, although $\delta^{13}C$ may not work depending on the source of the injected CO_2, radiocarbon or noble gas isotopes.

Continuous monitoring has shown that the concentration and flux of CO_2 (and other gases) varies with near-surface environmental changes, including in response to temperature, pressure and soil moisture as well as more deep-seated influences such as seismicity (e.g. Annunziatellis et al., 2003; Battani et al., 2010; Beaubien et al., 2013; Camarda et al., 2016; Etiope and Martinelli, 2002; Jones et al., In press; Schlömer et al., 2014). This is even true for injections tested at continuous rates, and values fluctuated at the CO_2 Field Lab even when the injection rate was increasing (Jones et al., 2014). This has implications in particular for the quantification of

emissions, as required by the Emissions Trading Scheme Directive (European Union, 2009).

6.2.1 Review of observations at natural CO_2 seepage sites

Natural CO_2 seeps occur both onshore and offshore and are evidence of similar trapping and migration mechanisms as applicable to the overburden to CO_2 storage sites. There are not many observations of offshore CO_2 seepage sites but almost all of those that have been reviewed in published literature are from volcanic regions, with the exception of the Salt Dome Juist. Sites where natural CO_2 seeps occur provide useful information about migration and storage of CO_2 in the subsurface. The flux rates at these sites are considered as anomalous and therefore not the usual background values that would be recognised elsewhere. They therefore provide the opportunity for testing characterisation and monitoring techniques that may be used at CO_2 storage sites to check their integrity. The sites described in this section are chosen because there is sufficient data available to enable a comparison.

Most naturally occurring CO_2 is the result of de-gassing of magma chambers, though it can also derive from dissolution of carbonate rocks, metamorphism, thermal alteration or degradation of organic material (McGinnis et al., 2011, Kirk 2011). Flux rates are highly variable ranging from a few grammes to a few kilogrammes per square metre per day.

The ability of gas to migrate through the sub-surface is controlled by the overlying sediments and whether there are easy pathways for the gas to travel along. Onshore CO_2 seeps present themselves in a number of scenarios including springs, mud pools and diffuse leaks through soil (Blackford et al. 2013b). CO_2 from onshore seeps is generally related to volcanic and metamorphic activities and degassing of the mantle (Blackford et al 2013b). Due to the dense nature of CO_2, vegetation may die where concentrations are high enough around the area of the seep at surface and prevailing wind conditions are insufficient to disperse the gas. The majority of offshore gas seeps emanate from bedrock fractures in volcanically active areas but there are also gas seeps emerging through soft sediments in hydrocarbon-bearing areas (Kirk, 2011). The sediments may be poorly consolidated and porous (e.g. sand or silt) or less permeable (e.g. clay) and gas may migrate and disperse in or accumulate beneath these layers. CO_2 produced within the subsurface offshore is commonly released as gas bubbles or CO_2-rich fluid from the seafloor and this can often result in pockmarks (Section 3.2.2.1) in soft sea bed sediments (Hoveland & Sommerville 1985, McGinnis et al., 2011, Kirk, 2011). Leaked CO_2 reduces the pH levels of sea water in localised areas close to the point of release resulting in more acidic conditions, which can have a detrimental effect on sea life ecosystems and organisms.

Table 6.1 summarises data from the natural sites that have been reviewed and the sites are described in more detail in Section 6.2.1. The original units (L d^{-1}) for flux rates, presented in the published work, have been included in the table to maintain the integrity of the data. Flux rates are also tabulated in tonnes (megagrammes), where appropriate, to enable comparison. Daily flux rates are plotted graphically using maximum rates where there is a range (for those sites that have values) in Figure 6.1.

Site	Flux rate ($x 10^6 l/d^{-1}$)	Flux rate ($x 10^6$ g d^{-1})	Flux rate (t/ year)	CO_2 source	Gas composition	Water Depth (m)	Temp (°C)	Salinity (TDS mg/l)	pH	Monitoring	Reference
Panarea	7 - 9	13.8 – 17.8	1670 - 8500	Linear faults & vents aligned with the faults	CO_2 98% H_2S 1.7%	Up to 30	46 -135 (discharge temp)	37,600 – 54,500	3-8	ACDP CTD Diver sampling	Tassi *et al.,* 2009 Caramanna 2010 Lombardi, 2010 Etiope *et al.,* 2007
Ischia, Italy	South side 1.4 (> 3000 m^2)	South side 2.8 (> 3000 m^2)	7.3	Mainly < 5 vents /m^{-2}	CO_2 90% to 95% N_2 3-6% No H_2S	Shallow <5 (warm water site in photic zone)	13 - 25 (sea-water ambient seasonal fluctuations)	380,000	7.4-8.2	Flux rates Gas composition Total Alkalinity Salinity Spatial and temporal pH Biological impact	Lombardi *et al.,* 2010 Hall-Spencer *et al.,* 2008
	North side 0.7 (> 2000 m^2)	North side 1.4 (> 2000 m^2)	5.5								Lombardi, 2010

Site	Flux rate ($x 10^6 l/d^{-1}$)	Flux rate ($x 10^6 g d^{-1}$)	Flux rate (t/ year)	CO_2 source	Gas composition	Water Depth (m)	Temp (°C)	Salinity (TDS mg/l)	pH	Monitoring	Reference
Champagne site, Mariana arc	0.9 (over 10 m^2)		8×10^8 (moles/year)	Vents	CO_2 90-98% H_2S 1% Trace H_2 and CH_4	1600	47-103 (discharge temp)		3.4 – 4.8	Vent fluid sampling from ROV Liquid droplet sampling CTD	Lupton *et al.,* 2006
Hatoma Knoll, Okinawa Trough				Vents	CO_2 95-98% H_2S 2-3%	682 - 1430	3.9 – 6.4 (bubble temp)	344,190	7 – 7.4	CTD Mapping of pH (400 x 400 m) HD Camera	Shitashima *et al.,* 2008
Salt Dome Juist, Southern German North Sea				Point source above dome		20	13 -15		6.8	ACDP ROV water sampling CTD ROV mounted camera	McGinnis *et al.,* 2011

Site	Flux rate ($x 10^6 l/d^{-1}$)	Flux rate ($x 10^6 g d^{-1}$)	Flux rate (t/ year)	CO_2 source	Gas composition	Water Depth (m)	Temp (°C)	Salinity (TDS mg/l)	pH	Monitoring	Reference
Florina	0.02 – 9.862 (m^{-2})	0.04 – 19.5 (per m-2)	7.3 – 3650	Gas vents and carbonated springs		NA onshore site	NA	NA	NA	Soil gas CO_2 concentrations CO_2 flux Botany Soil microbiology	Koukouzas *et al.,* 2015 Ziogou *et al.,* 2013

Table 6.1 Seepage rates and observational data at natural sites (adapted after Kirk, 2011)

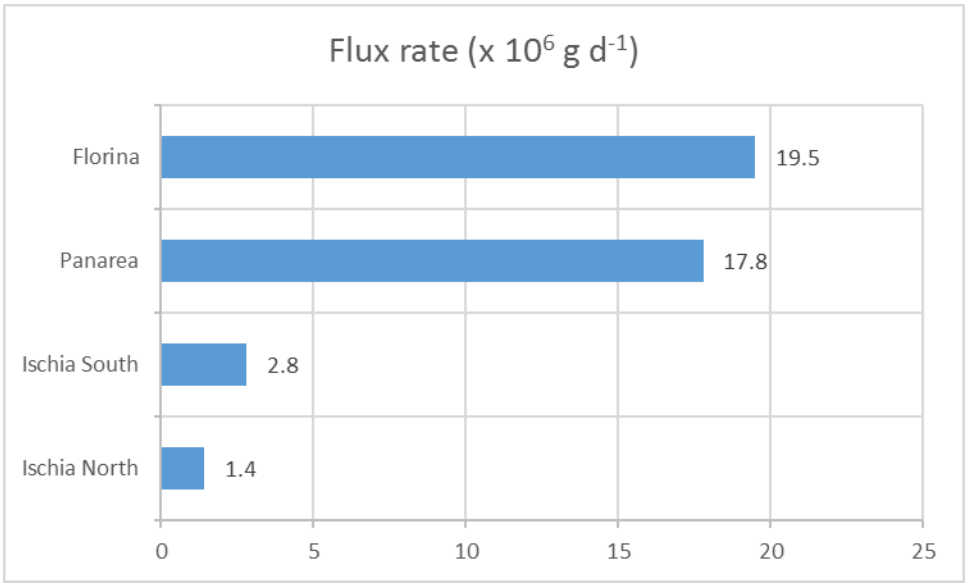

Figure 6.1 Graph showing maximum daily flux rates in megagrammes per day (equivalent to tonnes per day) at four of the natural analogue sites.

6.2.1.1 Panarea

Panarea is the smallest of the Aeolian Islands, a volcanic arc composed of seven islands and ten seamounts in the southern Tyrrhenian Sea, South Italy (Tassi et al., 2009). The island is part of a calcalkaline volcanic-island arc above a north-west-dipping subduction zone set in a deep Neogene to recent intra-orogenic basin that opened during the growth of a fold and thrust belt in the region (Argnani & Savelli. 1999). The volcanic activity is the result of the subduction zone that developed during the Quaternary and has been active up to at least 2002 (Tassi et al., 2009). The sea bed around Panarea comprises high-K, calcalkaline, dacite and porphyritic basaltic-andesite and the sea floor is loosely to partially consolidated Holocene sand and conglomerate formed due to erosion of emerging islets (Tassi et al., 2009). Vents occur along north-north-east and north-west trending fault systems in the fumarolic field which is located approximately 2.5 kilometres east of the island (Tassi et al., 2009).

Several cruises have acquired geophysical and oceanographic data and carried out monitoring of seabed geomorphological features and gas escape. Patterns in the water column have been observed and modelled using current meters, Acoustic Doppler Current Profiler (ADCP), Remotely Operated Vehicle (ROV), divers' observations and high-resolution bathymetry (Aliani et al., 2010). Sampling of free and dissolved gas has been carried out by scuba divers using canisters that have been pressurised with air to above hydrostatic pressure. Flow rates are measured by recording the time it takes for a canister to fill up with gas (Caramanna et al., 2010, Aliani et al., 2010). Flux rates from studies by Aliani et al. (2010) are in the order of 8.3×10^8 g d^{-1} (grams per day). Flux measurements by Caliro et al. (2004) have been taken annually since 1985, from which an estimate of a constant flux rate of 0.13 to 0.18×10^8 g d^{-1} has been made. Flux rates during a degassing event in 2002, where large amounts of gas (mainly CO_2) were suddenly released from the sea bed, were estimated to be 200×10^8 g d^{-1} but this slowly decreased to 7.9×10^7 g d^{-1} after about

two months (Caliro et al., 2004). Prior to this event, the activity at Panarea is described as the mild degassing of hydrothermal fluids (Esposito et al. 2010).

Monitoring of temperatures suggests that though vent temperatures are high, quick mixing with sea-water results in rapid cooling (Aliani et al., 2010). A drop in pH values around the vents indicates a change to acidic conditions, which is confirmed by corrosion of shell organisms and skin irritation reported by divers (Aliani et al., 2010). It is difficult to estimate the amount of water being emitted from the system and therefore how much gas is escaping because chemical reactions with sea-water plus circulation of seawater around vent areas complicate analysis of source of gas (Aliani et al., 2010).

Geochemical analyses in the 1980's reveal gas compositions are representative of a hydrothermal system (low H_2/CH_4 ratios), but during a 2002 degassing event compositions were analysed that showed increased magmatic gas input related to a volcanic event (Caliro et al., 2004).

6.2.1.2 Ischia

Ischia Island is part of the same island arc as Panarea and is the result of the uplift of a resurgent block which is bounded by high-angle normal and reverse faults where intermittent 'trap-door' style uplift causes seismicity and hydrothermal variations (Molin et al., 2003). This type of structure is characterised by concentric faulting which initially forms a dome geometry. Venting along the faults allows volcanic eruptions and a central block is lifted and then subsides during active and dormant periods respectively. Ischia is an example of a cold venting area in the Tyrrhenian Sea where vents to the south of the Castello d'Aragonese peninsula (on the east of the island) emit 2.8×10^6 g d^{-1} 8of gas over an area of 3000 square metres and vents in the north of the peninsula emit 1.4×10^6 g d^{-1} over an area of 2000 square metres (Hall-Spencer et al., 2008; Lombardi, 2010). The vents lie on the foreshore of the peninsula closest to the main part of the island. Gas emitted in this area contains 90 – 95 % carbon dioxide and 3 - 6 % N_2 with no H_2S (Hall-Spencer et al., 2008, Lombardi, 2010).

Vent gases are collected for analysis using pre-evacuated glass flasks. Spatial and temporal variability in pH, total alkalinity and salinity have also been investigated by analysis of regularly collected samples in various weather conditions. A series of mesocosm experiments (laboratory conditions) and species analysis (near vents) were carried out to assess the effects of lowered pH conditions on flora and fauna (Hall-Spencer et al., 2008).

6.2.1.3 Champagne Site (Mariana Arc)

The Champagne site is a CO_2-rich hydrothermal offshore site located in the northern Mariana Arc, south of Japan. It lies approximately 80 metres west-north-west of the top of the north-west Eifuku volcano in a water depth of about 1600 metres (Lupton et al., 2006).

At the Champagne site a vent is discharging hot (103°C) gas-rich milky fluid and, from an area in the same field, cold (<4°C) water droplets coated with a milky film that escape from cracks in the sea bed. The film around these droplets is thought to be hydrate, which forms when CO_2 comes into contact with water under the specific

pressure and temperatures observed here. The sea floor from which the water droplets are released comprises mainly pumice and a sulphur-rich sediment (Lupton et al. 2006).

Vent fluids were sampled using gas-tight bottles collected using an ROV. The water droplets are composed of 98% CO_2. Lupton et al. (2006) propose the high concentration is due to degassing of a magma chamber, with the rising CO_2 cooling on its way to the sea bed and mixing with CO_2-rich water and a CO_2 hydrate layer beneath the sediment surface. They suggest a hydrate layer provides a cap containing the liquid CO_2 within the subsurface and, if penetrated, it will release the CO_2 layer beneath.

The vent fluids have a similar concentration to the water droplets and both contain a small amount of H_2S although this is slightly higher in the water droplets. The composition of the CO_2 provides evidence that approximately 90% of the CO_2 is from marine carbonates and the remainder is from mantle processes (Lupton et al., 2006).

This site has an estimated flux rate of 8×10^8 moles/year of liquid CO_2 droplets over an area of 10 square metres where approximately 300 rising droplet streams were counted (Lupton et al., 2006).

6.2.1.4 Hatoma Knoll (Okinawa Trough)

The Hatoma Knoll is located in the south-west of the Okinawa Trough in the East China Sea. This site is a caldera, approximately 400 metres in diameter and 120 metres in height, and includes a hydrothermal vent (Shitashima et al., 2008). Clear hydrothermal fluids are vented inside the caldera area and CO_2 droplets are dispersed in several areas of the site (Ischibashi et al., 2015). Active hot vents are mostly composed of anhydrite whereas inactive vents are mainly of barite composition (Ishibashi et al., 2015).

A Remotely Operated Vehicle (ROV) was deployed by Shitashima et al. (2008) to monitor and collect CO_2-rich droplets. The ROV was fitted with a Conductivity-Temperature-Depth sensor (CTD) and a high-definition observation camera. Hydrothermal fluid temperatures up to 301°C have been recorded (Ishibashi et al., 2015). The size and rise-rate of the CO_2 droplets decreased as they rose up through the water column eventually leaving only a small amount of CO_2 hydrate which eventually dissolved.

There is also an in situ sensor to measure salinity and pH. Only localised pH depressions are detected over the venting sites and the pH of the surrounding sea-water is similar to that of the CO_2 droplets at pH 7.539 (Shitashima et al., 2008).

The CO_2 droplets are composed of 95 to 98 % CO_2, with 2 to 3 % H_2S and small amounts of methane and helium.

6.2.1.5 Salt Dome Juist

The CO_2 seep above Salt Dome Juist (studied by McGinnis et al. 2011) is located in the German sector of the southern North Sea in a water depth of about 20 metres approximately 30 kilometres from the East Frisian Island of Juist. It formed in a system of deep Quaternary valleys and depressions formed by repeated glaciations, which

have been filled with Pleistocene organic matter. A complicated system of salt diapirs and faulting at depth has been characterised using geophysical data. Sediments on the sea bed in this area are mostly fine- to medium-grained sand containing shell fragments.

During a boat survey carried out by McGinnis et al. (2011) an ADCP and CTD profiler were deployed and dissolved gases analysed from sea water samples. The water around the site was well mixed, water temperature between 13 to 15°C and pH levels approximately 6.8, whereas normal background values would be between 7.8 and 8.4 (McGinnis et al., 2011). Dissolved oxygen levels were close to saturation and methane concentrations were close to background levels. CO_2 values were approximately 10 to 20 times higher than normal background levels (McGinnis et al., 2011).

The source and mechanism of the CO_2 seep at Salt Dome Juist are unknown and CO_2 bubbles have not been detected (McGinnis et al., 2011).

6.2.1.6 Florina

The onshore Florina Basin in north-west Greece is a north-north-west—trending graben containing Neogene sandstone and conglomerate (Ziogou et al., 2013; Koukouzas et al., 2015). The basin-fill comprises vertically stacked reservoirs of limestone and sandstone (Koukouzas et al., 2015). The CO_2 in the Florina basin is from a magmatic-hydrothermal source (Ziogou et al., 2013). CO_2 accumulates in fine-grained Miocene fluvial sandstones and Mesozoic limestones (Koukouzas et al., 2015). Florina is a naturally sourced commercial CO_2 field that has produced in the region of 20 to 30 thousand tonnes of CO_2 per annum (Beaubien et al., 2005). CO_2 accumulations occur at three depths (296 - 338 m, 366 - 372 m and 380 - 409 m) and occur at low pressures (Koukouzas et al., 2015) but due to a lack of cap rock in areas where Tertiary clay and silts are not present the gas has migrated to the surface (Beaubien et al 2005). The CO_2 migrates via faults and fractures until it reaches the water table (Koukouzas et al., 2015). The CO_2 that reaches the surface is driven by high-heat and water flow. It is a water-dominated system and CO_2 is eventually emitted via carbonate-rich springs and gas vents (Koukouzas et al., 2015). Soil gas CO_2 concentration anomalies are aligned along a direction similar to that of major faults in the basin (Koukouzas et al., 2015) which shows that the faults are instrumental to the migration of CO_2 to the surface. Temporally variable gas flux rates in this area indicate that leakage may be episodic (Blackford et al., 2013a; Koukouzas et al., 2015).

In a study carried out as part of the RISCS project the methods used to monitor CO_2 and its near surface impacts at Florina were soil gas concentration, CO_2 flux, botany and soil microbiology. CO_2 flux and CO_2 soil gas were measured along a 25-metre transect that started at the centre of a CO_2 vent. CO_2 flux measurements taken at 0 – 3.25 metres from the vent had values between 2 000 and 10 000 g m^{-2} d^{-1}. At distances of 3.25 to 8.25 metres from the vent values were much lower at 40 to 700 g m^{-2} d^{-1}. At distances from the vent, between 8.25-25 metres, CO_2 flux values remained fairly stable at 40 to 20 g m^{-2} d^{-1} (Ziogou et al., 2013). A botanical survey suggests that some of the plant species have adapted to long-term exposure to the CO_2-enriched environment. Soil gas CO_2 concentrations were measured at depths of 20 centimetres, 50 centimetres and 70 centimetres along the same 25 metre transect (Ziogou et al.,

2013). The readings, taken at a depth of 20 centimetres, show high concentrations near the vent, decreasing values along the transect away from the vent to background levels (approximately 1 %) at a distance of 10 metres (Ziogou et al., 2013). CO_2 concentrations at 50 and 70 centimetre depths remain much higher than at shallower depth along the transect reaching background levels at about 20 metres from the vent (Ziogou et al., 2013).

6.3 Review of processes and rates of migration through overburden – controlled release experiments

It is important to assess the potential long-term behaviour of CO_2 in the subsurface including the overburden (e.g. migration pathways and geochemical rock interactions) before starting a geological storage project. It is also a basic regulatory requirement for all carbon capture and storage projects to verify there will be no significant effects on the environment or human health. Experimental release sites enable a comparison of leakage rates in different contexts and this is useful for evaluation of localised impacts.

Surface monitoring methods have been utilised at several controlled release sites which include soil gas concentration, soil flux, groundwater monitoring, atmospheric monitoring, plant biology, microbial monitoring and electric resistivity. These techniques have proven successful at the sites on which they have been deployed. Surface monitoring techniques are effective for characterising known leaks as demonstrated by experiments carried out at controlled CO_2 release facilities (Feitz et al., 2014b). They are effective in providing water chemistry analysis, quantifying the leak and for mapping the extent of the leak and the direction in which it migrates.

6.3.1 Summary of the controlled release sites

There are a few controlled CO_2 release experiments that have been carried out to investigate the behaviour of CO_2 in the subsurface and in particular in the overburden. These include: the QICS project (Quantifying and Monitoring Potential Ecosystem Impacts of Geological Carbon Storage) offshore Scotland, UK; CO_2 Field Lab, Norway; Ginninderra, Canberra, Australia; Ressacada Farm, Florianopolis city, Brazil; Zero Emission Research and Technology Centre (ZERT), Montana, USA; ASGARD, Nottingham, UK; Grimsrud Farm, Norway.

Each site deployed a suite of differing monitoring techniques summarised in Table 6.2.

Site	QICS	CO_2 Field Lab	Ginninderra	Ressacada	ZERT	ASGARD	Grimsrud
Soil gas		X	X	X	X	X	X
CO_2 flux	X	X	X	X	X	X	X
Soil analysis			X		X		
Eddy covariance		X	X	X	X		
CO_2 laser		X	X				
Electrochemical analysers						X	
Noble gas tracers			X		X		
Isotope tracers				X			X
Electrical resistivity				X			
Airborne hyperspectral imaging			X		X		
In-field phenotyping			X				
Microbial soil genomics			X	X		X	
Biological stress (plants)				X	X	X	X
Water chemistry	X			X	X		
Atmospheric CO_2 (other method)							X
Seismic reflection data	X						

Table 6.2 Comparison of monitoring techniques used at controlled release sites.

6.3.1.1 QICS Project

QICS was the world's first project to undertake a controlled release of CO_2 from beneath the seabed. The site chosen for the experiment was Ardmucknish Bay, a small bay open to the Firth of Lorne on the west coast of Scotland. This experiment addressed issues relating to how CO_2 flows through shallow marine sediments, the ecological impacts in shallow sediments and the water column and tools suitable to detect and monitor potential leaks.

A sub-horizontal injection borehole was drilled from the shore to a depth of 11 metres so that the overlying sediment layers remained undisturbed (Taylor et al., 2014). Injection started at a low rate in order to monitor the pressure at the injection point but because bubble streams were observed after the first three hours the rate was gradually increased until the maximum wellhead pressure was reached (Taylor et al., 2014). The experiment took place over a period of 37 days with a total of 4.2 tonnes of CO_2 injected into the sediments (Taylor et al., 2015; Dewar et al. 2015; Cevatoglu et al., 2015).

Three hours after injection commenced streams of bubbles were observed escaping from the sea bed, eventually more than 35 separate bubble streams were detected, using multibeam bathymetry imaging which also revealed the presence of pockmarks, at the maximum injection rate (Dewar et al. 2015; Cevatoglu et al., 2015). Pockmarks

generated by the QICS release were also recorded by video- and photographic observations. High-resolution seismic data imaged the CO_2 accumulating in sediments above the injection point (Cevatoglu et al., 2015), both as thin layers and within a 'gas-chimney' (Figure 3.12). Significant acoustic blanking also occurred with a vertical unreflective zone beneath the injection point. Two years later repeat seismic surveys were acquired. Intriguingly, these showed remnants of the trapped CO_2 layers, but the vertical gas chimney (and its associated acoustic blanking) had disappeared.

The QICS controlled release experiment therefore demonstrates both short-term buoyancy-driven flow in the sedimentary column and also longer term stabilisation as dissolution processes take over with differing rates of dissolution in the dispersed CO_2 of the chimney compared with more highly saturated CO_2 in the layers.

6.3.1.2 CO_2 Field Lab

The CO_2 Field Lab project performed a controlled release at a depth of 20 metres onshore in Norway. The site chosen for injection was situated on the Svelvik Ridge in a very heterogeneous, unconsolidated highly permeable sand and gravel deposit, underlain by layers of sand, silt and clay (Barrio et al., 2013). The sand is a fully water-saturated aquifer below a vadose zone of about one metre depth.

A baseline survey measuring surface gas and ground penetrating radar was carried out prior to injection. Soil gas concentrations and fluxes were low, showing CO_2 concentrations mainly below 1% and fluxes at less than 8 g m^2 d^{-1} (Barrio et al., 2013; Jones at el 2014).

The experiment injected 1.7 tonnes of CO_2 over a period of one week via an injection well drilled at a 45^0 angle. The aims were to detect and if possible quantify the migrated CO_2 concentration in the soil, to evaluate the sensitivity of the deployed monitoring tools and to practise the monitoring methods before applying them to a proposed deeper controlled release. Various methods were used to monitor gas (flux and concentrations), water (chemistry and isotopes) and borehole geophysics (resistivity, gamma ray, sonic logs etc.) some of which were continuous and some intermittent.

Flux measurements at the CO_2 Field Lab were taken over the initial area of escape on a one-metre grid. An eight metre-diameter zone was mapped with high fluxes up to 1886 g m^{-2} d^{-1} (Jones et al., 2014). A further surface breach was detected three days after injection was initiated, at a distance of about 13 metres to the north-east of the injection point, in a soil gas sample (Barrio et al., 2013, Jones et al., 2014). CO_2 concentrations reached 97% and flux readings reached up to 922 g m^{-2} d^{-1} by day four of the release. Flux measurements declined as soon as injection was halted, however CO_2 was found in samples close to the injection point both during and after injection. CO_2 concentrations around the venting points continued to increase slightly before a decline was seen.

6.3.1.3 The Ginninderra controlled release facility

The Ginninderra controlled release facility operated by Geoscience Australia and CO_2CRC was designed to evaluate different near surface monitoring techniques in the detection and quantification of CO_2 leaks. Monitoring techniques used at controlled release sites in other countries may not be as effective at the Ginninderra site due to

it having a completely different climate to other controlled release sites and considerably different soils (Feitz et al 2014a).

Three release experiments injecting CO_2 at the same rate each time were conducted at this site in early 2012 (dry season) late 2012 (wet season) and late 2013 (dry season). CO_2 was released from a 100 metre-long horizontal pipe with five release slots that has been installed at a depth of two metres. Four different crops were sown in two-metre wide plots for the late 2012 experiments and two different crops were sown in the 2013 experiment.

Daily flux rates reached up to 3.25 log g m^{-2} d^{-1} (Feitz et al. 2014a) this is around 1780 g m^{-2} d^{-1}.

6.3.1.4 Ressacada Farm

Ressacada Farm located in Florianopolis is the first controlled release site in Brazil which has been developed and run by Santa Catarina Federal University (UFSC), fully sponsored by PETROBRAS Research Center (CENPES). The experimental area consists mainly of Quaternary deposits which are mostly unconsolidated sands, though lenses of clay occur within the sandy layers (Moreira et al., 2014). There is also a shallow unconfined aquifer that occurs at depths between 0.4 and 1.3 metres (Moreira et al., 2014). This area has naturally high CO_2 fluctuations which could complicate quantification and leakage detection in a CO_2 leakage situation.

CO_2 was continuously injected over a period of 12 consecutive days. A total of 33 kilogrammes of CO_2 was injected over the lifetime of the controlled release experiment (Moreira et al., 2015).

CO_2 flux measurements reached 270 µmol m^{-2} s^{-1} (micromole per square metre per second) a notable increase from background levels of 34 µmol m^{-2} s^{-1} (Oliva et al., 2014). Flux readings did return to background levels after injection ceased. The highest flux rates were observed nine days after injection started (Oliva et al., 2014), though there were only very small changes observed in atmospheric fluxes and concentrations measured by eddy covariance (Moreira et al., 2015). The flux measurements were spatially consistent with the resistivity data and the groundwater quality parameters which determine the lateral migration of CO_2 in the shallow (approximately 50 cm depth) subsurface (Moreira et al., 2014).

Electrical resistivity values around the injection well increased by about 50% (measured as a percentage in relation to background values) during CO_2 injection, although the largest anomaly recorded reached 100% in an area to the south-west of the injection well (Oliva et al., 2014).

6.3.1.5 Zero Emission Research and Technology Center (ZERT)

The ZERT site is located in Bozeman, Montana, USA where a range of monitoring techniques have been deployed to measure onset and recovery times during a controlled CO_2 leak.

A 100-metre-long horizontal well was installed at the site in 2007 at a depth of 1.3 to 2.5 metres below the surface within the groundwater aquifer (Fessenden *et al.,* 2010).

The well has six 70-centimetre-long slots from which CO_2 is released during the experiments.

Controlled releases at this site occurred in the summers of 2007 and 2008 for varying durations and injection rates. Injection rates were chosen to challenge detection methodologies (Spangler *et al.,* 2010).

6.3.1.6 Artificial Soil Gassing and Response Detection (ASGARD) site

The ASGARD site is a University of Nottingham facility where plots of 2.5 square metres have been set up to investigate the effects of controlled injection of CO_2 into the soil. As part of the EC Seventh Framework Programme RISCS (Research into Impacts and Safety in Carbon Storage) project, CO_2 was continuously injected into the plots over a two-year period and the site was monitored over three years. The effects of elevated CO_2 in soil on crops, soil microbiology, soil flux and CO_2 concentration have been investigated. A range of crops were used: a grass/clover mix was established in eight plots plus two different crops were sown each year on the remaining plots: spring-sown barley and oilseed rape in 2010; beetroot and spring wheat in 2011 (Smith et al., 2013).

6.3.1.7 Grimsrud Farm

The Grimsrud Farm site was operated by Bioforsk as part of the EU RISCS project. The site is located south-east of Oslo in Norway. The experiment was set up by excavating plots, six metres by three metres, to a depth of 85 centimetres. T-shaped pipes were installed in the base at one end of each plot (Moni and Rasse, 2014). The plots were filled with a 45 centimetre-thick layer of sand and 40 centimetres of local clayey soil to the surrounding ground level. The plots were disc-ploughed and sown with oats at the same time as the rest of the field (Moni and Rasse 2014).

CO_2 with ^{13}C signature used as a tracer was injected at one end of the plot with the objective of creating a CO_2 gradient across the plot. CO_2 concentration and ^{13}C analysis, CO_2 fluxes and their isotopic signatures, atmospheric CO_2 and plant weights were all analysed.

6.3.2 Comparison of the controlled CO_2 release sites

The sites chosen for controlled CO_2 releases have been designed differently, with depths varying from 0.6 to 20 metres with four sites using a horizontal slotted wells, one site using a slotted vertical well and two sites using wells inclined at 45 degrees to inject CO_2 into the subsurface. All test sites inject CO_2 into a sand-rich sediment with the exception of the QICS project, which has sand and gravel at sea bed and Grimsrud which is overlain by a clay-dominated soil. QICS is currently the only example of an offshore controlled release site. **Error! Reference source not found.** provides a comparison of the controlled release facilities reviewed

Site	QICS	CO_2 Field Lab	Ginninderra	Ressacada	ZERT	ASGARD	Grimsrud
Location	UK	Norway	Australia	Brazil	US	UK	Norway
On/offshore	offshore	onshore	onshore	onshore	onshore	onshore	onshore
Depth of Release (m)	11	20	2	8	1.2 – 2.5	0.6	0.85
Well orientation	horizontal	45^0 inclined	horizontal	vertical	horizontal	45^0 inclined	horizontal
CO_2 injection rate (kg d^{-1})	10 - 210	120 - 420	144 - 288	2.2 - 3.6	100 - 300	3 – 8.5 (1 - 3 l min^{-1})	3 – 5.7 (1 - 2 l min^{-1})
Injection duration (days)	37	6		12	7 - 27	730	Approx. 64
Soil type	Fine laminated mud overlain by 2 metres of fine silty sand with 1-2 m of sand and gravel at sea bed	Sand	Sandy loams and clays with occasional coarse gravel	Sand with clay lenses	Alluvial sandy gravel deposits	Sandy, silty soil	45 cm thick sandy layer overlain by 40 centimetres local clayey soil
Time to CO_2 surface breakthrough (days)	< 1	~ 1	< 1	5	< 1		
CO_2 Flux chamber measurements (g m^{-2} d^{-1})	8-31.8 kg d^{-1}	1886		1015 (Max 267 µmol m^{-2} s^{-1})	~3100	500 - 2000	590 - 826

Site	QICS	CO_2 Field Lab	Ginninderra	Ressacada	ZERT	ASGARD	Grimsrud
CO_2 concentration (%)		97	Up to 1780			Seasonal average between 44 and 57	36 - 55
Percentage of CO_2 released detected at surface/sea bed	15						39 – 52

Table 6.3 Comparison of controlled release facility sites (Blackford et al., 2014; Jones et al., 2014; Feitz et al., 2014a; Moreira at el. 2014; Spangler et al., 2010; Smith et al., 2013; Moni and Rasse, 2014).

6.3.2.1 Injection rates

All of the experiments used different rates of injection with some keeping the rates low, e.g. at Ressacada they were between 2.2 to 3.6 kg d^{-1} to avoid any fracturing of the sediments which could have resulted in preferential pathways being formed (Moreira et al, 2014).

At the QICS and the CO_2 Field Lab sites, injection was started at very low rates, which were gradually increased over three or four increments (Taylor et al., 2015, Jones et al., 2014) to manage the pressure at the wellhead.

Three of the sites injected at a constant rate over the lifetime of the experiment, these were ZERT, ASGARD and Grimsrud. All had different experiment durations between approximately 10 and 700 days.

6.3.2.2 Flux measurements

Most sites showed an increase in flux measurements from background conditions once CO_2 injection commenced, though higher flux measurements were detected after increased CO_2 concentrations were observed in the sub-surface (between 20-50 cm). At Ressacada Farm, flux readings peak at day nine during injection where rates are almost eight times that of the background levels (Moreira et al., 2014). All sites then see a gradual decrease back to background conditions once CO_2 injection stopped. At the QICS site, where many bubble streams were observed escaping from the sea bed, the levels of CO_2 in the sea water around emission sites did not significantly deviate from background readings except for within a high-CO_2 plume within the water-column (Blackford et al., 2014). This shows that natural water circulation is effective at mixing and dispersing CO_2 that was expelled through the sea floor. Recovery from this experimental release was however evident within days to weeks of the cessation of injection (Blackford et al. 2014).The footprint produced by soil flux at the surface for all the sites is generally smaller than that produced by soil concentration in the sub-surface, usually in the top 20-50 centimetres of sediment.

Some sites (Ginninderra, ASGARD, Grimsrud, ZERT and Ressacada and the CO_2 Field Lab) report that weather has an effect on CO_2 flux. In contrast to the CO_2 Field Lab, it appears that CO_2 flow at Ginninderra is less effected by wet weather conditions and flow at this site is lower under dry conditions (Feitz et al 2014a; Jones et al., 2014).

To compare daily flux rates to daily injection rates, most sites (Grimsrud, ASGARD, ZERT and CO_2 Field Lab) show a low average percentage of injected CO_2 is detected at surface (less than 20% of CO_2). The QICS and Ressacada sites have a higher detection rate at more than 35%.

6.3.2.3 Water quality

Acidification within the groundwater at Ressacada Farm, CO_2 Field Lab and the ZERT site was confirmed by a change in pH levels in the monitoring wells (Oliva et al., 2014, Apps et al., 2011, Gal et al., 2013).

The offshore release site for the QICS project observed chemical changes due to the controlled release of CO_2 in sediment pore waters from 2 to 25 centimetres depth

during the final week of injection, which continued for a further two weeks after injection stopped (Blackford et al., 2014).

6.3.2.4 Leakage patterns

All the sites show a similar pattern in their leakage behaviour in that the CO_2 was initially detected in the near surface in localised hotspots or zones that are generally between one and ten metres in diameter. High CO_2 concentrations rapidly reduce to background levels away from the hotspot.

It seems that even though a rigorous site appraisal may be carried out, it is difficult to predict where these hotspots may occur. In the CO_2 Field Lab experiment, leakage was detected quite close to the injection wellhead during the first day of injection (Barrio et al., 2013, Gal et al., 2013, Jones et al., 2014). This was not expected as the site appraisal suggested that it was likely to reach a bedding plane between geological formations at a depth of 15 metres and then travel along the bedding plane until it reached the surface (Gal et al., 2013).

An important soil property for controlling breakthrough time and flux rates is permeability (Spangler et al., 2010). The CO_2 appears to travel along higher permeability pathways and is emitted from discrete, relatively small seepage points, the location of which is very difficult to predict. Similar patterns are also observed at natural CO_2 seepage sites (Feitz et al., 2014b).

6.3.2.5 Hyperspectral imaging

Airborne deployed instruments fitted with CO_2 sensors have shown potential to find the location of seeps. This technique was deployed at both Ginninderra and ZERT. At the ZERT site there is a correlation between seeps detected using soil flux techniques and those detected using hyperspectral imaging (Feitz et al., 2014b). Vegetation damage caused by CO_2 exposure was successfully located using this technique at Ginninderra (Feitz et al., 2014b).

6.3.2.6 Percentage of CO_2 released detected at surface/sea bed

Not all of the sites have attempted to calculate the amount of CO_2 to reach the surface, which is frequently underestimated, especially when closed chamber systems are used to measure fluxes.

Flux measurements were taken acoustically on a 24-hour rolling-average basis at the QICS site, which suggested that 15% of CO_2 was released in gaseous form at the sea bed. It is believed that 85% of the CO_2 passed through the sea bed in a dissolved phase or is still trapped in the sub-surface (Taylor et al., 2015).

The Grimsrud site estimates that they managed to measure between 39 – 52% of the total amount of CO_2 injected (Moni and Rasse, 2014).

6.3.3 Comparison of the controlled release sites: summary

The controlled release facilities discussed above have shown that the near-surface monitoring techniques were able to detect elevated levels of CO_2 even with relatively low fluxes in the soil, water and atmosphere.

One thing that stands out is that even though sites have varying depths, injection rates and background conditions, prediction of where CO_2 is likely to occur first in a leakage event can be extremely difficult. What is common with all controlled release sites and natural seepage sites is the pattern of distribution of leaks, which appear as hotspots that are difficult to detect. Once a leak has been discovered, near-surface monitoring techniques are an effective way to quantify the leak, map the leak extent and understand the behaviour of CO_2 accumulation.

Isotopic monitoring of soil CO_2 fluxes as deployed at Grimsrud and Ressacada increases CO_2 detection sensitivity (Moni and Rasse, 2014; Moreira et al., 2014) and this is particularly useful in areas where there are naturally high background levels of CO_2, e.g. at Ressacada Farm.

6.4 Lessons learnt from experiments and natural leakages

1. Areas of seeps range from metres to hundreds of metres across, the largest being in volcanic areas, which may not be relevant to CO_2 storage. Seeps are most commonly metres to tens of metres across and therefore characterisation observations and subsequent monitoring systems are needed that can identify seeps of this size.
2. Controlled release sites and natural seepage sites show a similar pattern of distribution in that leaks are initially localised to areas between one and tens of metres in diameter.
3. Flux rates measured at seepage sites are highly variable, from very low (around 100 g m^{-2} d^{-1}), close to background levels to high (around 100 kg m^{-2} $d^{-1}$and higher) in volcanic regions and extremely high (up to 1 kt m^{-2} d^{-1}) where CO_2 is being released from open boreholes. High rates in and around boreholes, faults or fractures are likely to be easily picked up by monitoring. Fluxes from CO_2 leakage in a sedimentary environment are most likely to fall in the range from 100 g m^{-2} d^{-1} to tens of kg m^{-2} d^{-1}.
4. Thorough investigation and appraisal of the overburden can be carried out using a variety of monitoring technologies; however, it is difficult to predict migration pathways and the location of breakthrough at surface above a storage site as highlighted by the CO_2 Field Lab project. This means a monitoring plan needs to be flexible in its approach to take possible deviations into account.
5. Quantification of CO_2 techniques require further refinement; it is very difficult to calculate the amount of the injected CO_2 that has actually reached the surface in a leakage event at the experimental sites. Flux rates in natural systems can be variable due to changes in water depth and pressure or weather conditions as well as the fact that CO_2 can be dispersed in the water system or prevailing wind directions over longer periods. Estimates of total emissions in volcanic areas are likely to require direct measurements coupled with modelling (including Gaussian simulations).
6. Even in an area where a controlled release experiment is being conducted and CO_2 is expected to be observed in the sub-surface and at the surface finding small

surface leaks can be difficult. Finding such leaks over the large extent of a full-scale storage site is one the biggest characterisation and monitoring challenges.

7. The characterisation and monitoring tools tested at both natural and experimental sites will be applicable for characterisation and monitoring at storage sites. The tools should be deployed on a site-specific basis and it is beneficial to choose tools that are complimentary to one another to allow verification of data. The tools used are sensitive enough to detect very small readings (down to the gram scale) and so are capable of picking up the smallest of leak (though not expected) from a storage site.
8. Leakage rates from experimental sites and natural systems appear to be of a similar order of magnitude. At experimental sites, CO_2 is injected at very shallow depths into formations we are expecting to leak, whereas in a full-scale storage site CO_2 is injected at a suitable depth into a site that should have an effective cap rock (not expected to leak). The amounts of CO_2 injected at experimental release sites are very small compared to the considerable volumes that would be injected for a commercial-scale CCS project. The volumes of CO_2 that have been observed reaching the surface from experimental sites are an extremely small amount (tonnes per year) when compared to a commercial-scale project that will be injecting millions of tonnes of CO_2 for permanent storage.

7 Summary, recommendations and knowledge gaps

7.1 Summary

Fluid migrates through geological strata driven by pressure or density differences within hydraulically connected pore space. Fluids, such as fresh or saline groundwater or hydrocarbons, migrate laterally and vertically within porous and permeable rock types until contained by impermeable strata and structures. Vertical and lateral fluid flow within a layered sequence of sedimentary strata may be substantially enhanced by high-permeability flow pathways. However, geological features and structures may be present that are barriers to subsurface fluid migration within the overburden to CO_2 storage sites. The overburden is defined here as the entire geological succession above the target reservoir formation with the lowermost stratum forming the primary seal formation.

The presence of natural oil, gas and CO_2 fields proves that strata can contain fluids and gasses over extended periods of geological time. The presence of natural seeps of oil, gas and CO_2 also shows that, in some cases, the overburden containment system fails to retain buoyant fluids. The site selection process and risk/consequence assessments for a CO_2 storage project need to identify those strata that will contain CO_2, and understand the potential rates and environmental signatures of seepage.

Geological and man-made features that are potential pathways or barriers to CO_2 migration in the overburden and an assessment of computational modelling of that flow are outlined below (Section 7.1.1). The character of the overburden sequences to five CO_2 storage or injection sites is summarised and those features that promote containment of subsurface fluids are highlighted (Section 7.1.2). The processes and rates of fluid migration and the timescales over which they operate are reviewed (Section 7.1.3). The potential for the overburden strata to trap migrating CO_2-bearing fluids is summarised in Section 7.1.4, and an overview of the lessons learned from experimental releases of CO_2 and natural seepage sites is presented in Section 7.1.5.

7.1.1 Pathways and barriers to overburden migration

Geological features and processes that have the potential to bypass impermeable seal rocks, enhance migration or form barriers to subsurface fluid flow to promote trapping of injected CO_2 include: faults and fractures; geological fluid flow pathways with relatively higher permeability; large-scale geomorphological features. Wellbores have the potential to be man-made seal rock bypass pathways, connecting the storage reservoir directly with the overburden strata. The pathways and barriers will be relevant to the assessment of risk of the migration of CO_2 in the overburden whether it is in dense phase, gaseous phase or dissolved in groundwater.

7.1.1.1 Geological faults and fractures

The principal geological pathways that might enable migration within the overburden by bypassing the primary seal rocks are fractures and faults. Although there is much evidence for fluid flow along faults, there is also evidence of faults acting as effective seals, from diagenetic mineral precipitation that seals fault rock, fault gouge production

and strain hardening that decreases fault zone permeability. Measured flux rates of naturally occurring CO_2 along faults are high, however, these are derived from magmatic and hydrothermal systems and do not provide a good analogue for CO_2 migration through the overburden of a storage site (Table 3.1). Faults (and mass movement deposits) may also form barriers that inhibit flow through the overburden. Whether such features are sealing or non-sealing to flow is dependent on the properties of the lithologies or sediment types juxtaposed across the fault (or basal surface of the mass flow deposit).

7.1.1.2 Geological fluid flow pathways

Evidence of natural migration of fluids through the overburden, over geological timescales, can be seen from the development of specific geological structures in the subsurface, such as chimneys, and in offshore areas from the development of pockmarks, mud volcanoes, sand or carbonate mounds and authigenic carbonate precipitation near or at the sea bed. The type of structure generated is dependent on a variety of parameters such as the source of fluid, the flow type, the structural setting and the nature of the sediment through which the fluid flows.

Chimney structures

Chimney structures are vertical conduits, typically tens to hundreds of metres in diameter and up to one kilometre or more in height, providing a pathway through thick, low-permeability overburden successions. They are common in sedimentary basins and known from hydrocarbon exploration as possible conduits for hydrocarbon migration. Seismic survey data reveal near-vertical chimneys that may culminate in pockmarks or gas-bearing mound features at the sea bed. Chimneys and pipes are recorded around the globe. They have been studied in the North Sea, where some occurrences of natural gas in the water column have been partly connected to source sediments through faults and chimney structures. A lack of data on the properties of chimney features has been identified as a key research target and several studies are investigating chimney structures in the North Sea at the date of this review.

Pockmarks

Pockmarks at the sea bed are considered the most frequent expression of focused fluid seepage of gases, such as methane, hydrogen sulphide and CO_2. The presence of pockmarks, as evidence of former or present day fluid migration, is well known worldwide from within both hydrocarbon-bearing basins and non-hydrocarbon provinces. They occur only in strata and settings suitable for their formation, mostly in fine-grained unconsolidated sediment, and can be locally very abundant although they occupy less than 5% of the entire UK sector of the North Sea. The detection of pockmarks is dependent on the deployment of high-resolution geophysical survey equipment, so their current known apparent distribution is mainly within economically developed areas. Non-random distribution of pockmarks may be associated with underlying faults, buried channels, tunnel valleys and mass movement deposits. The observation of pockmark structures at the sea bed should not be assumed to be evidence of current fluid flow, since they may be relict structures, and observation or survey of bubble streams is required to confirm active flow.

7.1.1.3 Large-scale geomorphological features

Large-scale, erosional geomorphological features in the shallow subsurface may act as either high-permeability flow pathways or barriers that inhibit migration though the overburden. Two types of geomorphological discontinuity that are tens of kilometres in extent are considered in detail in this review, submarine mass movement deposits and tunnel valleys, because of their distribution and association with evidence of fluid flow.

Submarine mass movement deposits

Submarine mass movement deposits can represent a significant stratigraphic component of many ancient and modern continental margins and have a worldwide distribution. The composition of the sediment matrix, its effective porosity and permeability will vary markedly between each type of deposit and so assessment of their role to enhance migration or trapping of fluid in the subsurface should be undertaken. Mass movement deposits may act as high-permeability pathways, if they are predominantly coarse grained, or baffles if they contain fine-grained, low-permeability mud layers.

Glacial tunnel valleys

Glacial tunnel valleys are of particular interest for overburden fluid migration since they are known to occur in onshore and offshore areas where geological storage or injection of CO_2 is in operation or planned. They are kilometre-scale erosional geomorphological features seen as open at the surface or infilled and buried in the shallow subsurface, to depths of 500 metres in the North Sea. Buried tunnel valleys form very extensive networks in north-west Europe; individual valleys display lengths of 125 kilometres or greater with implications for potential migration routes over large distances. North Sea tunnel valleys are also observed to cross-cut one another, with multiple generations of valleys forming apparently complex networks. The influence of tunnel valleys and their potential to enhance or impede fluid flow within the overburden in glaciated areas requires an understanding of their distribution, morphology and fill. However, since there is currently a lack of borehole samples very little is known about the fluid flow properties of tunnel valley fill in offshore areas.

7.1.1.4 Hydrofracturing and glacitectonic faults

Hydrofracture systems provide clear evidence of the passage of pressurised groundwater. Loading by glaciers and ice sheets typically results in the development of a pressurised hydrogeological system that can trigger hydraulic fracturing of the underlying sediments and bedrock. Potential migration pathways are created along faulted surfaces, and displacement of strata by rafting disrupts lateral seals to allow flow through more permeable material. Sediment-filled fractures, fluid escape structures and folding and faulting associated with hydrofracturing and glacitectonism are relatively common within areas of former glaciated terrane in the UK, northern Europe, Canada, Scandinavia and Russia. Evidence of glacitectonic deformation is recorded in areas where CO_2 storage is operational or planned, for example onshore in Canada and offshore in the North Sea. The effect of subglacial loading on groundwater systems is modelled to extend to 1500 metres depth in the Netherlands. Glacigenic fault zones can be tens of kilometres in length and although the maximum

depth of faulting is hundreds of metres it is typically much shallower. Although the possibility of enhanced migration is confined to the shallowest overburden strata it should not be discounted in geologically recently glaciated terranes.

7.1.1.5 Wellbores

Wellbores are designed, constructed and abandoned to preserve hydraulic isolation between intervals penetrated by the well and to prevent undesired fluid flow into or out of the wellbore. However, wellbores represent one of the main threats to storage containment since all CO_2 storage sites will contain at least one well and some may be penetrated by hundreds of wells. Despite careful design, losses in wellbore integrity can occur as a result of subsequent physical and chemical changes in and around the wellbore and/or construction defects. Wells abandoned prior to the inception of CO_2 storage at a locality will not have been designed specifically to withstand such operations. Pathways may exist along the interfaces between the well cement and geological formation, through the cement, along the interface between the cement and well casing, along the cement and metal casing interface of an abandonment plug and through the abandonment plug itself (Figure 3.25).

Abandoned wellbores may maintain their integrity and not necessarily provide a direct pathway for migration of CO_2 through the overburden to the surface, but it can be a very challenging process to establish this. A conservative approach to risk assessment is generally taken, so wells may be classified as 'higher risk' because there is insufficient information available to characterise and assess their integrity. Well integrity studies assess the rate of cement alteration rather than fluid migration or leakage and predicted alteration does not necessarily equate to barrier degradation since improved barrier properties are also reported. Alteration by diffusion through the cement matrix, in a scenario considered to be typical of CO_2 storage, is considered to be extremely slow and not a threat to well integrity. Fracture sealing may be more common than fracture opening because of the long residence times of the reaction fluids. Field-scale studies found that a well with questionable integrity sustained hydraulic isolation despite indications from core logging of large changes in integrity which, therefore, need not identify an increased risk of leakage. Study of CO_2-EOR wells found that well age, operational mode, completion intervals, or presence of acid gas in the produced fluids did not have a statistically detrimental effect on integrity. Unanticipated wellbore-related leakage has occurred in the USA where past records were inadequate to properly locate all wells in the area of interest. Wells for CO_2-EOR have been in operation for relatively short timescales compared to the period anticipated to demonstrate long-term containment at a CO_2 storage site. The risk of leakage may, therefore, be better understood from simulations that can predict the behaviours of well barriers over much longer time periods. An estimate of leakage rates along abandoned well bores, based on a few hundred simulations, found extremely small amounts of the total injected CO_2 might flow up the wellbore. Small-scale cement or casing leaks may be small (mostly less than 0.1 tonnes per year) or up to 100 tonnes per year but potentially of longer duration than large-scale leakage events.

7.1.1.6 Modelling of migration

Modelling of the migration of CO_2 in the overburden above a storage site is problematic because the leakage is always, to an extent, unexpected. Permitting of the operation would not have been possible if there was a known flow pathway through the overburden to the surface through which CO_2 was predicted to travel. The models reviewed either estimate maximum amounts of leakage from small, unpredictable pathways or, with hindsight, determine further information about a known leak from an existing operation. Computational modelling of CO_2 leakage and migration in the overburden and of the relationship between mechanism and expected rates is considered for flow through faults and fractures (**Error! Reference source not found.**), abandoned wellbores (**Error! Reference source not found.**) and via chimneys.

Large faults are detected during site characterisation while smaller faults, not discernible by seismic survey could also pose some level of risk to CO_2 storage operations. Ideally, prediction or simulation of flow through a 'static', geometrical fault model should be coupled with 'dynamic' geomechanical modelling to incorporate reactivation of existing or opening of new fractures by pressure changes associated with CO_2 injection. A sample of computational studies on CO_2 leakage through faults indicates increasing the length, aperture and permeability of a fault increases the potential flow rate through it. Stratal permeability also has an impact on the amount of pressure that is generated from an injection operation, which can then have a knock-on effect on the geomechanical stability and enable wider opening of fractures. Modelling of flow via abandoned wellbores is generally considered to be more localised than through faults and therefore more predictable, providing that the locations of historical wellbores are known. The key assumption to determine leakage rates through wellbores is the permeability, in which bi-modal distribution is typically applied. Two distinct categories, either intact well-bonded cement or degraded and/or poorly bonded cement are applied to appropriate sections of a wellbore. There have been many attempts to find computationally cheap solutions to the complex system of CO_2 leakage. Stochastic methods are the method of choice for simplified models with low computational cost to analyse the impact of uncertainty in wellbore permeability and provide confidence intervals for leakage rates.

7.1.2 Storage site overburden sequences

Review and comparison of the character of the overburden strata at five selected operational or planned CO_2 storage sites highlights a number of common features. The storage sites reviewed are the offshore Sleipner and Snøhvit projects and planned Goldeneye Field site and the onshore Ketzin pilot CO_2 injection project, Germany, and the Field Research Station in Alberta, Canada. The common feature of all these major CO_2 storage demonstration sites is injection into a porous and permeable storage formation. This unit is usually capped by a series of shale or clay lithologies, which act to seal the storage complex. Additionally, there are multiple secondary sealing units in the overburden sequence. These typically comprise low-permeability shale, clay or evaporite lithologies which act to seal the storage formation. Porous strata within the overburden sequence can act as secondary storage formations, should any injected

CO_2 bypass the primary seal rocks. The structure of the overburden sequence is commonly flat lying or shallowly inclined and little affected by faulting. Although fault structures are mapped in the overburden to the Snøvhit CO_2 storage project, site characterisation investigations indicate they are sealing to fluid flow and pressure propagation.

7.1.3 Rates of migration through the overburden

Evidence of rates of migration through the overburden are drawn from measurement and modelling of CO_2 flux from faults, methane flux at natural seepage sites and studies of the integrity of hydrocarbon and CO_2 wells.

7.1.3.1 Migration through faults

The factors that control fluid migration are common to both across-fault and vertical migration of fluids along fault zones. Stratigraphic juxtaposition, fault zone geometry, character of the damage zone, fault rock composition and post-deformation diagenesis all influence the likely along-fault and vertical flow properties. Natural seepage rates for CO_2 derived from magmatic and hydrothermal sources along faults (Table 3.1) give a useful range for the flux rates that can be transmitted, although it is not clear whether they provide good analogues for migration above CO_2 storage sites. The natural seep studies (Table 6.1) do provide some useful indications of how CO_2 might migrate through overburden faults. Some of the surface leakage has been associated with faults and low-level seismicity, indicating that seismic activity is responsible for facilitating along-fault migration. Modelling studies of CO_2 leakage along faults (Table 3.4) suggest variable fluxes, reflecting significant uncertainty in fault parameters and different injection rates. Simulated leakage rates which are comparable to those seen at natural analogue sites require very high fault zone permeabilities to be invoked.

7.1.3.2 Gas flux via geological fluid flow structures

Marine methane gas seeps are a widespread phenomenon; however, very few gas seepage rate measurements have been made (Table 3.1). Fluid flux can be spatially and temporally variable with several seeps exhibiting periodic and discontinuous ('on–off') flow rate characteristics. Seepage rates may be modified by tide and ocean swell changes, and potentially by earthquakes. Flux from a single seep is mostly small but the total marine contribution of methane gas flux has been estimated to be about 50 million tonnes per year from sea bed seeps, of which 30 million tonnes per year reaches the atmosphere. Methane flux rates from individual fluid flow features, where measured, are negligible but the cumulative total for a number of seeps may be notable. A study of the Tommeliten seepage area in Norway indicates approximately 26 tonnes of methane gas is being released each year (Hovland and Thomsen, 1989). The measured flux rates of naturally occurring methane gas inform our understanding of fluid flow through the overburden but are not directly relevant to the migration of CO_2 due to the contrast in physical and chemical properties of the two gases. CO_2 is more soluble than methane in aqueous solution and so a much greater proportion will be retained during migration through the overburden by dissolution.

7.1.3.3 Wellbore potential migration rates

Although there are relatively few records relating to actual wellbore leakage rates, data examined from analogue sites (Figure 3.26 and Table A1) suggest that both the rate and duration should be assessed. Although preliminary indications of the rate of flow in reverse-flow (blow-out) events could be high, one thousand tonnes per year or more, they are likely to leak for much less than a year. Smaller cement or casing leaks, mostly measured as one kilogramme a year or much less, could have lower rates of flow but potentially be of longer duration if not detected or mitigation is not cost effective.

7.1.4 Overburden trapping potential

The three dominant processes that can affect the natural attenuation of CO_2 migrating through the overburden are physical trapping, potential mineral precipitation and hydrodynamic trapping. The physical migration of CO_2 through the overburden will be controlled by viscous, capillary and gravity forces, which will determine the potential for secondary accumulation and lateral migration within a highly permeable lithology or fault. Simulations of fault-controlled CO_2 migration indicate that the greatest attenuation is likely to occur in permeable layers near to the storage reservoir.

Heterogeneity within the overburden, i.e. a wide range of permeability values, will increase the rate of dissolution and higher capillary threshold pressure increases the trapping potential of secondary aquifers through residual trapping and dissolution. The formation of secondary accumulations, whilst providing secondary trapping potential, may also provide further routes to leakage if high-permeability pathways connect these secondary accumulations to the surface. Fluxes to the surface are balanced by the size of these secondary accumulations and the permeability of connecting pathways.

Evidence for physical trapping by fault-controlled migration can be drawn from studies of natural CO_2-rich groundwaters. Extensional faults in south-east Utah can act as conduits for CO_2-bearing fluids, however, where low-permeability rocks occur in the hanging wall, the same structure can be a barrier to flow and so promote trapping. Exsolution of CO_2 to free gas phase significantly increases at depths shallower than 650 metres.

Dissolution of CO_2 to form acidic fluids is also the precursor to mineral dissolution and trapping in the overburden. Reaction of the weakly acidic fluids will initially dissolve carbonate and oxy-hydroxide mineral phases and subsequently silicate minerals, although at relatively slow rates, as supported by evidence of feldspar dissolution in south-east Utah. Field investigations also support the likelihood of re-precipitation of carbonate minerals to increase mineral trapping even in fine-grained rocks.

CO_2 dissolution and sinking of the saturated or partly saturated pore water has the potential to trap large volumes, although the mechanism may take thousands of years. However, in dynamic systems with active groundwater flow in the overburden dissolution may be more extensive.

Simulations of leakage along faults suggest that variable permeability values along a fault can reduce the rate of fracture flow and increase the potential for CO_2 dissolution. The amount of CO_2 reaching the surface after leaking through a highly permeable

fracture can be reduced if the fracture intersects suitably permeable formations within the subsurface. Modelling indicates the amount of CO_2 reaching the surface is lower when the fracture intersects a greater number of rock layers with high permeability values.

Hydrate formation may play an important role in trapping CO_2 within the overburden of a storage site in geological situations of elevated pressures and cool temperatures. Geographical locations where this might be possible include shallower sediments below the floors of deep cold oceans and below permafrost, should such regions be considered for storage. In these settings CO_2 hydrate could play an important role as both a primary storage phase, and/or a secondary chemical containment mechanism for unintended upward migration of CO_2 through the overburden. A preliminary assessment of the location and thickness of sediments indicates that CO_2 hydrate is not stable in sediments below the relatively shallow waters around the UK and north-west Europe under present-day conditions.The potential for CO_2 hydrate formation has particular application for higher latitude regions, such as northern areas of Canada.

7.1.5 Lessons learnt from experiments and natural leakages

Observations made of natural CO_2 seepage at six sites and at seven experimental CO_2 releases were reviewed and compared. The natural seeps are mostly (five) from volcanic regions and so are not suitable to indicate background values of CO_2 flux for a storage site; although they are useful to establish characterization and monitoring methods. By contrast, the controlled experimental sites are mostly onshore where the experimental method and monitoring of environmental impact is more readily achieved. Key lessons learned by comparison of the experimental releases and natural seepage sites are summarized in the following numbered points.

1. Surface seepage is most likely to be localised, within areas metres to tens of metres across. The migration pathways, and hence location of surface seeps, are very hard to predict even for well-characterised sites. Monitoring systems are therefore needed that can identify seeps at least tens of metres across within the large areas above storage sites. Controlled release sites and natural seepage sites show a similar pattern of distribution in that leaks are initially localised to areas between one and tens of metres in diameter.
2. Flux rates measured at natural seepage sites and experimental and accidental releases are highly variable, from very low rates close to background levels (around 0.0001 t m^{-2} d^{-1}), to very high rates (up to 1 Mt m^{-2} d^{-1}) where CO_2 has been released from open boreholes. High rates in and around boreholes, faults or fractures are likely to be easily detected. Fluxes from CO_2 leakage in a sedimentary environment are most likely to range from natural background to around 10 kilogrammes per square metre per day (10 kg m^{-2} $d^{-1)}$.
3. Quantification of CO_2 seepage is possible with existing methods but is still likely to need further refinement; flux rates vary over time in natural systems and even in subsurface release experiments with constant injection rates. Estimates of total emissions will need to account for both spatial and temporal variability.

7.2 Recommendations for overburden characterisation methods

7.2.1 Characterisation of overburden faults and fractures

High-resolution 3D seismic reflection data is recommended as the most effective method to identify and map the geometry of overburden faults with throws in the order of 10 metres or more. More deeply focused seismic surveys, aimed at the underlying storage reservoir intervals, commonly offer poorer imaging of the shallow overburden within a few hundred metres of the surface. Deep-focused seismic survey data should be combined with high frequency 3D or 2D seismic surveys if faults extend to the near surface, to more accurately determine the near-surface fault geometry. Analysis of structural seismic amplitude attributes, such as variance and 'ant-tracking', may be used to aid interpretation of faults, and to identify small-offset faults that may be more difficult to interpret using conventional cross-sectional seismic amplitude displays. Such attributes can be rendered onto interpreted horizon surfaces to display fault-horizon intersections at successive stratigraphic depths.

Borehole image logs, such as the Ultrasonic Borehole Imaging (UBI), or Formation Micro Imager (FMI) logs, can be used to identify faults and fractures intersected by the well. The logging tools are used to generate ultrasonic or electric images of the borehole walls and are commonly used to identify faults and fractures. Imaging of such features can be limited in near-vertical wells because the trajectory is only likely to intersect structures that are shallowly inclined. Deviated wells, which are themselves shallowly inclined or near-horizontal, will generally intersect a greater number of faults and fractures if they are present. The image logs allow the identification of small fractures, which can be invaluable in characterising potential fluid migration pathways in both the storage reservoir and in the overburden. Of particular importance is the identification of any preferential disposition of fault structures developed within the overburden, including those that are too small to be resolved by the seismic survey data. Borehole log data can provide information on the propensity for faulting, the orientation of faults and fractures, the widths of fault damage zones and, potentially, the nature of the fracture fill. High-resolution temperature logs can be used to identify any faults that are active conduits for fluid flow.

Interpretation of borehole image logs to identify borehole breakouts and drilling-induced tensile fractures is recommended to determine the relative orientation of the present day principal stresses acting on the overburden. Knowledge of the principal stress directions is essential to predict the mechanical integrity of faults and fractures and to determine the orientation of fault structures relative to the in situ stresses. The relationship between the orientation of existing structures and the prevailing stress field can be used to assess the likelihood that the fault may or may not be a prospective fluid-flow pathway.

Coring through faults is usually only undertaken in research boreholes, however, drilling through faults and acquiring core, although challenging, could be an option if an understanding of overburden fault properties is deemed critical to the characterisation of fluid-flow pathways.

7.2.2 Characterisation of chimney features

High-resolution 3D seismic surveys, operating with high frequency seismic sources, are recommended for characterisation of chimney features in the overburden. Currently, chimney features are characterised using large 3D seismic survey 'cubes' that have been acquired to characterise different target strata. This lack of optimisation means that accurate characterisation of chimney features in the overburden is far from optimal. Acquisition of survey data using seismic sources with higher frequencies than those used for deeply focused strata would offer a significant improvement in the vertical resolution of the data. Improved, high-frequency imaging would also inform interpretation of the internal structure of the vertical pathway.

In situ measurements of the internal hydraulic properties of chimneys are currently lacking. Acquisition of such data would offer insights into possible fluid flow rates and experimental work to core into a chimney by the STEMM-CCS project is invaluable to a wide scientific community. The planned data acquisition and coring and sampling will provide the first database of geomechanical, geophysical and hydraulic properties of a chimney structure. In future, the STEMM-CCS drilling and logging studies, acquired alongside geophysical data, will enable researchers to better parameterise vertical fluid conduits and estimate remnant saturations in chimney structures.

7.2.3 Characterisation of tunnel valleys and other glacial features

High-resolution, 3D seismic reflection data is recommended to provide the best data from which to identify and characterise subsurface glacial geomorphological features. Tunnel valleys, in particular, which may form preferential fluid flow pathways, are laterally variable over hundreds of kilometres and require imaging methods that can capture this lateral variation in map view. Tunnel valleys are often found to form cross-cutting networks, also requiring 3D data to understand the relationship between superimposed valleys. 3D seismic reflection data specifically designed to image the shallow section of the overburden to depths of hundreds of metres, i.e. with a high frequency seismic source, provide the best opportunity to characterise the infill of the tunnel valleys. However, 3D seismic data acquisition is very costly and so it is recommended that characterisation of geomorphological features in the overburden is undertaken using 3D seismic data acquired to image the deeper subsurface for other purposes, such as the oil and gas exploration industry. 2D seismic reflection data may also be used to image tunnel valleys, and high-resolution (high frequency source) 2D seismic is also suitable for characterising tunnel valley infill. Onshore, electro-magnetic methods may be used to image buried features such as tunnel valleys and to provide information on the coarseness and conductivity of the valley infill. Continually cored boreholes are required to ground-truth the internal valley infill, but remain prohibitively expensive, particularly offshore where, to date, no scientific drilling has been carried out through buried tunnel valleys.

7.2.4 Characterisation of glacitectonic structures

Characterisation for assessment of onshore glacitectonic structures as potential fluid pathways is best achieved by a detailed description and analysis of the deformation structures in onshore geological exposures. The observations may be made from

naturally exposed sections, such as coastal cliffs, incised river sections or similar, and/or man-made excavations in quarries and trial pits. Standard field techniques should be followed as routinely used by structural geologists.

The use of Unmanned Aerial Vehicles (UAVs) or 'drones' to capture high-resolution air photographs and/or video imagery is recommended as they can be used to create detailed 3D models of glacitectonic structures exposed in large cliff sections and quarries. When aerial photographic image acquisition is undertaken in conjunction with a Global Positioning System (GPS) survey the resultant models can be fully orthorectified and tied-in to any available subsurface geophysical data using commercially available 3D modelling packages.

The lateral and vertical extent of large-scale glacitectonic structures in the subsurface, both onshore and offshore, can also be investigated by interpretation of high-resolution 2D and 3D seismic reflection data.

These recommended approaches provide the best methods to identify and characterise the subsurface structure within a glacitectonised terrane. Glacitectonic thrust complexes can comprise several generations of cross-cutting folds and thrust faults, and can be traced laterally for hundreds of metres to tens of kilometres. Characterisation of these complex systems requires imaging methods that can capture this variation both horizontally (plan view) and vertically (cross section). 3D seismic reflection data specifically designed to image the shallow section of the overburden to depths to hundreds of metres, i.e. with a high-frequency seismic source, provides the best method to characterise the 3D structure of the overburden.

7.2.5 Characterisation of wellbore integrity

A series of consecutive activities are recommended to characterise the integrity of wellbores in the overburden to CO_2 storage sites. The objectives are to identify and characterise which wellbores, if any, are perceived as potential flow pathways for CO_2 migration in the overburden and to understand the risks they pose. Further activities include mitigating overburden flow risks and monitoring, appropriately, to allow timely preventative or remedial actions.

Wellbores that have the potential to enhance CO_2 migration through the overburden should be identified. The location and depths of wells within the storage area will have previously been investigated, as these are required as input to geological models to characterise the site. Simulations that model CO_2 injection and migration will encompass scenarios that are most likely, as well as those end-member scenarios that are least likely. These simulations can help to identify those wellbores expected to be within the predicted extent of the CO_2 plume. Scenarios that conceptually analyse the potential for linking up of different leakage paths will also be informative. For example, wellbores may not penetrate the storage reservoir itself but intersect dipping permeable overburden formations that, in turn, link to a gas chimney in the shallow subsurface. Such processes can highlight and prioritise the wellbores that require further characterisation to assess their risk to storage containment.

The integrity of wellbores that have the potential to enhance CO_2 migration through the overburden should be characterised. Documentary information of the design,

completion and abandonment of the identified wellbores should be reviewed for information on borehole and casing sizes and depths, cemented intervals and cement types and thickness. Original casing tests and logs of cement bond presence and quality and other information may be available. The effort required to achieve wellbore characterisation from legacy data should not be underestimated since this can be a non-trivial activity (Section 7.3.4). At this stage of characterisation, additional downhole integrity logs and tests could be performed in non-abandoned wellbores to which the storage operator has access.

The likelihood of wellbores enhancing CO_2 migration through the overburden should be assessed. This will include characterising the fluids, temperature and pressures in and around the identified at-risk wellbores to understand the effects that physical loading and chemical reactions may have on the wellbores. Commonly, the effects can be assessed through geomechanical and geochemical models if the dynamic system is sufficiently well understood. If not, relevant parameters and behaviours may be deduced through laboratory tests on relevant samples and field-scale studies. This can be a time-consuming and expensive activity, but can inform and so improve confidence in the results of geomechanical stability and geochemical modelling (Section 7.3.4).

Mitigation activities may be possible where the assessment of the identified wellbores indicates poor integrity that might enhance CO_2 migration in the overburden. For boreholes that remain accessible, it may be possible to mitigate identified leakage pathways through downhole maintenance such as cement squeeze jobs (Section 3.5.2.1). Site storage design and strategy could be modified to reduce the physical and chemical load on at-risk wellbores. Access to some wellbores will not be possible if they have been plugged and abandoned. The possibility of re-entering abandoned boreholes to mitigate leakage risks is considered in Section 7.3.4.

Monitoring of any wellbores that remain at-risk as potential CO_2 flow pathways is recommended. This might include, for example, downhole and annular pressure monitoring of accessible boreholes and surface-based subsurface monitoring targeted within the vicinity of abandoned wells. Integration of monitoring and modelling results, to regularly update the understanding of the enhanced migration potential, and to detect ‘early warning’ of unexpected migration is also recommended.

7.2.6 Numerical modelling for overburden characterisation

Characterisation methods can benefit from numerical modelling and is recommended to enable assessment of the dependence of leakage rates on particular parameters. Knowledge of the significance of each parameter, determined by numerical modelling, provides information to assess the importance of precise characterisation for every variable.

7.2.7 Characterisation to establish near-surface soil gas and gas flux baselines

Understanding of baseline gas concentration and flux condition is important for assessing any future emissions that might result in the unlikely event of leakage from CO_2 storage. This needs to encompass both temporal (e.g. diurnal, seasonal, event-driven) and spatial variability. Baseline knowledge helps to identify potentially

anomalous gas concentration and flux values during the operational phase of a CO_2 storage site that require further examination to ascertain whether they are due to leakage or not. Baseline flux values also need to be subtracted from gross measurements of flux for more accurate estimation of any emissions to the atmosphere or into sea-water due to storage site operation. Baseline definition is relevant to both onshore and offshore sites.

A combination of complementary technologies, based on the techniques and methods used at natural and experimental sites, are recommended to strengthen verification of results. Baseline characterisation and monitoring techniques need to be able to cover a range of scenarios by assessing areas between metre-scale and kilometre-scale as well as small-scale to large-scale fluxes.

In the event of detecting anomalous gas concentrations or fluxes, methods are required to determine the source of the gas to ascertain if there is leakage of injected CO_2. Gas ratios and stable or radiogenic isotopes (C and noble gases) have been shown to be successful for source attribution. The determination of source may vary depending on site characteristics and the source of the injected CO_2.

7.3 Knowledge gaps

7.3.1 Faults and fractures knowledge gaps

Currently there is a lack of quantitative parameterisation and attribution to adequately describe detailed fault architecture in three-dimensions. Numerical models of fluid-flow through faults are dependent on relevant input data to appropriately represent a fault and so generate realistic output. Quantitative ‘description’ is needed to parameterise fault zone heterogeneities such as thickness and distribution of small-scale faults, fault displacement and the distribution of fault rock properties within the fault zone.

The prediction by mathematical algorithms of fault sealing properties, such as Shale Gouge Ratio, has been shown to be consistent with observations of hydrocarbon column heights and differential pressure gradients across faults. However, the effectiveness of such algorithms to estimate the location of small areas where low permeability fault rock may be absent or very thin has not been rigorously tested using outcrop studies. Dockrill and Shipton (2010) show that fault seal algorithms may not sufficiently describe fault permeability distributions. Understanding the effectiveness of fault-seal algorithms would benefit from further studies of well-exposed faults, especially those that exhibit evidence of past fluid-flow. Additionally, cataclasis and grain-crushing are not explicitly accounted for in fault-seal algorithms, and neither has the impact of such processes been comprehensively assessed.

Faults may have experienced multiple episodes of both normal and reverse movement, which would be expected to have a significant impact on the efficacy of predictive fault-seal algorithms. There is a paucity of published case studies investigating the impact of fault reactivation and inversion on the effectiveness of fault seal algorithms.

The generally accepted convention that critically stressed faults are those that are most likely to allow preferential along-fault fluid-flow has been questioned by several

authors (Laubach et al., 2004; Sathar et al., 2012; Cuss et al., 2015). This questioning has led to debate about where and why some faults do not follow the accepted convention. There are a number of areas of uncertainty, including the geometry of a fault at scales less than the resolution of the characterisation data, potentially heterogeneous fault rock frictional properties, in situ stress variations and pore pressure distributions, and host-rock rheology. An appraisal is needed of how these factors might combine to complicate the prediction of critically stressed faults.

A lack of understanding of the role of polygonal faults in present day fluid-flow is considered to be an important knowledge gap. The overburden to many prospective CO_2 storage formations in the North Sea contains polygonally faulted strata (Section 3.1.2.3). However, it is not known whether such structures would be conduits to upward fluid flow at the present day and, if so, the lithological sequence and subsurface conditions needed to permit fluid flow.

7.3.2 Fluid flow features knowledge gaps

Contrasting with the present wealth of information on worldwide pockmark occurrence, the initiation of a large pockmark has never been directly observed and little is known about their longer-term activity and persistence. To assess pockmark field longevity and evolution, it would be vital to constrain the frequency of pockmark formation, and if applicable, pockmark demise, which would require repeat high-resolution swath bathymetric surveys.

A major unknown are in the in situ fluid flow properties of gas 'chimneys' which can be well in excess of a kilometre in height, allowing them to straddle thick overburden successions. In some cases the seismically imaged features are linked to overlying pockmarks at the seabed. This relationship is indicative of significant contemporary fluid flux and high transient permeability, suggesting they have formed conduits for large-scale gas or fluid migration at some point in their history. There is no record in the public domain of any chimney having been sampled in situ, but rare field exposures of exhumed examples suggest that they comprise pipe-like structures with disturbed strata and complex anastomosing fracture networks. However, their fluid flow properties, either when they are actively flowing, or in a state of natural dormancy, are not understood. A number of new projects (Section 3.2.1) aim to study the in situ properties of both natural methane gas and induced CO_2 chimneys. These projects offer the opportunity to better characterise vertical fluid flow pathways, enabling an improved understanding of in situ features. Developing a better understanding of both the broad- and fine-scale properties of chimneys would offer reduced uncertainty in monitoring and modelling of fluid conduits. A geophysical monitoring program which investigates the structure and properties of the chimney to derive seismic velocity and anisotropic properties would be of great use to the research community. Undertaking these studies alongside electromagnetic monitoring methodologies should offer a unique insight into the residual fluid distribution.

7.3.3 Overburden characterisation knowledge gaps

In order to better characterise the overburden an emphasis on logging and monitoring in boreholes above the reservoir zone is required. This would offer improved

characterisation of the region above the storage site. A continued understanding of the importance of downhole pressure monitoring, at both the reservoir level, and in the zone immediately overlying the CO_2 store would result in improvement in flow and geomechanical models of storage sites. Additionally, the thresholds for leakage detection would be easier to determine with a better characterised, and monitored, overburden.

7.3.4 Well integrity knowledge gaps

Knowledge gaps in the characterisation of wellbore integrity are associated with the challenges of access to the necessary legacy well records. It is often not possible to fully characterise the risk of fluid migration via wellbores because of the lack of well records. Record keeping and retrieval systems depend on the regulatory requirements, guidelines and company policies at the storage location, so characterisation difficulties will vary from site to site. Nevertheless anecdotally, many sites worldwide have found the process of characterising wellbore integrity a complex process. Difficulties range from insufficient legacy records to characterise integrity of individual wells to assimilating vast quantities of legacy records for sites with hundreds of wells. In particular, characterising the integrity of wellbores that have been abandoned, or to which there is no access, will not be possible without non-trivial re-drilling to re-enter the wellbore.

Knowledge gaps in the understanding of the wellbore integrity are also associated with the difficulties in obtaining the necessary information with which to make an assessment. Data required to assess the containment threat and which are lacking include:

- The hydraulic properties of wells are often not publicly available, as field operators rarely release data unless they are required to do so by regulation.
- Observational evidence needed to validate predictive models on the long-term effects of CO_2 at a field-scale is lacking. Currently, direct testing by borehole wall sampling risks compromising wellbore integrity, although the sample hole is plugged afterwards.
- Incomplete understanding of the coupled chemical, physical stressors, transport and flow properties particularly along barrier interfaces and the potential protective or detrimental effects.

Mitigation of poor well integrity, where it threatens containment, requires an understanding of how to ‘cheaply’ and effectively deal with a wellbore that lacks sufficient characterisation information, has suspect integrity or monitoring has indicated to be leaking. Re-entering old wells to re-abandon them will be very expensive and there is thought to be relatively little industry experience of such operations. There is little existing experience because prior to CO_2 storage there were likely to have been few instances where it would have been necessary to re-enter and re-abandon a well. Effectiveness and cost-benefit of such operations are also not known.

Knowledge gaps related to ‘at risk’ wellbores include the ability to monitor the integrity of abandoned wellbores and the ability of surface-based techniques to detect subsurface wellbore leakage.

7.3.5 Modelling knowledge gaps

Some of the largest challenges in modelling flow in the overburden are based around characterisation. The volume of overburden that might be affected by migration can be large and complex and so identifying appropriate parameter values for each storage site is the most difficult stage of the modelling and the most sensitive for predicting rates of leakage.

There are also a wide range of CO_2 reservoir types with very different properties relating to leakage pathways. This makes comparison and verification of numerical models difficult.

The two main pathways through which potential CO_2 leakage is modelled are faults and fractures and abandoned wellbores, as discussed above. Properties and characterisation methods for other possible pathways, e.g. chimneys, are less readily available and there is, therefore, a current lack of numerical modelling of CO_2 flow associated with these features.

The models are only as reliable as the characterisation of the site. Numerical models give precise results for the parameters input to within a given tolerance, but the applicability of the modelling to a specific site depends on the reliability of the input parameters. Modelling is especially useful with uncertainty quantification and can also be used with hindsight to determine parameters from a known leak.

7.3.6 Glacitectonic deformation and hydrofracturing knowledge gaps

Although there is clear field evidence that glacitectonic structures act as fluid pathways during deformation, their subsequent conductivity to near-surface hydrocarbon migration and/or groundwater systems remains poorly understood.

Hydrofractures in glacial environments provide clear evidence of the passage of pressurised meltwater that, once formed, could theoretically be reactivated. However, the overpressures required to initiate hydrofracturing, the nature of the fluid flow within these systems and the volumes of water they transmit remain uncertain.

7.3.7 Trapping by CO_2 hydrate formation knowledge gaps

This review shows there is potential for CO_2 hydrate formation in the overburden if CO_2 were to migrate out of a deep geological storage facility, under appropriate pressure and temperature conditions. However, quantitative data are needed to inform an assessment of the processes involved and prediction of CO_2 trapping by hydrate formation. Areas for research to provide the necessary detailed data are as follows:

1) Produce realistic climate models for prospective storage sites at high latitude. These should include assessments of likely permafrost depths.
2) Produce accurate thermal models for the sites of interest (both onshore and offshore). These should include:

As a starting point, an accurate assessment of current temperature profiles;

Time-dependent models for temperature profiles through the geosphere, especially if injected CO_2 is out of thermal equilibrium with the reservoir horizon or overlying rocks. These may require the generation of new data on properties such as the thermal conductivity and heat capacity of relevant rock types.

3) Investigate likely gas compositions and migration rates within the overburden, and assess whether they will facilitate hydrate formation if pressure/temperature conditions are suitable.

4) Ascertain whether hydrate formation and disassociation will affect the physical properties of the overburden.

The suggested investigations should lead to an improved understanding of the potential for CO_2 hydrate formation within the overburden above a deep geological store of CO_2. Ultimately, this should allow us to ascertain whether CO_2 hydrate formation will be a possible benefit or of neutral consequence for the long-term isolation of CO_2.

7.3.8 Wide-area near-surface soil gas and gas flux characterisation knowledge gaps

There is as yet no reliable method capable of detecting small fluid seeps efficiently and at reasonable cost across the whole surface area of a full-scale storage site. This is a desirable goal given that potential locations of seepage are very difficult to predict based on our present imperfect understanding of migration pathways.

7.3.8.1 Importance of diffuse seepage

There are indications from isotope data of low levels of seepage from experimental sites away from the more obvious seepage features, which were undetectable by gas concentration and flux measurements. What is not clear is how widespread this more diffuse seepage is and whether it results in the emission of significant amounts of CO_2. There are plans to investigate this in the European (Horizon 2020) project ENOS (Enabling Onshore CO_2 Storage in Europe).

7.3.8.2 Fault seepage

Although there has been some recent work on natural seepage along faults in sedimentary basins, such as that in the Paradox Basin in the USA, Florina Basin in Greece and on the Bongwana Fault in South Africa, there remain gaps in knowledge. The likely flux rates of seepage from CO_2 storage could be better constrained by concentrating on the closest analogues to storage sites. Whilst it is known that seepage only occurs in higher permeability zones, along a small proportion of total fault length, better understanding of why this is so would improve the capability to predict where leakage might occur and hence where monitoring would best be concentrated.

8 References

Aber, J. S. 1985. The character of glaciotectonism. *Geologie en Mijnbouw 64*, 389-395.

Aber, J.S., Croot, D.G. and Fenton, M.M. 1989. Glaciotectonic Landforms and Structures. *Kluwer, Dordrecht*.

Akbarabadi, M. and M. Piri 2013. Relative permeability hysteresis and capillary trapping characteristics of supercritical CO_2/brine systems: An experimental study at reservoir conditions. *Advances in Water Resources* 52: 190-206

Andresen K.J. (2012) Fluid flow features in hydrocarbon plumbing systems: what do they tell us about the basin evolution? *Marine Geology*, pp. 1–20.

Aliani, S., Bortoluzzi, G., Caramanna, G and Raffa, F. 2010. Seawater dynamics and environmental settings after November 2002 gas eruption off Bottaro (Panarea, Aeolian Islands, Mediterranean Sea). *Continental Shelf Research* 30, 1338–1348

Allan, U.S. 1989. Model for hydrocarbon migration and entrapment within faulted structures. *AAPG Bulletin* 73 (7), 803–811.

Allison, M L. 2001. Hutchinson, Kansas: A Geologic Detective Story. *Geotimes*, Vol. October 2001.

Altman, S. J., Aminzadeh, B., Balhoff, M. T., Bennett, P. C., Bryant, S. L., Cardenas, M. B., Chaudhary, K., Cygan, R. T., Deng, W., Dewers, T., DiCarlo, D. A., Eichhubl, P., Hesse, M. A., Huh, C., Matteo, E. N., Mehmani, Y., Tenney, C. M. and Yoon, H. 2014. Chemical and Hydrodynamic Mechanisms for Long-Term Geological Carbon Storage. *Journal of Physical Chemistry C*., 118(28), 15103-15113.

Andersen, L.T., Hansen, D.L. and Huuse, M. 2005. Numerical modelling of thrust structures in unconsolidated sediments: implications for glaciotectonic deformation. *Journal of Structural Geology* 27, 587-596.

Annunziatellis, A., Beaubien, S.E., Ciotoli, G. and Lombardi, S. 2004. A comparison of leaking and non-leaking CO_2 reservoirs as natural analogues for geological CO_2 sequestration (Sesta and Latera geothermal fields, central Italy). *Presented at the 32nd International Geological Congress, August 20-28, Florence, Italy*.

Annunziatellis, A, Beaubien, S E, Bigi, S, Ciotoli, G, Coltella, M and Lombardi, S. 2008. Gas migration along fault systems and through the vadose zone in the Latera caldera (central Italy): Implications for CO_2 geological storage. *International Journal of Greenhouse Gas Control*, Vol. 2, 353-372.

Antonellini, M.A., Aydin, A. and Pollard, D.D. 1994. Microstructure of deformation bands in porous sandstones at Arches National Park, Utah. *Journal of Structural Geology*, 16 (7), 941–959.

Aoyagi, R., Kitamura, O., Itaoka, K., Igawa, S. and Suzuki, S. 2011 Study on the role of simulation of possible leakage from geological CO_2 storage in sub-seabed for environmental impact assessment. *Energy Procedia* 4, 3881–3888.

Argent, J.D., Stewart, A., Green, P.F. and Underhill, J.R. 2002. Heterogeneous exhumation in the Inner Moray Firth, UK North Sea: constraints from new AFTA® and seismic data. *Journal of the Geological Society, London* 159, 715–729.

Argnani, A and Savelli, C. 1999. Cenozoic volcanism and tectonics in the southern Tyrrhenian Sea space-time distribution and geodynamic significance. *Journal of Geodynamics* 27. 409-432

Arts, R. J., Eiken, O., Chadwick, R.A., Zweigel, P., Van Der Meer, L. and Zinszner, B., 2004, Monitoring of CO_2 injected at Sleipner using time-lapse seismic data. *Energy*, 29, 1383–1392.

Arts, R.J., Baradello, J.L., Girard, J.F., Kirby, G., Lombardi, S., Williams, P. and Zaja, A. 2009. Results of geophysical monitoring over a “leaking” natural analogue site in Italy. *Energy Procedia* 1, 2269–2276.

Assayag, N., Bickle, M., Kampman, N. and Becker, J., 2009. Carbon isotope constraints on CO_2 degassing in cold-water geyser, Green river, Utah. *Energy Procedia* 1, 2361–2366.

Astorri, F., Beaubien, S.E., Ciotoli, G. and Lombardi, S. 2002. An assessment of gas emanation hazard using a geographic information system and geostatistics. *Health Physics* 82, 358–366.

Auken, E, Doetsch, J, Fiandaca, G, Christiansen, A V, Gazoty, A, Cahill, A G and Jakobsen, R. 2014. Imaging subsurface migration of dissolved CO_2 in a shallow aquifer using 3-D time-lapse electrical resistivity tomography. *Journal of Applied Geophysics*, Vol. 101, 31-41.

Aydin, A. 1978. Small faults formed as deformation bands in sandstone. *Pure and Applied Geophysics* 116, 913–930.

Aydin, A. 2000. Fractures, faults, and hydrocarbon entrapment, migration and flow. *Marine and Petroleum Geology* 17, 797–814.

Azar, J.J. and Samuel, G.R., 2007. *Drilling engineering*. PennWell Books, Tulsa, OK, USA. ISBN-13: 978-1-59370-072-0.

Bachu, S, and Watson, T L. 2006. Possible indicators for CO_2 leakage along wells. *8th International Conference on Greenhouse Gas Control Technologies*, June 19-22, Trondheim, Norway.

Bachu, S, and Watson, T L. 2009. Review of failures for wells used for CO_2 and acid gas injection in Alberta, Canada. *Energy Procedia,* 3531-3537.

Bachu, S. 2013. Drainage and imbibition CO_2/brine relative permeability curves at in situ conditions for sandstone formations in western Canada. *Ghgt*-11. T. Dixon and K. Yamaji. 37: 4428-4436.

Bachu, S. 2015. Review of CO_2 storage efficiency in deep saline aquifers. *International Journal of Greenhouse Gas Control 40*: 188-202.

Baer, J. and Rigby, J. 1978. Geology of the Crystal geyser and environmental implications of its effluent, Grand County, Utah. *Utah Geology* 5, 125–130.

Bakker, M.A.J. and van der Meer, J.J.M. 2003. Structure of a Pleistocene push moraine revealed by ground-penetrating radar: the eastern Veluwe Ridge, the Netherlands. In Bristow, C.S., Jol, H.M. (Eds.). *Ground penetrating radar in sediments*. Geological Society of London Special Publications, 211, 143-151.

Bakker, M.A.J. 2004. The internal structure of Pleistocene push moraines. *PhD thesis*, Queen Mary University of London. Published by TNO Built Environment and Geosciences, Geological Survey of the Netherlands. ISBN 90-9020270-6.

Ballas, G., Fossen, H. and Soliva, R. 2015. Factors controlling permeability of cataclastic deformation bands and faults in porous sandstone reservoirs. *Journal of Structural Geology* 76, 1–21.

Baristeas, N., Anka, Z., di Primio, R., Rodriguez, J.F., Marchal, D. and Dominguez, F., 2012, Distribution of hydrocarbon leakage indicators in the Malvanas basin, offshore Argentine continental margin, *Marine Gology*, 332-334, 56-74.

Barrio, M., Børresen, M H., Girard, J-F., Jones, D G., Kuras, O., Pezard, P., Baudin, E., Buddensiek, M. and Bakk. A. 2013. Overview of CO_2FielLab: Field laboratory for monitoring and safety assessment. *Second Brazilian Congress on CO_2 in the Oil, Gas and Biofuels Industries*, April, 2013, Rio de Janeiro.

Barrio, M, Bakk, A, Grimstad, A-A, Querendez, E, Jones, D G, Kuras, O, Gal, F, Girard, J-F, Pezard, P, Depraz, L, Baudin, E, Børresen, M H and Sønneland, L. 2014. CO_2 Migration Monitoring Methodology in the Shallow Subsurface: Lessons Learned from the CO_2FIELDLAB Project. *Energy Procedia*, Vol. 51, 65-74.

Barr, D. 2007. Conductive faults and sealing fractures in the West Sole gas fields, southern North Sea. In: Jolley, S.J., Barr, D., Walsh, J.J. and Knipe, R.J. (eds) *Structurally Complex Reservoirs*. Geological Society, London, Special Publications 292, 431–451.

Barton, C.A., Zoback, M.D. and Moos, D. 1995. Fluid flow along potentially active faults in crystalline rock. *Geology* 23 (8), 683–686.

Bateson, L, Vellico, M, Beaubien, S E, Pearce, J M, Annunziatellis, A, Ciotoli, G, Coren, F, Lombardi, S and Marsh, S. 2008. The application of remote-sensing techniques to monitor CO_2-storage sites for surface leakage: Method development and testing at Latera (Italy) where naturally produced CO_2 is leaking to the atmosphere. *International Journal of Greenhouse Gas Control*, Vol. 2, 388-400.

Battani, A, Deville, E, Faure, J L, Jeandel, E, Noirez, S, Tocqué, E, Benoît, Y, Schmitz, J, Parlouar, D, Sarda, P, Gal, F, Le Pierres, K, Brach, M, Braibant, G, Beny, C, Pokryszka, Z, Charmoille, A, Bentivegna, G, Pironon, J, de Donato, P, Garnier, C, Cailteau, C, Barrès, O, Radilla, G and Bauer, A. 2010. Geochemical Study of Natural CO_2 Emissions in the French Massif Central: How to Predict Origin, Processes and Evolution of CO2 Leakage. *Oil and Gas Science and Technology – Revue de l'Institut Français du Pétrole*, Vol. 65, 615-633.

Beaubien, S.; Lombardi, S.; Ciotoli, G.; Annuziatellis, A.; Hatziyannis, G.; Metaxas, A. and Pearce, J.. 2005. Potential hazards of CO2 leakage in storage systems : learning

from natural systems. In: Rubin , E.S., (ed.) *Greenhouse Gas Control Technologies 7*. Oxford, UK, Elsevier, 551-560.

Beaubien, S E, Ciotoli, G, Coombs, P, Dictor, M C, Krüger, M, Lombardi, S, Pearce, J M and West, J M. 2008. The impact of a naturally occurring CO_2 gas vent on the shallow ecosystem and soil chemistry of a Mediterranean pasture (Latera, Italy). *International Journal of Greenhouse Gas Control*, Vol. 2, 373-387.

Beaubien, S E, Jones, D G, Gal, F, Barkwith, A K A P, Braibant, G, Baubron, J C, Ciotoli, G, Graziani, S, Lister, T R, Lombardi, S, Michel, K, Quattrocchi, F and Strutt, M H. 2013. Monitoring of near-surface gas geochemistry at the Weyburn, Canada, CO_2-EOR site, 2001–2011. *International Journal of Greenhouse Gas Control*, Vol. 16, Supplement 1, S236-S262.

Benediktsson, I.O., Möller, P., Ingólfsson, O., van der Meer, J.J.M., Kjær, K.H. and Krüger, J. 2008. Instantaneous end moraine and sediment wedge formation during the 1890 glacier surge of Brúarjökull, Iceland. *Quaternary Science Reviews* 27, 209–234.

Bentham, M.S., Green, A. and Gammer, D. 2013. The occurrence of faults in the Bunter Sandstone Formation of the UK sector of the Southern North Sea. *Energy Procedia* 37, 5101–5109.

Berndt, C., Bünz, S. and Mienert, J. 2003. Polygonal fault systems on the mid-Norwegian margin: a long-term source for fluid flow. In: Van Rensbergen, P., Hillis, R.R., Maltman, A.J. and Morley, C.K. (eds) *Subsurface Sediment Mobilization*. Geological Society, London, Special Publications 216, 283–290.

Bigi, S., Battaglia, M., Alemanni, A., Lombardi, S., Campana, A., Borisova, E. and Loizzo, M. 2013. CO_2 flow through a fractured rock volume: Insights from field data, 3D fracture representation and fluid flow modelling. *International Journal of Greenhouse Gas Control* 18, 183–199.

Birkedal, K.A., Hauge, L.P., Graue, A. and Ersland, G. 2015. Transport mechanisms for CO_2-CH_4 exchange and safe CO_2 storage in hydrate-bearing sandstone. *Energies*, 8, 4073-4095, doi:10.3390/en8054073.

Bjørlykke, K., Høeg, K., Faleide, J.I. and Jahren, J. 2005. When do faults in sedimentary basins leak? Stress and deformation in sedimentary basins; examples from the North Sea and Haltenbanken, offshore Norway. *AAPG Bulletin* 89 (8), 1019–1031.

Blackford J., Beaubien S., Foekema E., Gemeni V., Gwosdz S., Jones D., Kirk K., Lions J., Metcalfe R., Moni C., Smith K., Steven M., West J. and Ziogou F. 2013a. A guide to potential impacts of leakage from CO_2 storage. *D5.2b, Revision: 5. RISCS Consortium.*

Blackford, J.; Hattam, C.; Widdicombe, S.; Burnside, N.; Naylor, M.; Maul, P.; Kirk, K.; Wright, I.. 2013b. CO_2 leakage from geological storage facilities: environmental, societal and economic impacts, monitoring and research strategies. *In: Gluyas, J.; Mathias, S., (eds.) Geological storage of carbon dioxide (CO_2): Geoscience, technologies, environmental aspects and legal frameworks. Sawston, Cambridge, Woodhead Publishing,* 149-178, 380pp.

Blackford, J., Stahl, H., Bull, J M., Bergès, B J P., Cevatoglu, M., Lichtschlag, M., Connelly, D., James, R H., Kita, J., Long, D., Naylor, M., Shitashima, K., Smith, D., Taylor, P., Wright, I., Akhurst, M., Chen, B., Gernon, T M., Hauton, C., Hayashi, M., Kaieda, H., Leighton, T G., Sato, T., Sayer, M D J., Suzumura, M., Tait, K., Vardy, M E., White P R. and Widdicombe, S. 2014. Detection and impacts of leakage from sub-seafloor deep geological carbon dioxide storage. *Nature Climate Change* 4, 1011-1016.

Bluemle, J.P. and Clayton, L. 1983. Large-scale glacial thrusting and related processes in North Dakota. *Boreas 13*, 279-299.

Boetius, A., Ravenschlag, K., Schubert, C.J., Rickert, D., Widdel, F., Gieseke, A., Amann, R., Jørgensen, B.B., Witte, U. and Pfannkuche, O. 2000. A marine microbial consortium apparently mediating anaerobic oxidation of methane. *Nature,* 407(6804), 623-626.

Bogdanov, Y.A., Sagalevitch, A.M., Vogt, P.R., Mienert, Y., Sundvor, E., Krane, K., Lein, A.Y., Egorov, A.V., Pepesypkin, V.I., Cherkashev, G.A. and Gebruk, A.V., 1999. The Håkon Mosby Mud Volcano in the Norwegian Sea: results of comprehensive investigations with submersibles. Okeanologiya, 39(3), pp.412-419

Boles, J.R., Clark, J.F., Leifer, I. and Washburn, L. 2001. Temporal variation in natural methane seep rate due to tides, Coal Oil Point area, California. *Journal of Geophysical Research* 106, 27077–27086.

Boulton, G.S. and Caban, P. 1996. Groundwater flow beneath ice sheets, part II; Its impact on glacier tectonic structures and moraine formation. *Quaternary Science Reviews 14*, 563-587.

Bretan, P., Yielding, G. 2003. Using calibrated shale gouge ratio to estimate hydrocarbon column heights. *AAPG Bulletin* 87, 397–413.

Bretan, P. and Yielding, G. 2005. Using buoyancy pressure profiles to evaluate uncertainty in fault-seal calibration. In: Boult, P. and Kaldi, J. (eds) *Evaluating Fault and Cap Rock Seals*. AAPG Hedberg Series 2, 151–162.

Bretan, P., Yielding, G., Mathiassen, O.M. and Thorsnes, T. 2011. Fault-seal analysis for CO_2 storage: an example from the Troll area, Norwegian Continental Shelf. *Petroleum Geoscience* 17, 181–192.

Brooke, C.M., Trimble, T.J. and Mackay, T.A. 1995. Mounded shallow gas sands from the Quaternary of the North Sea: analogues for the formation of sand mounds in deep water Tertiary sediments?. Geological Society, London, *Special Publications*, 94(1), 95-101.

Brooks, A.J., Kenyon, N.H., Leslie, A., Long, D. and Gordon, J.E., 2011. Scottish Natural Heritage Commissioned Report No. 430 “Characterising Scotland’s marine environment to define search locations for new Marine Protected Areas” Part 2, Heritage. 205pp.

Broster, B.E.and Seaman, A.A. 1991. Glacigenic rafting of weathered granite: Charlie Lake, New Brunswick. *Canadian Journal of Earth Sciences 28*, 649–654.

Brothers, L.L., Kelley, J.T., Belknap, D.F., Barnhardt, W.A., Andrews, B.D. and Maynard, M.L. 2011. More than a century of bathymetric observations and present-day shallow sediment characterization in Belfast Bay, Maine, USA: Implications for pockmark field longevity. *Geo-Marine Letters 31*, 237–248.

Brunet, J-P.L., Li, L., Zuleima, K.T. and Huerta, N.J. 2016. Fracture opening or self-sealing: Critical residence time as a unifying parameter for cement–CO_2–brine interactions International *Journal of Greenhouse Gas Control 47,* 25–37

Buenz, S., Tasianas, A., Karstens, J., Berndt, C., Darcis, M. and Flemisch B., 2012, Sub-seabed CO_2 Storage: Impact on marine ecosystems (ECO_2), Milestone Report (MS12): geological models for industrial storage sites, University of Tromsø, Norway, GEOMAR Helmholtz Centre for Ocean Research Kiel, Germany and University of Stuttgart, Germany

Bünz, S., Mienert, J. and Berndt, C., 2003. Geological controls on the Storegga gas-hydrate system of the mid-Norwegian continental margin. *Earth and Planetary Science Letters 209*, 291–307.

Bünz, S. and Institutt for Geologi, Universitetet i Tromsø. 2011. *UNIVERSITY OF TROMSØ cruise report Tromsø – Longyearbyen, 01-07-11 to 14-07-11, R/V Helmer Hanssen ; Part 1* Institutt for Geologi, Universitetet i Tromsø, Tromsoe, Norway, 28 pp.

Bünz, S. 2013. *R/V Helmer Hanssen Cruise No. 2013007 - Part I, University of Tromsø cruise report, Tromsø – Longyearbyen, 08-07-13 to 21-07-13* Institutt for Geologi, Univ. i Tromsø, Tromsø, 33 pp. DOI 10.3289/CR_ECO2_24445.

Burke. H., Phillips, E.R., Lee, J.R. and Wilkinson, I.P. 2009. Imbricate thrust stack model for the formation of glaciotectonic rafts: an example from the Middle Pleistocene of north Norfolk, UK. *Boreas* 38, 620–637.

Burnol, A., Thinon, I,, Ruffine, L. and Herri, J.-M. 2015. Influence of impurities (nitrogen and methane) on the CO_2 storage capacity as sediment-hosted gas hydrates – Application in the area of the Celtic Sea and the Bay of Biscay. *International Journal of Greenhouse Gas Control* 35 (2015) 96–109.

Burnside, N.M., Shipton, Z.K. and Ellam, R.M. 2007. Using spring deposits to track the evolution of fluid pathways through faults; Little Grand Wash Fault and Salt Wash Graben, Utah, USA. *Presented at GSA Annual Meeting, Geological Society of America, Denver, October 28*–31.

Cahill, A G and Jakobsen, R. 2013. Hydro-geochemical impact of CO_2 leakage from geological storage on shallow potable aquifers: A field scale pilot experiment. *International Journal of Greenhouse Gas Control*, Vol. 19, 678-688.

Cahill, A G, Marker, P and Jakobsen, R. 2014. Hydrogeochemical and mineralogical effects of sustained CO_2 contamination in a shallow sandy aquifer: A field-scale controlled release experiment. *Water Resources Research*, Vol. 50, 1735-1755.

Caine, J.S., Evans, J.P. and Forster, C.B. 1996. Fault zone architecture and permeability structure. *Geology* 24 (11), 1025–1028.

Caliro, S., Caracausi, A., Chiodini, G. Ditta, M., Italiano, F., Longo, M., Minopoli, C., Nuccio, P. M., Paonita, A. and Rizzo, A. 2004. Evidence of a recent input of magmatic gases into the quiescent volcanic edifice of Panarea, Aeolian Islands, Italy. *Geophysical Research Letters*, Vol. 31, L07619.

Canals, M., Lastras, G., Urgeles, R., Casamor, J.L., Mienert, J., Cattaneo, A., De Batist, M., Haflidason, H., Imbo, Y. and Laberg, J.S., 2004. Slope failure dynamics and impacts from seafloor and shallow sub-seafloor geophysical data: case studies from the COSTA project. *Marine Geology* 213, 9–72.

Caramanna, G., Fietzek, P. and Maroto-Valer, M. 2011. Monitoring techniques of a natural analogue for sub-seabed CO_2 leakages. *Energy Procedia* 4, 3262–3268.

Cardellini, C, Chiodini, G and Frondini, F. 2003. Application of stochastic simulation to CO_2 flux from soil: Mapping and quantification of gas release. *Journal of Geophysical Research*, Vol. 108, 2425.

Carey, J. W., Wigand, M., Chipera, S J., WoldeGabriel, G., Pawar, R., Lichtner, P C., Wehner, S C., Raines, M A., Guthrie Jr, G D. 2007. Analysis and performance of oil well cement with 30 years of CO_2 exposure from the SACROC Unit, West Texas, USA *International Journal of Greenhouse Gas Control* 1, 75 – 85

Carneiro, J.F. 2009. Numerical simulations on the influence of matrix diffusion to carbon sequestration in double porosity fissured aquifers. *International Journal of Greenhouse Gas Control* 3(4), 431–443.

Carroll, S. A., Keating, E., Mansoor, K., Dai, Z., Sun, Y., Trainor-Guitton, W., Brown, C. and Bacon, D. 2014. Key factors for determining groundwater impacts due to leakage from geologic carbon sequestration reservoirs. *International Journal of Greenhouse Gas Control*, Vol. 29, 153-168.

Carroll, S., Carey, J. W., Dzombak, D., Huerta, N J., Li, L., Richard, T., Um, W., Walsh, S D.C. and Zhang, L. 2016. Review: Role of chemistry, mechanics, and transport on well integrity in CO_2 storage environments, *International Journal of Greenhouse Gas Control* 49, 149-160.

Carroll, S., Mansoor, K. and Sun, Y. In press. Framing monitoring needs to detect leakage from wells to the overburden. *Energy Procedia*.

Cartwright, J., James, D. and Bolton, A. 2003. The genesis of polygonal fault systems: a review. In: Van Rensbergen, P., Hillis, R.R., Maltman, A.J. and Morley, C.K. (eds) *Subsurface Sediment Mobilization*. Geological Society, London, Special Publications 216, 223–243.

Cartwright J., Huuse M. and Aplin, A. 2007 Seal bypass systems. *AAPG Bulletin* 91:1141–1166.

Cartwright, J. 2014. Are outcrop studies the key to understanding the origins of polygonal fault systems? *Geology* 42 (6), 559–560.

Cavanagh, A. and Rostron, B. 2013. High-resolution simulations of migration pathways and the related potential well risk at the IEAGHG Weyburn Midale CO_2 storage project. *International Journal of Greenhouse Gas Control*, Vol. 16, Supplement 1, S15-S24.

Celia, M. A., Bachu, S., Nordbotten, J. M., Kavetski, D. and Gasda, S. E. 2006. A risk assessment tool to quantify CO_2 leakage potential through wells in mature sedimentary basins. *Proceedings of the 8th Confernce on Greenhouse Gas Technologies 20-25*.

Cevatoglu, M., Bull, J. M., Vardy, M. E., Gernon, T. M., Wright, I. C., and Long, D. 2015. Gas migration pathways, controlling mechanisms and changes in sediment physical properties observed in a controlled sub-seabed CO_2 release experiment. *International Journal of Greenhouse Gas Control* 38, 26-43 DOI:10.1016/j.ijggc.2015.03.005.

Chadwick, R.A. 1986. Extension tectonics in the Wessex Basin, southern England. *Journal of the Geological Society* 143, 465–488.

Chadwick, R. A., Kirby, G.A., Holloway, S., Gregersen, U., Johannessen, P.N., Zweigel, P. and Arts, R., 2002. Saline Aquifer CO_2 Storage (SACS2). Final Report: Geological Characterisation (Work Area 1). *British Geological Survey Commissioned Report*, CR/02/153C.

Chadwick, R. A., Arts, R., Eiken, O., Kirby, G.A., Lindeberg, E. and Zweigel, P., 2004, 4D seismic imaging of a CO_2 bubble at the Sleipner Field, central North Sea, in R. J. Davies, J. A. Cartwright, S. A. Stewart, M. Lappin, and J. R. Underhill, eds., *3D seismic technology: Application to the exploration of sedimentary basins*, Geological Society, 311–320.

Chadwick, R.A., Zweigel, P., Gregersen, U., Kirby, G.A., Holloway, S. and Johannessen, P.N. 2004. Geological reservoir characterization of a CO_2 storage site: The Utsira Sand, Sleipner, northern North Sea. *Energy* 29, 1371–1381.

Chadwick, R. A., Arts, R. and Eiken, O., 2005, 4D seismic quantification of a CO_2 plume at Sleipner, North Sea, in A. G. Dore, and B. Vining, eds., *Petroleum geology: Northwest Europe and global perspectives*, Geological Society, 1385–1399.

Chadwick, R. A., Noy, D., Arts, R. and Eiken, O., 2009, Latest time-lapse seismic data from Sleipner yield new insights into CO_2 plume development, in Energy Procedia, no. 1, issue 1: Greenhouse gas control technologies 9, *9th International Conference on Greenhouse Gas Control Technologies*, 2103–2110.

Chadwick R.A. and Eiken, O. 2013. Offshore CO_2 storage: Sleipner natural gas field beneath the North Sea (Chapter 10). In: Gluyas, J. and Mathias, S. (eds) *Geological storage of carbon dioxide (CO_2) – Geoscience, technologies, environmental aspects and legal frameworks.* Woodhead Publishing Ltd.

Chadwick, R. A., Marchant, B. P. and Williams, G. A. 2014. CO 2 storage monitoring: leakage detection and measurement in subsurface volumes from 3D seismic data at Sleipner. *Energy Procedia*, *63*, 4224-4239.

Chadwick, R.A., Williams, G.A. and White, J.C. 2016. High resolution imaging and characterisation of a CO_2 layer at the Sleipner CO_2 Storage operation using time-lapse seismics. *First Break*, 34, 79-87.

Chand, S., Thorsnes, T., Rise, L., Brunstad, H., Stoddart, D., Bøe, R., Lågstad, P., and Svolsbru, T. 2012. Multiple episodes of fluid flow in the SW Barents Sea (Loppa

High) evidenced by gas flares, pockmarks and gas hydrate accumulation. *Earth and Planetary Science Letters 331–332*, 305–314.

Chand, S., Crémière, A., Lepland, A., Thorsnes, T., Brunstad, H. and Stoddart, D. 2016. Long-term fluid expulsion revealed by carbonate crusts and pockmarks connected to subsurface gas anomalies and palaeo-channels in the central North Sea. *Geo-Marine Letters*, 1-13.

Chang, K.W., Minkoff, S.E. and Bryant, S.L., 2009. Simplified model for CO_2 leakage and its attenuation due to geological structures. *Energy Procedia* 1, 3453–3460.

Checkai, D., Bryant, S. and Tao, Q. 2013. Towards a Frequency Distribution of Effective Permeabilities of Leaky Wellbores, *Energy Procedia* 37 (2013) 5653 – 5660

Chester, F.M. and Logan, J.M. 1986. Ultracataclasite structure and friction processes of the Punchbowl Fault, San Andreas system, California. *Pure and Applied Geophysics* 124, 199–221.

Chiaramonte, L., Zoback, M.D., Friedmann, J. and Stamp, V. 2008. Seal integrity and feasibility of CO_2 sequestration in the Teapot Dome EOR pilot: geomechanical site characterization. *Environmental Geology* 54, 1667–1675.

Chiaramonte, L., White, J.A. and Trainor-Guitton, W. 2015. Probabilistic geomechanical analysis of compartmentalization at the Snøhvit CO_2 sequestration project. *Journal of Geophysical Research: Solid Earth* 120 (2), 1195–1209.

Childs, C., Walsh, J.J., Manzocchi, T., Strand, J., Nicol, A., Tomasso, M., Schöpfer, M.P.J. and Aplin, A.C. 2007. Definition of a fault permeability predictor from outcrop studies of a faulted turbidite sequence, Taranaki, New Zealand. In: Jolley, S.J., Barr, D., Walsh, J.J. and Knipe, R.J. (eds) *Structurally Complex Reservoirs*. Geological Society, London, Special Publications 292, 235–258.

Childs, C., Manzocchi, T., Walsh, J.J., Bonson, C., Nicol, A. and Schöpfer, M.P.J. 2009. A geometric model of fault zone and fault rock thickness variations. *Journal of Structural Geology* 31, 117–127.

Chiodini, G., Frondini, F., Kerrick, D.M., Rogie, J., Parello, F., Peruzzi, L. and Zanzari, A.R. 1999. Quantification of deep CO_2 fluxes from central Italy. Examples of carbon balance for regional aquifers and of soil diffuse degassing. *Chemical Geology* 159, 205–222.

Chiodini, G. and Frondini, F. 2001. Carbon dioxide degassing from the Albani Hills volcanic region, Central Italy. *Chemical Geology* 177, 67–83.

Chiodini, G., Frondini, F., Cardellini, C., Granieri, L., Marini, L. and Ventura, G. 2001. CO_2 degassing and energy release at Solfatara volcano, Campi Flegrei, Italy. *Journal of Geophysical Research: Solid Earth* 106 (B8), 16213–16221.

Cita, M.B., Ryan, W.B.F. and Paggi, L., 1981. Prometheus mud breccia. An example of shale diapirism in the western Mediterranean Ridge. Annales Geologiques des Pays Helle- niques 30, 543–570.

Conley, S., Franco, G., Faloona, I., Blake, D. R., Peischl, J. and Ryerson, T. B. 2016. Methane emissions from the 2015 Aliso Canyon blowout in Los Angeles, CA *Science* 10.1126/science.aaf2348 (2016).

Corcoran, D.V. and Doré, A.G. 2002. Depressurization of hydrocarbon-bearing reservoirs in exhumed basin settings: evidence from Atlantic margin and borderland basins. In: Doré, A.G., Cartwright, J.A., Stoker, M.S., Turner, J.P. and White, N. *Exhumation of the North Atlantic Margin: Timing, Mechanisms and Implications for Petroleum Exploration*. Geological Society, London, Special Publications 196, 457–483.

Corona, F.V. 2005. Fault trap analysis of the Permian Rotliegend gas play, Lauwerzee Trough, NE Netherlands. In: Dóre, A.G. and Vining, B.A. (eds) *Petroleum Geology: North-West Europe and Global Perspectives–Proceedings of the 6th Petroleum Geology Conference*. Geological Society, London, Petroleum Geology Conference Series, 327–335.

Cotterill, C.J., Phillips, E., James, L., Forsberg, C.F., Tor Inge Tjelta, T.I., Carter, G. and Dove, D. In press. The evolution of the Dogger Bank, North Sea: a complex history of terrestrial, glacial and marine environmental change. *Quaternary Science Reviews*.

Croot, D.G. 1987. Glaciotectonic structures: a mesoscale mode of thin-skinned thrust sheets? *Journal of Structural Geology 9*, 797, 808.

Crow, W., Carey, J.W., Gasda, S., Williams, D.B. and Celia, M. 2010. Wellbore integrity analysis of a natural CO_2 producer, *International Journal of Greenhouse Gas Control* 4, 186-197.

Cuss, R.J. and Harrington, J.F. 2016. An experimental study of the potential for fault reactivation during changes in gas and pore-water pressure. *International Journal of Greenhouse Gas Control*, 53, 41–55.

Cuss, R.J., Milodowski, A. and Harrington, J.F. 2011. Fracture transmissivity as a function of normal and shear stress: First results in Opalinus Clay. *Physics and Chemistry of the Earth* 36, 1960–1971.

Cuss, R.J., Harrington, J.F., Noy, D.J., Sathar, S. and Norris, S. 2015. An experimental study of the flow of gas along synthetic faults of varying orientation to the stress field: Implications for performance assessment of radioactive waste disposal. *Journal of Geophysical Research: Solid Earth* 120, 3932–3945.

D'Alessandro, W., Bellomo, S., Brusca, L., Karakazanis, S., Kyriakopoulos, K. and Liotta, M. 2011. The impact on water quality of the high carbon dioxide contents of the groundwater in the area of Florina (N. Greece). 135-143 in *Advances in the Research of Aquatic Environment*. N. Lambrakis, G. Stournaras and K. Katsanou (editors).Springer Berlin Heidelberg.) *Environmental Earth Sciences*,

Dance, T. and Paterson L. 2016. Observations of carbon dioxide saturation distribution and residual trapping using core analysis and repeat pulsed-neutron logging at the CO_2CRC Otway site. *International Journal of Greenhouse Gas Control* 47: 210-220.

Dando, P.R., Austen, M.C., Burke, R.A., Kendall, M.A., Kennicutt II, M.C., Judd, A.G., Moore, D.C., O'Hara, S.C.M., Schmaljohann, R. and Southward, A.J., 1991. Ecology

of a North Sea pockmark with an active methane seep. *Marine Ecology Progress* Series 70, 49–63.

Davy, B., Pecher, I., Wood, R., Carter, L. and Gohl, K., 2010. Gas escape features off New Zealand: Evidence of massive release of methane from hydrates. *Geophysical Research Letters*, 37, L21309.

Dimitrov, L.I. 2002. Mud volcanoes - the most important pathway for degassing deeply buried sediments. *Earth-Science Reviews*, 59, 49-76.

Dimitrov, L.I., Woodside, J., 2003. Deep-sea pockmark environments in the Eastern Mediterranean. *Marine Geology*, 195, 263-276.

Denchik, N, Pezard, P A, Neyens, D, Lofi, J, Gal, F, Girard, J-F and Levannier, A. 2014. Near-surface CO_2 leak detection monitoring from downhole electrical resistivity at the CO_2 Field Laboratory, Svelvik Ridge (Norway). *International Journal of Greenhouse Gas Control*, Vol. 28, 275-282.

Deremble, L, Loizzo, M, Huet, B, Lecampion, B, and Quesada, D. 2011. Stability of a leakage pathway in a cemented annulus. *Energy Procedia*, Vol. 4, 5283-5290.

Cavarretta, G., Gianelli, G., Scandiffio, G. and Tecce, F. 1985. Evolution of the Latera geothermal system ll: Metamorphic hydrothermal mineral assemblages and fluid chemistry. *Journal of Volcanology and Geothermal Research* 26, 337–364.

Dewar, M., Sellami, N. and Chen, B. 2015. Dynamics of rising CO_2 bubble plumes in the QICS field experiment: Part 2 – Modelling. *International Journal of Greenhouse Gas Control* 38, 52-63

de Vries, D F H and Bernardo, C H. 2011. Spatial and temporal variability in atmospheric CO_2 measurements. *Energy Procedia*, Vol. 4, 5573-5578.

Di, P., Feng, D. and Chen, D., 2014. Temporal Variation in Natural Gas Seep Rate and Influence Factors in the Lingtou Promontory Seep Field of the Northern South China *Sea. Terr. Atmos. Ocean. Sci*. 25, 665–672.

Dockrill, B. and Shipton, Z.K. 2010. Structural controls on leakage from a natural CO_2 geologic storage site: Central Utah, USA. *Journal of Structural Geology* 32, 1768–1782.

Dore, A.G., 1995. Barents Sea Geology, Petroleum Resources and Commercial Potential. Arctic, 48, 207-221.

Dowdeswell, J.A. and Ottesen, D., 2013. Buried iceberg ploughmarks in the early Quaternary sediments of the central North Sea: a two-million year record of glacial influence from 3D seismic data. *Marine Geology*, *344*, pp.1-9.

Duguid, A., Carey, J. W. and Butsch, R. 2014. Well integrity assessment of a 68 year old well at a CO_2 injection project *Energy Procedia* 63 5691 – 5706

Duguid, A., Guo, B. and Nygaard, R. In press. Well integrity assessment of monitoring wells at an active CO2-EOR flood. *Energy Procedia*. GHGT-13, Lausanne, Switzerland, November 2016. Technical session 4B.

Duran, E.R., R. di Primio, Z. Anka, D. Stoddart and B. Horsfield, 2013. 3D-basin modelling of the Hammerfest Basin (South Western Barents Sea): A quantitative

assessment of petroleum generation, migration and leakage. *Marine Petroleum Geol*., 45: 281-303. DOI: 10.1016/j.marpetgeo.2013.04.023

Eidvin, T., Jansen, E., Rundberg, Y., Brekke, H. and Grogan, P., 2000. The upper Cainozoic of theNorwegian continental shelf correlated with the deep sea record of the Norwegian Sea and the North Atlantic. *Marine and Petroleum Geology* 17, 579–600.

El-Maghraby, R. M. and M. J. Blunt, 2013. Residual CO_2 Trapping in Indiana Limestone. *Environmental Science & Technology* 47(1): 227-233.

Ennis-King, J. and L. Paterson, 2003. Rate of dissolution due to convective mixing in the underground storage of carbon dioxide. In Gale, J. and Kaya, Y. *Greenhouse Gas Control Technologies*, Vols I and II, Proceedings, 1653-1656.

Ennis-King, J. and L. Paterson. 2005. Role of convective mixing in the long-term storage of carbon dioxide in deep saline formations. *SPE Journal* 10(3): 349-356.

Esposito, A., Anzidei, M., Atzori, S., Devoti, R., Giordano, G. and Pietrantonio, G. G. 2010. Modeling ground deformations of Panarea volcano hydrothermal/geothermal system (Aeolian Islands, Italy) from GPS data. *Bulletin of Volcanology*, 72, 609–621

Etiope, G. 2015. Natural Gas Seepage: The Earth's Hydrocarbon Degassing. Springer. pp. 199.

European Union, 2009. Directive 2009/29/EC of the European Parliament and of the Council of 23 April 2009 amending Directive 2003/87/EC so as to improve and extend the greenhouse gas emission allowance trading scheme of the Community. Official Journal of the European Union, L 140/64, 5.6.2009.

Evans, J.P. 1990. Thickness–displacement relationships for fault zones. *Journal of Structural Geology* 12, 1061–1065.

Evans, K.F. 2005. Permeability creation and damage due to massive fluid injections into granite at 3.5 km at Soultz: 2. Critical stress and fracture strength. *Journal of Geophysical Research* 110, B04204.

Fader, G.B.J. 1991. Gas-related sedimentary features from the eastern Canadian continental shelf. *Continental Shelf Research*, 11, 1123-1153.

Færseth, R.B. 2006. Shale smear along large faults: continuity of smear and the fault seal capacity. *Journal of the Geological Society, London* 163, 741–751.

Farajzadeh, R., Salimi, H., Zitha, P. and Bruining, H. 2007 Numerical simulation of density-driven natural convection in porous media with application for CO_2 injection projects. *Int. J. Heat Mass Transf*. 50(25-26), 5054– 5064.

Farrell, N.J.C., Healy, D. and Taylor, C.W. 2014. Anisotropy of permeability in faulted porous sandstones. *Journal of Structural Geology*, Volume 63, June 2014, Pages 50–67. http://dx.doi.org/10.1016/j.jsg.2014.02.008

Faulkner, D.R., Lewis, A.C. and Rutter, E.H. 2003. On the internal structure and mechanics of large strike-slip fault zones: field observations of the Carboneras fault in southeastern Spain. *Tectonophysics* 367 (3–4), 235–251.

Faulkner, D.R., Jackson, C.A.L., Lunn, R.J., Schlische, R.W., Shipton, Z.K., Wibberley, C.A.J. and Withjack, M.O. 2010. A review of recent developments

concerning the structure, mechanics and fluid flow properties of fault zones. *Journal of Structural Geology* 32, 1557–1575.

Feitz, A, Jenkins, C, Schacht, U, McGrath, A, Berko, H, Schroder, I, Noble, R, Kuske, T, George, S, Heath, C, Zegelin, S, Curnow, S, Zhang, H, Sirault, X, Jimenez-Berni, J and Hortle, A. 2014a. An assessment of near surface CO_2 leakage detection techniques under Australian conditions. *Energy Procedia*, Vol. 63, 3891-3906.

Feitz, A J, Leamon, G, Jenkins, C, Jones, D G, Moreira, A, Bressan, L, Melo, C, Dobeck, L M, Repasky, K and Spangler, L H. 2014b. Looking for leakage or monitoring for public assurance? *Energy Procedia*, Vol. 63, 3881-3890.

Feitz, A, Fomin, T, Ransley, T, Pevzner, R, Milovan Urosevic, Harris, B, Adam Bailey, Schacht, U and Hortle, A. In Press. The CO_2CRC Otway shallow CO_2 controlled release experiment: Site suitability assessment. *Energy Procedia*.

Ferrill, D.A., Winterle, J., Wittmeyer, G., Sims, D., Colton, S. and Armstrong, A. 1999. Stressed Rock Strains Groundwater at Yucca Mountain, Nevada. *GSA Today* 9 (5), 1–8.

Fichler, C., Henriksen, S., Rueslaatten, H. and Hovland, M., 2005. North Sea Quaternary morphology from seismic and magnetic data: indications for gas hydrates during glaciation? *Petroleum Geoscience*, *11*(4), pp.331-337.

Finkbeiner, T., Zoback, M., Flemings, P. and Stump, B. 2001. Stress, pore pressure, and dynamically constrained hydrocarbon columns in the South Eugene Island 330 Field, northern Gulf of Mexico. *AAPG Bulletin*, 85 (6) 1007–1031.

Fisher, Q.J. and Knipe, R.J. 2001. The permeability of faults within siliciclastic petroleum reservoirs of the North Sea and Norwegian Continental Shelf. *Marine and Petroleum Geology* 18, 1063–1081.

Förster, A., Norden, B., Zinck-Jørgensen, K., Frykman, P., Kulenkampff, J., Spangenberg, E., Erzinger, J., Zimmer, M., Kopp, J., Borm, G., Juhlin, C., Cosma, C.-G. and Hurter S. 2006. Baseline characterization of the CO_2SINK geological storage site at Ketzin, Germany. *Environmental Geosciences*, 13(3), 145-161.

Fossen, H., Schultz, R.A., Shipton, Z.K. and Mair, K. 2007. Deformation bands in sandstone: a review. *Journal of the Geological Society* 164, 755–769.

Fossen, H. and Rotevatn, A. 2016. Fault linkage and relay structures in extensional settings – A review. *Earth-Science Reviews*, Vol. 154, 14–28.

Freeman, S.R., Harris, S.D. and Knipe, R.J. 2008. Fault Seal Mapping – incorporating geometric and property uncertainty. In: Robinson, A., Griffiths, P., Price, S., Hegre, J. and Muggeridge, A. (eds) *The Future of Geological Modelling in Hydrocarbon Development*. Geological Society, London, Special Publications 309, 5–38.

Fulljames, J.R., Zijerveld, L.J.J. and Franssen, R.C.M.W. 1997. Fault seal processes: systematic analysis of fault seals over geological and production timescales. In: Møller-Pedersen, P. and Koestler, A.G. (eds) *Hydrocarbon Seals: Importance for Exploration and Production*. Norwegian Petroleum Society (NPF), Special Publication 7, 51–59.

Furnival, S., Wright, S., Dingwall, S., Bailey, P., Brown, A., Morrison, D. and De Silva, R. 2014. Subsurface Characterisation of a Saline Aquifer Cited for Commercial Scale CO_2 Disposal. *Energy Procedia* 63, 4926–4936.

Furre, A. K., Kiær, A., and Eiken, O., 2015. CO_2-induced seismic time shifts at Sleipner, *Interpretation*, 3(3), 23–35.

Fyfe, J.A. 1986. Fisher (56°N–02°E) 1:250,000. Quaternary Geology Map Sheet. British Geological Survey.

Gafeira, J. 2010. Submarine mass movement processes on the North Sea Fan as interpreted from the 3D seismic data. Unpublished PhD thesis, University of Edinburgh.

Gafeira, J., Long, D., Scrutton, R. and Evans, D. 2010. 3D seismic evidence of internal structure within Tampen Slide deposits on the North Sea Fan: are chaotic deposits that chaotic? *Journal of the Geological Society*, 167(3), 605-616.

Gafeira, J. and Long, D., Diaz-Doce, D., 2012. Semi-automated characterisation of seabed pockmarks in the central North Sea. *Near Surface Geophysics* 10, 303–314.

Gafeira, J. and Long, D. 2015. Geological investigation of pockmarks in the Scanner Pockmark SCI area. Peterborough. *JNCC Report 570*.

Gal, F, Brach, M, Braibant, G, Jouin, F and Michel, K. 2011. CO_2 escapes in the Laacher See region, East Eifel, Germany: Application of natural analogue onshore and offshore geochemical monitoring. *International Journal of Greenhouse Gas Control*, Vol. 5, 1099-1118.

Gal, F, Brach, M, Braibant, G, Bény, C and Michel, K. 2012. What can be learned from natural analogue studies in view of CO_2 leakage issues in Carbon Capture and Storage applications? Geochemical case study of Sainte-Marguerite area (French Massif Central). *International Journal of Greenhouse Gas Control*, Vol. 10, 470-485.

Gal, F., Proust, E., Humez, P., Braibant, G., Brach, M., Koch, F., Widory, D. and Girard, J-F. 2013. Inducing a CO_2 leak into a shallow aquifer (CO_2FieldLab EUROGIA+ project): Monitoring the CO_2 plume in groundwaters. *Energy Procedia* 37, 3583 – 3593.

Gartrell, A., Zhang, Y., Lisk, M. and Dewhurst, D. 2003. Enhanced hydrocarbon leakage at fault intersections: An example from the Timor Sea, Northwest Shelf, Australia. *Journal of Geochemical Exploration* 78–79, 361–365.

Gartrell, A., Zhang, Y., Lisk, M. and Dewhurst, D. 2004. Fault intersections as critical hydrocarbon leakage zones: Integrated field study and numerical modelling of an example from the Timor Sea, Australia. *Marine and Petroleum Geology* 21, 1165–1179.

Gasda, S.E. Nordbotten, J. M., Celia, M.A. 2008. Determining effective wellbore permeability from a field pressure test: a numerical analysis of detection limits. *Environmental Geology* 54,1207-15.

Gasda, S. E., Zhang, J.Z. and Celia, M.A. 2011. Analysis of in-situ wellbore integrity data for existing wells with long term exposure to CO_2 *Energy Procedia* 4 5406–5413

Gatliff, R.W., Richards, P.C., Smith, K., Graham, C.C., McCormack, M., Smith, N.J.P., Long, D., Cameron T.D.J., Evans, D., Stevenson, A.G., Bulat, J. and Ritchie, J.D. 1994. The Geology of the central North Sea. *United Kingdom Offshore Regional Report*, British Geological Survey, HMSO, London. 118 pp.

Gaus, I., Azaroual, M. and Czernichowski-Lauriol, I. 2005. Reactive transport modelling of the impact of CO_2 injection on the clayey cap rock at Sleipner (North Sea). *Chem. Geol*. 217, 319–337.

Gay, A., Lopez, M., Cochonat, P. and Semondadz, G. 2004. Polygonal faults-furrows system related to early stages of compaction – Upper Miocene to recent sediments of the Lower Congo Basin. *Basin Research* 16, 101–116.

Gay, A. and Berndt, C. 2007. Cessation/reactivation of polygonal faulting and effects on fluid flow in the Vøring Basin, Norwegian Margin. *Journal of the Geological Society*, 164(1), 129-141.

Gay, A., Mourgues, R., Berndt, C., Bureau, D., Planke, S., Laurent, D., Gautier, S., Lauer, C. and Loggia, D., 2012. Anatomy of a fluid pipe in the Norway Basin: Initiation, propagation and 3D shape, *Marine Geology*, 332-334, 75-88.

Gehrmann, A., Hüneke, H., Meschede, M. and Phillips, E. 2016. 3D microstructural architecture of deformed glacigenic sediments associated with large-scale glacitectonism, Jasmund Peninsula (NE Rügen), Germany. *Journal of Quaternary Science* DOI: 10.1002/jqs.2843.

Gemmer, L., Huuse, M., Clausen, O.R. and Nielsen, S.B., 2002. Mid-Palaeocene palaeogeography of the eastern North Sea basin: integrating geological evidence and 3D geodynamic modelling. *Basin Research 14*, 329–346.

Gibbard, P.L., 1988. The history of the great northwest European rivers during the past three million years. *Philosophical Transactions of the Royal Society*, London, Series B 318, 559–602.

Ginsburg, G.D. and Soloviev, V.A. 1994. Mud volcano gas hydrates in the Caspian Sea. *Bulletin Geological Society Denmark 41*, 95–100.

Goudinho, F. In press-a. Integration results of soil CO_2 flux and subsurface gases in the Ressacada Pilot site, Southern Brazil. *Energy Procedia*.

Goudinho, F. In press-b. CO_2MOVE Project: the new Brazilian Field Lab fully dedicated to CO_2 MMV experiments. *Energy Procedia*.

Goulty, N.R. 2008. Geomechanics of polygonal fault systems: a review. *Petroleum Geoscience* 14, 389–397.

Gouveia, F.J., Johnson, M.R., Leif, R.N. and Friedmann, S.J. 2005. Aeromagnetic measurement and modelling of the mass of CO_2 emissions from Crystal Geyser, Utah. *Lawrence Livermore National Laboratory Report* UCRL-TR-211870.

Govindan, R., Korre, A. and Durucan, S. 2013. Application of an Unsupervised Methodology for the Indirect Detection of CO_2 Leakages Around the Laacher See in Germany using Remote Sensing Data. *Energy Procedia* 37, 4057-4064.

Graham, A., Lonergan, L. and Stoker, M. 2007. Evidence for Late Pleistocene ice stream activity in the Witch Ground Basin, central North Sea, from 3D seismic reflection data *Quaternary Science. Review*, 26 pp. 627–643.

Graham, A.G., Stoker, M.S., Lonergan, L., Bradwell, T. and Stewart, M.A., 2011. The Pleistocene glaciations of the North Sea basin. In In: Ehlers, J., Gibbard, P.L., Hughes, P.D. (Eds.), *Quaternary Glaciations: Extent and Chronology: a Closer Look. Developments in Quaternary Science*, vol. 15. Elsevier, pp. 261-278.

Gregersen, U. and Johannessen, P.N., 2007, Distribution of the Neogene Utsira Sand and the succedding deposits in the vIking Graben area, North Sea. *Marine and Petroleum Geology* 24, 591-606.

Griffiths, P.A., Allen, M.R., Craig, J., Fitches, W.R. and Whittington, R.J. 1995. Distinction between fault and salt control of Mesozoic sedimentation on the southern margin of the Mid-North Sea High. In: Boldy, S.A.R. (Ed.) *Permian and Triassic Rifting in Northwest Europe*. Geological Society, London, Special Publications 91, 145–159.

Grude, S., Landrø, M., and Osdal, B. 2013. Time-lapse pressure-saturation discrimination for CO_2 storage at the Snøhvit field. *International Journal of Greenhouse Gas Control* 19, 369-378.

Grude, S., Landrø, M., White, J.C. and Torsæter, O. 2014 CO_2 saturation and thickness predictions in the Tubåen Fm., Snøhvit field, from analytical solution and time-lapse seismic data. *International Journal of Greenhouse Gas Control*, 29. 248-255.

Guen, Y.L., Huot, M., Loizzo, M. and Poupard, O., 2011. Well integrity risk assessment ofKetzin injection well (Ktzi-201) over a prolonged sequestration period. In:*10th International Conference on Greenhouse Gas Control Technologies*, vol. 4,pp. 4076–4083.

Hall-Spencer, JM, Rodolfo-Metalpa, R, Martin, S, Ransome, E, Fine, M., Turner, SM, Rowley, SJ, Tedesco, D and Buia, M-C. 2008. Volcanic carbon dioxide vents show ecosystem effects of ocean acidification. *Nature* Vol. 454, p. 96-99.

Hammer, Ø., Webb, K.E. and Depreiter, D., 2009. Numerical simulation of upwelling currents in pockmarks, and data from the Inner Oslofjord, Norway. *Geo-Marine Letters,* 29(4), pp.269-275.

Hampton, M. a., Lee, H.J. and Locat, J., 1996. Submarine landslides. Reviews of Geophysics 34, 33.

Haney, M M, Snieder, R, Sheiman, J and Losh, S. 2005. A moving fluid pulse in a fault zone. *Nature*, Vol. 437, 46.

Hansen, O., Gilding, D., Nazarian, B, Osdal, B., Ringrose, P., Kristoffersen, J-B, Eiken, O. and Hansen, H. 2013. Snøhvit: The history of injecting and storing 1 Mt CO_2 in the fluvial Tubåen Fm. *Energy Procedia* 37, 3565-3573.

Harding, R. and Huuse, M. 2015. Salt on the move: Multi stage evolution of salt diapirs in the Netherlands North Se. *Marine and Petroleum Geology* 61, 39–55.

Harp, D R, Pawar, R, Carey, J W, and Gable, C W. 2016. Reduced order models of transient CO_2 and brine leakage along abandoned wellbores from geologic carbon sequestration reservoirs. *International Journal of Greenhouse Gas Control*, Vol. 45, 150-162.

Harrington, J.F., Noy, D.J., Horseman, S.T., Birchall, D.J., and Chadwick, R.A., 2010, Laboratory study of gas and water flow in the Nordland Shale, Sleipner, North Sea. In: Grobe, M., Pashin, J., and Dodge, R. (eds) Carbon Dioxide Sequestration in Geological Media – State of the science. *AAPG Studies in Geology* v. 59, p. 521–543.

Harris, C., Williams, G., Brabham, P., Eaton, G. and McCarroll, D. 1997. Glaciotectonized Quaternary sediments as Dinas Dinlle, Gwynedd, North Wales, and the bearing on the style of deglaciation in the eastern Irish Sea. *Quaternary Science Reviews 16*, 109-127.

Heath, J.E., Lachmar, T.E., Evans, J.P., Kolesar, P.T. and Williams, A.P., 2009. Hydrogeo-chemical characterization of leaking, carbon dioxide-charged fault zones in east-central Utah, with implications for geologic carbon storage. In: Mcpherson, B.J., Sundquist, E.T. (Eds.), *Carbon Sequestration and Its Role in the Global Carbon Cycle*. American Geophysical Union, Washington, DC, pp.147–158.

Heath, J. E., Dewers, T. A., McPherson, Bjol, Nemer, M. B. and Kotula, P. G. 2012. Pore-lining phases and capillary breakthrough pressure of mudstone caprocks: Sealing efficiency of geologic CO2 storage sites. *International Journal of Greenhouse Gas Control*, 11, 204-220.

Heggland, R. and Nygaard, E. 1998. Shale intrusions and associated surface expressions—examples from Nigerian and Norwegian deepwater areas. In: Proc. Offshore Technology Conference. Houston, TX, vol. 1, pp. 111–124.

Hennings, P., Allwardt, P., Paul, P., Zahm, C., Reid, R. Jr., Alley, H., Kirschner, R., Lee, B. and Hough, E. 2012. Relationship between fractures, fault zones, stress, and reservoir productivity in the Suban gas field, Sumatra, Indonesia. *AAPG Bulletin* 96 (4), 753–772.

Hepple, R.P. and Benson, S.M. 2005. Geologic storage of carbon dioxide as a climate change mitigation strategy: performance requirements and the implications of surface seepage. *Environmental Geology 47*, 576-585.

Hermanrud, C., Halkjelsvik, M.E., Kristiansen, K., Bernal, A. and Strömbäck, A.C. 2014. Petroleum column-height controls in the western Hammerfest Basin, Barents Sea. *Petroleum Geoscience* 20, 227–240.

Herring, A. L., Andersson, L. and Wildenschild D. 2016. Enhancing residual trapping of supercritical CO2 via cyclic injections. *Geophysical Research Letters* 43(18): 9677-9685.

Hillier, A.P. 2003. The Leman Field, Blocks 49/26, 49/27, 49/28, 53/1, 53/2, UK North Sea. In: Gluyas, J.G. and Hichens, H.M. (eds) *United Kingdom Oil and Gas Fields, Commemorative Millennium Volume*. Geological Society, London, Memoirs 20, 761–770.

Hillis, R.R., Thomson, K. and Underhill, J.R. 1994. Quantification of Tertiary erosion in the Inner Moray Firth using sonic velocity data from the Chalk and the Kimmeridge Clay. *Marine and Petroleum Geology* 11, 283–293.

Hirst, B, Gibson, G, Gillespie, S, Archibald, I, Podlaha, O, Skeldon, K D, Courtial, J, Monk, S and Padgett, M. 2004. Oil and gas prospecting by ultra-sensitive optical gas detection with inverse gas dispersion modelling. *Geophysical Research Letters*, Vol. 31, art. no.-L12115.

Hirst, B, Jonathan, P, González del Cueto, F, Randell, D and Kosut, O. 2013. Locating and quantifying gas emission sources using remotely obtained concentration data. *Atmospheric Environment*, Vol. 74, 141-158.

Hood, J.W. and Patterson, D.J. 1984. Bedrock aquifers in the northern San Rafael Swell area, Utah, with special emphasis on the Navajo Sandstone. *State of Utah Department of Natural Resources Technical Publication* 78, p.128.

Hovland, M. and Sommerville, J.H. 1985. Characteristics of two natural gas seepages in the North Sea. *Marine and Petroleum Geology* 2, 319–326.

Hovland, M. and Judd, A.G. 1988. Seabed pockmarks and seepages: impact on geology, biology, and the marine environment. *Graham and Trotman Limited*, London, UK.

Hovland, M. and Thomsen, E. 1989. Hydrocarbon-based communities in the North Sea? *Sarsia*, 74, 29-42.

Hou, Z, Bacon, D H, W., E D, Lin, G, Fang, Y, Ren, H, and Fang, Z. 2014. Uncertainty analyses of CO_2 plume expansion subsequent to wellbore CO_2 leakage into aquifers. *International Journal of Greenhouse Gas Control*, Vol. 27, 69-80.

Huang, Z-Q., Winterfield, P.H., Xion, Y., Wu, Y-S., and Yao, J. 2015. Parallel simulation of fully-coupled thermal-hydro-mechanical processes in CO_2 leakage through fluid-driven fracture zones. *International Journal of Greenhouse Gas Control* 34, 39–51.

Huerta, N. J., Carey, J. W., Carroll, S., Dzombak, D., Harp, D., Li, L., Richard, T., Walsh, S. D. C., Um, W. and Zhang, L. 2016. Well Integrity in CO_2 Storage Operations: Current Understanding and Open Questions; NRAP-TRS-I-007-2016; *NRAP Technical Report Series*; U.S. Department of Energy, National Energy Technology Laboratory: Albany, OR; p 48.

Huerta, N. J., Hesse, M. A., Bryant, S. L., Strazisar, B. R. and Lopano, C. 2016. Reactive transport of CO2-saturated water in a cement fracture: Application to wellbore leakage during geologic CO2 storage. *International Journal of Greenhouse Gas Control* 44, 276-289.

Hull, J. 1988. Thickness Displacement Relationships for Deformation Zones. *Journal of structural geology* 10 (4), 431–435.

Humez, P., Audigane, P., Lions, J., Chiaberge, C. and Bellenfant, G. 2011. Modelling of CO_2 Leakage up Through an Abandoned Well from Deep Saline Aquifer to Shallow Fresh Groundwaters. *Transport in Porous Media*, Springer Verlag, 2011, 90 (1), pp.153-181.

Humez, P, Négrel, P, Lagneau, V, Lions, J, Kloppmann, W, Gal, F, Millot, R, Guerrot, C, Flehoc, C, Widory, D and Girard, J-F. 2014. CO_2–water–mineral reactions during CO_2 leakage: Geochemical and isotopic monitoring of a CO_2 injection field test. *Chemical Geology*, Vol. 368, 11-30.

Huuse, M. and Lykke-Andersen, H. 2000. Overdeepened Quaternary valleys in the eastern Danish North Sea: morphology and origin. *Quaternary Science Reviews 19*, 1233-1253.

IEAGHG. 2005. A review of natural CO_2 occurrences and releases and their relevance to CO_2 storage. *IEAGHG Report 2005/8.*

IEAGHG. 2015. Review of offshore monitoring for CCS projects. *IEAGHG Technical Report*, 2015/02.

IEAGHG. 2016. Fault permeability. *IEAGHG Technical Report*, 2016/13.

IEAGHG. In press. A Summary Report of the Monitoring and Modelling Networks Combined Meeting. Edinburgh, July 2016.

Iding, M. and Blunt, M.J. 2011. Enhanced solubility trapping of CO_2 in fractured reservoirs. *Energy Procedia* 4, 4961–4968.

Iglesias, J., Ercilla, G., García-Gil, S. and Judd, A.G., 2010. Pockforms: An evaluation of pockmark-like seabed features on the Landes Plateau, Bay of Biscay. *Geo-Marine Letters* 30, 207–219.

Ingrassia, M., Martorelli, E., Bosman, a., Macelloni, L., Sposato, A. and Chiocci, F.L. 2015. The Zannone Giant Pockmark: First evidence of a giant complex seeping structure in shallow-water, central Mediterranean Sea, Italy. *Marine Geology* 363, 38–51.

IPCC. 2005. Special Report on Carbon Dioxide Capture and Storage. Metz, B., Davidson, O., De Coninck, H., Loos, M. and Meyer, L.,Intergovernmental Panel on Climate Change, Geneva (Switzerland). Working Group III.

Isaksen, D. and Tonstad, K. 1989. A revised Cretaceous and Tertiary lithostratigraphic nomenclature for the Norwegian North Sea, *NPD Bulletin* 5, Oljedirektoratet.

Ishibashi, J-i., Ikegami, F., Tsuji, T. and Urabe, T. 2015. Hydrothermal Activity in the Okinawa Trough Back-Arc Basin: Geological Background and Hydrothermal Mineralization. *In: Ishibashi, J-i., Okino, K. and Sunamura, M. (Editors). Subseafloor Biosphere Linked to Hydrothermal Systems. TAIGA Concept*. 337-359.

Ishii, E. 2015. Predictions of the highest potential transmissivity of fractures in fault zones from rock rheology: Preliminary results. *Journal of Geophysical Research: Solid Earth* 120, 2220–2241.

Italiano, F., Favara, R., Etiope, G. and Favali, P. 2001. Submarine emissions of greenhouse gases from hydrothermal and sedimentary areas. *Presented at the Water-rock Interaction Conference 2001. Proceedings of the 10th International Symposium, Swets and Zeitlinger, Lisse.*

Ivanov, M. K., Limonov, A .F. and Van Weering, T.C., 1996. Comparative characteristics of the Black Sea and Mediterranean Ridge mud volcanoes. *Marine Geology*, *132* (1-4), 253-271.

Ivanova, A., Kashubin, A., Juhojuntti, N., Kummerow, J., Henninges, J., Juhlin, Ch., Lüth, S. and Ivandic, M. 2012. Monitoring and volumetric estimation of injected CO_2 using 4D seismic, petrophysical data, core measurements and well logging: a case study at Ketzin, Germany. *Geophysical Prospecting*, 60, Pages 957 - 973, doi: 10.1111/j.1365-2478.2012.01045.x.

Jakobsen, P.R. 1996. Distribution and intensity of glaciotectonic deformation in Denmark. *Bulletin of the Geological Society of Denmark 42*, 175–185.

Azar, J.J. and Samuel, G. R. 2007. Drilling Engineering. PennWell Books, Tulsa, OK, USA. ISBN-13: 978-1-59370-072-0.

Johnson, J. W., Nitao, J. J. and Morris, J. P. 2004. Reactive transport modeling of cap-rock integrity during natural and engineered CO_2 storage. *Carbon Dioxide Capture for Storage in Deep Geologic Formations* 2, 787.

Johnson, G, Hicks, N, Bond, C E, Gilfillan, S M V, Jones, D, Kremer, Y, Lister, R, Nkwane, M, Maupa, T, Munyangane, P, Robey, K, Saunders, I, Pearce, J, Shipton, Z K and Haszeldine, R S. In press. Detection and understanding of natural CO_2 releases in KwaZulu-Natal, South Africa. *Energy Procedia*.

Jolley, S.J., Dijk, H., Lamens, J.H., Fisher, Q.J., Manzocchi, T., Eikmans, H. and Huang, Y. 2007. Faulting and fault sealing in production simulation models: Brent Province, northern North Sea. *Petroleum Geoscience* 13, 321–340.

Jones, D G, Barlow, T, Beaubien, S E, Ciotoli, G, Lister, T R, Lombardi, S, May, F, Möller, I, Pearce, J M and Shaw, R A. 2009. New and established techniques for surface gas monitoring at onshore CO_2 storage sites. *Energy Procedia*, Vol. 1, 2127-2134.

Jones, D G, Barkwith, A K A P, Hannis, S, Lister, T R, Gal, F, Graziani, S, Beaubien, S E and Widory, D. 2014. Monitoring of near surface gas seepage from a shallow injection experiment at the CO_2 Field Lab, Norway. *International Journal of Greenhouse Gas Control*, Vol. 28, 300-317.

Jones, D G, Beaubien, S E, Blackford, J C, Foekema, E M, Lions, J, De Vittor, C, West, J M, Widdicombe, S, Hauton, C and Queirós, A M. 2015. Developments since 2005 in understanding potential environmental impacts of CO_2 leakage from geological storage. *International Journal of Greenhouse Gas Control*, Vol. 40, 350-377.

Jordt, A., Zelenka, C., von Deimling, J.S., Koch, R. and Koser, K., 2015. The Bubble Box: Towards an Automated Visual Sensor for 3D Analysis and Characterization of Marine Gas Release Sites. *Sensors* 15, 30716–30735.

Jørgensen, F., Lykke-Andersen, H., Sandersen, P.B., Auken, E. and Nørmark, E., 2003. Geophysical investigations of buried Quaternary valleys in Denmark: an integrated application of transient electromagnetic soundings, reflection seismic surveys and exploratory drillings. *Journal of Applied Geophysics*, 53(4), pp.215-228.

Judd, A.G., 2001. Pockmarks in the UK sector of the North Sea. UK Department of Trade and Industry *Technical Report* TR_002.

Judd, A.G. and Hovland, M., 2007. Seabed Fluid Flow: Impact on Geology, Biology and the Marine Environment. *Cambridge University Press*, Cambridge.

Juhlin, C., Giese, R., Zinck-Jørgensen, K., Cosma, C., Kazemeini, H., Juhojuntti, N., Lüth, S., Norden, B. and Förster, A. 2007. 3D baseline seismics at Ketzin, Germany: the CO_2SINK project. *Geophysics*, *72*(5), B121-B132.

Jung, N.H., Han, W.S., Watson, Z.T., Graham, J.P. and Kim, K.Y. 2014. Fault-controlled CO_2 leakage from natural reservoirs in the Colorado Plateau, East-Central Utah. *Earth and Planetary Science Letters* 403, 358–367.

Jung, N.-H., Han, W.S., Han, K., and Park, E. 2015. Regional-scale advective, diffusive, and eruptive dynamics of CO_2 and brine leakage through faults and wellbores, *J. Geophys. Res. Solid Earth*, 120, 3003–3025.

Kampman, N., Bickle, M., Becker, J., Assayag, N. and Chapman, H., 2009. Feldspar dissolu-tion kinetics and Gibbs free energy dependence in a CO_2-enriched groundwater system, Green River, Utah. *Earth Planet. Sci. Lett*.284, 473–488.

Kampman, N., Burnside, N.M., Shipton, Z.K., Chapman, H.J., Nicholl, J.A., Ellam, R.M. and Bickle, M.J., 2012. Pulses of carbon dioxide emissions from intracrustal faults following climatic warming. *Nat. Geosci*.5, 352–358.

Kampman, N., Bickle, M.J., Wigley, M., Dubacq, B., 2014a. Fluid flow and CO_2–fluid–mineral interactions during CO_2-storage in sedimentary basins. *Chem. Geol*.369, 22–50.

Kampman, N., Maskell, A., Chapman, H.J., Bickle, M.J., Evans, J.P., Purser, G., Zhou, Z., Gattacceca, J., Schaller, M., Bertier, P., Chen, F., Turchyn, A.S., Assayag, N., Rochelle, C. and Busch, A., 2014b. Drilling and sampling a natural CO_2reservoir: implications for fluid flow and CO_2–fluid–rock reactions during CO_2migration through the overburden. *Chem. Geol*.369, 51–82.

Kampman, N., Busch A., Bertier P., Snippe J., Hangx, S. Pipich, V., Z. Di, Rother, G., Harrington, J.F. Evans, J.P., Maskell, A., Chapman, H.J. and Bickle, M.J. 2016 Observational evidence confirms modelling of the long-term integrity of CO_2-reservoir caprocks. *Nature Communications*.

Karstens, J. and Berndt, C., 2015, Seismic chimneys in the Southern Viking Graben – Implications for paleo fluid migration and overpressure evolution, *Earth and Platnetary Science Letters*, 412, 88-100.

Kayen, R. E. and Lee, H. J. 1993. Slope stability in regions of sea-floor gas hydrate: Beaufort Sea continental slope. *Bulletin. U.S. Dept. of the Interior*, U.S. Geological Survey, 97-103

Kazemeini, S. H., Juhlin, C., and Fomel, S. 2010. Monitoring CO_2 response on surface seismic data; a rock physics and seismic modeling feasibility study at the CO_2 sequestration site, Ketzin, Germany. *Journal of Applied Geophysics*, *71*(4), 109-124.

Keating, E, Dai, Z, Dempsey, D and Pawar, R. 2014. Effective detection of CO_2 leakage: a comparison of groundwater sampling and pressure monitoring. *Energy Procedia*, Vol. 63, 4163-4171.

Keating, E, Pawar, R and Dempsey, D. In press. Pressure monitoring to detect fault rupture due to CO2 injection. *Energy Procedia*.

Kenyon, N. H., Ivanov, M. K., Akhmetzhanov, A. M. and Akhmanov, G. G. (Eds.), 2000. Multidisciplinary Study of the Geological Processes on the North East Atlantic and Western Mediterranean Margins. IOC Technical Series 56, UNESCO

Kempka, T., Kühn, M., H. Class, H., Frykman, P., Kopp, A., Nielsen, C.M., and Probst P. 2010. Modelling of CO_2 arrival time at Ketzin–Part I. *International Journal of Greenhouse Gas Control*, *4*(6), 1007-1015.

Kim, GY., Yi, BY., Yoo, DG., Ryu, BJ. and Riedel, M. 2011. Evidence of gas hydrate from downhole logging data in the Ulleung Basin, East Sea. *Mar Petrol Geol* 28:1979–1985.

King, L.H. and MacLean, B., 1970. Pockmarks on the Scotian Shelf. *Bulletin of the Geological Society of America* 81, 3141–3148.

Kirby, G.A., Chadwick, R.A. and Holloway, S. 2001. Depth mapping and characterisation of the Utsira Sand saline aquifer, central and northern North Sea. *BGS Commissioned Report* CR/01/218.

Kirk, K. 2011. Natural CO_2 flux literature review for the QICS project. *British Geological Survey Commissioned Report, CR/11/005.* 38pp.

Kjær, K.H., Larsen, E., van der Meer, J., Ingólfsson, Ó., Krüger, J., Benediktsson, Ì. Ö., Knudsen, C.G. and Schomacker, A. 2006. Subglacial decoupling at the sediment/bedrock interface: a new mechanism for rapid flowing ice. *Quaternary Science Reviews 25*, 2704–2712.

Klusman, R W. 2011. Comparison of surface and near-surface geochemical methods for detection of gas microseepage from carbon dioxide sequestration. *International Journal of Greenhouse Gas Control*, Vol. 5, 1369-1392.

Kohl, B. and Roberts, H. H., 1994. Fossil foraminifera from four active mud volcanoes in the Gulf of Mexico. *Geo-Marine Letters*. 14, 126– 134.

Konno, U., Tsunogai, U., Nakagawa, F., Nakaseama, M., Ishibashi, J., Nunoura, T. and Nakamura, K. 2006. Liquid CO_2 venting on the seafloor: Yonaguni Knoll IV hydrothermal system, Okinawa Trough. *Geophysical Research Letters*, 33, L16607, 5pp.

Kopf, A.J., 2002. Significance of mud volcanism. Reviews of Geophysics 40, 52.

Koukouzas, N., Tasianas, A., Gemeni, V., Alexopoulos, D. and Vasilatos, C. 2015. Geological modelling for investigating CO_2 emissions in Florina, Greece. *Open Geosciences* 7, 465–489.

Krevor, S, Perrin, J-C, Esposito, A, Rella, C and Benson, S. 2010. Rapid detection and characterization of surface CO_2 leakage through the real-time measurement of

δ^{13}C signatures in CO_2 flux from the ground. *International Journal of Greenhouse Gas Control*, Vol. 4, 811-815.

Krevor, S., Pini, R., Li, B. X. and Benson, S. M. 2011 Capillary heterogeneity trapping of CO_2 in a sandstone rock at reservoir conditions. *Geophysical Research Letters* **38**.

Kristensen, T.B., Piotrowski, J.A., Huuse, M., Clausen, O.R. and Hamberg, L., 2008. Time-transgressive tunnel valley formation indicated by infill sediment structure, North Sea–the role of glaciohydraulic supercooling. *Earth Surface Processes and Landforms*, *33*(4), pp.546-559.

Krüger, M, Jones, D, Frerichs, J, Oppermann, B I, West, J, Coombs, P, Green, K, Barlow, T, Lister, R, Shaw, R, Strutt, M and Möller, I. 2011. Effects of elevated CO_2 concentrations on the vegetation and microbial populations at a terrestrial CO_2 vent at Laacher See, Germany. *International Journal of Greenhouse Gas Control*, Vol. 5, 1093-1098.

Kuhlmann, G., Adams, S., Anka, Z., Campher, C., di Primio, R. and Horsfield, B., 2011. 3D petroleum systems modelling within a passive margin setting, Orange Basin, blocks 3 / 4, offshore South Africa—implications for gas generation, migration and leakage. *South African Journal of Geology* 114 (3–4), 387–414. http://dx.doi.org/10.2113/gssajg.114.3-4.387

Kuske, T, Jenkins, C, Zegelin, S, Mollah, M and Feitz, A. 2013. Atmospheric Tomography as a Tool for Quantification of CO_2 Emissions from Potential Surface Leaks: Signal Processing Workflow for a Low Accuracy Sensor Array. *Energy Procedia*, Vol. 37, 4065-4076.

Kvenvolden, K. A., 1993. Gas hydrates – geological perspective and global change. Reviews of Geophysics, 31 (2) (1993), pp. 173–187

Kvenvolden, K., Lorenson, T. and Reeburgh, W., 2001. Attention turns to naturally occurring methane seepage. *Eos* 82, 457–458.

LaForce, T., Ennis-King, J., Boreham, C. and Paterson, L. 2015. Residual CO2 saturation estimate using noble gas tracers in a single-well field test: The CO2CRC Otway project (vol 26, pg 9, 2014). *International_Journal_of_Greenhouse_Gas_Control* 41: 358-358.

Lance, S., Henry, P., Le Pichon, X., Lallemant, S., Chamley, H., Rostek, F., Faugères, J.-C., Gonthier, E. and Olu, K. 1998. Submersible study of mud volcanoes seaward of the Barbados accretionary wedge: sedimentology, structure and rheology. *Marine Geology*. 145, 255–292.

Langhi, L, Ross, A, Crooke, E, Jones, A, Nicholson, C and Stalvies, C. 2014. Integrated hydroacoustic flares and geomechanical characterization reveal potential hydrocarbon leakage pathways in the Perth Basin, Australia. *Marine and Petroleum Geology*, Vol. 51, 63-69.

Lassen, R N, Sonnenborg, T O, Jensen, K H and Looms, M C. 2015. Monitoring CO_2 gas-phase migration in a shallow sand aquifer using cross-borehole ground penetrating radar. *International Journal of Greenhouse Gas Control*, Vol. 37, 287-298.

Laubach, S.E., Olson, J.E. and Gale, J.F.W. 2004. Are open fractures necessarily aligned with maximum horizontal stress. *Earth and Planetary Science Letters* 222, 191–195.

Lee, K-K, Lee, S H, Yun, S-T and Jeen, S-W. 2016. Shallow groundwater system monitoring on controlled CO_2 release sites: a review on field experimental methods and efforts for CO_2 leakage detection. *Geosciences Journal*, Vol. 20, 569-583.

Lehner, F.K. and Pilaar, W.F. 1997. The emplacement of clay smears in synsedimentary normal faults: inferences from field observations near Frechen, Germany. In: Møller-Pedersen, P. and Koestler, A.G. (eds) *Hydrocarbon Seals: Importance for Exploration and Production*. Norwegian Petroleum Society (NPF), Special Publication 7, 39–50.

Leifer, I. and MacDonald, I., 2003. Dynamics of the gas flux from shallow gas hydrate deposits: Interaction between oily hydrate bubbles and the oceanic environment. *Earth and Planetary Science Letters* 210, 411–424.

Leifer, I. and Boles, J., 2005. Measurement of marine hydrocarbon seep flow through fractured rock and unconsolidated sediment. *Marine and Petroleum Geology* 22, 551–568.

Leveille, G.P., Knipe, R., More, C., Ellis, D., Dudley, G., Jones, G., Fisher, Q.J. and Allinson, G. 1997. Compartmentalization of Rotliegendes gas reservoirs by sealing faults, Jupiter Fields area, southern North Sea. In: Ziegler, K., Turner, P. and Daines, S.R. (eds) *Petroleum Geology of the Southern North Sea*. Geological Society, London, Special Publications 123, 87–104.

Lewicki, J. L., Birkholzer, J., and Tsang, C. 2006. Natural and industrial analogues for release of CO_2 from storage reservoirs: Identification of features, events, and processes and lessons learned. *Lawrence Berkeley National Laboratory*.

Lewicki, J.L., Birkholzer, J. and Tsang, C.F. 2007. Natural and industrial analogues for leakage of CO_2 from storage reservoirs: Identification of features, events, and processes and lessons learned. *Environmental Geology* 52 (3), 457–467.

Lewicki, J. L. and Hilley, G. E. 2009. Eddy covariance mapping and quantification of surface CO_2 leakage fluxes. *Geophysical Research Letters*, Vol. 36.

Lewicki, J. L. and Hilley, G. E. 2012. Eddy covariance network design for mapping and quantification of surface CO_2 leakage fluxes. *International Journal of Greenhouse Gas Control*, Vol. 7, 137-144.

Lewis, G., Knipe, R.J. and Li, A. 2002. Fault seal analysis in unconsolidated sediments: a field study from Kentucky, USA. In: Koestler, A.G. and Hunsdale, R. (eds) *Hydrocarbon Seal Quantification*. NPF Special Publication 11, 243–253.

Limonov, A.F., Woodside, J. M. and Ivanov, M. K. (Eds.), 1994. Mud volcanism in the Mediterranean and Black Seas and shallow structure of the Eratosthenes Seamount. Initial results of the geological and geophysical investigations during the Third UNESCO-ESF “Training Through Research” Cruise of RV Gelendzhik, June–July 1993. *UNESCO Reports in Marine Sciences*, 64. 173 pp

Lindeberg, E.; Bergmo, P., Torsaeter, M. and Grimstad, A-A. In press. The Aliso Canyon methane well leakage as an analogue for worst case CO_2 leakage and quantification of acceptable storage loss, *Energy Procedia*, GHGT-13 Lausanne, Switzerland, November 2016, poster 269.

Lindeberg, E. and D. Wessel-Berg 1997. Vertical convection in an aquifer column under a gas cap of CO_2. *Energy Conversion and Management*, 38: S229-S234.

Lindsay, N.G., Murphy, F.C., Walsh, J.J. and Watterson, J. 1993. Outcrop studies of shale smear on fault surfaces. In: Flint, S.S. and Bryant, I.D. (eds) *The Geological Modelling of Hydrocarbon Reservoirs and Outcrop Analogues*. International Association of Sedimentologists, Special Publication 15, 113–123.

Lions, J, Devau, N, de Lary, L, Dupraz, S, Parmentier, M, Gombert, P and Dictor, M-C. 2014. Potential impacts of leakage from CO_2 geological storage on geochemical processes controlling fresh groundwater quality: A review. *International Journal of Greenhouse Gas Control*, Vol. 22, 165-175.

Liu, F., Lu, P., Griffith, C., Hedges, S.W., Soong, Y., Hellevang, H. and Zhu, C. 2012. CO_2–brine–caprock interaction: reactivity experiments on Eau Claire shale and a review of relevant literature. *International Journal of Greenhouse Gas Control* 7, 153–167.

Livingstone, S.J. and Clark, C.D., 2016. Morphological properties of tunnel valleys of the southern sector of the Laurentide Ice Sheet and implications for their formation. *Earth Surface Dynamics*, 4(3), p.567.

Locat, J., 2001. Instabilities along ocean margins: a geomorphological and geotechnical perspective. *Marine and Petroleum Geology* 18, 503–512.

Locat, J., Lee, H.J., 2002. Submarine landslides: advances and challenges. *Canadian Geotechnical Journal* 39, 193–212.

Lombardi, S. 2010. A resource for studying potential impacts, examining gas migration processes and testing monitoring techniques. *IEAGHG workshop: Natural releases of CO_2: Building knowledge for CO_2 storage Environmental Impact Assessments*. Maria Laach, Germany, 2nd – 4th November 2010.

Lombardi, S, Annunziatellis, A, Beaubien, S E, Ciotoli, G and Coltella, M. 2008. Natural analogues and test sites for CO_2 geological sequestration: experience at Latera, Italy. *First Break*, Vol. 26, 39-43.

Lonergan, L., Cartwright, J., Laver, R. and Staffurth, J. 1998. Polygonal faulting in the Tertiary of the central North Sea: implications for reservoir geology. In: Coward, M.O., Daltaban, T.S. and Johnson, H. (eds) *Structural Geology in Reservoir Characterization*. Geological Society, London, Special Publications 127, 191–207.

Løseth H, Gading M and Wensaas L. 2009. Hydrocarbon leakage interpreted on seismic data. Mar Petrol Geol 26:1304–1319.

Løseth, H., Wensaas, L., Arntsen, B., Hanken, N., Basire, C. and Graue, K., 2011. 1000 m long gas blow-out pipes. *Marine and Petroleum Geology 27*, 1047–1060.

Lucier, A., Zoback, M., Gupta, N. and Ramakrishnan, T.S. 2006. Geomechanical aspects of CO_2 sequestration in a deep saline reservoir in the Ohio River Valley region. *Environmental Geosciences* 13 (2), 85–103.

Luhar, A K, Etheridge, D M, Leuning, R, Loh, Z M, Jenkins, C R and Yee, E. 2014. Locating and quantifying greenhouse gas emissions at a geological CO_2 storage site using atmospheric modeling and measurements. *Journal of Geophysical Research: Atmospheres*, Vol. 119, 2014JD021880.

Lupton, J., Butterfield, D., Lilley, M., Evans, L., Nakamura, K., Chadwick Jr., W., Resing, J., Embley, R., Olson, E., Proskurowski, G., Baker, E., de Ronde, C., Roe, K., Greene, R., Lebon, G. and Young, C. 2006. Submarine venting of liquid carbon dioxide on a Mariana Arc volcano. *Geochem. Geophys. Geosyst., 7*, Q08007.

Lynch, R., E. McBride, T. Perkins, and Wiley, M. 1985. Dynamic kill of an uncontrolled CO_2 well, *Journal of Petroleum Technology*, vol 37, issue 07. Pp 1,267 - 1,275.

Maestro, A., Barnolas, A. and Somoza, L. 2002. Geometry and structure associated to gas-charged sediments and recent growth faults in the Ebro Delta (Spain). *Marine Geology,* 186: 351–368.

Makurat A., Torudbakken B, Monsen K., and Rawlings C. 1992. Cenezoic uplift and caprock Seal in the Barents Sea: fracture modelling and seal risk evaluation. *SPE Annual Technical Conference and Exhibition, 4-7 October*, Washington, D.C

Manceau, J. C., Hatzignatiou, D. G., de Lary, L., Jensen, NB, and Reveillere, A 2014. Mitigation and remediation technologies and practices in case of undesired migration of CO_2 from a geological storage unit-Current status *International Journal of Greenhouse Gas Control*, 22, 272-290.

Manceau, J.C., Tremosa, J., Lerouge, C., Gherardi, F., Nussbaum, C., Wasch, L.J., Alberic, P., Audigane, P. and Claret, F., 2016. Well integrity assessment by a 1:1 scale wellbore experiment: Exposition to dissolved CO_2 and overcoring. *International Journal of Greenhouse Gas Control* 54 258–271

Manzocchi, T., Childs, C. and Walsh, J.J. 2010. Faults and fault properties in hydrocarbon flow models. *Geofluids* 10 (1–2), 94–113.

Marrett, R. and Allmendinger, R.W. 1990. Kinematic analysis of fault-slip data. *Journal of structural geology* 12 (8), 973–986.

Martinez, M. J., Newell, P., Bishop J, E. and , Turner, D Z. 2013. Coupled multiphase flow and geomechanics model for analysis of joint reactivation during CO_2 sequestration operations. *International Journal of Greenhouse Gas Control*, Vol. 17, 148-160.

Martínez-Carreño, N. and García-Gil, S., 2013. The Holocene gas system of the Ría de Vigo (NW Spain): Factors controlling the location of gas accumulations, seeps and pockmarks. *Marine Geology* 344, 82–100.

Maslin, M., Owen, M., Day, S. and Long, D., 2004. Linking continental-slope failures and climate change: Testing the clathrate gun hypothesis. Geology 32, 53–56.

Mayo, A.L., Shrum, D.B. and Chidsey, T.C., 1991. Factors contributing to exsolving carbon dioxide in ground water systems in the Colorado plateau, Utah. In: Chidsey,

T.C. (Ed.), *Geology of East-Central Utah*. Utah Geological Survey, Salt Lake City, pp.335–341.

McCrone, C.W., Gainski, M. and Lumsden, P.J. 2003. The Indefatigable Field, Blocks 49/18, 49/19, 49/23. 49/24, UK North Sea. In: Gluyas, J.G. and Hichens, H.M. (eds) *United Kingdom Oil and Gas Fields, Commemorative Millennium Volume*. Geological Society, London, Memoirs 20, 741–747.

McGinnis, D.F., Schmidt, M., DelSontro, T., Themann, S., Rovelli, L., Reitz, A. and Linke, P. 2011. Discovery of a natural CO_2 seep in the German North Sea: Implications for shallow dissolved gas and seep detection. *Journal of Geophysical Research* 116, C03013.

Mildren, S.D., Hillis, R.R., Lyon, P.J. and Meyer, J.J. 2005. FAST: A New Technique for Geomechanical Assessment of the Risk of Reactivation-related Breach of Fault Seals. In: Boult, P. and Kaldi, J. (eds) *Evaluating fault and cap rock seals*. AAPG Hedberg Series 2, 73–85.

Milkov, A., 2000. Worldwide distribution of submarine mud volcanoes and associated gas hydrates. *Marine Geology* 167, 29–42.

Mingxing B, Zhichao Z and Xiaofei F. 2016. A review on well integrity issues for CO_2 geological storage and enhanced gas recovery, *Renewable and Sustainable Energy Reviews*, Volume 59, June 2016, Pages 920-926.

Miocic, J.M., Gilfillan, S.M.V., McDermott, C. and Haszeldine, R.S. 2013. Mechanisms for CO_2 leakage prevention – a global dataset of natural analogues. *Energy Procedia* 40, 320–328.

Molin, P., Acocella, V. and Funiciello. 2003. Structural, seismic and hydrothermal features at the border of an active intermittent resurgent block: Ischia Island (Italy). *Journal of Volcanology and Geothermal Research* 121, 65-81

Moni, C. and Rasse, D. 2013. Simulated CO_2 leakage experiment in terrestrial environment: Monitoring and detecting the effect on a cover crop using ^{13}C analysis. *Energy Procedia* 37, 3479 – 3485.

Moni, C. and Rasse, D. 2014. Detection of simulated leaks from geologically stored CO_2 with ^{13}C monitoring. *International Journal of Greenhouse Gas Control* 26, 61–68.

Moran, S.R., Clayton, L., Hooke, R., Fenton, M.M. and Andriashek, L.D. 1980. Glacier-bed landforms of the prairie region of North America. *Journal of Glaciology 25*, 457-473.

Moreau, J. and Huuse, M., 2014 Infill of tunnel valleys associated with landward-flowing ice sheets: The missing Middle Pleistocene record of the NW European rivers? *Geochemistry Geophysics Geosystems* 15, 1-9

Moreira, A C d C A, Musse, A P S, Rosário, F d, Lazzarin, H S C, Cavelhão, G, Chang, H K, Oliva, A, Landulfo, E, Nakaema, W M, Melo, C L, Bressan, L W, Ketzer, J M, Constant, M J, Spangler, L H and Dobeck, L M. 2014. The First Brazilian Field Lab Fully Dedicated to CO_2 MMV Experiments: From the Start-up to the Initial Results. *Energy Procedia*, Vol. 63, 6227-6238.

Moreira, A. Almeida, J C., Oliveira, S., Nakaema, W., Landulfo, E., Rosario, F, Musse, A.P., Bruno, M. and Correa, S. 2015. Preliminary results of the atmospheric leakage dispersion modelling of the Brazilian CO_2 Pilot. *WIT Transactions on Ecology and The Environment*, Vol 195, 391-402.

Morris, A., Ferrill, D.A. and Henderson, D.B. 1996. Slip-tendency analysis and fault reactivation. *Geology* 24 (3), 275–278.

Morton, A.C. 1979. The provenance and distribution of the Paleocene sands of the Central North Sea. *Journal of Petroleum Geology* 2, 11–21.

Moscardelli, L. and Wood, L., 2008. New classification system for mass transport complexes in offshore Trinidad. Basin Research 20, 73–98.

Mosawy, R., Thomas, S., Adcock, K. and Biddick, K., 2006. Athena Site Survey and Habitat Assessment Survey *UKCS, Block 14, Project Ref. 6880* for Senergy / Ithaca Energy (UK) Ltd.

Murton, B.J. and Biggs, J., 2003. Numerical modelling of mud volcanoes and their flows using constraints from the Gulf of Cadiz. *Marine Geology* 195, 223–236.

NASCENT. 2005. Natural analogues for the geological storage of CO_2. *British Geological Survey Report*.

Nakajima, T, Xue, Z, Chiyonobu, S, and Azuma, H. 2014. Numerical simulation of CO_2 leakage along fault system for the assessment of environmental impacts at CCS site. *Energy Procedia*, Vol. 63, 3234-3241.

Nelson, E.B., 2012. Well cementing fundamentals. *Oilfield Review*, Summer 2012: 24, No.2., p 59-60. [Accessed October 2016].

Neumann, P P, Asadi, S, Bennetts, V H, Lilienthal, A J and Bartholmai, M. 2013. Monitoring of CCS Areas using Micro Unmanned Aerial Vehicles (MUAVs). *Energy Procedia*, Vol. 37, 4182-4190.

Newell, D L, Larson, T E, Perkins, G, Pugh, J D, Stewart, B W, Capo, R C and Trautz, R C. 2014. Tracing CO_2 leakage into groundwater using carbon and strontium isotopes during a controlled CO_2 release field test. *International Journal of Greenhouse Gas Control*, Vol. 29, 200-208.

Newton, R., Cunningham, R. and Schubert, C. 1980. Mud volcanoes and pockmarks: seafloor engineering hazards or geological curiosities?, in: Offshore Technology Conference, 5-8 May 1980. Houston, Texas.

Newton, C., Shipp, R., Mosher, D.C. and Wach, G.D., 2004. Importance of mass transport complexes in the Quaternary development of the Nile fan, Egypt, in: *Offshore Technology Conference*. Houston, Texas, p. 10.

Nicol, A., Childs, C., Walsh, J.J. and Schafer, K.W. 2013. A geometric model for the formation of deformation band clusters. *Journal of Structural Geology* 55, 21–33.

Nicol, A., Seebeck, H., Field, B. and McNamara, D. 2015. Fault Permeability Study. IEA/CON/15/230. *GNS Science Consultancy Report 2015/206*. 125pp.

Nicot, J.-P., Oldenburg, C.M., Houseworth, J.E. and Choi, J.-W., 2013. Analysis ofpotential leakage pathways at the Cranfield, MS, U.S.A., CO_2sequestration site. *International Journal of Greenhouse Gas Control* 18, 388–400.

Nogues, J P, Court, B, Dobossy, M, Nordbotten, J M and Celia, M A. 2012. A methodology to estimate maximum probable leakage along old wells in a geological sequestration operation. *International Journal of Greenhouse Gas Control*, Vol. 7, 39-47.

Nordbotten, J M, Celia, M A, and Bachu, S. 2004. Analytical solution for leakage rates through abandoned wells. *Water Resources Research*, Vol. 40, 1-10.

Nordbotten, J. M., Celia, M. A., Bachu, S. and Dahle, H. K. 2005. Semianalytical solution for CO_2 leakage through an abandoned well. *Environmental Science and Technology*, Vol. 39, 602-611.

Norden, B. and Frykman, P. 2013. Geological modelling of the Triassic Stuttgart Formation at the Ketzin CO_2 storage site, Germany. *International Journal of Greenhouse Gas Control*, *19*, 756-77.

Nouzé, H., Contrucci, I., Foucher, J.-P., Marsset, B., Thomas, Y., Thereau, E., Normand, A., Le Drezen, E., Didailler, S., Regnault, J.-P., Le Conte, S., Guidart, S., Lekens, W., Dean, S. and Throo, A., 2004. Premiers résultats d'une étude géophysique sur le flanc nord des glissements de Storegga (Norvège). *Comptes Rendus de l'Académie des Sciences de Paris 336*, 1181–1189.

Oliva, A., Moreira, A., Chang, H K., Rosário, F., Musse, A., Melo, C., Bressan, L Ketzer, J., Contant, M., Lazzarin, H., Cavelhão, G. and Corseuil, H. 2014. A comparison of three methods for monitoring CO_2 migration in soil and shallow subsurface in the Ressacada Pilot site, Southern Brazil. *Energy Procedia* 63, 3992 – 4002.

Olu-Le Roy, K., Caprais, J.C., Fifis, A., Fabri, M.C., Galéron, J., Budzinsky, H., Le Ménach, K., Khripounoff, A., Ondréas, H. and Sibuet, M., 2007. Cold-seep assemblages on a giant pockmark off West Africa: Spatial patterns and environmental control. *Marine Ecology* 28, 115–130.

Ors, O. and Sinayuc, C. 2014. An experimental study on the CO_2-CH_4 swap process between gaseous CO_2 and CH_4 Hydrate in porous media. *Journal of Petroleum Science and Engineering*, 119, 156–162.

Osborne, M.J. and Swarbrick, R.E., 1997. Mechanisms for generating overpressure in sedimentary basins: a reevaluation. AAPG Bull. 81 (6), 1023e1041.

Osdal, B., Zadeh, H.M., Johansen, S. and Gilding, D. 2013, CO_2 saturation and Thickness Prediction from 4D Seismic Data at the Snøhvit Field. *75th EAGE Conference and Exhibition,* London.

Osdal, B., Zadeh, H.M., Johansen, S., Gonzalez, R.R. and Waerum, G.O. 2014, Snøhvit CO_2 Monitoring using Well Pressure Measurement and 4D Seismic. *Fourth EAGE CO_2 Geological Storage Workshop*, Stavanger.

Ostanin I., Anka Z., di Primio R. and Bernal A. 2012. Identification of a large Upper Cretaceous polygonal fault network in the Hammerfest basin: implications on the reactivation of regional faulting and gas leakage dynamics, SW Barents Sea. *Marine Geology*, 332–334:109–125.

Ostanin I., Anka Z., di Primio R. and Bernal A. 2013. Hydrocarbon plumbing systems above the Snohvit gas field: structural control and implications for thermogenic methane leakage in the Hammerfest Basin, SW Barents Sea. *Marine and Petroleum Geology* 43:127–146. doi:10.1016/j.marpetgeo.2013.02.012

Ottesen, D., Rise, L., Andersen, E.S., Bugge, T. and Eidvin, T., 2009. Geological evolution of the Norwegian continental shelf between 61°N and 68°N during the last 3 million years. *Norwegian Journal of Geology* 89, 251–265.

Overeem, I., Weltje, G.J., Bishop-Kay, C. and Kroonenberg, S.B. 2001. The Late Cenozoic Eridanos delta system in the Southern North Sea Basin: a climate signal in sediment supply? *Basin Research* 13, 293–312.

Pawar, R. J., Bromhal, G. S., Carey, J. W, Foxall, W, Korre, A, Ringrose, P. S., Tucker, O., Watson, M. N. and White, J. A. 2015. Recent advances in risk assessment and risk management of geologic CO2 storage. *International Journal of Greenhouse Gas Control* 40, 292–311.

Peacock, D.C.P. and Sanderson, D.J. 1994. Geometry and development of relay ramps in normal fault systems. *AAPG Bulletin* 78, 147–165.

Pearce, J M, Baker, J, Beaubien, S, Brune, S, Czemichowski-Lauriol, I, Faber, E, Hatziyannis, G, Hildenbrand, A, Krooss, B M, Lombardi, S, Nador, A, Pauwels, H and Schroot, B M. 2003. Natural CO_2 accumulations in Europe: Understanding long-term geological processes in CO_2 sequestration. *Greenhouse Gas Control Technologies*, Vols i and ii, Proceedings, 417-422.

Pearce, J., Czernichowski-Lauriol, I., Lombardi, S., Brune, S., Nador, A., Baker, J., Pauwels, H., Hatziyannis, G., Beaubien, S. and Faber, E. 2004. A review of natural CO_2 accumulations in Europe as analogues for geological sequestration. In: Baines, S.J. and Worden, R.H. (eds) *Geological Storage of Carbon Dioxide*. Geological Society, London. Special Publications 233, 29–41.

Pearce, J M. 2006. What can we learn from natural analogues? - An overview of how analogues can benefit the geological storage of CO_2. Advances in the Geological Storage of Carbon Dioxide: *International Approaches to Reduce Anthropogenic Greenhouse Gas Emissions*, Vol. 65, 129-139.

Pedersen, S.A.S. 1987. Comparative studies of gravity tectonics in Quaternary sediments and sedimentary rocks related to fold belts. In: Jones, M.E., Preston, R.M.F. (Eds.), Sediment Deformation Mechanisms. *Geological Society of London, Special Publication 29,* pp. 43–65.

Pedersen, S.A.S. 2005. Structural analysis of the Rubjerg Knude Glaciotectonic Complex, Vendsyssel, northern Denmark. *Geological Survey of Denmark and Greenland Bulletin 8*, 192 pp.

Pedersen, S.A.S. 2014. Architecture of Glaciotectonic Complexes. *Geosciences 2014*, 4, 269-296.

Pedersen, S.A.S. and Boldreel, L.O. 2016. Glaciotectonic deformations in the Jammerbugt and the glaciodynamic development in the eastern North Sea. *Journal of Quaternary Science*.

Petersen, C. J., Bünz, S., Hustoft, S., Mienert, J. and Klaeschen, D. 2010. High-resolution P-Cable 3D seismic imaging of gas chimney structures in gas hydrated sediments of an Arctic sediment drift. *Marine and Petroleum Geology,* 27, 1981-1994.

Pettinelli, E., Beaubien, S.E., Zaja, A., Menghini, A., Praticelli, N., Mattei, E., Di Matteo, A., Annunziatellis, A., Ciotoli, G. and Lombardi, S. 2010. Characterization of a CO_2 gas vent using various geophysical and geochemical methods. *Geophysics* 75, B137–B146.

Pezard, P A, Denchik, N, Lofi, J, Perroud, H, Henry, G, Neyens, D, Luquot, L and Levannier, A. 2016. Time-lapse downhole electrical resistivity monitoring of subsurface CO_2 storage at the Maguelone shallow experimental site (Languedoc, France). *International Journal of Greenhouse Gas Control*, Vol. 48, Part 1, 142-154.

Phillips, E.R., Evans, D.J.A. and Auton, C.A. 2002. Polyphase deformation at an oscillating ice margin following the Loch Lomond Readvance, central Scotland, UK. *Sedimentary Geology* 149, 157-182.

Phillips, E. and Merritt, J. 2008. Evidence for multiphase water-escape during rafting of shelly marine sediments at Clava, Inverness-shire, NE Scotland. *Quaternary Science Reviews* 27, 988–1011.

Phillips, E., Lee, J.R. and Burke, H. 2008. Progressive proglacial to subglacial deformation and syntectonic sedimentation at the margins of the Mid-Pleistocene British Ice Sheet: evidence from north Norfolk, UK. *Quaternary Science Reviews 27*, 1848-1871.

Phillips, E., Lee, J.R. and Evans, H.M. 2011. Glacitectonics – Field Guide. *Quaternary Research Association*, Pontypool.

Phillips, E., Everest, J. and Reeves, H. 2013. Micromorphological evidence for subglacial multiphase sedimentation and deformation during overpressurized fluid flow associated with hydrofracturing. *Boreas* 42, 395-427.

Phillips, E. and Hughes, L. 2014. Hydrofracturing in response to the development of an overpressurised subglacial meltwater system during drumlin formation: an example from Anglesey, NW Wales. *Proceedings of the Geologists' Association 125*, 296–311.

Phillips, E., Evans, D.J.A., Atkinson, N. and Kendall, A. In press. Structural architecture and glacitectonic evolution of the Mud Buttes cupola hill complex, Southern Alberta, Canada. *Quaternary Science Reviews*.

Pfannkuche, O., 2005. *Cruise Report ALKOR 259: Methane Cycle at Shallow Gaseous Sediments in the Central North Sea*. GEOMAR, Kiel. 42pp.

Pilcher, R. and Argent, J., 2007. Mega-pockmarks and linear pockmark trains on the West African continental margin. *Marine Geology* 244, 15–32.

Piotrowski, J.A., 2006. Groundwater under ice sheets and glaciers. In: Knight, P.G. (Ed.), *Glacier Science and Environmental Change*. Blackwell, Oxford, pp. 50–60.

Pittman, E.D. 1981. Effect of fault-related granulation on porosity and permeability of quartz sandstone, Simpson Group (Ordovician) Oklahoma. *AAPG Bulletin* 65, 2381–2387.

Porter, J.R., Knipe, R.J., Fisher, Q.J., Farmer, A.B., Allin, N.S., Jones, L.S., Palfrey, A.J., Garrett, S.W. and Lewis, G. 2000. Deformation processes int eh Britannia Field, UKCS. *Petroleum Geoscience* 6, 241–254.

Prior D. B., Doyle, E. H. and Kaluza, M. J., 1989. Evidence for sediment eruption on deep sea floor, Gulf of Mexico. Science 243, 517– 519.

Pruess, K., 2005. Numerical simulation of CO_2 leakage from a geologic disposal reservoir, including transitions from super- to sub-critical conditions, and boiling of liquid CO_2. *Society of Petroleum Engineers Journal*, 237–248.

Pruess, K., 2008. Leakage of CO_2 from geologic storage: role of secondary accumulation at shallow depth. *International Journal of Greenhouse Gas Control* 2, 37–46.

Pruess, K., 2011. Modeling CO_2 leakage scenarios, including transitions between super- and sub-critical conditions, and phase change between liquid and gaseous CO_2. *Energy Procedia* 4, 3754–3761.

Rahman, T., Lebedev, M., Barifcani, A. and Iglauer, S. 2016. Residual trapping of supercritical CO2 in oil-wet sandstone. *Journal of Colloid and Interface Science* 469: 63-68.

Ramachandran, H., Pope, G.A. and Srinivasan, S. 2014. Effect of thermodynamic phase changes on CO_2 leakage. *Energy Procedia* 63, 3735–3745.

Rebesco, M., Hernández-Molina, F.J., Rooij, D. and Van Wåhlin, A., 2014. Contourites and associated sediments controlled by deep-water circulation processes: State-of-the-art and future considerations. *Marine Geology* 352, 111–154.

Reeburgh, W.S., 2007. Oceanic methane biogeochemistry. *Chemical Reviews* 486–513.

Rijsdijk, K. F., McCarroll, D., Owen, G., van der Meer, J.J.M. and Warren, W. P. 1999. Clastic dykes in glacigenic diamicts: Evidence for subglacial hydrofracturing from Killiney Bay, Ireland. *Sedimentary Geology 129*, 111-126.

Rise, L., Bellec, V.K., Chand, S. and Bøe, R., 2015. Pockmarks in the southwestern Barents Sea and - Finnmark fjords. *Norwegian Journal of Geology* 263–282.

Roberts, D.H., Dackombe, R.V. and Thomas, G.S.P. 2006. Palaeo-ice streaming in the central sector of the British-Irish Ice Sheet during the Last Glacial Maximum: evidence from the northern Irish Sea Basin. *Boreas 36*, 115-129.

Robertson, E.C. 1983. Relationship of fault displacement to gouge and breccia thickness. *American Institute of Mining Engineers Transactions* 35, 1426–1432.

Rochelle, C.A. and Long, D. 2008. Gas hydrate stability in the vicinity of a deep geological repository for radioactive wastes: A scoping study. *British Geological Survey Report, OR/08/073*, 24pp.

Rochelle, C.A., Camps, A.P., Long, D., Milodowski, A., Bateman, K., Gunn, D., Jackson, P., Lovell, M.A., and Rees, J. 2009. Can CO_2 hydrate assist in the underground storage of carbon dioxide? *Geological Society, London, Special Publications*, v. 319; p. 171-183.

Rochelle, C.A. and Milodowski, A.E. 2013. Carbonation of borehole seals: comparing evidence from short-term lab experiments and long-term natural analogues. *Applied Geochemistry* 30, 161–177, 10.1016/j.apgeochem.2012.09.007.

Romanak, K D, Bennett, P C, Yang, C and Hovorka, S D. 2012. Process-based approach to CO_2 leakage detection by vadose zone gas monitoring at geologic CO_2 storage sites. *Geophysical Research Letters*, Vol. 39, L15405.

Romanak, K D, Wolaver, B, Yang, C, Sherk, G W, Dale, J, Dobeck, L M and Spangler, L H. 2014. Process-based soil gas leakage assessment at the Kerr Farm: Comparison of results to leakage proxies at ZERT and Mt. Etna. *International Journal of Greenhouse Gas Control*, Vol. 30, 42-57.

Ruprecht, C., Pini, R., Falta, R., Benson, S. and Murdoch, L. 2014. Hysteretic trapping and relative permeability of CO2 in sandstone at reservoir conditions. *International Journal of Greenhouse Gas Control* 27: 15-27.

Rutqvist, J. 2012. The geomechanics of CO_2 storage in deep sedimentary formations. *Geotechnical and Geological Engineering*, Vol. 30, 525-551.

Sakai, H., Gamo, T., Kim, E.S., Tsutsumi, M., Tanaka, T., Ishibahi, J., Wakita, H., Yamano, M. and Oomori T. 1990. Venting of carbon dioxide-rich fluid and hydrate formation in mid-Okinawa Trough Backarc Basin, *Science*, 248, 1093–1096.

Sathar, S., Reeves, H.J., Cuss, R.J. and Harrington, J.F. 2012. The role of stress history on the flow of fluids through fractures. *Mineralogical Magazine* 76 (8), 3165–3177.

Schilling, F., Borm, G., Würdemann H., Möller, F. and Kühn, M. 2009. Status report on the first European on-shore CO_2 storage site at Ketzin (Germany). *Energy Procedia*, *1*(1), 2029-2035.

Schlömer, S, Möller, I and Furche, M. 2014. Baseline soil gas measurements as part of a monitoring concept above a projected CO_2 injection formation—A case study from Northern Germany. *International Journal of Greenhouse Gas Control*, Vol. 20, 57-72.

Schneider Von Deimling, J., Rehder, G., Greinert, J., McGinnnis, D.F., Boetius, A. and Linke, P., 2011. Quantification of seep-related methane gas emissions at Tommeliten, North Sea. *Continental Shelf Research* 31, 867–878.

Schneider Von Deimling, J., Linke, P., Schmidt, M. and Rehder, G., 2015. Ongoing methane discharge at well site 22/4b (North Sea) and discovery of a spiral vortex bubble plume motion. *Marine and Petroleum Geology* 68, 718–730.

Schroder, I F, Zhang, H, Zhang, C and Feitz, A J. 2016. The role of soil flux and soil gas monitoring in the characterisation of a CO_2 surface leak: A case study in Qinghai, China. *International Journal of Greenhouse Gas Control*, Vol. 54, Part 1, 84-95.

Schoell, M. 1980. The hydrogen and carbon isotopic composition of methane from natural gases of various origins. *Geochimica et Cosmochimica Acta*, 44(5), 649-661.

Schroot, B.M. and Schüttenhelm, R.T.E. 2003. Expressions of shallow gas in the Netherlands North Sea. *Geologie en Mijnbouw* 82 (1), 91–105.

Schroot, B.M., Klaver, G.T. and Schüttenhelm, R.T.E. 2005. Surface and subsurface expressions of gas seepage to the seabed – examples from the southern North Sea. *Marine and Petroleum Geology* 22, 499–515.

Sejrup, H.P., Aarseth, I. and Haflidason, H., 1991. The Quaternary succession in the northern North Sea. *Marine Geology*, 101, 103-111.

Sherk, G W, Romanak, K D, Dale, J, Gilfillan, S M V, Haszeldine, R S, Ringler, E S, Wolaver, B D and Yang, C. 2011. The Kerr Investigation: Final Report. Findings of the investigation into the impact of CO_2 on the Kerr Property. *International Performance Assessment Centre for geologic storage of Carbon Dioxide (IPAC-CO_2)*, pp. 181.

Shell, 2011. Static Model (Aquifer)*. ScottishPower CCS Consortium UK Carbon Capture and Storage Demonstration Competition Report*, UKCCS – KT – S7.22 – Shell – 001, p. 37

Shipton, Z.K., Evans, J.P., Dockrill, B., Heath, J., Williams, A., Kirchner, D. and Kolesar, P.T. 2004. Analysis of CO_2 leakage through 'low-permeability' faults from natural reservoirs in the Colorado Plateau, east-central Utah. In: Baines, S.J. and Worden, R.H. (eds) *Geological Storage of Carbon Dioxide*. Geological Society, London. Special Publications 233, 43–58.

Shipton, Z.K., Evans, J.P., Dockrill, B., Heath, J., Williams, A., Kirchner, D. and Kolesar, P.T. 2005. Natural leaking CO_2-charged system as analogs for failed geologic storage reservoirs. In: Thomas, D.C. and Benson, S.M. (eds) *Carbon Dioxide Capture for Storage in Deep Geologic Formations*. Elsevier, New York, 699–712.

Shipton, Z.K., Soden, A.M., Kirkpatrick, J.D., Bright, A.M. and Lunn, R.J. 2006. How thick is a fault? Fault displacement-thickness scaling revisited. *Earthquakes: Radiated Energy and the Physics of Faulting* 170, 193–198.

Shitashima, K, Maeda, Y, Koike, Y and Ohsumi, T. 2008. Natural analogue of the rise and dissolution of liquid CO_2 in the ocean. *International Journal of Greenhouse Gas Control* 2, p. 95-104.

Sibson, R.H. 1990. Conditions for fault-valve behaviour. In: Knipe, R.J. (Ed.) *Deformation mechanisms, Rheology and Tectonics*. Geological Society, London. Special Publications 54, 15–28.

Sigman, D.M., Hain, M.P. and Haug, G.H. 2010. The polar ocean and glacial cycles in atmospheric CO_2 concentration. *Nature*, 466, 47-55.

Slater, G. 1927. Structure of the Mud Buttes and Tit Hills in Alberta. *Bulletin of the Geological Society of America 38*.

Slater, G. 1931. The structure of the Bride Moraine, Isle of Man. *Proceedings of the Liverpool Geological Society 14*, 186-196.

Sloan, E. D., Koh, C.A., 2007. Clathrate Hydrates of Natural Gases, CRC Press, Boca Raton, 752 pp.

Sminchak, J.R., Moody, M., Theodos, A., Larsen, G. and Gupta, N. 2014. Investigation of Wellbore Integrity Factors in Historical Oil and gas Wells for CO_2 Geosequestration in the Midwestern U.S., *Energy Procedia*, Volume 63, Pages 5787-5797.

Smith, K L, Steven, M D, Jones, D G, West, J M, Coombs, P, Green, K A, Barlow, T S, Breward, N, Gwosdz, S, Krüger, M, Beaubien, S E, Annunziatellis, A, Graziani, S and Lombardi, S. 2013. Environmental impacts of CO_2 leakage: recent results from the ASGARD facility, UK. *Energy Procedia*, Vol. 37, 791-799.

Snippe, J. and Tucker, O. 2014. CO_2 fate comparison for depleted gas field and dipping saline aquifer. In Dixon, T., Herzog, H., Twinning, S. 12th International Conference on Greenhouse Gas Control Technologies, GHGT-12, *Energy Procedia*, 63, 5586-5601.

Somoza, L., Medialdea, T., León, R., Ercilla, G., Vázquez, J.T., Farran, M., Hernández-Molina, J., González, J., Juan, C. and Fernández-Puga, M.C. 2012. Structure of mud volcano systems and pockmarks in the region of the Ceuta Contourite Depositional System (Western Alboran Sea). *Marine Geology,* 332-334, 4-26.

Soroush, M., Wessel-Berg, D., Torsaeter, O. and Kleppe, J. 2014. Investigating residual trapping in CO_2 storage in saline aquifers - application of a 2D glass model, and image analysis. *Energy Science & Engineering* 2(3): 149-163.

Soter, S. 1999. Macroscopic seismic anomalies and submarine pockmarks in the Corinth-Patras Rift, Greece. *Tectonophysics,* 308, 275–290.

Spangler, L, Dobeck, L, Repasky, K, Nehrir, A, Humphries, S, Barr, J, Keith, C, Shaw, J, Rouse, J, Cunningham, A, Benson, S, Oldenburg, C, Lewicki, J, Wells, A, Diehl, J R, Strazisar, B, Fessenden, J, Rahn, T, Amonette, J, Barr, J, Pickles, W, Jacobson, J, Silver, E, Male, E, Rauch, H, Gullickson, K, Trautz, R, Kharaka, Y, Birkholzer, J and Wielopolski, L. 2010. A shallow subsurface controlled release facility in Bozeman, Montana, USA, for testing near surface CO_2 detection techniques and transport models. *Environmental Earth Sciences*, Vol. 60, 227-239.

Sperrevik, S., Gillespie, P.A., Fisher, Q.J., Halvorsen, T. and Knipe, R.J. 2002. Empirical estimation of fault rock properties. In: Koestler, A.G. and Hunsdale, R. (eds) *Hydrocarbon Seal Quantification*. Norwegian Petroleum Society (NPF), Special Publication 11, 109–126.

Steinich, G. 1972. Endogene Tektonik in den Unter-Maastricht-Vorkommen auf Jasmund (Rügen). In: *Geologie 20, Beiheft 71/72*, S. 1 - 207. Berlin.

Stewart, M., Lonergan, L. and Hampson, G., 2012. 3D seismic analysis of buried tunnel valleys in the Central North Sea: tunnel valley fill sedimentary architecture. *Geological Society, London, Special Publications*, *368*(1), pp.173-184.

Stewart, M.A., Lonergan, L. and Hampson, G., 2013. 3D seismic analysis of buried tunnel valleys in the central North Sea: morphology, cross-cutting generations and glacial history. *Quaternary Science Reviews*, *72*, pp.1-17.

Stewart, S. A. and Davies, R. J. 2006. Structure and emplacement of mud volcano systems in the South Caspian Basin. *AAPG Bulletin* 90, 771–786.

Stoker, M.S. and Bent, A.J.A., 1987. Lower Pleistocene deltaic and marine sediments in boreholes from the central North Sea. *Journal of Quaternary Science* 2, 87–96.

Stoker, M.S., Balson, P.S., Long, D. and Tappin, D.R., 2011. An overview of the lithostratgraphical framework for the Quaternary deposits on the United Kingdom continental shelf. *British Geological Survey Research Report, RR/11/03* (48 pp)

Streit, J.E. and Hillis, R.R. 2004. Estimating fault stability and sustainable fluid pressures for underground storage of CO_2 in porous rock. *Energy* 29, 1445–1456.

Streit, J.E. and Watson, M.N. 2005. Estimating rates of potential CO_2 loss from geological storage sites for risk and uncertainty analysis. *Presented at the 7th International Conference on Greenhouse Gas Control Technologies, Vancouver, Canada*.

Streit, J.E. and Watson, M.N. 2007. Final risk assessment report for the FutureGen project environmental impact statement. October 2007 revision. *US Department of Energy Report*.

Talukder, A.R., 2012. Review of submarine cold seep plumbing systems: Leakage to seepage and venting. *Terra Nova* 24, 255–272.

Tasianas, A., Mahl, L., Darcis, M., Bünz, S. and Class, H. Simulating seismic chimney structures as potential vertical migration pathways for CO_2 in the Snøhvit area, SW Barents Sea: model challenges and outcomes. 2016. *Environmental Earth Sciences* 2016; Volum 75 (504). ISSN 1866-6280.s doi: 10.1007/s12665-016-5500-1.

Tassi, F, Capaccioni, B, Caramanna, G, Cinti, D, Montegrossi, G, Pizzino, L, Quattrocchi, F and Vaselli, O. 2009. Low-pH waters discharging from submarine vents at Panarea Island (Aeolian Islands, southern Italy) after the 2002 gas blast: Origin of hydrothermal fluids. *Applied Geochemistry*, Volume 24, Issue 2, February 2009, p. 246-254.

Taylor, P., Stahl, H., Vardy, M E., Bull, J M., Akhurst, M., Hauton, C., James, R H., Lichtschlag, A., Long, D., Aleynik, D., Toberman, M., Naylor, M., Connelly, D., Smith, D., Sayer, M D J., Widdicombe, S., Wright, I C. and Blackford, J. 2015. A novel sub-seabed CO_2 release experiment informing monitoring and impact assessment for geological carbon storage. *International Journal of Greenhouse Gas Control*, 38, 3-17.

Tao, Q. and Bryant, S. L. 2014. Well permeability estimation and CO_2 leakage rates *International Journal of Greenhouse Gas Control* 22 (2014) 77–87

Teige, G.M.G. and Hermanrud, C. 2004. Seismic characteristics of fluid leakage from an under-filled and overpressured Jurassic fault trap in the Norwegian North Sea. *Petroleum Geoscience* 10, 35–42.

Tewksbury, B.J., Hogan, J.P., Kattenhorn, S.A., Mehrtens, C.J. and Tarabees, E.A. 2014. Polygonal faults in chalk: Insights from extensive exposures of the Khoman Formation, Western Desert, Egypt. *Geology*, 42, 479–482.

Thomas, G.S.P., Chiverrell, R.C., Huddart, D., Long, D. and Roberts, D.H. 2006. The Ice Age In: Chiverrell RC and Thomas GSP (eds.). A New History of the Isle of Man: Volume 1 Evolution of the natural landscape. *Liverpool University Press*, 126-219.

Thomas, G.S.P. and Chiverrell, R.C. 2007. Structural and depositional evidence for repeated ice-marginal oscillation along the eastern margin of the Late Devensian Irish Sea Ice Stream. *Quaternary Science Reviews 26*, 2375-2405.

Thomas, G.S.P. and Chiverrell, R.C. 2011. Styles of structural deformation and syntectonic sedimentation around the margins of the Late Devensian Irish Sea Ice Stream: the Isle of Man, Llyn Peninsula and County Wexford. In Phillips, E., Lee, J.R., Evans, H.M. (Eds.). 2011. *Glacitectonics – Field Guide. Quaternary Research Association*.

Tizzard, L., 2008. The Contribution to Atmospheric Methane from Sub-Seabed Sources in the UK Continental Shelf. *University of Newcastle*.

Todd, B.J., Shaw, J. and Valentine, P.C., 2016. Submarine glacial landforms on the Bay of Fundy–northern Gulf of Maine continental shelf. *Geological Society, London, Memoirs*, 46(1), pp.429-436.

Torabi, A. 2014. Cataclastic bands in immature and poorly lithified sandstone, examples from Corsica, France. *Tectonophysics* 630, 91–102.

Trautz, R. C., Pugh, J. D., Varadharajan, C., Zheng, L., Bianchi, M., Nico, P. S., Spycher, N. F., Newell, D. L., Esposito, R. A., Wu, Y., Dafflon, B., Hubbard, S. S. and Birkholzer, J T. 2012. Effect of Dissolved CO_2 on a Shallow Groundwater System: A Controlled Release Field Experiment. *Environmental Science and Technology*, Vol. 47, 298-305.

Trevisan, L., Pini, R., Cihan, A., Birkholzer, J. T., Zhou, Q. L. and Illangasekare, T. H., 2015. Experimental analysis of spatial correlation effects on capillary trapping of supercritical CO_2 at the intermediate laboratory scale in heterogeneous porous media. *Water Resources Research* 51(11): 8791-8805.

Trium Inc. and Chemistry Matters. 2011. Site Assessment (SW-30-05-13-W2M), near Weyburn, Saskatchewan. *Trium Environmental Inc. and Chemistry Matters, Project Number: T10-167-CEN*, pp. 50.

Tueckmantel, C., Fisher, Q.J., Grattoni, C.A. and Aplin, A.C. 2012. Single- and two-phase fluid flow properties of cataclastic fault rocks in porous sandstone. *Marine and Petroleum Geology* 29 (1), 129–142.

Underhill, J.R. and Woodcock, N.H. 1987. Faulting mechanisms in high-porosity sandstones; New Red Sandstone, Arran, Scotland. In: Jones, M.E. and Preston, R.M.F. (eds). *Deformation of sediments and Sedimentary Rocks*. Geological Society, London, Special Publication 29, 91–105.

Underschultz, J.R. 2016. Linking capillary and mechanical seal capacity mechanisms. *Petroleum Geoscience,* 23, 3–9.

van der Meer, J.J.M., Kjær, K. and Krüger, J. 1999. Subglacial water-escape structures, Slettjökull, Iceland. *Journal of Quaternary Science* 14, 191–205.

van der Meer, J.J.M., Kjær, K.H., Krüger, J., Rabassa, J. and Kilfeather, A.A. 2008. Under pressure: clastic dykes in glacial settings. *Quaternary Science Reviews* 28, 708-720.

Van der Vegt, P., Janszen, A. and Moscariello, A., 2012. Tunnel Valleys: current knowledge and future perspectives. In: Huuse, M., Redfern, J., Le Heron, D.P., Dixon, R.J., Moscariello, A., Craig, J. (Eds.), Glaciogenic Reservoirs and Hydrocarbon Systems. *Geological Society Special Publication*, vol. 368, pp. 75-97.

van der Wateren, F.M. 1985. A model of glacial tectonics, applied to the ice-pushed ridges in the central Netherlands. *Bulletin of the Geological Society of Denmark 34*, 55-77.

van der Wateren, F.M. 1987. Structural geology and sedimentology of the Dammer Berge push moraine, FRG. In: J.J.M. van der Meer (ed.). *Tills and Glaciotectonics*. Balkema, Rotterdam, 157-182.

van der Wateren, D. F. M. 1995. Processes of glaciotectonism. In Menzies, J. (ed.): Glacial Environments, Vol. 1: Modern Glacial Environments: Processes, *Dynamics and Sediments*, 309–335. Butterworth-Heinemann, Oxford.

van Gijssel, K. 1987. A lithostratigraphic and glaciotectonic reconstruction of the Lamstedt Moraine, Lower Saxony (FRG). In: J.J.M. van der Meer (ed.). *Tills and Glaciotectonics*. Balkema, Rotterdam, 145-155.

Van Hulten, F.F.N. 2010. Geological factors effecting compartmentalization of Rotliegend gas fields in the Netherlands. In: Jolley, S.J., Fisher, Q.J., Ainsworth, R.B., Vrolijk, P.J. and Delisle, S. (eds) *Reservoir Compartmentalization*. Geological Society, London. Special Publications 347, 301–315.

Van Landeghem, K.J.J., Niemann, H., Steinle, L.I., Reilly, S.S.O., Huws, D.G. and Croker, P.F., 2015. Geological settings and seafloor morphodynamic evolution linked to methane seepage. Geo-Marine Letters 35, 289–304.

Vaughan-Hirsch, D. P., Phillips, E., Lee, J. R. and Hart, J. K. 2013. Micromorphological analysis of poly-phase deformation associated with the transport and emplacement of glaciotectonic rafts at West Runton, north Norfolk, UK. *Boreas 42*, 376–394.

Vaughan-Hirsch, D.P. and Phillips, E.R. 2016. Mid-Pleistocene thin-skinned glaciotectonic thrusting of the Aberdeen Ground Formation, Central Graben region, central North Sea. *Journal of Quaternary Science DOI*: 10.1002/jqs.2836.

Vejbaek, O.V. 2008. On dis-equilibrium compaction as the cause for Cretaceous-Paleogene over-pressures in the Danish North Sea. *AAPG Bulletin* 92, 165–180.

Vialle, S., Druhan, J.L. and Maher, K. 2016. Multi-phase flow simulation of CO_2 leakage through a fractured caprock in response to mitigation strategies. *International Journal of Greenhouse Gas Control* 44, 11–25.

Voltattorni, N., Sciarra, A., Caramanna, G., Cinti, D., Pizzino, L. and Quattrocchi, F. 2009. Gas geochemistry of natural analogues for the studies of geological CO_2 sequestration. *Applied Geochemistry* 24, 1339–1346.

Walsh, J.J. and Watterson, J. 1991. Geometric and kinematic coherence and scale effects in normal fault systems. In: Roberts, A.M., Yielding, G. and Freeman, B. (eds) *The Geometry of Normal Faults*. Geological Society, London. Special Publications 56, 193–203.

Wang, H., Ren, Y., Jia, J. and Celia, M A. 2015. A probablistic collocation Eulerian-Lagrangian localized adjoint method on sparse grids for assessing CO_2 leakage through wells in randomly heterogeneous porous media. *Computer Methods in Applied Mechanics and Engineering*, Vol. 292, 35-53.

Watson, M.N., Boreham, C.J. and Tingate, P.R. 2004. Carbon dioxide and carbonate cements in the Otway Basin: implications for geological storage of carbon dioxide. *APPEA Journal* 44 (1), 703–720.

Watson, F.E., Mathias, S.A., van Hunen, J., Daniels, S.E. and Jones, R.R. 2012. Dissolution of CO_2 From Leaking Fractures in Saline Formations. *Transport in Porous Media*, 94, 729-745

Watson, Z.T., Han, W.S., Keating, E.H., Jung, N.H. and Lu, M. 2014. Eruption dynamics of CO_2-driven cold-water geysers: Crystal, Tenmile geysers in Utah and Chimayó geyser in New Mexico. *Earth and Planetary Science Letters* 408, 272–284.

West, J.M., Jones, D.G., Annunziatellis, A., Barlow, T.S., Beaubien, S.E., Bond, A., Breward, N., Coombs, P., de Angelis, D., Gardner, A., Gemeni, V., Graziani, S., Green, K.A., Gregory, S., Gwosdz, S., Hannis, S., Kirk, K., Koukouzas, N., Krüger, M., Libertini, S.; Lister, T.R., Lombardi, S., Metcalfe, R., Pearce, J.M., Smith, K.L., Steven, M.D., Thatcher, K. and Ziogou, F. 2015. Comparison of the impacts of elevated CO_2 soil gas concentrations on selected European terrestrial environments. *International Journal of Greenhouse Gas Control*, 42. 357-371.

White DJ. 2014. Toward quantitative CO_2 storage estimates from time-lapse 3D seismic travel-times: An example from the IEAGGH Weyburn-Midale monitoring and storage project. *International Journal of Greenhouse Gas Control* 2014; 16S: S95-S102.

White, J.C., Williams, G.A.; Grude, S. and Chadwick, R. A. 2015 Utilizing spectral decomposition to determine the distribution of injected CO_2 at the Snøhvit Field. *Geophysical Prospecting*, 63 (5). 1213-1223.

Wilkinson, M., Gilfillan, M.V., Haszeldine, R.S. and Ballentine, C.J., 2009. Plumbing the depths: testing natural tracers of subsurface CO_2origin and migration, Utah. In: Grobe, M., Pashin, J.C., Dodge, R.L. (Eds.), *Carbon Dioxide Sequestration in Geologic Media-State of the Science*. American Association of Petroleum Geologists, pp.619–634.

Williams, G., Brabham, P., Eaton, G. and Harris, C., 2001. Late Devensian glaciotectonic deformation at St Bees, Cumbria: a critical wedge model. *Journal of the Geological Society 158*, 125–135.

Williams, J.D.O., Holloway, S. and Williams, G.A. 2014. Pressure constraints on the CO_2 storage capacity of the saline water-bearing parts of the Bunter Sandstone Formation in the UK Southern North Sea. *Petroleum Geoscience* 20, 155–167.

Williams, J.D.O., Fellgett, M.W., Kingdon, A. and Williamson, J.P. 2015. *In-situ* stress orientations in the UK Southern North Sea: Regional trends, deviations and detachment of the post-Zechstein stress field. *Marine and Petroleum Geology* 67, 769–784.

Williams, J.D.O. and Gent, C.M.A. 2015. Shallow Gas Offshore Netherlands – The Role of Faulting and Implications for CO_2 Storage. *Presented at the Fourth International Conference on Fault and Top Seals, Alméria, Spain, 20–24th September.* Mo FTS P04.

Williams, J.D.O., Fellgett, M.W. and Quinn, M.F. 2016. Carbon dioxide storage in the Captain Sandstone aquifer: determination of in situ stresses and fault-stability analysis. *Petroleum Geoscience* 22, 211–222.

Wiprut, D. and Zoback, M.D. 2000. Fault reactivation and fluid flow along a previously dormant normal fault in the northern North Sea. *Geology* 28 (7), 595–598.

Woodside, J. M., Ivanov, M. K. and Limonov, A.F. (Eds.), 1997. Neotectonics and fluid flow through seafloor sediments in the Eastern Mediterranean and Black Seas—Parts I and II. IOC Technical Series, 48, UNESCO.

Worsley D., Johansen R. and Kristensen S.E. 1988 The Mesozoic and Cenozoic succession of Tromsøflaket In: Dalland A., Worsley D., Ofstad K. (eds) A lithostratigraphic scheme for the Mesozoic and Cenozoic Succession Offshore Mid and Northern Norway. *Norwegian Petroleum Directorate Bulletin* No. 4, pp 42–65

Worum, G., van Wees, J-D., Bada, G., van Balen, R.T., Cloetingh, S. and Pagnier, H. 2004. Slip tendency analysis as a toll to constrain fault reactivation: A numerical approach applied to three-dimensional fault models in the Roer Valley rift system (southeast Netherlands). *Journal of Geophysical Research* 109 (B02401).

Yang, Q, Matter, J, Stute, M, Takahashi, T, O'Mullan, G, Umemoto, K, Clauson, K, Dueker, M E, Zakharova, N, Goddard, J and Goldberg, D. 2014. Groundwater hydrogeochemistry in injection experiments simulating CO_2 leakage from geological storage reservoir. *International Journal of Greenhouse Gas Control*, Vol. 26, 193-203.

Yielding, G., Freeman, B. and Needham, D.T. 1997. Quantitative fault seal prediction. *AAPG Bulletin* 81 (6), 897–917.

Yielding, G., Bretan, P. and Freeman, B. 2010. Fault seal calibration: a brief review. In: Jolley, S.J., Fisher, Q.J., Ainsworth, R.B., Vrolijk, P.J. and Delisle, S. (eds) *Reservoir Compartmentalization*. Geological Society, London. Special Publications 347, 243–255.

Yielding, G. 2012. Using probabilistic shale smear modelling to relate SGR predictions of column height to fault-zone heterogeneity. *Petroleum Geoscience* 18, 33–42.

Zahasky, C, and Benson, S. 2014. A simple approximate semi-analytical solution for estimating leakage of carbon dioxide through faults. *Energy Procedia*, Vol. 63, 4861-4874.

Zanella, E. and Coward, M.P. 2003. Structural Framework. In: Evans, D., Graham, C., Armour, A. and Bathhurst, P. (eds) *The Millennium Atlas: Petroleum Geology of the Central and Northern North Sea*. Geological Society, London. 45–59.

Zeidouni, M., Hovorka, S. D., and Shi, K. W. (2016). Tracer test to constrain CO2 residual trapping and plume evolution. *Environmental Earth Sciences* 75(22).

Zhang, M. and Bachu, S. 2011. Review of integrity of existing wells in relation to CO_2 geological storage: What do we know?, *International Journal of Greenhouse Gas Control,* Volume 5, Issue 4, Pages 826-840.

Ziogou, F., Gemeni, V., Koukouzas, N., De Angelis, D., Libertini, S., Beaubien, S.E., Lombardi, S., West, J., Jones, D.G., Coombs, P., Barlow, T.S., Gwosdz, S. and Krüger, M. 2013. Potential environmental impacts of CO_2 leakage from the study of natural analogue sites in Europe. *Energy Procedia* 37, 3521–3528.

Zuo, L. and S. M. Benson 2014. Process-dependent residual trapping of CO_2 in sandstone. *Geophysical Research Letters* 41(8): 2820-2826.

Appendices

Appendix 1 Table A1 Selected Leakage Rates along Wellbores at Analogues Sites: Gas Storage or CO_2 producers

Study summary	Study objective and design	Leakage rate results	Comments or relevance to CO_2 storage
Type of study: Numerical **Fluid(s):** CO_2 and brine **Site:** Cranfield, MS, USA **Reference:** Nicot et al., 2013	A semi-analytical solution was used to assess wellbore leakage risk at Cranfield CO_2-EOR site. CO_2 and brine mass flow rates at the ground surface were calculated. Flow pathways up abandoned wells that are considered include behind the casing via an annulus and/or permeable pathways through damaged cement.	0.9 t/year per well, i.e. **5.8 x 10^{-6} t/year**. This represents 0.0002 % of the injection rate. The models suggest that up to 2 of the 17 wells in the study area could be leaking, the rest are effectively sealed.	Mitigating factors include: a) a tested well that showed poor cement bond log was nevertheless found to be maintaining isolation b) annulus pathways may self-seal via formation cave in or swelling mechanisms b) multiple permeable zones above the injection would likely "blead off' fluids rising through an unsealed casing-rock annulus, particularly those pressure depleted by production.
Type of study: Field **Fluid(s):** CO_2 and brine **Site:** Cranfield, MS, USA **Reference:** Duguid et al., 2014	Hydraulic isolation in a 68 year old wellbore was assessed using field data. Various wireline geophysical logs and pressure tests were run. Fluid and sidewall core samples were also taken to measure strength and permeability properties.	The well was found to be **hydraulically isolating** over the interval that identified as having poor isolation from the field data. The remedial cement squeeze job was therefore unnecessary.	A wellbore identified as having poor integrity and presenting a leakage risk nevertheless still provided a barrier to potential CO_2 migration. The integrity was better than field data suggested.

Study summary	Study objective and design	Leakage rate results	Comments or relevance to CO_2 storage
Type of study: Numerical **Fluid(s):** CO_2 and brine **Site:** Generic **Reference**: Harp et al., 2016,	A Reduced Order Model estimates CO_2 and brine leakage rates into an overlying thief zone, aquifer and all the way to surface.	Maximum leakage rate into the overburden aquifer for CO_2 was 0.008 kg/s, equivalent to **252 t/year**; and for brine the rate was much less than 0.001kg/s , equivalent to **< 31.5 t/year**	An extremely small fraction of the total injected CO_2 leaks up the wellbore. The most important input parameter was the permeability assigned to the wellbore.
Type of study: Field and numerical **Fluid(s):** CO_2 and brine **Site:** Generic. Field data from 314 CH_4 wells. **Reference:** Tao and Bryant, 2014 & Checkai et al., 2013	CO_2 wellbore leakage flux and flow rates through cement, casing, or formation defects were computed. Estimates and ranges of pathway permeabilities and apertures were created using Monte Carlo simulations of Surface Casing Pressures or Vent Flow field data from a study of 314 hydrocarbon gas wells across 6 fields.	Leakage range spanned 0.01 kg/m^2/year to 5 t/m^2/year for individual wells. The majority of leakage rates, per well, were less than 1 kg/year (**0.001 t/year**) and highest rates were less than **0.1 t/year**.	90% of fluxes were less than 0.1 t/m^2/year i.e. less than large natural CO_2 fluxes such as Crystal geyser, USA or from volcanic vents in Germany and Hungary. Leakage path permeability was the most important parameter, compared to leakage depth and other parameters examined.
Type of study: Numerical **Fluid(s):** CO_2 and brine **Site:** Ketzin, Germany **Reference:** Le Guen et al., 2011	A numerical study to assess risk of leakage via the plugged and abandoned former CO_2 injection well after 1000 years. Model results show CO_2 saturation in the wellbore cavity, casing annulus and cement for 2 pressure scenarios. The high pressure case intends to represent a hypothetical large scale site. The low pressure case is intended to be relevant to the pilot scale site studied.	Zero leakage for the low pressure case. In the hypothetical, high pressure case, CO_2 saturations reach the surface via cement leaching and casing corrosion processes after less than 500 years, indicating a leakage pathway to surface.	If a high pressure case was ever envisaged at this site, mitigating actions prior to plugging and abandonment would be required to reduce leakage risks.

Study summary	Study objective and design	Leakage rate results	Comments or relevance to CO_2 storage
Type of study: Numerical **Fluid(s):** CO_2 and brine **Site:** Paris Basin, France **Reference:** Humez et al*.,* 2011	Multiphase reactive transport model (TOUGH REACT) used to study the geochemical impact of CO_2 and brine leakage into a freshwater aquifer. Leakage through a hypothetical leaky well 100 m from injection well for 5 years is considered, with assumed pathways along the cement-rock interface.	After 90 days the CO_2 reached the overlying aquifer at a rate of 0.2 kg/s, increasing to 1.1 kg/s after 5 years. . Equivalent to **6307 to 34,690 t/year**. Accompanying brine flow rate decreased from 0.019 kg/s after 90 days to 0.003 kg/s after 3 years, Equivalent to **94.6 t/year** brine after 5 years injection and simulation.	Basic sensitivity analysis shows that the leakage rate depends strongly on the distance, void volume and residual trapping between the injector and leaking well and the permeability of the leaking wellbore. For example, if the leaky well is positioned more than 500 m from the injector, the leakage rate becomes negligible.
Type of study: Field **Fluid(s):** CH_4 and C_2H_6 (methane and ethane) **Site:** Aliso Canyon, CA, USA **Reference:** Conley et al*.,* 2016	A field-monitoring study to determine the leakage rate from a blown-out well in a natural gas storage facility for emissions accounting. CH_4 concentration was measured through time via aircraft-borne sensors on 13 flights during the leak period. Ground-collected air samples were also analysed. Aliso canyon gas storage facility has 115 wells in total. The single-well blow-out event described here lasted 112 days (3 months), from November 2015 to February 2016.	Leakage rates were up to 60 t/hr CH_4 & 4.5 t/hr C_2H_6 (ethane) for the first 6 weeks, decreasing thereafter to 20 t/hr CH_4. Equivalent to **0.53 Mt/year** decreasing to **0.18M t/year** Post-kill residual leak rate <1 t/hr, consistent with typical non-zero leak rates from other similar facilities US-wide. Equivalent to less than **0.009 Mt/year.**	This event was temporarily the largest known anthropogenic point source of CH_4 in the USA. Approximately 100 kt was released in total, which represents 3% of the storage facility capacity. The wellbore blowout was eventually stopped, or ‘killed’, by drilling a relief well that intersected the affected well above the reservoir depth to deliver ‘kill-fluids’. 7 previous attempts to kill the well via original wellbore failed because of complexities in the fluid pathway to the base of the well.

Study summary	Study objective and design	Leakage rate results	Comments or relevance to CO_2 storage
Type of study: Numerical **Fluid(s):** CO_2 based on field data from CH_4 well **Site:** Aliso Canyon, CA, USA **Reference:** Lindeberg et al., *(In press*)	Modelling to investigate hypothetical equivalent CO_2 leakage rates based on a CH_4 wellbore blowout. Reservoir and well models were matched to the observed CH_4 gas escape from the Alison Canyon wellbore blowout and those parameters were used to simulate a similar hypothetical incident with CO_2. The wellbore flow was modelled as 2 phase flow in pipes.	The CH_4 leakage rate of 15 kg/s became 9.11 kg/s CO_2**.** Equivalent to **0.3 Mt/year** CO_2, based on the CH_4 leakage rate of 0.5 Mt/year (Conley et al., 2016). Note that the leak duration was for approximately 3 months.	A lower leakage rate and lower total lost was found for CO_2 than for natural gas: 57.33 Mt 0.37% of the CO_2 stored was lost compared to 94.5 Mt or 2.8% of the stored CH_4. Remediation at the CO_2 blowout would likely be easier because of the lower well pressure at rupture point. Note that the well bore set up at Aliso Canyon was complex and unlike any that would be used at a CO_2 storage site.
Type of study: Field **Fluid(s):** CO_2 **Site:** Sheep Mountain, CO, USA **Reference:** Lynch et al*.,* 1985, reviewed in Lewicki et al., 2006	Field measurement of leakage from a wellbore blow out of a well being drilled as a CO_2 producer at the Sheep mountain natural CO_2 field. The blowout in 1982 resulted in CO_2 flowing from the surface wellhead and also leaking from fractures in the ground around the drill site.	The CO2 leakage rate was calculated to be at least 5.6×10^6 m^3/day, i.e. equivalent to 10,500 t/day and **3.8 Mt/year.** Note that the leak duration was 17 days.	The high flow rate complicated the first 2 attempts to stop (kill) the flow. Flow was eventually controlled by the dynamic injection of drag-reduced brine followed by mud.

Study summary	Study objective and design	Leakage rate results	Comments or relevance to CO_2 storage
Type of study: Field **Fluid(s):** CO_2 and brine **Site:** Crystal Geyser, UT, USA **Reference:** Gouveia et al*.,* 2005, reviewed in Lewicki et al., 2006	An abandoned oil exploration well from 1935 provides a pathway for CO_2-charged water. Crystal Geyser is 1 of several boreholes drilled in the basin for water or oil that now discharge CO_2-rich water. Eruption patterns have varied through time and are reviewed in Jung et al., 2015. Atmospheric CO_2 concentrations were measured along with wind speed and directions on a grid 25 – 100 m from the site. Gaussian modelling was used to estimate the leakage rate.	224-500 t/day during eruptions, when geysers were around 20 m high, and erupting approximately every 12 hours. 15 t/day during pre-eruptive events. The annual leakage rate was estimated at **12 kt/year**.	Wellbore abandonment procedure is not reported and it is thought that only surface casing is in place. Studies at geysering sites allow improved understanding of CO_2-brine flow rates and geysering behaviour via open wellbores.
Type of study: Numerical **Fluid(s):** CO_2 and brine **Site:** Crystal Geyser, UT, USA **Reference:** Jung et al*.,* 2015	See above for geyser description. A regional-scale simulation model using TOUGH2/EC incorporates CO_2-brine flow up a major fault and along the crystal geyser wellbore. The model replicated the geyser-like wellbore leakage behaviour and matched field-measured flow rates. Leakage rate of brine and CO_2 gas from wellbore at surface.	Computed flux coincided with field measurements. During geysering behaviour maximum flow rates of CO_2 gas was 0 - 8.5 x 10^3 g/m^2/d; and brine was 0-2.1 x 10^5 g/m^2/d.	Of the 3 well based parameters varied, changing the matrix permeability had the greatest effect. Changing wellbore porosity or radius had comparatively little effect.

Study summary	Study objective and design	Leakage rate results	Comments or relevance to CO_2 storage
Type of study: Field and numerical **Fluid(s):** CO_2 and brine **Site:** Crystal Geyser, UT, USA **Reference:** Watson et al., 2014	Down-hole, in situ measurements of pressure and temperature were used to calculate leakage rates of the geyser-flow of brine and CO_2 up 3 abandoned boreholes in Utah, USA: Crystal Geyser (see above). Tenmile Geyser is an abandoned oil exploration well near Crystal Geyser, but with an eruption to quiescent time ratio 17-50 times less than Crystal Geyser. Chimayo Geyser was a well drilled for residential water extraction. Its eruption to quiescent time ratio is half that of Tenmile Geyser.	CO_2 leakage rates at: Crystal Geyser, UT, USA: $4.77 \pm 1.92 \times 10^3$ t year. **3-7kt/year** Tenmile Geyser, UT, USA: $6.17 \pm 1.73 \times 10^1$ t/year. **4.44-7.9t/year** Chimayo Geyser, NM, USA: $6.54 \pm 0.57 \times 10^1$ t/year. **5.97-7.11t/year.**	CO_2 leakage via the geysering was greater than the diffuse or fault leakage in the vicinity of this natural CO_2 release area. However, note that in a CO_2 storage scenario, mitigating discharge from a well would be likely to be a much easier process, than remediating the non-anthropogenic pathways.
Type of study: Field **Fluid(s):** CO_2 and CH_4 **Site:** Torre Alfina, Italy **Reference:** Ferrara and Stephani 1978, reviewed in Lewicki et al., 2006	A geothermal exploration well blew out in 1973 during drilling resulting in free flow of fluid (primarily gas) to surface. After the well was shut in, numerous areas of CO_2 surface emissions occurred via permeable pathways through the overburden because there was no casing in place yet. Atmospheric CO_2 concentrations were measured within a 250 m diameter of the well over a 53 day-survey to estimate the leakage rate. The leakage was controlled by completely cementing the well.	More than 300 t/hr of fluid, primarily CO_2 gas was released. Equivalent to **2.63 Mt/year**. The total release was around 25 kt of CO_2. Note that the release period <1 year.	This blow out (and that at Sheep Mountain) occurred during drilling into a pressurised natural CO_2 reservoir. It is therefore only relevant to a CO_2 storage scenario if a) if records of storage site location were lost, pressure in the reservoir had not dissipated and future exploration holes pierced them b) in the highly unlikely case that uncased and still open wells exist in the storage site vicinity.

Study summary	Study objective and design	Leakage rate results	Comments or relevance to CO_2 storage
Type of study: Field **Fluid(s):** CH_4 **Site:** Leroy, WY, USA **Reference:** Araktingi et al., 1984, reviewed in Lewicki et al., 2006	Casing corrosion caused failure of a well in a gas storage facility in 1973. Gas migrated horizontally through the overburden to another well where it migrated vertically along the outside of the well casing and bubbled out at surface. Leakage was later found via another well casing and at surface nearby a few years later. Some leaks continued when storage pressures were reduced, suggesting a secondary shallow accumulation may have built up. Post 1981 leakage was controlled by keeping the storage injection pressure below a threshold value. CH_4 leakage rates were estimated by modelling pressure data in combination with the time it took for tracers injected to reach the surface.	The average annual leakage rate from 1976-1981 was 3 x 10^6 m^3/year Equivalent to **0.2 Mt/year** and 3 % of gas the gas stored.	These findings could be used as an analogue for 'worst-case' behind-casing annular flow rates for old abandoned wells with no records of cement across overburden permeable intervals. Note that current abandonment procedures would generally require cement across overburden permeable intervals and that if such wells were found during site characterisation they would likely require remediation or a change in site to reduce the leakage risks. This site could also have relevance for leakage mitigation by dropping the reservoir pressure e.g. by back-producing some of the CO_2 stored.

Appendix 2 Table A2: List of Pockmarks and Other Negative Fluid Escape Features Reported in Shallow-Water Sites (<200 M). Compiled By Ingrassia Et Al. (2015). Water Depth, Width and Vertical Relief Values in Metres (M). NA, Data Not Available

ID	*Location*	*Sea/Ocean*	*Water depth (m)*	*Width (m)*	*Vertical relief (m)*	*Origin/process*	*Sea floor features*	*Reference*
1	Braemar field, Orkney Islands	North Sea	120	5 -130	0.5 - 5	Biogenic gas	Pockmark field	Hartley, 2005
2	Tommeliten seepage area, Norwegian	North Sea	65-75	3-5	NA	Gas associated to salt diapirs	Pockmark field	Hovland and Thomsen, 1989
3	Scanner Pockmark, United Kingdom	North Sea	172	900-450	22	NA	Pockmark field	Dando et al. 1991; Jones, 1993; Dando, 2001
4	Eastern Skagerrak	North Sea	200	200-500	20-25	Biogenic	Giant pockmark	Hovland, 1992
5	Norwegian Trench, Norway	North Sea	100 - 500	400	45	Mixed biogenic/thermogenic bottom current	Elongate depressions	Bøe et al., 1998
6	Oregon shelf, USA	Pacific Ocean	132	NA	5	Biogenic	Pockmark field	Juhl and Taghon, 1993
7	Hecate Strait,Canada	Pacific Ocean	130-135	30-160	2-10	Thermogenic	Pockmark chain	Barrie et al., 2011
8	Santa Barbara seep, Usa	Pacific Ocean	120	500		Hydrocarbon gases	Giant pockmark	Davis and Spies, 1980; Montagna et al., 1989
9	Cascadia continental margin	Pacific Ocean	150	100	NA	Methane emission	Giant pockmark	Salmi et al., 2011
10	Kagoshima Bay, Japan	Pacific Ocean	200	5000	NA	Hydrothermal fluid	Crater-like depression	Yamanaka et al., 2013
11	Passamaquoddy Bay, Canada	Gulf of Maine	35-81	1-300	29	Biogenic methane	Pockmark field	Wildish et al., 2008
12	Dnepr Paleo-delta	Black Sea	90-100	100	3	Stratigraphically controlled flow	Elongated depression	Naudts et al., 2006

ID	Location	Sea/Ocean	Water depth (m)	Width (m)	Vertical relief (m)	Origin/process	Sea floor features	Reference
13	Bulgarian continental shelf	Black Sea	160-240	50-200	1.5-7	NA	Pockmark field	Dimitrov and Dontcheva, 1994
14	Turkish shelf-Eastern	Black Sea	180-300	50-200	10-25	Gas-migration bottom current	Pockmark field	Cifci et al., 2003
15	Grand Banks, Fortune Bay	Atlantic Ocean	100-200	NA	NA	NA	Pockmark field	Fader, 1991
16	Louisiana Shelf, Louisiana	Gulf of Mexico	60-75	20-35	0.3-1.5	Thermogenic	Pockmark field	Sassen et al., 2003
17	Florida Middle Ground carbonate banks, West Florida	Gulf of Mexico	40 - 50	200	2 3	Groundwater seep	Depressions	Mallinson et al., 2014
18	Biscayne Bay, Florida	Atlantic Ocean	0-20	10-200	1-10	Groundwater seep	Depressions	Kramer et al., 2001
19	Abrolhos Bank, Brazil	Atlantic Ocean	20-50	10 -75	8-39	Gas and karst processes	Sinkhole-like structure	Bastos et al., 2013
20	Belfast Bay-Gulf of Maine	Atlantic Ocean	10-70	300	20	Biogenic gas	Giant pockmark	Kelley et al., 1994; Rogers et al., 2006
21	Virginia/North Carolina continental shelf	Atlantic Ocean	100-150	>1000	50	Thermogenic or biogenic	Giant pockmark	Driscoll et al., 2000; Newman et al., 2008
22	Malin shelf, Ireland	Atlantic Ocean	100-180	100-500	NA	NA	Pockmark field	Szpak et al., 2012
23	Eckernförde Bay, Germany	Baltic Sea	25	NA	NA	Groundwater seep	Pockmarks	Bussmann et al., 1999
24	Norton Sound, Alaska	Bering Sea	< 50	1-10	1	Biogenic	Pockmark field	Nelson et al., 1979; Sandstrom et al., 1983
25	West Spitsbergen continental margin	Arctic Sea	50-245	80-100	20-30	Thermogenic	Pockmarks	Rajan et al., 2012; Gentz et al., 2014

ID	Location	Sea/Ocean	Water depth (m)	Width (m)	Vertical relief (m)	Origin/process	Sea floor features	Reference
26	Hopen Island, Norwey	Barent sea	130-240	10-20	1	Thermogenic	Pockmark field	Solheim and Elverhoi, 1985
27	Berri Field	Arabian Gulf	30	80	1-5	Hydrocarbon gases	Pockmark field	Judd and Hovland, 2007
28	Strait of Hormuz	Arabian Gulf	80-100	10-40	8	Hydrocarbon gases	Pockmark field	Judd and Hovland, 2007
29	Western continental margin of India	Arabian Sea	25-75	80-130	0.75-2.5	Biogenic or thermogenic Gas	Pockmarks	Karisiddaiah and Veerayya, 2002
30	Izu Peninsula, Japan	Japan Sea	90-100	450	10	Volcanic gas emissions	Crater-like depression	Notsu et al., 2014
31	Yampi Shelf, Northwest Australia	Timor Sea	50-90	1-10	1-2	Hydrocarbon gases	Pockmark field	Rollet et al., 2006
32	Yellow Sea continental shelf	Yellow Sea	80-100	500	4-12	Thermogenic gases	Crater-like depression	Jeong et al., 2004
33	Columbretes Islands	Western Mediterranean	80-90	300?	NA	NA	Giant pockmark	Munoz et al., 2005
34	Patras Gulf, Western Greece	Gulf of Corinth	20-40	25-250	0.5-15	Gas venting	Pockmark field	Hasiotis et al., 1996; Christodoulou et al., 2003; Marinaro et al., 2006
35	Santorini Island, Greece	Aegean sea	200	1700	505	Explosive silicic volcanism	Crater-like depression	Cantner et al., 2014
36	Prinos Bay, Thasos Island	Aegean Sea and the Ionian Sea	6-25	25	3	Groundwater seep or thermogenic	Pockmarks	Newton et al., 1980
37	Bonaccia Field, Italy	Aegean Sea and the Ionian Sea	100	NA	NA	NA	Pockmark field	Conti et al., 2002; Geletti et al., 2008

ID	Location	Sea/Ocean	Water depth (m)	Width (m)	Vertical relief (m)	Origin/process	Sea floor features	Reference
38	Northern Israel continental shelf	Eastern Mediterranean	< 120	NA	NA	NA	Pockmark field	Schattner et al., 2012
39	Izmir Gulf, Turkey	Aegean sea	40-50	20-180	1-7	Biogenic gas	Pockmark field	Dondurur et al., 2011
40	Iskenderun Bay, south-east Turkey	Eastern Mediterranean	80-82	35	0.5-1.5	Biogenic	Pockmark field	Garcìa-Garcìa et al., 2004
41	Jabuka Trough	Adriatic Sea	180-250	30-500	1-6	Probably thermogenic	Pockmark field	Geletti et al., 2007
42	Apulian continental shelf, Italy	Adriatic Sea	50-105	10-150	0.5-20	Groundwater seep	Depressions	Taviani et al., 2012
43	Panarea Islands, Italy	Tyrrhenian Sea	7-15	15	9	Hydrothermal fluid	Crater-like depression	Anzidei et al., 2005; Esposito et al., 2006; Aliani et al., 2010

IEA Greenhouse Gas R&D Programme

Pure Offices, Cheltenham Office Park, Hatherley Lane,
Cheltenham, Glos. GL51 6SH, UK

Tel: +44 1242 802911 mail@ieaghg.org
www.ieaghg.org